CRANFIELD UNIVERSITY

Department of Informatics and Sensors

Optimisation of Wireless Communication System

by

Exploitation of Channel Diversity

Khalid Iqbal

Supervisor:

R. F. Ormondroyd

CRANFIELD UNIVERSITY

Department of Informatics and Sensors

PhD THESIS

Academic Year 2004-2008

Khalid Iqbal

Optimisation of Wireless Communication System by Exploitation of Channel Diversity

Supervisor: R. F. Ormondroyd

July 2008

ACKNOWLEDGEMENTS

I would like to thank all those who helped me throughout my PhD. I wish to express my sincere gratitude to my supervisor Professor Richard Ormondroyd, for being the guiding force behind the research necessary for the completion of this thesis. Without his guidance, encouragement, support, ideas, and scientific enlightenment this work would not have been possible.

I also extend my sincere gratitude to Dr I.L Morrow and Dr Evan Hughes who as part of Thesis committee have been abundantly helpful and gave me a lot of valuable advice on my final oral exam and thesis. Furthermore, my great appreciation also goes to the management and staff of Department of Aerospace, Power and sensors for providing support and wonderful research environment.

Finally, I would like to thank my parents, my parents-in-law, my wife, children and my friends for all the encouragement and support they have provided me throughout my academic career. No words can express my gratitude to them.

ABSTRACT

Communication systems are susceptible to degradation in performance because of interference received through their side lobes. The interference may be deliberate electronic counter measure (ECM), Accidental RF Interference (RFI) or natural noise. The growth of interference communication systems have given rise to different algorithms, Adaptive array techniques offer a possible solution to this problem of interference received through side lobes because of their automatic null steering in both spatial and frequency domains. Key requirement for space-time architecture is to use robust adaptive algorithms to ensure reliable operation of the smart antenna. Space division multiple access (SDMA) involves the use of adaptive nulling to allow two or more users (mobiles) in the same cell to share same frequency and time slot. One beam is formed for each user with nulls in the direction of other users. Different approaches have been used to identify the interferer from desired user. Thus a ***basic model for determining the angle of arrival of incoming signals***, ***an appropriate antenna beam forming and adaptive algorithms*** are used for array processing.

There is an insatiable demand for capacity in wireless data networks and cellular radio communication systems. However the RF environment that these systems operate in is harsh and severely limits the capacity of traditional digital wireless networks. With normal wireless systems this limits the data rate in cellular radio environments to approximately 200 kbps whereas much higher data rates in excess of 25Mbps are required. A common wireless channel problem is that of frequency selective multi-path fading. To combat this problem, new types of wireless interface are being developed which utilise space, time and frequency diversity to provide increasing resilience to the channel imperfections. At any instant in time, the channel conditions may be such that one or more of these diversity methods may offer a superior performance to the other diversity methods. The overall aim of the research is to develop new systems that use a novel combination of smart antenna MIMO techniques and an advanced communication system based on advanced system configuration that could be exploited by IEEE 802.20 user specification approach for broadband wireless networking. The new system combines the Multi-input Multi-output communication system with frequency diversity in the form of an OFDM modulator. The benefits of each approach are examined under similar channel conditions and results presented.

TABLE OF CONTENTS

LIST OF FIGURES

LIST OF TABLES

LIST OF ABBREVIATIONS

ADSL	Asymmetric digital subscriber line
AoA	Angle of Arrival
AMPS	Advanced mobile phone system
AWGN	Additive White Gaussian Noise
AHG	Ad-hoc Group
BPSK	Binary Phase Shift Keying
BER	Bit-Error- Rate
BFN	Beam forming network
BLAST	Bell labs layered space-time
BS	Base Station
CMA	Constant Modulus Algorithm
CDMA	Code division multiple access
OFDM	Coded orthogonal freq division multiplexing
CSMA-CD	Carrier sense multiple access collision detect
D-BLAST	Diagonal Bell labs layered space-time
DLST	Diagonal layered space-time
DoA	Direction of Arrival
DSBSC	Double sideband suppressed carrier
DSSS	Direct sequence spread spectrum
FDMA	Frequency division multiple access
FHSS	Frequency hopped spread spectrum system
GA	Genetic Algorithm
GWSSUS	Gaussian Wide Sense Stationary Uncorrelated Scattering
GPRS	General Packet radio system
3GPP	3_{rd} generation partnership project
HLST	Horizontal layered space-time
H-BLAST	Horizontal Bell labs layered space-time
HSR	High sensitivity receiver
ISI	inter-symbol interference
ISDN	Integrated services digital network
ISM	Industrial, scientific and medical
LANs	Local area networks
LMS	Least mean square

LCMV	Linearly constrained minimum variance
LOS	Line of sight
LST	Layered space-time
MAN	Metropolitan area networks
MS	Mobile station
MISO	Multiple input single output
MIMO	Multiple input multiple output
MDDCM	Multi user double directional channel model
MSE	Mean square error
MSBS	Mobile Station Base Station
MMSE	Minimum mean square error
MVDR	Minimum variance distortionless response
ML	Maximum likelihood
MLSE	Maximum likelihood sequence estimation
NLMS	Normalized least mean square
NLOS	Non line of sight
NMPS	Nordic mobile phone system
OFDM	Orthogonal frequency division multiplexing
PCM	Pulse code modulation
PDAs	Personal digital assistants
PG	Path gain
PL	Path loss
PMR	Private mobile radio
RELP	Residually excited linear prediction vocoder
RMS	Root mean square
RF	Radio frequency
RLS	Recursive least mean square
SCM	Spatial channel model
SDMA	Space division multiple access
SFIR	spatial filtering for interference reduction
SIR	Signal to interference ratio
SIMO	Single input multiple output
SMS	Short message service
SNR	Signal to noise ratio
SNOI	Signal not of interest

SOI	Signal of interest
STBC	Space-time block codes
STC	Space-time coded
STTC	Space-time trellis codes
STTTC	Space-time turbo-trellis codes
TACS	Total access communication system
TOA	Time of Arrival
TDMA	Time division multiple access
ULA	Uniform Linear Array
VLST	Vertical layered space-time
VBLAST	Vertical Bell labs layered space-time
WLANs	Wireless local area networks

LIST OF SYMBOLS

$\mathbf{w}$	Beamforming weight vector
$(.)^{T}$	Stands for transpose
$(.)^{H}$	Stands for Hermitian
$(.)^{*}$	Stands for complex conjugate
σ^2	Noise variance
d	Spacing between adjacent antenna elements
f_d	Doppler frequency (Hertz)
t_s	Sampling time
θ	Direction of angle of arrival in degrees
a (θ)	Array response or steering vector for direction θ
λ	Carrier wavelength
$\mathbf{H}$	Matrix of channel coefficients
$h(t,\tau)$	Channel impuse response
τ	Delay variable.
j	Square root of –1
θ_{nmAOD}	Angle of departure for m^{th} subpath of n^{th} path
θ_{nmAOA}	Angle of arrival for m^{th} subpath of n^{th} path
$\|\mathbf{V}\|$	Magnitude of MS velocity vector
ϕ	Phase angle
α	Proportionality constant
μ	Forgetting factor that controls convergence of adaptive algorithms
$\mathbf{V}(\phi_s)$	Array response factor or steering vector in the look direction
$n(t)$	Receiver thermal noise
$d(t)$	Reference signal
$\mathbf{R}$	Correlation matrix of signal
$\hat{\mathbf{R}}$	Estimated correlation matrix
$\mathbf{R}_{ipn}$	Correlation matrix of interference plus noise only
(T_C)	Coherence time
(B_c)	Coherence bandwidth

(δ)	Phase shifter
P_t	Transmitter power
P_r	Reciever power
G_t	Transmit antenna gain
G_r	Receive antenna gain
θ_v	MS velocity vector
$\theta_{n,AoD}$	Angle of departure of n^{th} path
$\theta_{n,AoA}$	Angle of arrival of n^{th} path
Ω_{BS}	BS antenna array orientation with respect to North
Ω_{MS}	MS antenna array orientation with respect to North
$\Delta_{n,m}$	Offset for m^{th} sub-path of n^{th} path

Chapter -1

1 A historical perspective

1.1 Cellular Radio

The insatiable demand for mobile wireless connectivity worldwide over the past three decades has placed extreme demands on the RF spectrum that is needed to support these wireless networks. In the 1970s, the principal requirement for mobile radio was in support of private mobile radio (PMR) between a central base-station to mobile radios mounted in vehicles such as taxis, emergency service and police vehicles as well as public utility vehicles. Communications over this type of system were predominantly analogue voice communications using power efficient modulation schemes such as double-sideband suppressed carrier (DSBSC). The use of HF (3-30MHz) and VHF (30-300MHz) carrier frequencies provided reasonable ranges to support area coverage from the base-station transmitter, but the use of HF meant that spectrally efficient modulation schemes such as single-sideband (SSB) needed to be used and this placed severe limits on the obtainable bandwidth. Channelisation was invariably by means of frequency division multiple-access (FDMA) [2] and it was possible for this wide-area coverage scheme to meet the normal levels of traffic of that era because the user densities were so low.

In the 1980s, an entirely different type of mobile radio system was developed to support very much higher subscriber densities using voice communications. This type of system was called the cellular mobile radio [117]. It did not use wide area coverage base-stations, but many, overlapping, small area coverage areas called cells. High power wide area coverage transmitters of the PMR system are replaced by a great many lower power transmitters that are capable of covering the small area cell. In order to provide the higher system capacities needed to support the very high user densities, higher carrier frequencies in the UHF band (300-3000MHz) needed to be used. However, UHF signals are far easier to reflect and scatter than HF and VHF frequencies and so the mode of radiowave propagation at this frequency is substantially different than at HF. Propagation at this frequency is predominantly by a 'plane-earth' mechanism in which signal reception at a receiver is the vector sum of multiple signals from the direct path and reflected and scattered paths. This gives rise to a received signal that suffers deep fluctuations in the instantaneous signal as well as a mean signal level that suffers a very high attenuation with range according to a propagation law that has a $1/d^4$ relationship, where d is the separation between transmitter and receiver. Although it seems counter-intuitive that a very high path loss can be beneficial to the design and operation of the system, this is the situation for cellular radio. The aim of a

cellular approach is that by using small cells, the number of simultaneous calls within the cell is quite low, which naturally limits the required capacity of each basestation that serves each cell. However, because of the very high path loss, the signal strength rapidly decays over several cell diameters, so it is then possible to reuse the same frequency in a distant cell, without causing significant co-channel interference in that cell. Consequently, first generation cellular mobile radio was characterized by a robust, interference insensitive modulation scheme, frequency modulation (FM) and frequency reuse to maximize the spectral efficiency of the entire cellular system. Essentially, this system exploits the spatial domain to maximize the network capacity and provide an acceptable spectral efficiency. First generation cellular systems tested the practicality and demand for communications on the move and the growth in mobile phone sales was explosive. First generation systems were known by a number of different names depending on the origins of the equipment. In the US it was called advanced mobile phone system (AMPS) in Scandinavia it was the Nordic mobile phone system (NMPS) whilst in Europe it was known as the Total Access Communication System (TACS) [117]. First generation cellular radio provided a wireless interface to a conventional circuit-switched telecommunications system allowing mobile subscribers to communicate with traditional landlines as well as with other mobile subscribers. This was a major paradigm shift from the PMR, which was little more sophisticated than a walky-talky radio, albeit over extended ranges.

In the 1990s, second generation cellular mobile radios were developed to address the problem of demand, given the very tight availability of the spectrum for wireless systems. The new system recognized that some subscribers would wish to transmit or receive data files using the cellular radio as the air interface. Consequently, digital modulation schemes were adopted to facilitate data transmission by a minority of subscribers, the remainder communicating by voice. Voice signals were represented by a binary data stream using a digital vocoder and the signal was transmitted over the air-interface using digital modulation. In the European second generation cellular radio system called GSM [3], the vocoder used a technique called residually excited linear prediction vocoder (RELP), rather than the conceptually simpler pulse code modulation (PCM). This provided an acceptable speech transmission quality at a bit rate of 22.8kb/s (compared with 64kb/s for PCM). This meant that the data rate of each voice channel could be kept acceptably small to minimize the bandwidth of the transmitter. Digital transmission allowed a different form of subscriber multiple access to be used – namely time-division multiple access (TDMA) [117] rather than FDMA in which eight simultaneous users could be carried on a single carrier frequency. However, the system had the capability of operating on a number of different carrier

frequencies, simultaneously, thereby allowing upto 1000 subscribers to communicate with a base-station simultaneously. Because each handset used TDMA, it had to have a bandwidth that accommodated all eight digital signals simultaneously. For the GSM system using GMSK modulation and a RELP vocoder (as well as error control coding and channel sounding pilot bits), the bandwidth of each handset is 200kHz, resulting in an equivalent bandwidth per handset of 200kHz/8 users = 25kHz/user. This is the same equivalent bandwidth as first generation cellular radio systems.

Robust digital modulation with forward error correction coding combined with channel coding requires a lower signal to noise ratio (SNR) compared with analogue transmission schemes (typically by 5-10 times), allowing lower transmitter powers and reduced levels of mutual interference, thereby providing capacity enhancements compared with analogue schemes. Second generation cellular radio systems used for voice are circuit-switched. GSM provided a particular digital service called short message service (SMS), which allowed subscribers to exchange text messages. By choosing a preferential pricing tariff for such digital text services radically altered the use of mobile phones from a predominantly voice service to a text based service. Simultaneously, with the growth of the internet, there was also particular interest in the packet data services that GSM could provide. These packet data services were handled by a different, packet-switched, network called the general packet radio system (GPRS). Although GPRS is not yet as commercially successful as SMS, largely because a separate packet switched service provider is needed as well as the traditional circuit-switched operators for voice services, the development of wireless PDAs with small high resolution LCD screens that use the GSM air interface for data connectivity is beginning to increase demand for this type of service. To meet this demand, new enhanced packet-switched services are being developed where new, spectrally efficient, modulation schemes and the ability to concatenate multiple time slots are allowing GSM handsets to provide data rates over the air interface at rates of 64kbps – rivaling the rates provided by ISDN for landlines. Later generations of this system moved from 900MHz to 1800MHz carrier frequency, using lower power handsets and smaller cell sizes (as demanded by the higher carrier frequency and ease with which signals could be scattered). This system, known as DCS1800, was able to double the base station capacity from 1000 simultaneous calls to 2000 simultaneous callers.

In parallel with this development, Qualcomm in the US developed an entirely different cellular radio concept based on direct-sequence spread-spectrum techniques according to the IS95 interim standard. Having the trade name cdmaONE, this was the first mass-production code division multiple access (CDMA) cellular radio system. The cdmaONE system used a high-speed orthogonal binary sequence drawn from a Walsh-Hadamard set to

spread the bandwidth of the data bits of each user. Generally, each data bit was represented by a complete Hadamard sequence of L chips. Consequently the bandwidth of the spread-spectrum signal was expanded by L times. Each user is allocated a different orthogonal sequence but the spread-spectrum signal shares the same frequency band as the other signals. Consequently, even though each user has a much wider bandwidth (typically 1.2MHz), it does represent the bandwidth for L users, so the average bandwidth per user is comparable to other types of multiple access types. In the receiver, the wanted signal is extracted from the composite of user signals by correlating the received signal with a replica orthogonal sequence. Although Hadamard sequences have good orthogonality properties, their spectral properties were poor. To counter this, each transmission used a long pseudo-random sequence to randomize the signal. This signal did not provide additional spectrum spreading but ensured that the spectrum of the transmitted signal was approximately uniformly distributed across the transmission bandwidth. CDMA provides the advantage of flexibility in the way that different data rates could be handled and it offers a way to reduce the effect of multipath fading, as described below.

It was recognized in the late 1990s that techniques such as ADSL would provide much higher data rates than were possible for ISDN. However, the effect of multipath propagation, in particular the effect of the delay spread due to the spread in the arrival time of the multiple signal components introduced a fundamental limit to the data rate achievable from a second generation handset due to inter-symbol interference. Consequently, with delay spreads produced by a typical urban environment being around 5μs, the data rate of a GSM handset was limited to 270kbps in a 200 kHz bandwidth. In order to substantially improve the data rate achievable from cellular mobile radios when operating in a dispersive channel, a significant improvement in technology was needed to counter the effect of the channel. As with both the first and second generation cellular radio systems a number of different technologies were trialed, with the winners being wideband CDMA in Europe and CDMA2000 in the USA.

Both systems were based on code-division multiple access to allow individual subscribers to access the air interface and the technology allowed a very flexible approach to different data rates by each user. In third-generation cellular radio systems, packet data transmission was a key part of the system from the outset. Such is the inherent flexibility of the system that a single user can use any data rate from around 2Mbps down to a few kbps. In WCDMA [16], the reason why data can be sent at much higher rates than the coherence bandwidth of the channel is due to the use of a wideband direct-sequence spread-spectrum signal that uses a digital matched filter receiver to provide a correlation window that extends

over the period $\pm\tau_c$, where τ_c is the period of a single chip of the high-speed spread-spectrum code. Within this correlation window, all wanted signals are properly despread and then demodulated. However, any signal that falls outside this window, which includes delayed signals due to multipath propagation, are rejected. In this way, any multipath component that is delayed by more than the chip period is suppressed. This means that intersymbol interference due to multipath fading is also suppressed. With a typical minimum delay echo in an urban environment occurring about 1μs after the direct component, means that the chip duration of the spread-spectrum system must be shorter than 1μs. In WCDMA, the chip rate is 4.096 Mbps enabling each carrier to fit within a bandwidth of 5 MHz. Indeed, this means that WCDMA will reject multipath echoes that occur more than 0.2μsec from the direct path.

Third generation cellular radio provides a faster air interface in conjunction with the GPRS packet data system to provide enhanced wireless data connectivity to PDAs such as the Blackberry®. However, it has not captured the imagination of the market place in the same way as the original second-generation phones and sales remain sluggish.

1.2 Wireless local area networks

At around the same time that third-generation cellular radio was being developed a different approach to wireless connectivity was being taken by manufacturers traditionally associated with computer packet data networks. These manufacturers recognized the need for wireless connectivity of computers based on wireless local area networks (LANs) [6], particularly the interconnection of laptops to form computer clusters and laptops to desktops. The topology and mode of operation of such LANs is completely different from cellular radios. This is largely because of the packet-switched nature of the network, compared with circuit-switched networks for mobile cellular radios which means that the wireless access node does not have to handle multiple users simultaneously since the network access protocol handles multiple access using techniques such as carrier-sense multiple-access collision detect (CSMA-CD). These systems were characterized as being static, largely indoor, but requiring very high data rates. Nevertheless, multipath propagation due to reflections from floors, walls and office furniture was found to be the limiting factor to the achievable data rate, as for the case of cellular mobile radio. Although the delay-spread in a typical indoor environment is only of the order of tens of nanoseconds, since the required data rate is of the order 50 – 100Mb/s, it is clear that delay-spread places an upper limit on the maximum data rate. A key development in wireless local area networks was the development of the IEEE802.11 standard, often called WiFi in 1997.

WiFi is based on the Ethernet LAN protocol so that IP packets can be sent over the network. A number of different physical layer standards were proposed, based on the technology of the day. The original standard allowed data to be transferred over short ranges at rates of either 1Mbps or 2Mbps using either a direct-sequence spread-spectrum (DSSS) modulation scheme or a frequency hoped spread-spectrum system (FHSS). However by 1999 two new standards were approved to significantly improve the achievable data rate. The first standard to reach the marketplace was standard 802.11b, which used a high-rate DSSS system to achieve data rates of 11Mbps using the correlating receiver to mitigate the effect of the delay spread, as described above. However, standard 802.11a used a totally different approach to mitigating multipath fading using orthogonal frequency division multiplex (OFDM). This modulation scheme extended the achievable data rate to 54Mbps. In OFDM, the single high-speed data stream is multiplexed into a number of lower data streams. The number of parallel data streams dictates the rate of each stream so a 2.024Mbps data rate transmitted on 1024 carriers equates to a bit rate on each stream of only 2kbps. Each of these data streams is then modulated onto a separate carrier frequency and transmitted in parallel. The concept is that each low rate stream has a bit period that is many times longer than the delay spread so is little affected by the intersymbol interference due to the delay spread. The number of carriers used is largely determined by the prevailing delay spread, the original data rate and the coherence time of the channel, together with complexity issues of generating large numbers of carriers. In practice, the carriers are generated entirely in DSP using the inverse fast Fourier transform and they are coherently demodulated in the receiver in DSP using the fast Fourier transform. OFDM forms a major part of this thesis and is described in Chapter 7.

The original 802.11 standard operated in the unlicensed ISM frequency band at 2.4GHz. 802.11b also used the 2.4GHz ISM band, whereas in the US 802.11a used the much higher frequency 5GHz ISM band. The 80.11g standard, approved in 2001, used the 54Mbps OFDM modulation scheme but operated in the 2.4GHz ISM band. A number of manufacturer-specific implementations of the various 802.11 standards exist – each with different features, within the standard. Some, for example, use multiple antennas separated by about 10cms. These can be individually switched on, to ensure that one of the antennas is located in a signal peak (at 2.4GHz the typical distance between a peak and a trough is approx. 6cms). Alternatively, both antennas could be used as a simple spatial diversity system. The various equipments provided communication ranges of around 50m, depending on the physical environment.

In 2005, a new 'interim standard' was proposed called 802.11n. This standard also used multiple antennas, but configured as a multi-input multi-output (MIMO) configuration to provide capacity enhancement, rather than robustness through diversity. The 802.11n standard

arrived data rates of around 104Mbps, double the rate of the 802.11g standard. In essence, 802.11n recognizes the potential of exploiting the spatial domain, whilst OFDM modulation simultaneously exploits frequency diversity. MIMO systems form the heart of this thesis and will be described in detail in subsequent chapters.

In 1999, it was recognized that there was a commercial need for a wireless broadband system in support of metropolitan area networks. Others recognized the need for a 'last mile' data solution allowing broadband interconnectivity to the broadband internet without the need for wire connectivity (and the disruption that accompanies such an installation). The solution was two competing standards 802.16 (WiMAX) and 802.20 (WiBro). To date, only the 802.16 standard has been implemented and a number of variants to the standard have been developed. In contrast 802.20 has been beset by problems in arriving at a consensus standard, although it is important to recognize that the two standards do not solve the same WMAN problem. 802.20, for example, focuses on broadband connection to extremely high-speed vehicles, whereas 802.16 has its origins in broadband connection to buildings. However, the 802.16 standard has evolved to include connection to mobile units and later versions of the standard provide modifications that allow the wireless network to form *ad hoc* networks and reconfigurable networks. Equally importantly is a variant that allows WiMAX terminals to have a hand-off capability that allows WiMAX equipped computers (such as compact laptops) to roam from one access point to another without losing connection. The 802 protocol represents the MAC protocol that is used, so like 802.11, WiMAX also uses an Ethernet-like protocol that is able to provide support for IP. 802.16, in its simplest form, allows a home or office computer network based on Ethernet protocol to be connected to a backbone network wirelessly. There is no need to install an ADSL wire connection between the home/office and a local exchange. Ranges, therefore, are much further than for WiFi; being able to accommodate typically up to 15km range, or further with suitable antennas. Base-stations are assumed to be pole-mounted using antenna arrays to provide gain to meet the link budget. The customer premises antenna may also be a dish or antenna array mounted securely on the premises. Because such wireless systems are by their nature outdoors and 'public', security is much stronger than for WiFi. Like the 802.11 WiFi standard, 802.16 covers many different physical layer implementations to allow the system to be used in a variety of environments. In clear line-of-sight conditions, M'PSK and QAM modulation on a single carrier is used to provide spectrally efficient modulation in the 2.4 and 5 GHz ISM bands. Additionally, the system can also operate in licensed spectrum in the 2.4 and 5GHz bands. In conditions where multipath fading is known to be a severe problem, OFDM modulation is used to mitigate the frequency selective fading. This aspect forms a major part of this thesis and is described in

detail in Chapter 7. In order to accommodate different delay spreads found in different types of channel, the OFDM system can handle different types of modulation scheme which is achieved by using different OFDM block sizes (i.e. number of different simultaneous carriers).

The 802.16 standard, and potentially the 802.20 standard, pose a severe threat to the continued development of fourth-generation cellular radio and may represent the point at which mobile-cellular radio and wireless LANs converge. Mobile cellular radio has evolved to provide relatively high data rates that can provide connection of the device to the internet via GPRS. In contrast, WiMAX has achieved mobile connectivity for IP data networks. Yet by using voice over IP (VOIP) techniques, these promise to allow telephony connectivity to a PDA or similar device. In this thesis, the focus is on wireless MAN technology such as 802.16 and 802.20.

1.3 Exploitation of Space Diversity

It is clear from the historical development of wireless systems over the past three decades, that the performance of such systems has been enhanced through the use of diversity in the time, frequency and spatial domains. This thesis is concerned about the exploitation of diversity as a means of further enhancing wireless system performance. However, there are a great many ways in which diversity can be applied, and some of these methods are discussed in this thesis. In particular, the exploitation of the spatial domain is of current interest and this can be achieved using different configurations of antenna.

Smart antennas used in wireless communication systems can improve the capacity, performance and reliability by using either adaptive beamforming, diversity techniques or switched fixed beams. What is of particular interest, and which forms the main area of interest in this thesis is how an adaptive antenna system can change its mode of operation to optimise the use of wireless resources in a particular channel environment. When is it better to act like and adaptive beam former with interference nulling and when is it better to reconfigure the antenna so that it acts like a MIMO system, providing either enhanced diversity or capacity (or both)? For these types of application, the reconfigurable adaptive antenna can be considered to be a ‘smart antenna’, in which it is able to reconfigure itself in the context of the RF environment that the radio systems operate. However, the question arises as to whether an optimum exists.

This thesis focuses on the issue of optimisation of the smart antenna and in doing this the following areas have been considered as important enabling technologies for a future adaptive wireless system: smart antennas, space division multiple access (SDMA), MIMO techniques such as layered space-time Architectures such as BLAST (and the requirement for multi-user detection) and space-time block codes (STBC).

A smart antenna is composed of two or more antennas. The amplitude and phase of the signals received by all the antennas is combined in such a way so as to improve the reception of desired signal. The smart antenna is important for reducing the effects of intentional jamming signals, unintentional co-channel interference and multipaths [114]. Smart antennas are being used for improving the performance of wireless radio systems by suppressing the interfering signals and increasing the capacity of the systems. An important aspect of the smart antenna and its use in future wireless systems such as the cognitive radio is the ability to identify the direction of users so that the antenna can then beamform in those wanted directions. It is also necessary to identify the direction of unwanted signal so that the adaptive antenna can place nulls in these directions. Christodoulou and Naftali [23] describe the basic model for determining the angle of arrival for incoming signals, antenna beamforming and adaptive algorithms used for array processing.

The use of the smart antennas provides improvements when used with time division multiple access (TDMA) and code division multiple access (CDMA) digital communication systems [23]. In order to achieve the desired performance from wireless communication systems it is necessary to overcome the problems of multi-path fading, polarization mismatch and interference. An optimum solution to resolve these problems is to use the antenna array to improve the performance of a system in ***three different ways*** [30].

(i) By using diversity-combining techniques, which combine the signals from multiple antennas in such a way that it mitigates the multipath fading.

(ii) By using adaptive beamforming with antenna arrays, that provides capacity improvement through interference reduction and also mitigates the multipath fading. Adaptive arrays cancel or coherently combine multipath components of desired signal, and null out the interfering signals that have different directions of arrival from the desired signal.

(iii) By using switched fixed beams to achieve coarser pattern control than adaptive arrays. Two or more of the fixed beams can be used for diversity reception. Adaptive and switched beam antenna systems are referred to as ‘‘smart antennas’’ because of the dynamic system intelligence required for their operation.

The concept of space division multiple access (***SDMA***) has also been proposed in [127], where different co-channel signals are transmitted and received simultaneously through different spatial channels in order to improve the capacity of wireless communication system. The SDMA enables the users to use same communication channel simultaneously by forming individual radiation pattern for users. To achieve SDMA, smart antennas must carefully form

their radiation patterns to capture desired user and nullify the interfering users. Therefore, the smart antenna requires high accuracy in propagation channel response estimation. Therefore to form an effective radiation pattern in the downlink a smart antenna pattern that utilizes closed loop control and space-time coding (STC) technique is used [115]. At base station smart antenna comprises of set of sub-arrays and STC signal is fed to sub arrays and users at the same time. STC can estimate the channel response by transmitting signals from sub-arrays simultaneously thereby improving the system's throughput.

Central to the effective utilization of the spatial domain is the accurate model of radio wave propagation in the cellular and wireless LAN environments. There have been a large number of different channel models developed each with a different level of fidelity, as computational power has increased. Some of the important model developments include: Lee's model, the geometrically based single bounce (GBSB) statistical channel model, geometrically based circular model (macro-cell model), geometrically based elliptical model (micro-cell wideband model), Gaussian wide sense stationary uncorrelated scattering (GWSSUS) statistical channel model, Gaussian angle of arrival channel model, time varying vector channel model (Raleigh's model), modified Saleh Valenzuela's model and Ray tracing model used for antenna array communication systems are described in [45].

The concept of Multiple Input Multiple Output (***MIMO***) systems that represents an effective way to increase the user capacity in different non-line-of-sight and richly scattered RF environments is also receiving considerable attention [124]. Use of antennas both at the transmitting and receiving ends allows (i) an increase in capacity and spectral efficiency (ii) reduction in fading due to diversity (iii) increase in number of users and improved resistance to interference. Different approaches like space-time block code (STBC) technique and layered space-time architecture are considered in many papers [43] [132][134]. BLAST (Bell Labs Layered space time) as described in [43][134] is considered as a bandwidth-efficient approach, where co-channel streams of data are transmitted and received using multiple antenna elements at transmitting and receiving end thereby exploiting the spatial domain. Therefore Layered space-time architecture having equal number of antenna elements at both ends of link offers a tremendous capacity improvement. However, it must be recognized at the outset that this is only possible in richly scattered environments where Rayleigh and Rician fading have already had a very negative effect on the performance of the system. Consequently it is important to recognize at the outset that such system do not provide system improvements when compared with AWGN channels, but do help to restore the performance of the channel which has already been degraded by Rayleigh fading. The V-BLAST communication architecture has been implemented in real time environments in the Bell

laboratory [69]. The space-time block codes and VBLAST techniques are described further in Chapter 6.

1.4 Aims and Objectives of the Work described in this Thesis

The aim of this thesis is to examine how the various forms of diversity that exist for wireless systems can be exploited to provide capacity enhancements or improved robustness. The work is carried out in the context of wireless MAN systems such 802.16 WiMAX and 802.20, in which the wireless environment is predominantly outdoor in a richly scattered multipath fading environment. WiFi is not considered in this work.

In particular the use of s*mart antennas* in conjunction with different types of diversity such as frequency diversity and time diversity is considered based on antenna arrays that can self-reconfigure to adapt to user requirements in real time and/or in response to the changing wireless environment are being proposed for cellular wireless systems, wireless LANS and military communication systems. The broad aim of the work is to improve the performance of wireless systems by either providing improved robustness, increased number of callers or increased data rates for selected users. Therefore the aims and objectives of the research are:

a. To examine ways of optimizing the smart antenna to achieve and maintain the required performance metrics.
b. To look at the various ways in which spatial diversity can be exploited by a smart communications system using different techniques such as *SDMA* that forms highly directional beam towards wanted user and a null towards an interferer thus isolating them in space, *MIMO* systems that use dumb antennas and clever signal processing at the receiving end to resolve the problem of interference or *Opportunistic Communication* system that transmits to a user only when the channel conditions to that particular user are good.
c. Implementation of adaptive algorithms like LMS, NLMS and RLS in Matlab by forming main beam pattern in wanted direction while nulling out the interferers.
d. To exploit the diversity that is offered by multipath channels in terms of space, time and frequency diversity. As multipath propagation generates many bit errors due to the effect of ISI that occurs because of delay spread, So Diversity is the phenomenon that can be used in different ways to minimise the effects of ISI.
e. To exploit the time diversity by implementing Opportunistic communication system using omnidirectional and an adaptive antennas.
f. To select a standard channel model that provides different scenarios that are close to reality and can also support wide band MIMO systems.

g. To develop a MIMO system model based on selected standard channel model.
h. To provide an advanced system configuration that could be exploited by IEEE 802.20 user specification approach for broadband wireless networking, which is still in development.
i. To develop new system that uses a novel combination of smart antenna MIMO techniques and an advanced communication system based on OFDM technology using above selected standard channel model.

1.5 Thesis Outline

This thesis is mainly concerned with theory, design and implementation of broadband systems with different multipath propagation channel models employing error correction techniques, delay equalisation, adaptive antenna utilisation to isolate the wanted and interferers. Currently, one of the main developments in wireless networks is the *exploitation* of the diversity that is inherent in wireless channels that suffer from multipath propagation and signal scattering and this forms the main aim of this Thesis.

Chapter two introduces the concepts of modelling of digital communication systems and, especially, the wireless channel. The slow and fast fading characteristics are presented along with properties of flat fading and frequency selective fading. It also shows how scattering and multipath fading adversely affect the performance of a digital communication link, and the type of countermeasure techniques like channel coding, modulation techniques, phase estimation, delay equalizer and maximum likelihood detection that are needed to overcome the channel impairments to achieve a communication link with acceptable performance in terms of achievable bit error rates. A spatial channel model considered as realistic physical channel model has the capability of configuring the system with multiple antenna elements at transmitting and receiving end with applicability in different outdoor propagation like urban micro, suburban macro and urban macro environments has been described in detail along with factors that form the basis of selection of the channel model for the purpose of simulations.

Chapter three gives a detailed description of use of antenna array in communication system; the antenna array may well be *highly directional* so that signals arriving from one direction are received preferentially to signals arriving from a different direction. It is this directional behaviour of the antenna array that makes them so useful, and this aspect of the antenna array is discussed in chapter three. This chapter examines the use of the beamforming network as a means of optimising the signal to interference ratio of signal arriving from an angle θ when corrupted by a spatially random field and/or coherent interference signals at

specific angles of arrivals θ_i and this approach is appropriate when the signal source and the interference sources are stationary.

Chapter four gives the description of adaptive beamforming, when either the wanted signal or the coherent interference are moving the signal to interference ratio of signal arriving from an angle θ when corrupted by a spatially random field and/or coherent interference signals at specific angles of arrivals θ_i is not optimised. It is, of course, possible to treat each change of position of the signals as quasi-static sources in which the sources are assumed to be stationary over a given period where the angles of arrivals are being estimated prior to some form of optimal beam forming. The adaptive beamformer utilizes the optimum beamformer and this requires that the correlation matrix of the interference-plus-noise is known. Since this is generally not available *a priori*, it must be estimated from the received signals. In this case, a number of classical methods of adaptive algorithms have been developed that allow the antenna beam pattern to respond dynamically, to the changes in the position of the wanted and interference signal sources. In addition to that although there are many ways to improve the beamformer but in order to isolate the wanted user from an interferer by always forming a deep null in the direction of an interferer a novel method of optimising the weights with the help of Genetic algorithm and then using in the RLS adaptive algorithm is also implemented.

Chapter five describes the opportunistic communications system that uses a novel network protocol and only transmits to a user when the channel conditions to that particular user are good as compared to traditional communications systems, where the resources are allocated according to the demands of user without considering the quality of a channel as a result the channel capacity is lost when the channels get faded. The concept of multiuser diversity is exploited by opportunistic communication, where multiple users are communicating with common BS in the time varying fading channels while remaining in the same cell. It is assumed that channel state information is tracked at the receivers and fed back to the transmitters and scheduling in this case is done on the basis that a user with good channel conditions is only allowed to transmit to the BS. In this case, a number of algorithms in various fading environments using Rayleigh and spatial channel models employing omni-directional and adaptive antenna at the BS have been developed that allow the users to communicate with common BS, depending upon the condition of the channel of that particular user. This aspect of opportunistic communication is considered in this chapter.

Chapter six describes the types of MIMO systems and implementation with the help of space time block coded system and Layered space time architecture. Simulations of Matlab Rayleigh and spatial channel models using multiple antenna configurations at transmit and receive end have been implemented to show the BER vs SNR performance of the systems by

exploiting the effect of diversity in the system. The comparison of layered space time architecture (LST) and space time block code (STBC) systems is also drawn by simulation results of BER vs SNR. It is worth to note that STBC systems are better if BER performance improvement is required for fixed data rate, while LST systems are better for improvement of data rate based on the number of antennas at transmitting end as the data on all the transmitters is multiplexed.

In chapter seven the frequency diversity is exploited by orthogonal frequency division multiplexing (OFDM) systems and a new system has been developed that uses a novel combination of smart antenna multiple input and multiple output (MIMO) techniques based on OFDM technology using a realistic channel model that provides an advanced system configuration, which is exploited by IEEE 802.20 user specification approach for broadband wireless networking. In this chapter transmission of signal through mobile radio channel is described under different environments like flat fading and frequency selective fading. The multipath effect gives rise to intersymbol interference (ISI) as a result the transmission rate is affected so the use of guard intervals (GI) is necessary to combat the ISI. The BER performance of OFDM systems under different channel conditions due to the Doppler Effect is simulated. Different simulations of OFDM and OFDM-MIMO systems have been implemented using Matlab Rayleigh and Spatial Channel models. The importance of coding and interleaving in frequency selective fading channel is examined alongwith implementation of techniques such as viterbi-decoding, time interleaving and frequency interleaving to improve the system performance in terms of BER.

Conclusion and Summary of the work is given in chapter eight.

Chapter -2

2 Computer Simulation of Digital Communication Systems

2.1 Introduction

The aims of all current and future cellular radio and wireless LAN communication systems are to: (i) maximise the capacity of the wireless system, (ii) minimise the use of the spectrum needed to support that capacity, (iii) provide the necessary quality of service to guarantee adequate delivery of the data across the wireless interface (iv) provide a flexible and efficient means of accommodating variable data rates of all the users that will support new types of data services [1][24][31][124]. For multiple access systems, such as cellular radio and wireless LANs, this may involve providing adequate protection from other users of the wireless network or ensuring adequate recovery of all the data, subject to the effects of the wireless channel. Currently, one of the main developments in wireless networks is the *exploitation* of the diversity that is inherent in wireless channels that suffer from multipath propagation and signal scattering and this forms the main aim of this Thesis.

Current and future generation wireless systems are so complex, and have such strong interactions with the RF channel providing the air interface, that it is rare for any hardware to be developed until the system has undergone detailed appraisal using mathematical models and computer simulation. Since one of the aims of the research reported in this thesis is to examine how wireless LANs can exploit all aspects of the terrestrial RF channel by using adaptive modulation techniques to optimise their use of the time, frequency and spatial domains using detailed computer modelling, it is important that such aspects are examined. Chapter 2 introduces the concepts behind modelling digital communication systems and, especially, the wireless channel. It will show how scattering and multipath fading adversely affect the performance of a digital communication link, and the sort of techniques that are needed to overcome the channel impairments to achieve a communication link with acceptable performance in terms of achievable bit error rates.

2.2 Modelling Methods

Any computer model-based research into wireless communications, such as this, depends critically on the appropriateness and accuracy of the computer model of the wireless system, especially the wireless channel. It is very easy to obtain misleading results and draw erroneous conclusions regarding the appropriateness of a communication system by using an

RF channel model that is not representative of the true channel. The truthfulness of both the system model and the channel model is entirely dependent on the assumptions made. There are many reasons why models, especially channel models, may be over simplistic or even erroneous. A prime reason is the lack of adequate computing power. Another important reason is that the key mechanisms that affect the performance of a particular communication system may not be fully understood.

Considering the channel model, the generation of a truly representative model of an RF channel, including the noise and interference models that prevail in that channel and which are typical of multi-user cellular system operating in an urban canyon, for example, requires tremendous computing power to generate channel parameters that are statistically accurate. An accurate geometric model of fading, given the actual geography of the urban environment using techniques such as ray-tracing or a solution of the wave-equations, using the urban landscape to provide the boundary conditions either for the rays or the waves, is computationally intensive. It is only very recently that multi-processor and cluster computers have become available that have the necessary power and RAM to accurately model such environments. However, such models are still relatively rare within the research community. Generally, less comprehensive models are used that are optimised to model certain aspects of the channel (e.g. the Doppler or delay-spread) to some level of statistical accuracy.

Models of communication systems can be classified as either mathematical or physical [53][45]. Mathematical models may, in turn, be classified as being static or dynamic, deterministic or stochastic and discrete or continuous. Static models generally used fixed value parameters to define the system and channel, whereas dynamic models attempt to include changes in the parameters within the model.

A deterministic mathematical model solves the problem by obtaining a closed set of analytic functions that describe the operation of the communication system, such as the modulation scheme, and the channel, generally by making a number of important simplifying assumptions that make the development of the equations tractable. The advantage of this approach is that it is possible to characterise the system without recourse to powerful computers (often a scientific calculator will suffice) and if the mathematical model is sufficiently general, to be able to compare the performance of different variants of the system analytically. The major problem with this approach is that in order to make the development of the equations tractable, the assumptions that are needed may make the final model unrepresentative of the actual communication system and channel.

Major difficulties with deterministic mathematical models are in respect of the channel model. Whereas simple static channel models representing free-space propagation and

plane-earth propagation are straightforward to model, dynamic channel models are particularly difficult. Consequently, channel models of time-varying, frequency-selective fast-fading caused by multipath propagation can be very difficult to model and incorporate into mathematical systems models [58].

In contrast, a stochastic approach to mathematical modelling attempts, to simulate the entire communication system, including the transmitter, receiver, channel and noise. In essence, the computer model is a representation of the physical system, with the exception that the carrier frequency may be set to a lower value than the actual value to simplify the model. Continuous-time stochastic models may model the system using analogue computers and representative analogue noise sources (or equivalently, real-time simulation packages such as Simulink®), whereas discrete stochastic models represent all signals by discrete-time signal samples and all processes in the transmitter, receiver and channel are represented by digital signal processing techniques. In either case, the technique is referred to as a stochastic process, because the noise and interference are represented by random signals. Each run of the model will provide different results because of the random interference, but if sufficient runs are carried out, the average performance of the system can be obtained from the set of results. Such methods are often called Monte-Carlo methods. Thus, to estimate the bit error probability of a digital communication system, a discrete-time system is developed using data bits whose states are random, the modulators and demodulators are modelled as per the hardware and the signal samples are corrupted by samples of a random noise signal with a well-defined distribution, such as Gaussian. Each corrupted data bit is detected in a digital representation of the receiver, where it is possible to compare the state of the received bit to the state of the transmitted bit, to decide whether it is in error. If a sufficiently large number of bits are sent, the resulting error rate tends to the correct value for the average. Such an approach can provide increased authenticity of the system model, but a bit error rate of 1 error in 10^6 bits sent means that at least 5×10^6 bits need to sent through the model to be confident that the average error rate is accurate. Even on a modern PC, this can take 10 minutes or more, even for a relatively simple system.

Time-varying, frequency selective, stochastic models of multipath channels can be produced using digital analogues of the actual processes in the true channel, thereby replicating the randomly fading channel which has the same statistics as the true channel. Such channel models are only possible because a large body of experimental work has been carried out to establish the key parameters of different types of channel in different types of region (such as average number of paths and the delay profile) as well as the statistics defining the fades. Such experiments provide the statistical basis of the models. However, this type of

channel is only *representative* of a particular type of channel (for example a typical channel that has Rayleigh fading statistics, or a channel that has Rician fading statistics). It may include details such as independent multipath fading and the effect of Doppler, even the effect of spatial decorrelation, but, at best, it is a *typical* channel. Measurements of the channel characteristics in some area would not replicate these model characteristics, although the key parameters, such as fade depth, level crossing rate, and delay spread might have the correct values in a statistical sense.

Physical models, attempt to replicate the channel characteristics of a specific geographic region using detailed electromagnetic modelling of the environment to produce characteristics that are far more representative of what might be observed if an experimental observation of the channel characteristics were measured in that area. This is achieved by using the topography and buildings of that region as boundary conditions from which the actual signal propagation can be modelled either electromagnetically using the solutions to the wave equation, or quasi-optically using ray-tracing techniques. Whilst, it is undoubtedly true that this approach is the most accurate, it is the most computationally intensive.

In the following sections, different types of approach to communication system modelling is described briefly, and the principal features of a discrete stochastic channel model are provided, together with some preliminary simulation results.

2.2.1 A simple deterministic mathematical model of a digital communication system

To illustrate the comments made above, consider a simple digital communication system operating over an ideal free-space line-of-sight (LOS) channel [117]. For this type of channel, the path loss is represented by spherical signal spreading, where the signal power density is reduced as the power from the transmitter, P_t, spreads in all directions, subject to any directional constraints placed on the signal by the transmitter and receiver antennas which have directional gain, G_t and G_r, respectively. In this case, the static deterministic channel model representing the free-space loss, L_{FS}, takes the form:

$$L_{FS} = \lambda^2 / (4\pi d)^2 \tag{2.1}$$

where, d is the range and λ is the wavelength of the carrier signal. This model simply provides the mean path loss of the channel subject to the constraint of spherical spreading. More sophisticated free-space models may include various loss mechanisms, such as atmospheric loss, L_{atmos}, rain fading, L_{rain} and other miscellaneous losses, L_{misc}. In addition, it is also usual to include other important propagation effects such as tropospheric refraction,

which has an impact on unobstructed range. These additional effects may also be static deterministic models, or may involve time-varying parameters.

However, if it is assumed that radio-wave propagation is by a plane-earth mechanism, where there is both a direct component of the signal and one or more signals that are due to reflections off plane surfaces, the mathematical model for the path loss is entirely different from (2.1). In this case, a simplified mathematical analysis of plane-earth propagation provides an idealised mean path loss of the form [117]:

$$L_{PE} = \left(\frac{h_t h_r}{d^2} \right)^2 \tag{2.2}$$

Plane-earth propagation generally produces far higher propagation losses than free-space propagation and so it is vital to ensure that the correct model has been chosen from the outset.

Using either type of channel model, a mathematical model of the communication link can be developed that relates the mean power at the receiver, P_r, to the power at the transmitter, P_t:

$$P_r = P_t G_t G_r L_{FS} L_{atmos} L_{rain} L_{misc} \quad \text{or} \quad P_r = P_t G_t G_r L_{PE} L_{atmos} L_{rain} L_{misc} \tag{2.3}$$

Given an appropriate model for the noise and interference in the channel and receiver, this allows the mathematical model to specify the signal to noise ratio at the receiver detector. A simple noise model assumes that the only interference in the channel is the prevailing black body radiation that is collected by the antenna. This is amplified in the receiver and augmented with additional noise that is generated by the resistive and active components in the receiver. As a result, the noise at the detector is given by [24]:

$$N = kT_e B \tag{2.4}$$

where k is Boatman's constant, B is the equivalent noise bandwidth of the receiver and T_e is the equivalent 'temperature' of the receiver that takes into account the black-body radiation detected at the receiver antenna and the additional contributions to the noise in the receiver. Again, this model may be over simplistic.

A simple deterministic model for the communication system can also be developed in a similar manner. Assume that digital data is transmitted using M'ary phase shift keying:

$$x(t) = A\cos\left(\omega_c t + \phi(t)\right) \tag{2.5}$$

Where, $x(t)$ is the transmitted signal, ω_c is the carrier frequency and $\phi(t)$ is the phase shift impressed on the carrier by virtue of the digital modulation. The phase shift, $\phi(t)$ can take one of only M values in the range 0-360° depending on the order of the modulation. The M possible versions of (2.5) are each known as symbols and they represent the waveform that is transmitted for a given word of length $\log_2 M$. For example, for binary phase shift keying,

(BPSK), the phase $\phi(t)$ can take one of only two values: one representing the case when a '1' is sent and the other representing when a '0' is sent. In this case the period of the symbol and the period of the bit are the same For quadrature phase shift keying (QPSK) [139], $\phi(t)$ can take one of four values corresponding to whether the following data words are sent: '00', '01', '11' or '10' is sent. In this case the period of the symbol is twice that of each bit (i.e. the binary words comprise two bits).

The aim of the detector in the receiver is to measure the value of $\phi(t)$ (given that the signal is corrupted by noise) and decide which of the M possible values that $\phi(t)$ can take is the closest to the measured phase. This is known as a maximum likelihood receiver. The received data bits are then obtained from the detected symbol by a process of demapping. The resulting bit stream can then be compared to the original bit stream.

It is well known that in additive Gaussian noise, where the effect of phase rotation and distortion due to the receiver filters together with other distorting effects is ignored, the probability of detecting the correct phase of the carrier (and hence where the data bits are received in error or not) is given by [139]:

$$P_b = \frac{1}{\log_2 M}\left[1 - \left(\frac{B}{R_b}\right)^{1/2} \operatorname{erf}\left(\sin\left(\frac{\pi}{M}\right)\left(\frac{P_r}{N}\right)^{1/2}\right)\right] \tag{2.6}$$

where P_b is the probability of a bit error and R_b is the data rate used.

This equation assumes that the bits are generated randomly with equal probability and that the receiver is fully optimised to detect binary bits using a matched filter. Any deviation from this assumption will invalidate the model. Nevertheless, this model is often used to provide the best-case performance bound. Using (2.6) it is possible to show how the received signal level affects the probability of a data bit error from this entirely deterministic model, and this is shown in Figure 2.1 for different modulation orders, M. In this case, the noise bandwidth, B and data rate, R_b are normalised to: $R_b = B = 1$. The curves make two points. First, using a higher order modulation order allows higher bit rates to be transmitted whilst maintaining the transmission bandwidth, but since the signal power is proportional to the data rate, this requires a higher signal to noise power ratio (SNR) as a direct consequence. Second, higher order modulation schemes increasingly resemble analogue signals. As the modulation order increases, the likelihood of errors increases as the decision region for each symbol becomes much smaller, unless the noise variance is reduced. Consequently, in order to achieve a desired level of error probability, the SNR must improve significantly as the modulation increases.

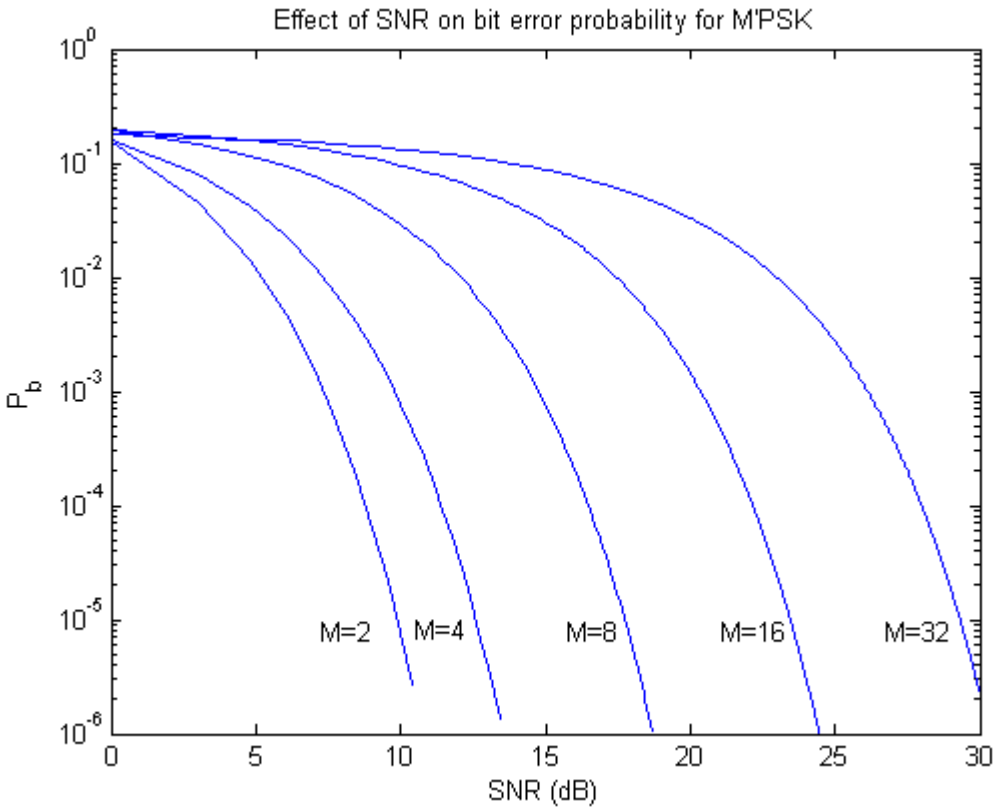

Figure 2.1: The effect of SNR on the bit error probability for different orders of M'PSK

It is possible to remove the effect of the data rate by normalising the SNR by the data rate, so that the signal is measured in terms of energy per bit. The effect of bandwidth changes can also be removed by representing the noise as a noise spectral density, such that SNR is represented as an equivalent E_b/N_0. Using these normalisations, an equivalent expression to (2.6) based on E_b/N_0 can be obtained [139]:

$$P_b = \frac{1}{\log_2 M}\left[1 - \text{erf}\left(\sin\left(\frac{\pi}{M}\right)\sqrt{\log_2 M}\left(\frac{E_b}{N_0}\right)^{1/2}\right)\right] \tag{2.6a}$$

Figure 2.2 shows the impact of this normalisation on the bit error characteristics for the same conditions given in the previous example. This set of characteristics is now independent of the data rate and transmission bandwidth and shows quite clearly that increasing the modulation order requires the noise density to be reduced, relative to the energy per bit because the decision region for each symbol has been reduced.

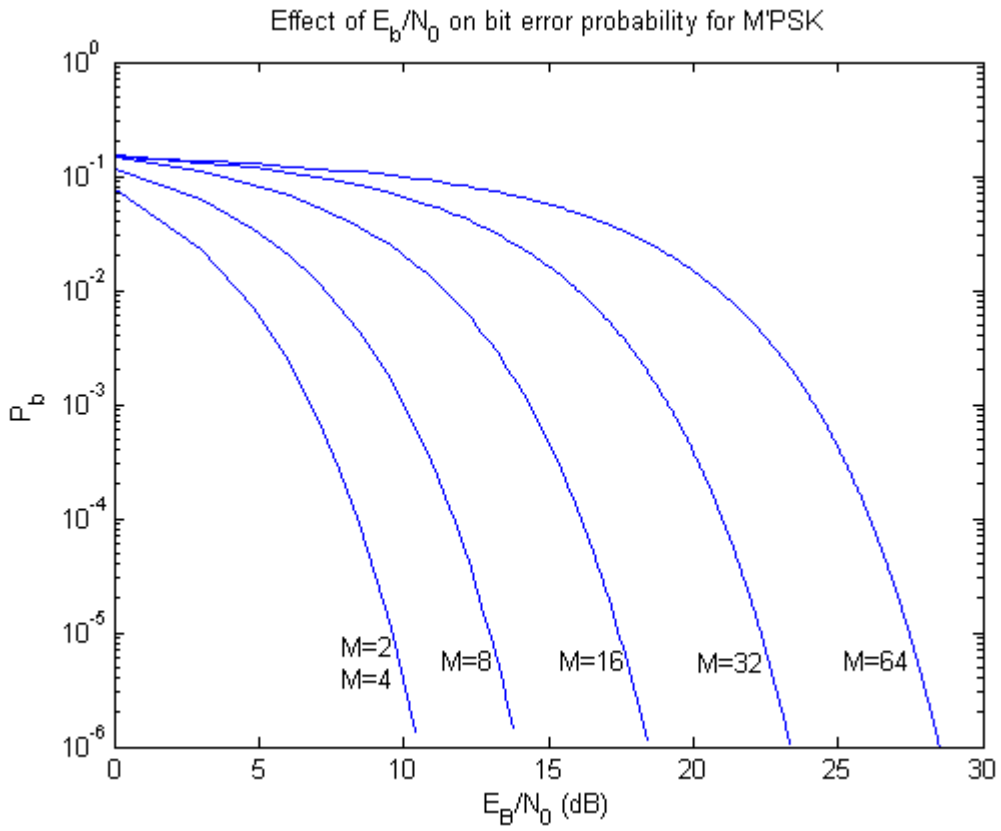

Figure 2.2: The effect of E_b/N_0 on the bit error probability for different orders of M'PSK

The channel is taken as a simple lossless channel in which the only impairment is additive noise. It is not necessary to use a computer to generate this performance model and the method can be used to estimate the minimum transmitter power needed to achieve a given level of bit error performance by using Figure 2.1 or Figure 2.2 to set the minimum level of received signal power to provide the required average error rate, and then to use value of P_r in (2.3) and either (2.2) or (2.1) to obtain the required transmitter power to achieve a stated range or to estimate the range given the transmitter power.

Similar mathematical expressions can be derived (under ideal conditions) to represent other digital modulation schemes, such as differential PSK or quadrature amplitude modulation, given below:

$$P_b = \frac{2}{\log_2 M}\left(\frac{M^{1/2}-1}{M^{1/2}}\right)\left[1-\text{erf}\sqrt{\frac{3B}{2R_b(M-1)}\left(\frac{P_r}{N}\right)^{1/2}}\right] \tag{2.7}$$

Such deterministic approaches to communications models are invaluable in providing a 'sanity check' when developing complex stochastic models to ensure that the simulations results are comparable to those expected theoretically for more idealised conditions. Figure 2.3 shows the performance of the QAM modulation scheme for different modulation orders as a function

of SNR. The key observation is that when M > 4 the required SNR for QAM to achieve a given error rate is lower than for M'PSK of a similar order, showing that the distance between constellation points is much larger for QAM than M'PSK for the same transmitter power. Figure 2.4 provides the error characteristics as a function of E_b/N_0

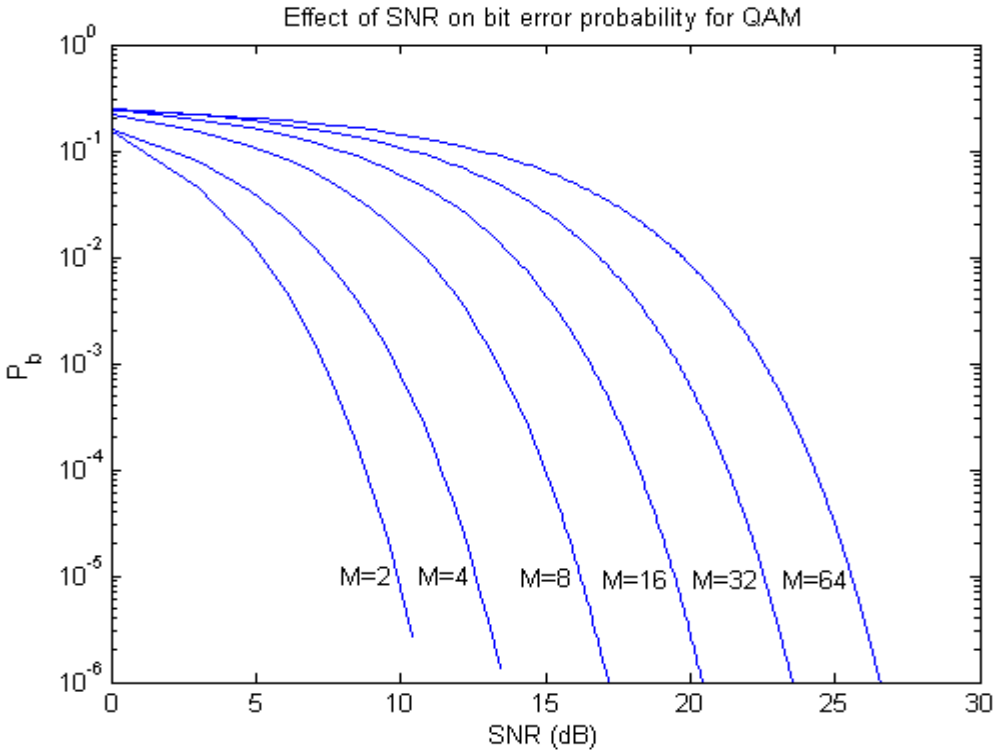

Figure 2.3: The effect of SNR on the bit error probability for different orders of QAM

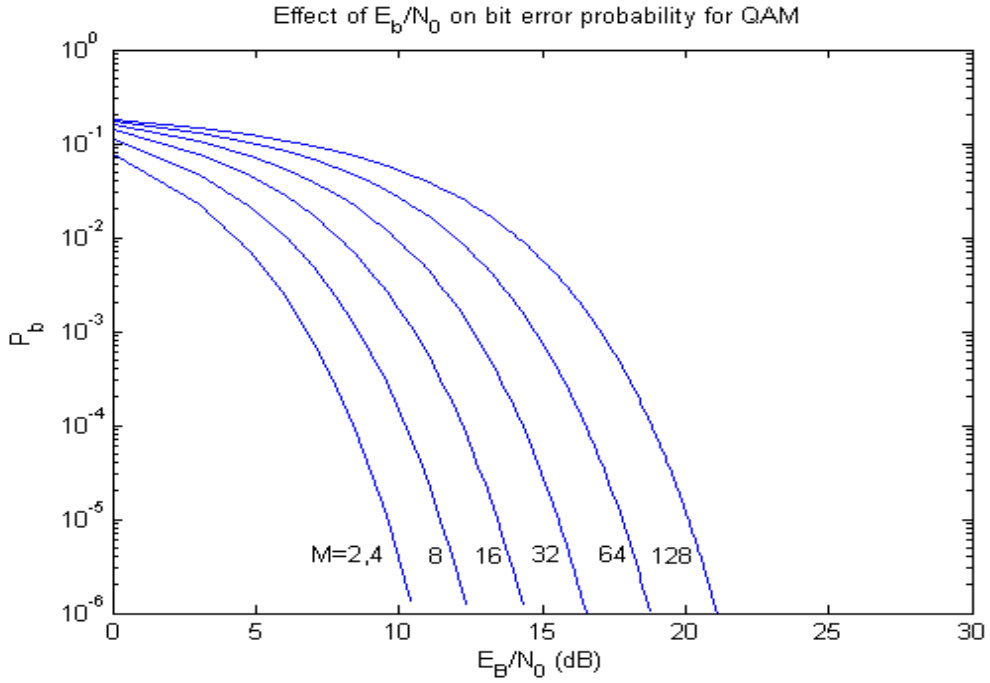

Figure 2.4: The effect of E_b/N_0 on the bit error probability for different orders of QAM

2.2.2 A simple stochastic model of a digital communication system

In contrast to the simple deterministic model detailed above, it is possible to achieve a similar result using a Monte-Carlo simulation of the digital communication system using sampled signals. A block diagram of the stochastic model is shown in Figure 2.5. It follows the hardware implementation, but uses digital signal processing algorithms to represent FEC coders and decoders, interleavers, modulators and demodulators etc. instead of hardware implementations.

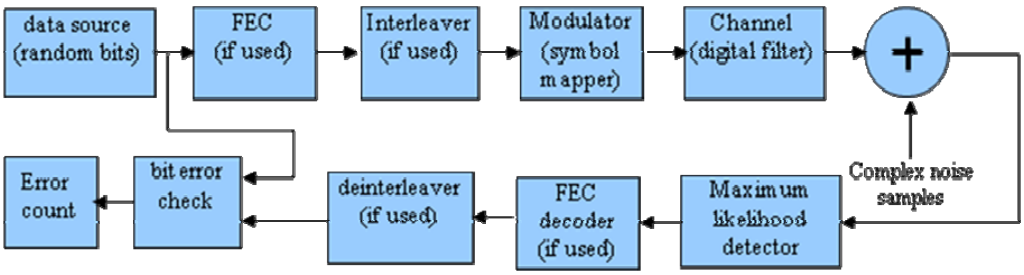

Figure 2.5: Schematic of a stochastic model of a communications system

2.2.2.1 Baseband equivalent signals

The basis of most stochastic models of a digital communication system is that they use a baseband equivalent model of the bandpass communication system [117]. The reason for this is as follows. Assume that the digital communication system operates at a carrier frequency of 1.8GHz and has a transmission bandwidth of 400KHz. The maximum frequency of this signal is 1.8002GHz. To model this as a discrete sampled signal, would require a minimum sampling rate of 2×1.8002GHz to meet Nyquist's sampling rate criterion, whereas the actual information that we need to model is only changing at a baseband rate of 200kHz. Indeed, the same information is being transmitted, irrespective of the actual carrier frequency. It is clear that the sampling rate is reduced as the carrier frequency is lowered, and a minimum sampling rate of 400kHz is needed when the carrier frequency is set to 0Hz. This is the basis of using a baseband equivalent model.

A general bandpass signal at a fixed carrier frequency can be expressed as:

$$x(t) = a(t)\cos\left(\omega_c t + \phi(t)\right) \tag{2.8}$$

This can be expressed in Cartesian form:

$$x(t) = x_I \cos(\omega_c t) - x_Q \sin(\omega_c t) \tag{2.9}$$

The corresponding complex baseband signal is defined as:

$$x(t) = a(t)\exp(j\phi(t)) \tag{2.10}$$

(i.e. the carrier frequency is set to zero)

and the corresponding Cartesian form of the baseband signal is:

$$x_{LP}(t) = x_I + jx_Q \tag{2.11}$$

(i.e. the baseband signal is simply the amplitude term of (2.8) corrected by the phase term, $\phi(t)$). A baseband model of a real band-pass signal is a complex-valued baseband signal that is processed throughout by complex valued operators (such as the signal modulator) and to which must be added baseband (i.e. complex-valued) noise and interference. The equivalent baseband noise is found as follows. The band-pass noise signal is given by:

$$\begin{aligned} n(t) &= r(t)\exp(j\phi(t))\exp(j\omega_c t) \\ &= n_I(t)\cos(\omega_c t) - n_Q(t)\sin(\omega_c t) \end{aligned} \tag{2.12}$$

where, $r(t)$, $n_I(t)$ and $n_Q(t)$ are independent random processes. Consequently, the baseband equivalent noise process is:

$$n_{LP}(t) = n_I(t) + jn_Q(t) \tag{2.13}$$

where, $\langle n_I^2(t)\rangle = \langle n_Q^2(t)\rangle = \langle n^2(t)\rangle$ (2.14)

For a sampled digital system, the noise can be represented as a sequence of complex-valued samples, $n(l)$, drawn from two, independent, random sequences $n_I(l)$ and $n_Q(l)$ (usually Gaussian distributed):

$$n_{LP}(l) = n_I(l) + jn_Q(l) \tag{2.15}$$

If the two random distributions from which $n_I(l)$ and $n_Q(l)$ are drawn each have unit variance, and the required total noise power is $N = \sigma^2$, where σ^2 is the required noise variance, then this is achieved by scaling the noise samples as follows:

$$n_{LP}(l) = \frac{\sigma}{\sqrt{2}} n_I(l) + j\frac{\sigma}{\sqrt{2}} n_{Q(l)} \tag{2.16}$$

Signal Source

In most simulations of digital communication systems, the signal is a random stream of ones and zeros drawn from random signal with a uniform distribution such that the probability of generating a one or zero equals 50%. This represents the baseband signal model.

2.2.2.2 Encryption, error correction and interleaving

If the transmitter uses encryption in the physical layer, the generated data bits can be modified using an algorithm that models the actual encryption process represented as some form of

digital state machine and implemented in software. Generally, encryption does not affect the data rate and the output of the encryption algorithm is also bits. The digital signal may then be coded in someway to provide error detection or error correction capability. It is not the purpose of this thesis to provide full details of FEC codes. There are many excellent texts that provide this detail [8][9][10] suffice it to say that there are many variants of coding algorithm including convolutional coding, block coding, such as BCH codes, Reed-Solomon and turbo codes which all provide error correction capability. In this thesis, convolutional codes are used, especially with OFDM waveforms, discussed in Chapter 7.

In all cases, error detection and correction codes operate by adding *redundancy* to the original data so the data rate at the coder output is much higher than the uncoded data rate at the coder input. The increase in the bit rate is called the code rate. A typical code rate for a convolutional coder is R = 1/2 or R = 1/3, corresponding to an output signalling rate that is twice or three times the original signalling rate, respectively[139]. This may involve an increase in the transmission bandwidth. Alternatively, higher order modulation schemes can be used that are able to transmit with a high spectral efficiency. For example, quaternary phase shift keyed modulation (QPSK) can transmit at 2bps per Hz. Consequently, a rate half convolutional coder, which doubles the signalling rate, can be used in conjunction with a QPSK modulator (which halves the bandwidth requirement), to create a convolutionally coded system with no increase in transmission bandwidth compared with the uncoded case. However, the penalty of using this arrangement is that the transmitter power must be twice as large as the uncoded case.

Taking the case of the convolutional coder, the convolutional code is generated by passing a data sequence through a multi-output state machine. The state machine is a set of shift registers whose outputs are modulo 2 additions of the shift register taps, as shown in figure 3.6 for an illustrative rate half coder. The taps define the coder. In this case the taps are given by 110 and 101 which are also represented in octal form as 6 and 7, respectively. The outputs of the coder are the convolution of the data stream with the impulse response of the coder. It will be seen that for each bit input into the coder, two bits are output. Three output and four output coders are possible. The number of coder outputs that need to be multiplexed onto the output port defines the code rate. It will be clear from Figure 2.6 that any particular output depends not only on the current bit that was input to the machine, but the 2 previous bits. Also, the coded data bit is represented not just by one output, but by both outputs. Consequently, the convolutional coder has both redundancy and memory. Thus an error in one data bit can be recovered by examining all six output symbols from that erroneous output bit. The constraint length defines the memory of the coder. In this case constraint length is

K=3. The larger the constraint length is, the more effective the ability of the coder to recover from errors. Similarly, the greater the number of outputs used to represent the input bit (i.e. the code rate), the greater the ability to recover from an error.

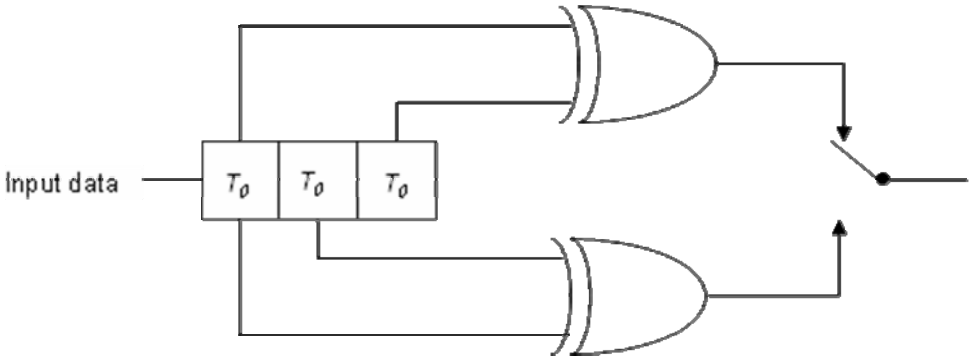

Figure 2.6: Schematic of a Rate=1/2, *K*=3 convolutional coder

Considering the convolutional coder as a state machine [117][139], a given sequence of inputs produces an output sequence in which certain output states are forbidden. If, due to transmission errors, a sequence is produced that contains these illegal states, the convolutional decoder in the receiver will detect these error states and can estimate where the error lies. Central to the decoder algorithm is the prior knowledge of the state machine that generated the original sequence. One possible (but impractical) decoder algorithm assumes that a finite block of encoded data is stored at the input of the decoder. Using the same state machine as in the encoder, the decoder regenerates output sequences for all possible states of the input block of data. The regenerated output sequences are then compared with the actual received sequence and the input pattern corresponding to the closest match represents the most likely input sequence that was sent. The amount of work involved increases exponentially with the length of the block. However, it will be apparent that the present bit depends only on the *K*-1 previous bits and so a much more efficient search process can be used. This is accomplished using a Viterbi decoder. Forward error correction (FEC) is entirely algorithmic and can be implemented using software, as here.

Many types of FEC are susceptible to burst errors, typical of the type of error found in fading channels. To minimise this problem, it is usual to *randomise* the FEC coded data prior to modulation and transmission using an *interleaver* [117]. In the receiver, a de-interleaver de-randomises the order of the data bits prior to passing the bits through the error correction decoder. The reason for this is that after interleaving, a burst error corrupts adjacent bits during transmission, but the de-interleaver then randomises the errors whilst simultaneously de-randomising the data bits. Many FEC algorithms are able to handle the

random errors that are so produced, especially convolutional coders. The penalty of the interleaver is that if the burst error lasts for many data symbols, the length of the interleaver may be very large causing a large delay in receiving and demodulating the data. A number of different types of interleaver exist. These are optimised to handle different types of burst error. A common interleaver is the block interleaver, shown in Figure 2.7.

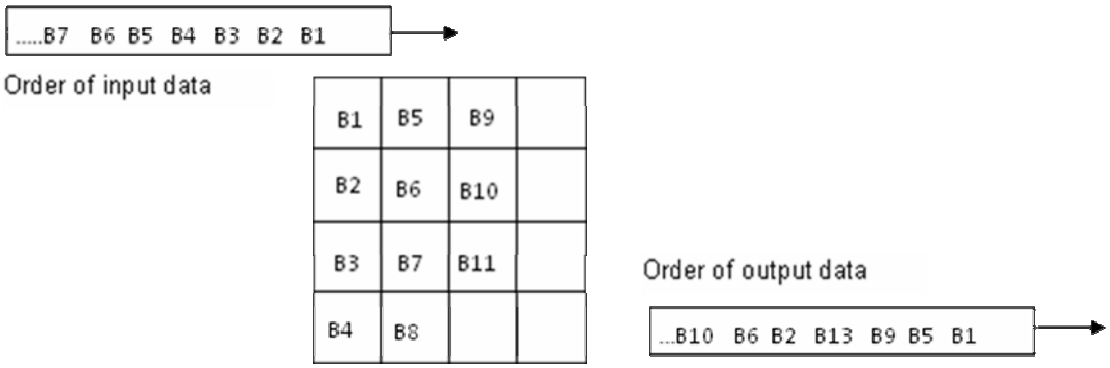

Figure 2.7: Schematic of a simple block interleaver

Here an array is populated by the data bits in column-by-column order. The array is then read out using a row-by-row order, as shown above. The de-interleaver in the receiver works in the opposite sense that the data is fed in row order and read out in column order.

2.2.2.3 Modulation

Having established the baseband signal model, digital modulation is simply a mapping process [139]. In this process, each of the *M* different digital symbols representing the alphabet of the modulation scheme has a unique point on the *constellation* of the modulation scheme corresponding to a particular Cartesian representation for x_I and x_Q in (2.11). The actual data stream is generally generated randomly with an equal probability of a '1' or '0' being generated.

The processed bits are arranged to form digital words of length $m = \log_2 M$, and by comparing these words with the alphabet, each word is represented by the corresponding complex value representing the Cartesian coordinate on the constellation. Three typical constellations are shown in Figure 2.8 representing BPSK, QPSK (4QAM) and 16QAM modulation schemes, which are extensively used in this Thesis. The radius of the constellation determines the power of the signal.

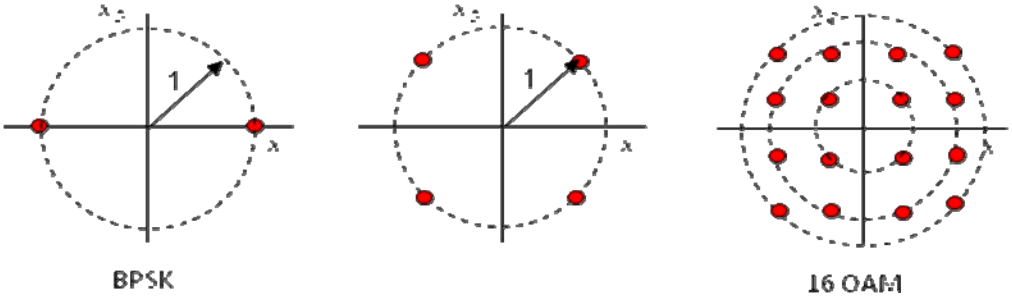

Figure 2.8: Constellations of 3 common digital modulation schemes

The modulated signals are normally scaled so that the average power in the transmitted signal is 1W (feeding into 1Ω).

The complex valued signal samples represent the transmitted symbols and these are operated on by the channel [60], which can be implemented as a digital filter, in which the channel coefficients are convolved with the data symbols

$$y(n)=\sum_{m=0}^{M-1} h(m-n)x(n) \tag{2.17}$$

where $h(m)$ is the channel impulse response, which is defined over M samples. Because, $x(n)$ is complex, $h(m)$ must also be complex, $h(m)=h_I(m)+jh_Q(m)$. The length of the impulse response, M, is defined by the longest multipath echo that is considered to have a significant impact on the data. For a simple non-fading channel, $M = 1$ and $h(0)$ has a constant value for all n set by the combined path losses such as defined by (2.1) or (2.2). For a simple fading channel, where the channel impulse response is much shorter than the symbol period, $M = 1$, but $h(0)$ is not constant, and changes with n at a rate determined by the movement of the radios within the channel. This type of channel is called a *flat-fading* channel because all the frequency components of the signal $x(n)$ are faded by the same amount. For the flat-fading case, the channel coefficient, $h(0)$, is a sequence of random variables drawn from a set with an appropriate distribution, such as Rayleigh or Rician. Channel modelling will be discussed in greater detail in a later section of this chapter. When $M > 1$, (i.e. the impulse response of the channel is longer than the symbol period this creates *frequency selective fading* because $h(m)$ is a transversal filter whose frequency characteristics are defined by the delay profile of the impulse response, $h(m)$. For static multipath, the M coefficients of $h(m)$ are fixed for all values of n. However, in a typical mobile radio multipath channel, the M coefficients vary randomly for each value of n.

Additive channel and receiver noise are modelled according to (2.16). Consequently the signal at the receiver is given by:

$$y(n)=\sum_{m=0}^{M-1} h(m-n)x(n)+\frac{\sigma}{\sqrt{2}}n_I(n)+j\frac{\sigma}{\sqrt{2}}n_Q(n) \tag{2.18}$$

where n_I and n_Q are samples drawn from two independent Gaussian random variables of unit standard deviation.

2.2.2.4 Digital Receiver

The baseband receiver (demodulator) is often implemented as a digital matched filter that employs a maximum-likelihood detector for recovery of the digital symbols from the noisy signal samples. This avoids the need for modelling filters in the transmitter or receiver. However, where these must be modelled for added fidelity, $y(n)$ in (2.18) will be first passed through an appropriate digital matched filter algorithm, such as a root-raised cosine filter [63].

The digital implementation of a baseband maximum likelihood detector involves comparing each of the received signal samples, $y(n)$, with every point on the constellation. The constellation point corresponding to the smallest distance between the sample and that point, is selected as the most likely digital symbol, which can then be rearranged as a bit stream and compared with the original bit stream to obtain the bit error rate. A schematic of the maximum-likelihood detector for QPSK is shown in Figure 2.9. In this figure, the actual complex-valued received signal sample is shown in blue (due to the effects of the path and noise) and its distance from each point on the QPSK constellation is found to be d_1, d_2, d_3 and d_4. In this case, the shortest distance is d_1, indicating that symbol 1, representing bits 01, is the most likely symbol sent.

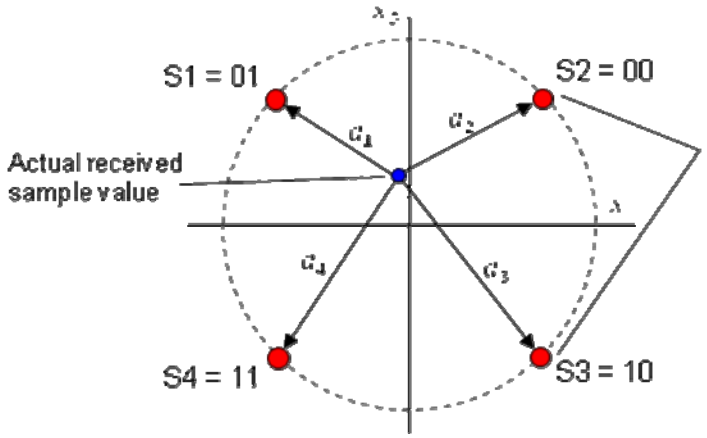

Figure 2.9: Schematic showing how the maximum likelihood detector works

2.2.3 Stochastic modelling of a digital communication system in an AWGN channel

Figure 2.10 shows the bit error probability performance of the same digital communication system detailed in Section 2.2.1, but using a stochastic model of the system.

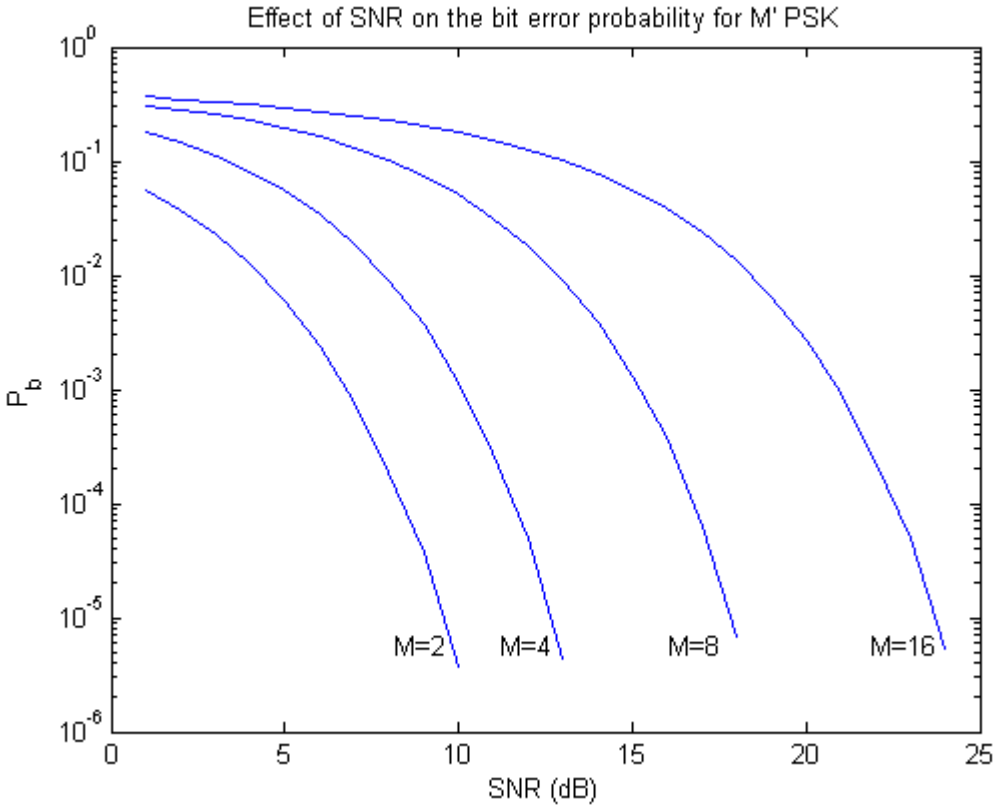

Figure 2.10: Effect of SNR on the BER of M'PSK modulation using computer simulation

As before, the noise bandwidth and data rate are normalised to: $R_b = B = 1$, and the results are shown for different orders of modulation, M. The channel is taken as a simple lossless channel in which the only impairment is additive noise with a Gaussian distribution. The model of the communication system was simulated using Matlab®. The results should be compared with the theoretical curves given in [139].

Figure 2.11shows the performance of the simulated communication system, in terms of the bit error probability, when QAM modulation is used, for the same parameters as above. The results should be compared with the theoretical performance curves shown in Figure 2.3.

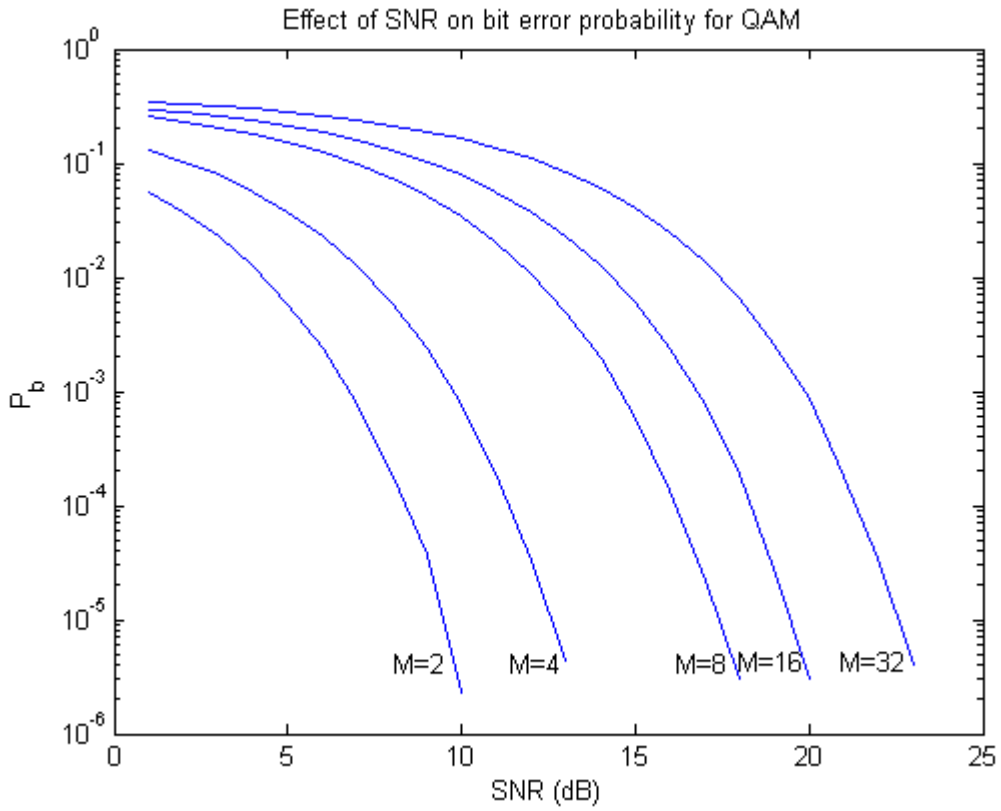

Figure 2.11: Effect of SNR on the BER of QAM modulation using computer simulation

There is excellent agreement between the theoretical and simulated system results for both the M'PSK and QAM systems. However, in order to have a measure of confidence in the error rate measurements at around 1 error in 10^6 bits sent, 5×10^6 bits were actually sent and each curve took 20mins to compute on a 2.8GHz PC.

Figure 2.12 shows the performance of the simulated communication system in terms of the bit error probability in AWGN, when a Rate = ½, convolutional coder is used. In this case, the *x* axis is normalised in terms of E_b/N_0 rather than SNR, where E_b is the energy per bit and N_0 is the noise spectral density. This removes the effect of the noise bandwidth and the data rate from the results. Each curve is obtained for a different constraint length, *K*. The constraint length represents the depth of the convolutional coder. For K=7, for example this represents the number of bits that the information contained in the current bit is being carried by (including that bit). The results show that the longer the constraint length, the greater the coding gain. However, by requiring that more coded symbols are examined to recover the information in the current symbol, the greater the workload in the receiver and the longer the processing delay (i.e. the additional coding gain is paid for by a far higher data processing requirement). This is in agreement with the qualitative discussion in Section 2.2.2. The

simulated results match the theoretical results for convolutionally coded data in AWGN very closely [139].

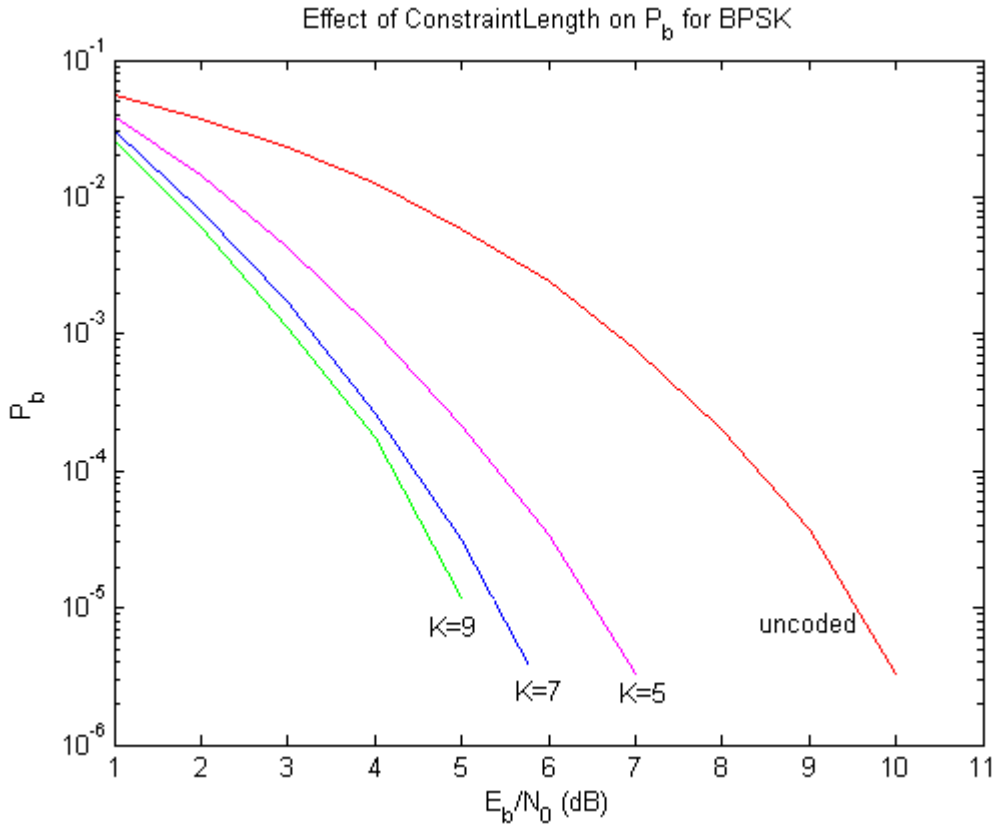

Figure 2.12: Effect of using a rate=1/2 convolutional coder on the bit error probability

Figure 2.13 shows the effect of code rate on the probability of a bit error for an AWGN channel. In this figure the constraint length was maintained at K=7. A rate of 1/3 requires that the output bit[1] rate is three times the input bit rate. This means that the information contained in the current bit is being carried by three coded streams, whereas for a rate = ½ code, the information is only being carried by two streams. This carries a considerable bandwidth penalty as well as an increased computational overhead. However, this is repaid in terms of a significantly reduced E_b/N_0 compared with the uncoded case or the rate = ½ coders to achieve a given bit error rate.

The simulation provides the expected result that the rate=1/2, K=7, convolutional coder provides ~3dB of coding gain compared to the uncoded case at $P_b = 10^{-6}$.

[1] Strictly, the output of the coder should be referred to as symbols rather than bits since the actual information smeared over the K-1 previous outputs and each bit is actually represented by R output pulses (where R is the code rate). However, the term 'bit' indicates that the coder output is binary valued.

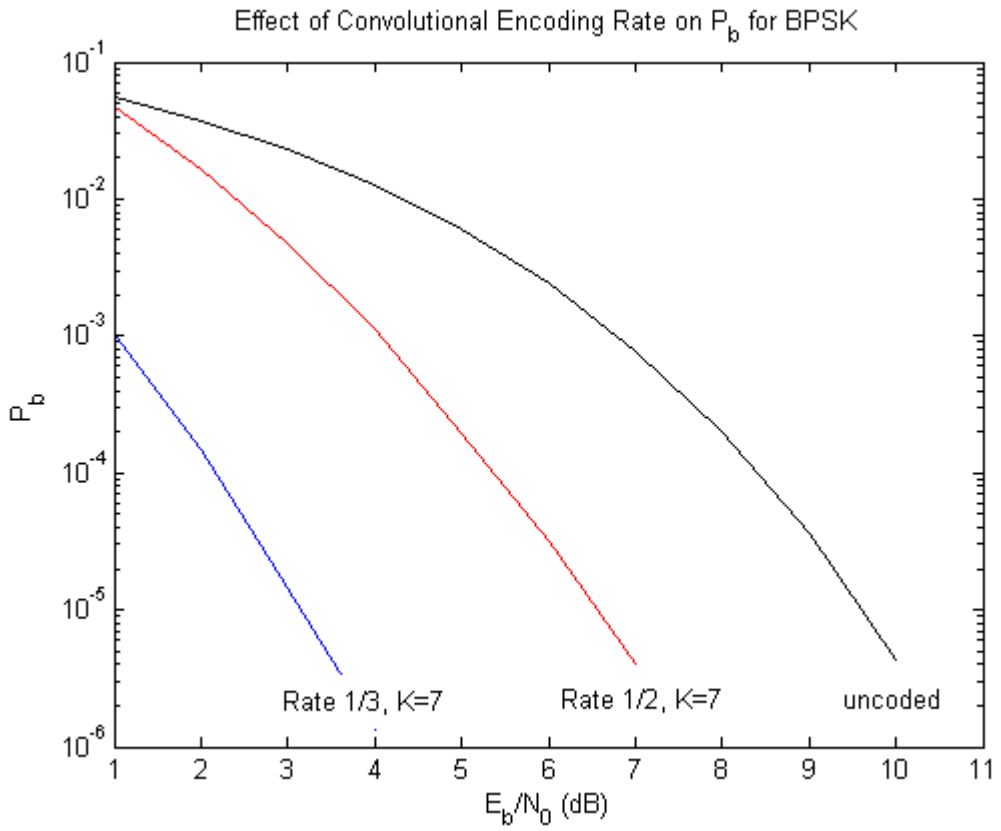

Figure 2.13: Effect of using different convolutional code rates on the bit error probability

2.3 Channel Models for Mobile and Wireless MANs

The channel environments of mobile cellular radio and wireless LANs/MANs share one aspect in common: the transmitter and receiver heights are generally low mounted so that there is inadequate Fresnel zone clearance to guarantee free-space propagation on a line-of-sight link. Because this condition cannot be met, the predominant propagation mode is, at best, *plane-earth* in which there is a strong interaction between a direct line-of-sight component and at least one reflected signal, giving rise to spatial fading where the signal components suffer destructive interference. At worst, propagation is non-line of sight in which the signal arrives at the receiver entirely by scattering, reflection and refraction.

Figure 2.14 shows a typical scenario where a basestation antenna is mounted at typically 10-20m in height transmitting to a mobile or wireless LAN node whose antenna is at a height of 2-5m. The signal comprises a direct component, and a signal that is reflected at a plane surface, such as the ground. For this highly idealised model, the received signal is the vector sum of the direct and reflected components [117].

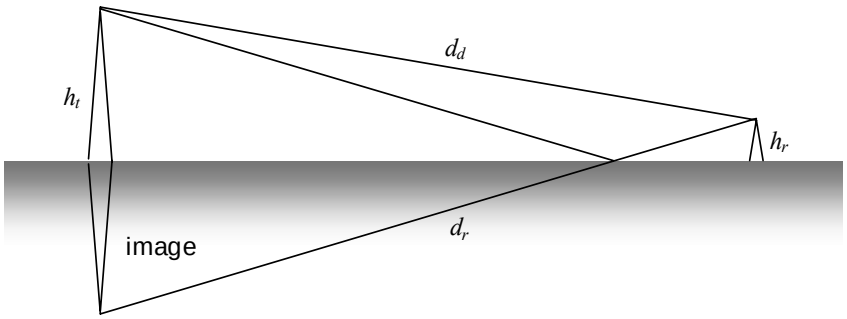

Figure 2.14: Schematic of idealised plane-earth propagation

The lengths of the direct and reflected components are simply:

$$d_d = \sqrt{d^2 + (h_t - h_r)^2} \cong d\left(1 + 0.5\left(\frac{h_t - h_r}{d}\right)^2\right)^{0.5} \quad \text{and} \quad d_r = \sqrt{d^2 + (h_t + h_r)^2} \cong d\left(1 + 0.5\left(\frac{h_t + h_r}{d}\right)^2\right)^{0.5} \tag{2.19}$$

The path length difference is

$$\Delta d = d_r - d_d \approx \frac{2h_t h_r}{d} \tag{2.20}$$

corresponding to a phase shift:

$$\Delta\phi = \frac{2\pi}{\lambda}\frac{2h_t h_r}{d} = \frac{4\pi h_t h_r}{d\lambda} \tag{2.21}$$

The received signal at the mobile/LAN node is:

$$\left|A_{total}\right| = \left|A_{direct} + A_{reflected}\right| = A_{direct}\left|1 + \rho e^{j\Delta\phi}\right| \tag{2.22}$$

The ratio between received power and the direct ray

$$\frac{P_r}{P_d} = \left|\frac{A_{total}}{A_{direct}}\right|^2 = \left|1 + \rho e^{j\Delta\phi}\right|^2 \tag{2.23}$$

where ρ is the reflection coefficient of the ground plane. Both the direct and reflected paths suffer spherical spreading:

$$P_d = P_t\left(\frac{\lambda}{4\pi d}\right)^2 \tag{2.24}$$

where P_t is the transmitter power. Inserting (2.24) into (2.23) and making the assumption that $\rho = -1$, yields:

$$P_r = P_t\left(\frac{\lambda}{4\pi d}\right)^2 \cdot \left|1 - e^{j\Delta\phi}\right|^2 = P_t\left(\frac{\lambda}{4\pi d}\right)^2 \left(1 - \cos\Delta\phi\right)^2 + \sin^2\Delta\phi \tag{2.25}$$

At relatively short distances of the mobile from the basestation, using (2.21), ϕ has a relatively large angle and the average power fluctuates widely from 0 (destructive interference) to 2. This is called the fading region. The extent of the fading region is given by:

$$R_{\max} = \frac{4h_t h_r}{\lambda} \tag{2.26}$$

As the mobile moves further from the basestation, ϕ becomes much smaller – approaching 0. In the limit $(1-\cos\Delta\phi)^2 + \sin^2\Delta\phi \approx \Delta\phi$ yielding [117]:

$$P_r = P_t\left(\frac{\lambda}{4\pi d}\right)^2 \Delta\phi = P_t\left(\frac{\lambda}{4\pi d}\right)^2\left(\frac{4\pi h_1 h_2}{\lambda d}\right)^2 = P_t\left(\frac{h_1 h_2}{d^2}\right)^2 \tag{2.27}$$

The equivalent path loss form of (2.25) is plotted in Figure 2.15 as a function of d, where the phase shift $\Delta\phi$ is obtained as a function of range using (2.21). In this figure, the chosen parameters are typical of a 2.4GHz WiMAX system, where h_t = 10m and h_r=5m and λ= 0.125m. These parameters yield a value for $R_{\max}$ = 1600m where there are large fluctuations in path loss due to constructive and destructive interference occurring every 20 or 30m and a mean reduction in signal strength that is proportional to $1/d^2$. Beyond this range, the power at the receiver falls off smoothly with range according to (2.27) (i.e. $1/d^4$).

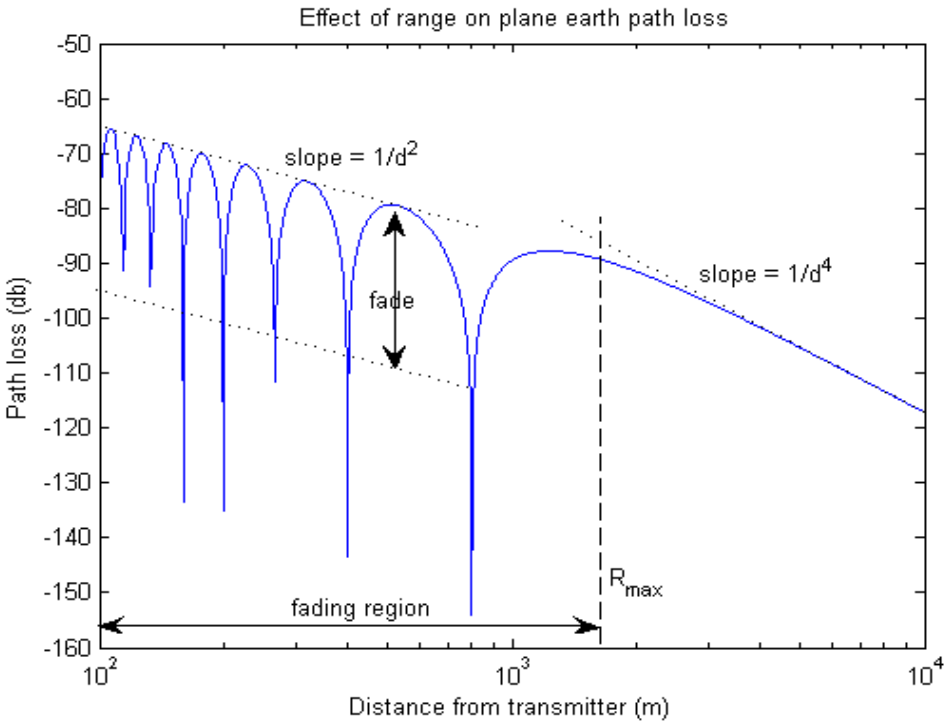

Figure 2.15: Variation of the path loss with range for the case h_t=10m, h_r=5m and f=2.4GHz

This equation forms the basis for many models of terrestrial propagation including the Murphy propagation model and the Egli propagation model where the transmitter and receiver ranges are quite large by virtue of a high transmitter power. A typical application where an Egli or Murphy model might be applicable is private mobile radio (PMR), typical of large area coverage from a central basestation to utility vehicles or the emergency services, where the service area might be 40-60km. However, for the case of mobile cellular radios, wireless LANs and wireless MANS, the transmitter powers are very limited (typically in the range 100mW-1W) and so generally do not operate in this limiting region, but in the much shorter fading region.

2.3.1 Fast and slow fading

For a mobile handset, it will be clear from (2.25) and Figure 2.15 that although multipath fading is a spatial phenomenon, it becomes translated into a temporal effect as the vehicle propagates through the fades. If the vehicle travels quickly through the fades, it results in a rapid fade, and conversely, when the vehicle or pedestrian travels through the region slowly, the fades occur much more slowly and the period that the receiver stays in the fade will be longer. This can create severe problems for the recovery of the data. It is clear from Figure 2.15 that fading is not truly random over a short time scale, but has some structure that is related to the vehicle speed. It is this observation that has allowed developments in wireless systems to be able to *estimate* the temporal variation of the channel characteristics and from this *predict* the likely behaviour of the channel over relatively short time periods (~milliseconds) so that the wireless system can *compensate* for the fluctuations in the path loss.

Although Figure 2.15 provides an excellent summary of fading in a terrestrial channel it does not provide any detail about the fading mechanisms that are known to exist from accurate field measurements that have been made over the past 30 years. In practice, the model defined by (2.25) is made more complicated by multiple reflections from many different plane surfaces such as buildings, billboards etc between the transmitter and the receiver. Objects larger than about 3m will act as scatterers for radio signals in the frequency range 1-2GHz, so that random scattering is an additional mechanism by which a radio signal can propagate to the receiver. Foliage and features such as bridges and tunnels together with large buildings provide additional sources of path attenuation.

It is well known from detailed measurements of practical wireless channels in different types of environments, such as urban, suburban and rural, that the time variation of

the envelope of a mobile receiver signal comprises of both fast fading and slow fading, as shown in Figure 2.16

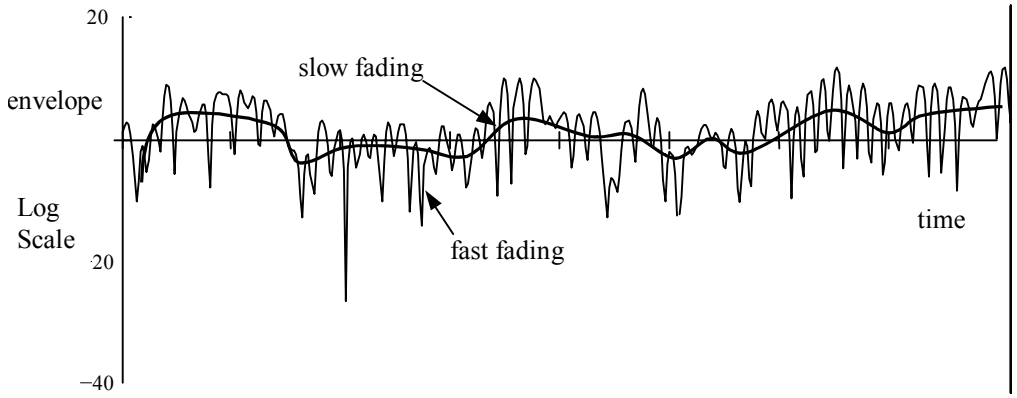

Figure 2.16: Typical variation of the envelope of an RF signal in a fading environment

Slow fading is generally due to a time-varying change in path loss, called shadow loss due to the handset signal being blocked by large buildings, tunnels etc. Field trials have shown that the statistics of the envelope fluctuations are often log-normal with a standard deviation of 5 to 12dB.

Fast fading is generally associated with multipath fading from multiple reflectors and scatterers. However, because it is rare for reflected signals to be reflected with a reflection coefficient $\rho = -1$, as required to create (2.25), the infinitely deep fades of Figure 2.15 are very unlikely, and the signal envelope has a random element to the fluctuations due to the different signal levels of each of the paths at the receiver antenna. As discussed above, the fade has structure, set by the vehicle speed. This is specified by the *channel coherence time*. The coherence time represents the period of time over which the channel statistics can be assumed to be stationary. It is this property of the fade that allows reliable communications to be established by a process of channel estimation and prediction, so that signal processing techniques such as phase and delay equalisation or signal diversity can be exploited.

The fluctuation in the signal envelope due to fast fades have been found to have a Rician distribution if there is a well-defined direct component to the signal, or a Rayleigh distribution if there is no line-of-sight path and the signal arrives at the receiver purely by scattering and reflections. If the geography is substantially different from normal urban and suburban environments, field trials have shown that the statistics may differ from Rayleigh or Rician. In case of a frequency selective channel as the channel is time varying so the characteristics may change fast due to the effect of Doppler when the user is moving. The response of a multipath propagation channel in time and freq domain is as depicted in Figure 2.17(a) and (b) respectively. Here a mobile user is travelling at a speed of 63.720kmph

corresponding to a Doppler of 161.60Hz at a carrier frequency of 2.4GHz, number of paths considered are 6 and time period per symbol is 0.2 μsec.

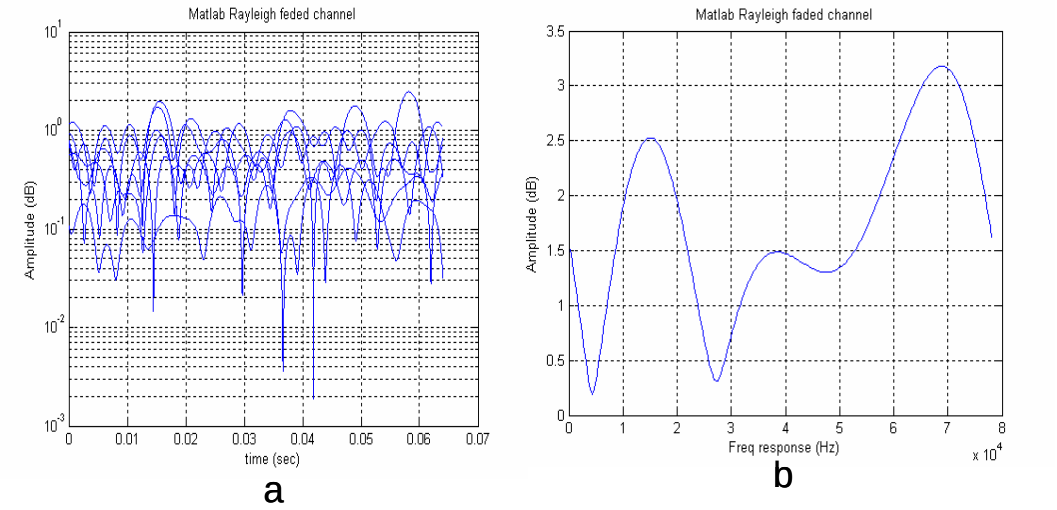

Figure 2.17: Response of multipath propagation channel in time and freq domain

2.3.2 Multipath propagation

The arrival at the receiver antenna of multiple reflected and scattered replicas of the transmitted signal, each delayed due to their different path lengths, together with random phase shifts, generates a multipath signal that can be considered as a single transmitted signal that is convolved with a channel model that has an impulse response that represents the principal echoes together with a continuum of the scattered signals as illustrated in Figure 2.18. The arrival time of the last of these echoes relative to the arrival time of the first signal is termed the maximum *delay spread* of the channel, τ_m. The delay spread depends on what is considered to be the longest significant path, which is subjective. An alternative definition, the normalised delay spread, represents the rms pulse width broadening factor:

$$\tau_N = \sqrt{\sum_{i=1}^{L} P_i \tau_i^2} \tag{2.28}$$

where P_i is the power in the ith path component, τ_i is the relative delay of the ith path and L is the total number of paths.

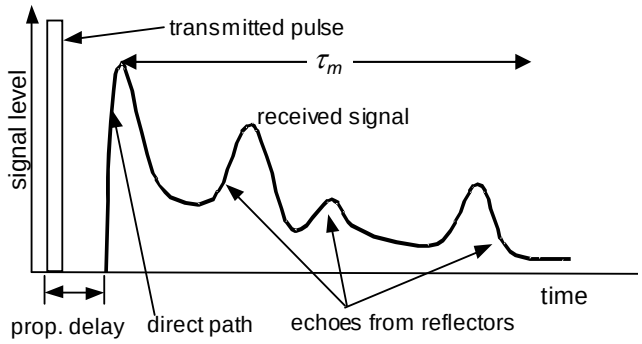

Figure 2.18: Schematic showing the delay spread of a signal due to multipath propagation

This parameter, together with the transmission bandwidth of the signal, determines whether the channel is 'narrowband' or 'wideband'. If the signal's bandwidth is narrower than the *coherence bandwidth* of the channel, $B_s << B_c = 1/(\tau_m)$, (i.e. the delay spread is much greater than the transmitted symbol period) then all the frequency components of the transmitted signal encounter nearly identical propagation delays and the channel is said to produce frequency non-selective, or flat, fading. This is called the narrowband approximation [63]. The coherence bandwidth represents the frequency separation at which the correlation coefficient between the attenuations of two signal components at these frequencies becomes less than 0.5 [11]. Although the channel is not frequency selective, the random fluctuation of the channel characteristics, ensure that it is time-varying.

If on the other hand, the transmission rate is sufficiently high such that some of the echoes of one symbol arrive at the same time as those of other consecutive symbols, the channel is termed wideband and the multipath propagation creates inter-symbol interference (ISI) which adversely affects successful recovery of the data. The impulse response creates a channel characteristic that is strongly frequency selective and the impulse response of these characteristics ensure that the channel model is time varying. The impulse response of a time-variant multipath channel can be written as [117]:

$$h(\tau, t) = \sum_{i=1}^{L} \alpha_i(t) e^{-j(\tau_i(t) + \phi_i(t))} \tag{2.29}$$

Where $\alpha_i(t)$, $\tau_i(t)$ and $\phi_i(t)$ are the amplitude, arrival time and phase of the received signal from the i^{th} path at time instant t, respectively. The rate at which both $\alpha_i(t)$ and $\phi_i(t)$ vary depends on the vehicle velocity cutting through the spatial fade pattern. Equivalently, this is related to the Doppler frequency shift of the carrier. The Doppler frequency shift is given by [117]:

$$f_D = \frac{v \cdot f_c}{c} \cdot \cos\theta_i \tag{2.30}$$

where v is velocity of the vehicle, f_c is the carrier frequency and θ_i is the angle of arrival of the RF signal relative to the velocity vector. The maximum Doppler frequency occurs when the signal arrives in the opposite direction to the velocity vector, when $f_{D_{\max}} = v/\lambda$. If it is assumed that the scattered signals arrive at the antenna from all angles with a uniform distribution, then the spectral distribution of the received carrier power due to the spread in Doppler is given by [13]

$$S(f_D) = \frac{-1}{2\pi f_m \sqrt{1-(f_D/f_m)^2}} \tag{2.31}$$

which is shown in Figure 2.19. The maximum Doppler frequency f_m represents the rate at which the nulls in the fast fade characteristics of Figure 2.16 occur and is represented as $f_m = \frac{v}{c}$, this is related to the channel coherence time, $T_c(t)$, as discussed earlier. This is given by [12] and represented as:

$$T_c(t) \approx \frac{9}{16\pi f_m} \tag{2.32}$$

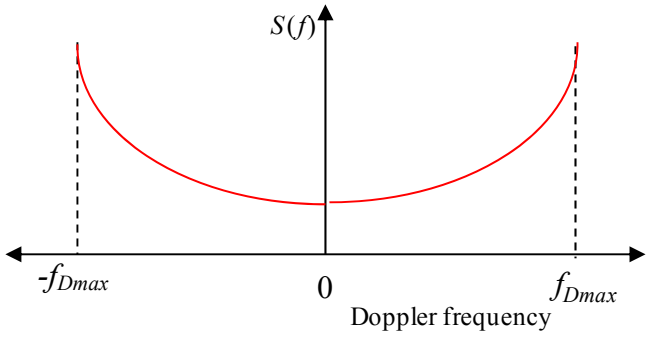

Figure 2.19: The spread in Doppler frequency due to the uniform distribution in the arrival angles of a scattered signal at the vehicle antenna – the Doppler power spectrum

2.3.3 Channel Modelling

The model presented here is based on the assumption that the multipath returns of the signal are uncorrelated and have complex-valued Gaussian distributions[2]. This model is more known as the Gaussian wide-sense stationary uncorrelated scatterers model (GWSSUS) [123]. A model for the narrowband (flat-fading) channel is first presented where the received signal echoes all arrive within short intervals of each other (relative to the sample interval) so that the impulse response of the channel may be modelled as a single multiplicative complex Gaussian random variable. A model of the multipath (wideband) channel based on that of the narrowband channel is then developed.

2.3.3.1 Narrowband Model

Although there are a number of different methods [58][117] of modelling a narrowband channel, the following is a widely adopted method, and was used widely in this research. The generation of the real and imaginary parts of the narrowband coefficient can be achieved by using two uncorrelated Gaussian distributed random numbers. These coefficients do not change infinitely quickly because of the finite coherence time of the channel, which is set by the vehicle velocity (2.32). One method of incorporating this effect is to note that the effect of vehicle motion is reflected in the Doppler power spectrum given by (2.31) and shown in Figure 2.19.

This is achieved in the model by separately filtering the real and imaginary random coefficients using *Doppler filters*. A schematic of the narrowband channel model is shown in Figure 2.20 below.

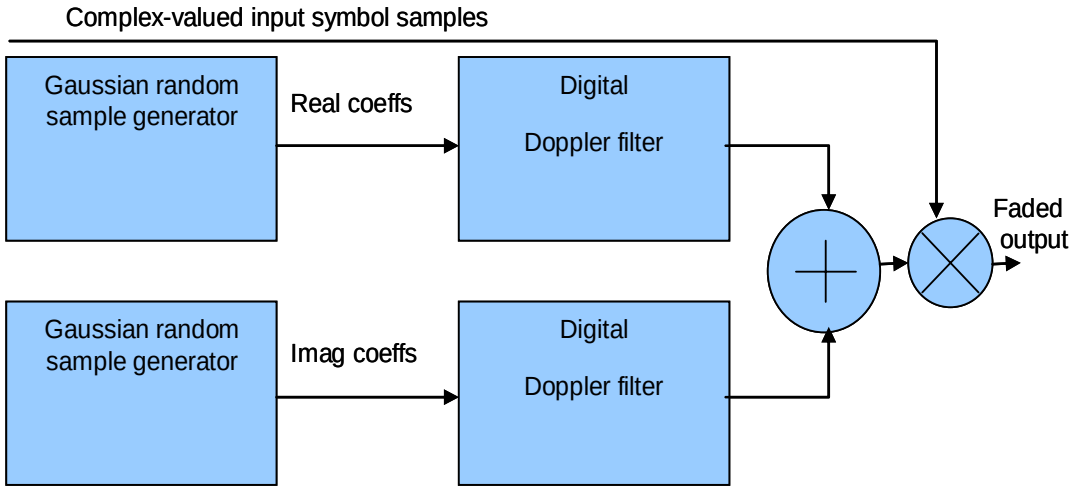

Figure 2.20: Schematic of the narrowband channel model

[2] This corresponds to the case where the magnitude of each path has a Rayleigh distribution and the phase is uniformly distributed over the range 0-2π.

The frequency characteristics of this filter match the characteristics of the Doppler spectrum given by (2.31). This limits the rate of change of the random coefficients to a rate that is set by the maximum Doppler frequency, $f_{D_{\max}}$. The inclusion of the filter does not affect the statistical distribution of the random numbers [11], but does affect their variances. This, however, can be corrected for by inserting an appropriate scaling factor [14]. Filtering inserts some correlation between the output samples and the amount of correlation changes according to the maximum Doppler frequency. The relationship between the cut-off frequency and the correlation factor is inversely proportional. The filtering of the random numbers may be done in either the frequency domain or the time domain as discussed below.

2.3.3.2 Time domain implementation

In this approach, the time-domain Gaussian numbers are convolved with the impulse response of the Doppler filter of equation (2.31). A time-domain filter, having the required Doppler spectrum, can be implemented using two cascaded second order filters. One filter represents a highly resonant second order filter tuned to ring at $f_{D_{\max}}$ and the other is a Butterworth filter shapes the spectrum to give a good approximation to (2.31). The *s*-domain approximation of this two-stage filter is given by [15]:

$$H(s) = \frac{1}{s^2 + \sqrt{2}s + 1} \cdot \frac{1}{s^2 + 0.02s + 1} \tag{2.33}$$

This form of frequency characteristic can be implemented as an IIR digital filter using Matlab to evaluate the difference equations. Recall, that two such filters are needed, one for the real part of the path coefficient and one for the imaginary part of the path coefficient. There are two particular problems with this approach. First, the resonant filter has an extremely long start-up transient, and the filtered random coefficients cannot be used until after this start up transient has elapsed. Second, the rate of change of the path coefficients is much slower than the sampling rate for the data so some form of multi-rate sampling system must be used in order to minimise the number of taps needed to implement the filter. A typical frequency characteristic for each Doppler filter is shown in Figure 2.21, below.

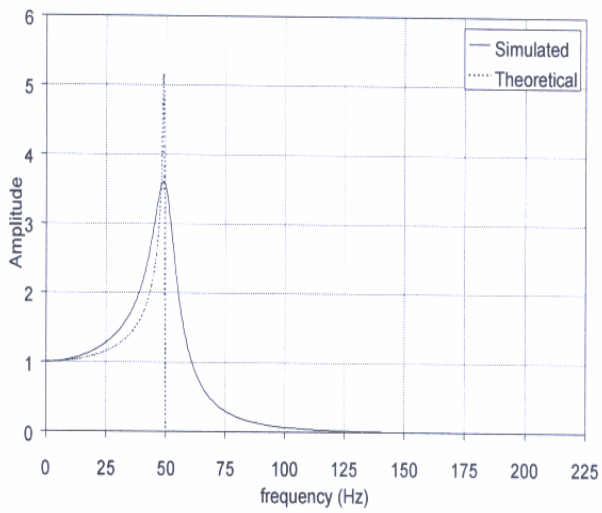

Figure 2.21: Characteristics of the digital Doppler filter used to filter the random channel coefficients

2.3.3.3 Frequency domain method

This method is based on the discrete Fourier transform, in which the real and imaginary parts of the complex multiplicative coefficient are multiplied by the Doppler transfer function of equation (2.31). Exploiting the fact that the Fourier transform of a Gaussian process is another Gaussian process this transformation is only needed once. This is a relatively simple process, as long as an efficient fast Fourier transform exists. This type of approach has a problem due to the bandwidth of the Doppler spectrum which is much smaller than the data bandwidth so a very large Fourier transform size is needed in order to ensure that a significant proportion of the input samples fall within the Doppler filter's bandwidth [11]. At the output of the Fourier transform, a scaling factor is used to ensure that the variance of the output samples is not changed. This method does not suffer from start-up transient problems, but a very large FFT is needed to provide an accurate narrowband filter.

2.3.3.4 Convolver method

This is the most practical method of implementing the Doppler filter because it is both computationally efficient and does not have a long start-up transient. This method is also based on the Doppler filter of (2.31). However, in this case, the frequency characteristic is represented as an equivalent impulse response, $h(t)$. The filtered sequence of random coefficients (both real and imaginary), are obtained by convolving the Gaussian random sequence with this impulse response:

$$y(t) = h(t) * x(t) \tag{2.34}$$

where * represents the convolution operation.

Figure 2.22 shows a typical time-variation of the real and imaginary path coefficients for a Doppler frequency of 10Hz. Note that each path coefficient still retains the Gaussian probability distribution of the unfiltered samples, but the variance is much lower due to the effect of the filter.

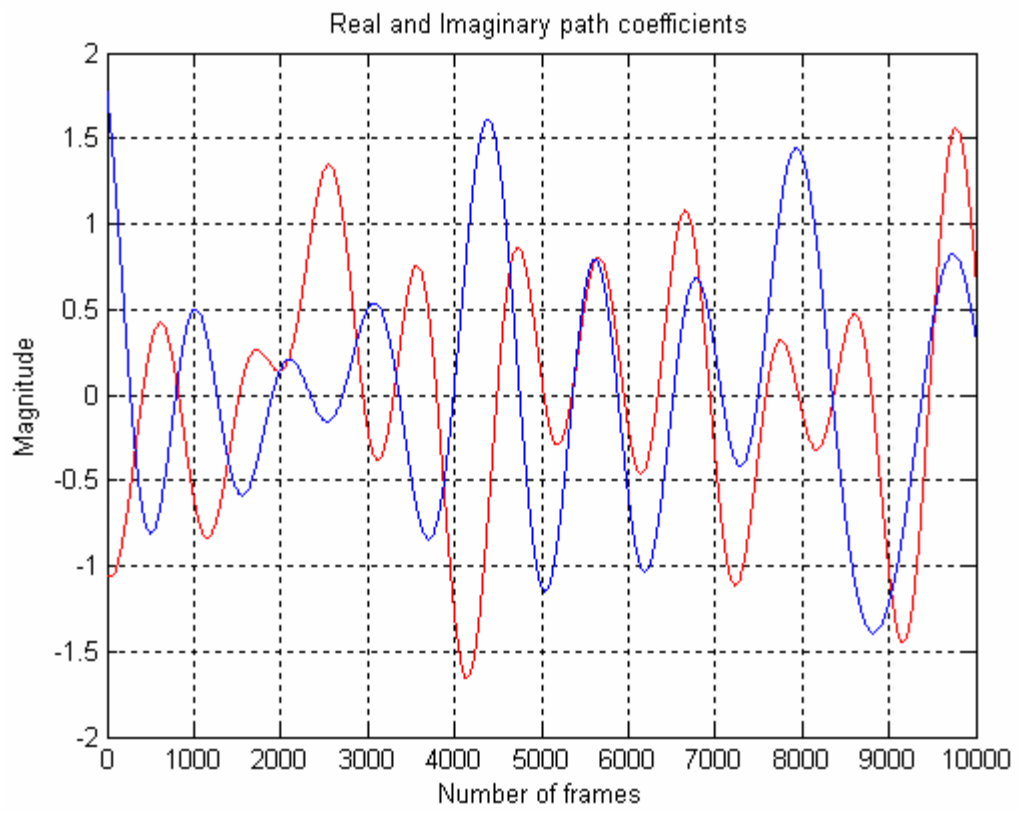

Figure 2.22: Typical variation of the real and imaginary path coefficients for a narrowband channel for a Doppler frequency of 10Hz.

2.3.3.5 Wideband Channel Model

This type of channel arises when the path delay differences are longer than the symbol duration resulting in the arrival of one symbol's echoes at the time of arrival of other consecutive symbols. The impulse response of such channel may be represented in discrete form as consisting of a number of delta functions whose amplitude has Rayleigh/Rician distribution. A typical wideband channel impulse response is shown in Figure 2.23, below.

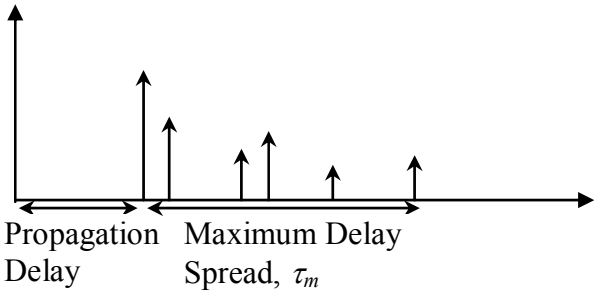

Figure 2.23: Typical impulse response for a wideband channel

Although various impulse response models have been used in the past, the best known ones are those of the COST 207 Standards Group, specified by the Group Special Mobile committee (GSM) for different environments, such as, typical urban, bad urban, rural and hilly terrain. The set of six tap GSM impulse responses for the two most common channel models are summarised in the Table 2-1 below:

Path	1	2	3	4	5	6
Spectrum	Rayleigh	Rayleigh	Rayleigh	Rayleigh	Rayleigh	Rayleigh
Delay μsec	0.0	0.2	0.4	0.6	15.0	17.2
Attenuation	0	2.0	4.0	7.0	6.0	12.0
Correlation	0	0	0	0	0	0

(a)

Path	1	2	3	4	5	6
Spectrum	Rayleigh	Rayleigh	Rayleigh	Rayleigh	Rayleigh	Rayleigh
Delay μsec	0.0	0.2	0.6	1.6	2.4	5.0
Attenuation	3.0	0.0	2.0	6.0	8.0	10.0
Correlation	0	0	0	0	0	0

(b)

Table 2-1 : Parameters of the COST 207 channel models for: (a) Hilly Terrain, (b) Typical Urban

Since the response of the channel outside the signal's bandwidth is of little importance, the channel can be sampled at the symbol rate leading to the tapped delay line model [123][117], as shown in Figure 2.24. When the baseband signal is applied to the series of delays, the output from each tap is multiplied by a time varying complex-valued path coefficient generated using the narrowband method shown earlier in Figure 2.20, *R,* that characterises the

fast fading and by a further gain, A, in order to keep the average power of that path at a certain wanted level. The outputs from all the taps are then added together using a complex summer and combined with some additive Gaussian noise before being passed to the output.

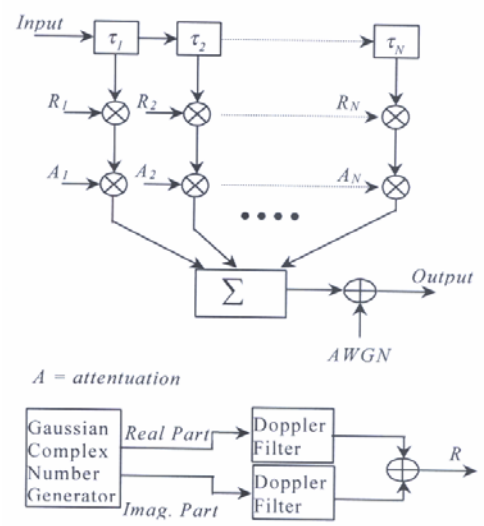

Figure 2.24: Schematic of the wideband channel Simulator

Figure 2.25 shows the time-frequency plane of the magnitude of the channel coefficient for a typical Rayleigh channel. This figure shows the temporal variation of the channel coefficient and the time-varying impulse response of the wideband channel model provides the frequency selective fading. Because the channel impulse response is constantly changing, the frequency response changes accordingly.

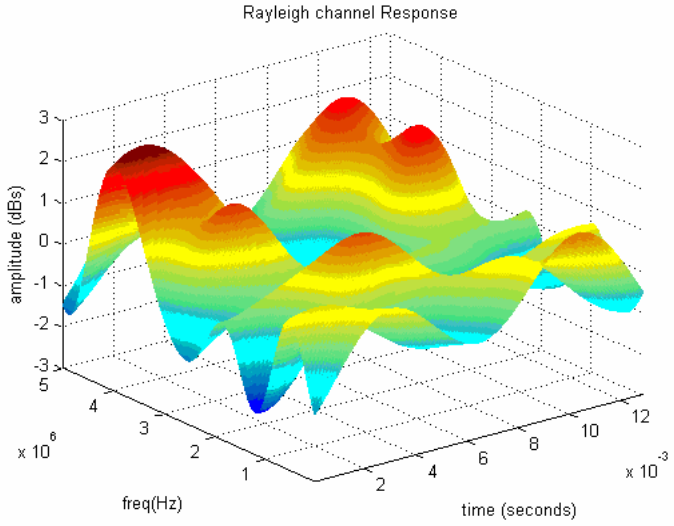

Figure 2.25: Time-frequency response of a typical wideband multipath channel

2.4 Multipath effects

In mobile radio environments, the surroundings such as houses, buildings or trees act as reflectors of radio waves as shown in Figure 2.26 below. Since the mobile antenna is well below the surroundings, so there is no direct line of sight path between transmitter and receiver. Propagation is mainly by scattering from these surfaces and by diffraction over or/and around these surfaces. These objects produce reflected signals with attenuated amplitudes and phases. If a modulated signal is transmitted, there are number of reflected waves of the transmitted signal each having different propagation delays arriving at the receiving antenna from different directions. These waves are called multipath waves and all these reflected waves arrive at the receiving antennas with different phases because of different angle of arrivals. When these reflected waves are collected by receiving antenna in space they are combined vectorially to give resultant signal, which can be large or small depending upon distribution of phases among the component waves. The challenges faced by wireless communication systems may be categorized as

a. Multipath propagation
b. Delay spread
c. Doppler spread

The multipath structure of a channel is quantified by its *delay spread*. Delay spread can be stated as the difference in time of arrival of first line sight wave and the last reflected wave of the multipath signal. When the delay spread is less than the duration of the symbol period then the channel is said to be frequency nonselective channel. However, when the delay spread is more than the time duration of a symbol period then the channel is said to be frequency selective due to existence of large variation in the channel characteristics. This delay spread gives rise to ISI that occurs because of the delayed signals that overlap the following symbols. As a result there could be significant BER because as and when the transmitted bits are increased the ISI increases thereby increasing the BER at the receiving end.

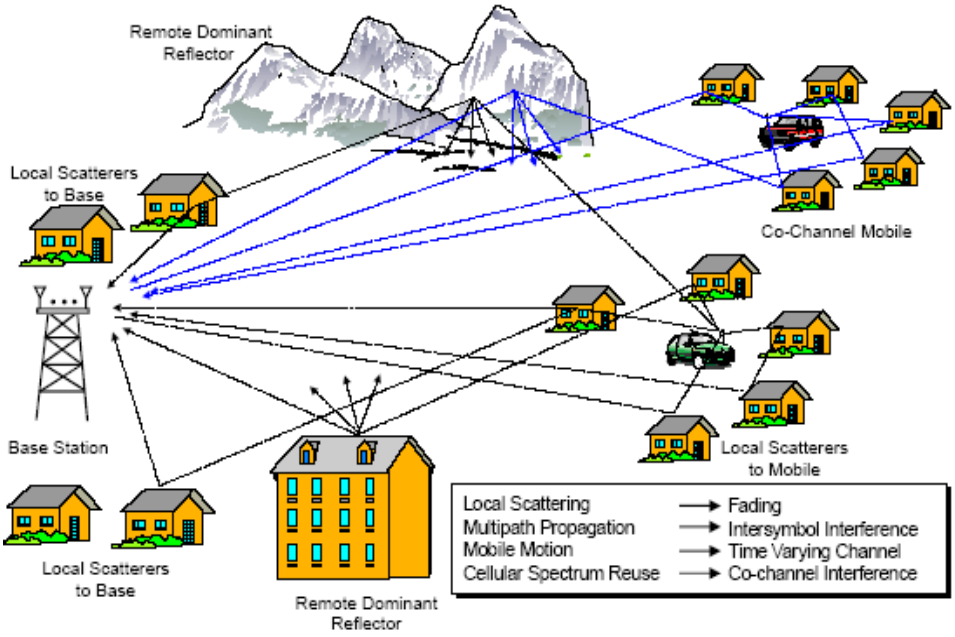

Figure 2.26: Multipath Environment

As shown in Figure 2.26, the reflection could be from closer buildings/obstacles causing short delay in addition to longer delay that is caused by the remote building/obstacles. Therefore the radio propagation channel in mobile communication systems can be regarded as a non linear function of the environment. Figure 2.26 shows a typical multipath environment and each multipath is charactersied by its amplitude a_l, phase ϕ_l, time delay τ_l, AoA and doppler shift f_d. The channel impulse response $\mathbf{h}(t,\tau)$ at any point in space for an omnidirectional antenna is represented as time vaying function and is given as [45]:

$$\mathbf{h}(t,\tau) = \sum_{l=0}^{L-1} a_l(t) e^{j\phi_l(t)} \delta(t - \tau_l(t)) \tag{2.35}$$

where, L is the total number of multipaths.

The received signal $\mathbf{r}(t)$ is achieved by convolution of transmitted signal $\mathbf{s}(t)$ with channel impulse response from (2.35) [63] and represented as

$$\mathbf{r}(t) = \int_{-\infty}^{+\infty} h(t,\tau)\mathbf{s}(t-\tau)d\tau + \mathbf{n}(t) \tag{2.36}$$

where $\mathbf{n}(t)$ is the complex Gaussian noise and integral limit is defined by the delay spread of the channel.

2.4.1 Doppler Effect

The phenomenon of Doppler Effect can be stated as whenever there is some movement in relation to transmitter and receiver, there is some change in the carrier frequency of the receiver carrier as a result gives rise to change in the Doppler [117]. The time variations, or the dynamic changes in the propagation path lengths, can be directly related to the Doppler effects that arise. The rate of change of phase, due to motion, is apparent as Doppler frequency shifts in each propagation path and to illustrate this, Physical interpretation of Doppler shift can be represented as shown in Figure 2.27.

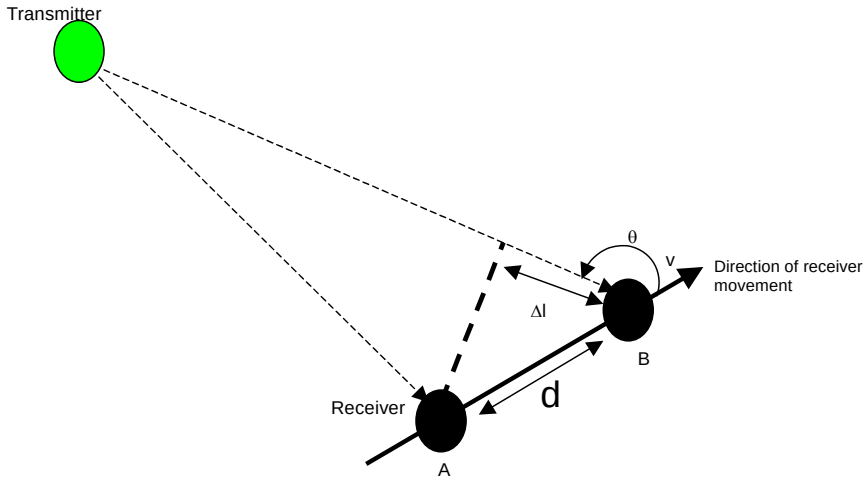

Figure 2.27: Doppler Effect

From Figure 2.27 it is seen that when a mobile moves with velocity v along the path AB, the distance between AB is represented by $d = v\Delta t$. The incremental change in path length of the wave represented by $\Delta l = d\cos\theta$, where θ is the spatial angle and phase change is therefore given as [117]:

$$\Delta\phi = -\frac{2\pi}{\lambda}\Delta l = -\frac{2\pi}{\lambda} d\cos\theta = -\frac{2\pi v\Delta t}{\lambda}\cos\theta \tag{2.37}$$

Hence apparent change in frequency i.e. Doppler shift is given by

$$f = -\frac{1}{2\pi}\frac{\Delta\phi}{\Delta t} = \frac{v}{\lambda}\cos\theta \tag{2.38}$$

Where, v is the velocity with which the receiver is moving, θ is the angle between the direction of movement of the receiver and the wave of propagation and λ is wavelength of the carrier. Therefore from (2.38) it is obvious that frequency shift depends on speed of the receiver, direction of movement and the carrier frequency corresponding to wavelength of the wave of propagation. The increase or decrease in the frequency dictates, whether the Doppler

shift is positive or negative thereby giving $f_m = \pm v/\lambda$ where f_m is the maximum Doppler shift.

2.4.2 Parameters of multipath Channels

2.4.2.1 Path Loss

Whenever a signal is transmitted from transmitter it gets attenuated and arrives at the receiver with different wavelengths because of reflection, refraction and scattering effects. It is expressed as given in [121]:

$$PL(dB) = 10\log\frac{p_t}{p_r} \tag{2.39}$$

where, p_t and p_r are the transmitted and received power respectively.

2.4.2.2 Time Delay Spread

The impulse response of a wireless channel varies randomly because of multipath reflections and scattering that occurs at random locations. The time delay spread can be defined as the difference in time of arrival of LOS component and the last multipath delayed component. Whenever the delay spread is greater than time duration of the symbol period the delay spread becomes large as result giving rise to generation of bit errors thereby decreasing the performance of the system. As shown in Figure 2.28 the main ray is preceded by second ray and the amount of power received is decreasing corresponding to the arrival of each ray. This occurs because of the fact that when the delay is more signal received is weaker because of travelling long path due to reflection from remote buildings/obstacles.

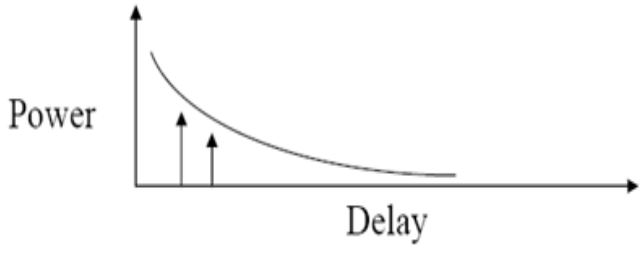

Figure 2.28: Exponential delay spread

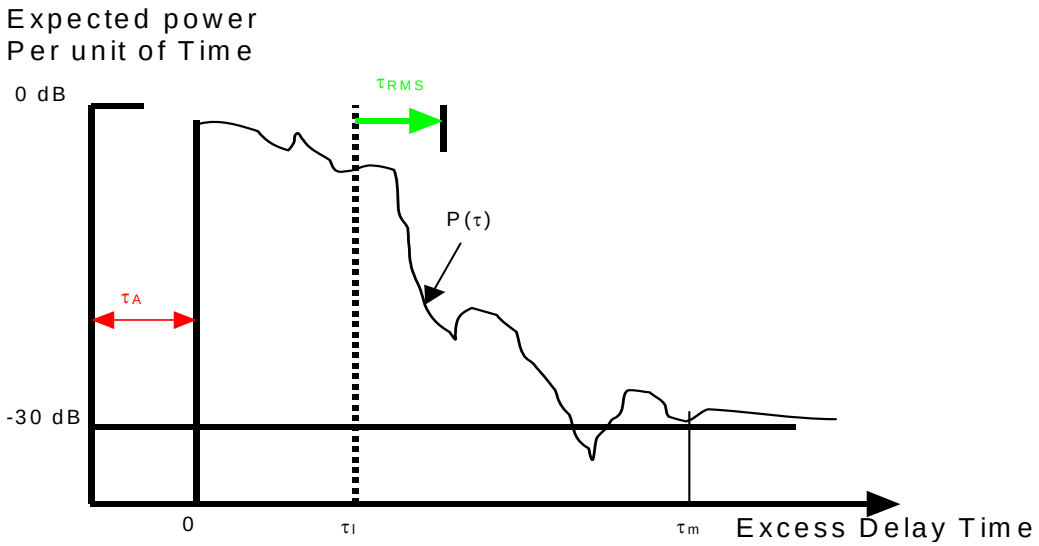

Figure 2.29: Power delay Profile and delay Parameters

2.4.2.2.1 First Arrival Delay (τ_A)

The first arrival delay denoted as τ_A is expressed as the arrival of first transmitted signal at the receiver. It is the minimum possible propagation path delay from transmitter to the receiver and usually measured at the receiver. It serves as reference delay and any delay that occurs after this reference delay is known as excess delay.

2.4.2.2.2 Mean Excess Delay (τ_l)

The mean excess delay can be defined as the first moment of the power delay profile that is related to the first delay, as shown in Figure 2.29. Mathematically it is expressed as given in [121]:

$$\tau_l = \int (\tau - \tau_A) P(\tau) d\tau \tag{2.40}$$

2.4.2.2.3 RMS Delay (τ_{RMS})

The RMS delay spread is the measure of delay spreads of multipaths and is defined as the standard deviation about the mean excess. It is expressed as:

$$[\tau_{RMS} = \int (\tau - \tau_l - \tau_A)^2 P(\tau) d\tau]^{1/2} \tag{2.41}$$

2.4.2.2.4 Maximum Excess Delay (τ_m)

The maximum excess delay is related to the power level of the signal corresponding to the threshold level. Whenever the signal falls below threshold level this is considered as a noise. In case of Figure 2.29 maximum excess delay is τ_m is the value for which $P(\tau)$ falls below threshold level (–30dB) of the peak value of the power of the signal.

2.4.2.2.5 Normalized Delay Spread (τ_n)

This is defined as ratio between maximum delay spread and first delay spread and is expressed as

$$\tau_n = \tau_m / \tau_A \tag{2.42}$$

when, $\tau_n \langle\langle 1$, the channel is considered as flat fading channel, whereas when τ_n approaches or exceeds unity, the channel is referred to as wideband time variant frequency selective channel.

2.4.2.3 Multipath delay spread

As the time domain description of a linear system is specified by impulse response of the system. When the channel is time variant, the impulse response is also time varying function [117][123]. If the complex envelope of the time variant impulse response is $\mathbf{h}(t,\tau)$ where τ is a delay variable, then complex envelope of the filter output $\mathbf{w}(t)$ can be obtained by convolving the input $\mathbf{z}(t)$ with impulse response. Mathematically from Figure 2.30 below the same can be represented as summation

$$\mathbf{w}(t) = \Delta\tau \sum_{m=1}^{n} \mathbf{z}(t - m\Delta\tau)\mathbf{h}(t, m\Delta\tau) \tag{2.43}$$

From Figure 2.30 it is seen that input is first delayed and then multiplied by the scattering gain.

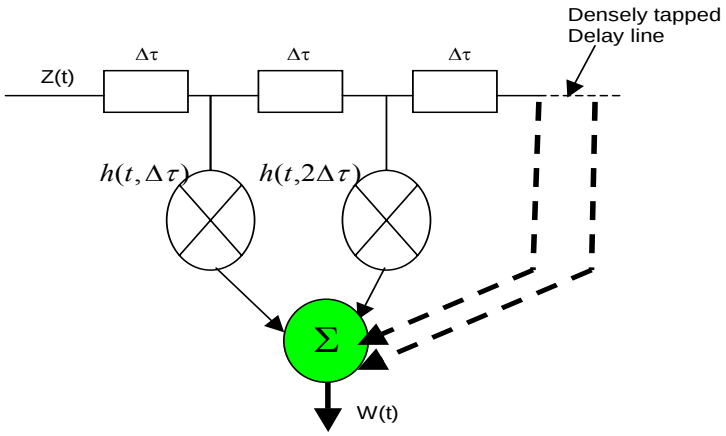

Figure 2.30: Linear time variant Channel using input delay spread function

2.4.2.4 Coherence Bandwidth

Coherence bandwidth denoted as B_c is defined as range of frequencies over which the characteristics of the channel are time invariant and channel is said to be a flat fading channel. It is also defined in terms of bandwidth over which the signal variation measured is almost 10% and is approximated as

$$B_c = \frac{1}{50\,\tau_{RMS}} \tag{2.44}$$

The real coherence bandwidth depends on the actual impulse response of the channel.

2.4.2.5 Coherence Time

Coherence time denoted as T_C and can be described as the time duration of the symbol over which the channel impulse response does not vary and remains constant. So the minimum signal duration at which the frequency dipersion becomes noticeable si inversely proportional to the magnitude of the maximum Doppler shift f_m by the signal. Similarly, the minimum signal duration at which time selective fading becomes apparent is related to the channel's coherence time $T_c(t)$, which is represented as in [12]

$$T_C = \frac{9}{16\pi f_m} \tag{2.45}$$

The behaviour of the channel is defined by Coherence time (T_C) and Coherence bandwidth (B_c)

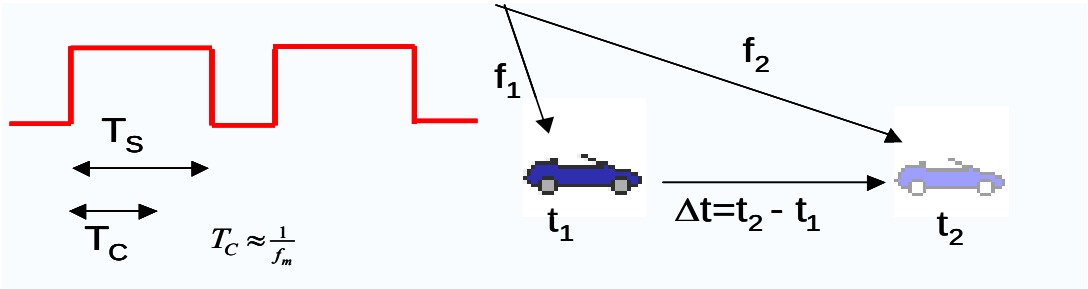

Figure 2.31: Coherence time representation

2.4.3 Coherence in spatial and temporal domain

The spatial and temporal domain coherence of the system is related to the phase characteristics of the system. Therefore it can be stated that the concept of coherence is based on the stability of the variation in phase of the system. Spatial coherence dictates the similarity of signals at different points in the space whereas temporal coherence dictates the similarity between two signals at different time intervals. When there is an array of antenna elements used at receiving end to form main beam in the direction of wanted users by the process of spatial filtering. However noise, interference and also other delayed signals arriving from different directions other than the direction of wanted user resulting into ISI are suppressed.

2.5 Diversity

In the previous section the phenomenon of spatial and temporal coherence has been discussed. Here it is emphasised that since buildings and other obstacles in built up areas are considered as scatterers of the signal. Whenever there is some correlation between different incoming components of the signal waves, there is lot of fluctuation of the signal in the channel thereby giving rise to decrease in the signal power to an extent that this signal power drops significantly and the channel is said to be in a deep fade. In order to reduce the effects of fading, *Diversity* is a common technique that can be applied either at BS or MS in order to achieve low BER at some cost. In wireless communication systems different diversity methods are used to achieve the better performance of a system. The most important diversity techniques identified by [62][63] are classified as (i) time diversity that is because of the doppler spread (ii) frequency diversity that occurs due to delay spread and (iii) spatial or the antenna diversity.

Since fading in the channel is mostly due to phase difference between different echoes so is most likely to find the fading on different antennas separated by few wavelengths apart completely uncorrelated and this phenomenon is called *antenna diversity*. On the other hand in case of *frequency diversity*, the information signal is transmitted simultaneously at different

frequencies. In order to achieve the best performance it is important to transmit at frequencies separated by at least coherence bandwidth of the channel. In case of *time diversity* the signal is transmitted simultaneously in different time slots, and in order to achieve the desired performance of the system these time slots are separated by at least the coherence time of the channel.

2.5.1 Time Diversity

In case of time diversity as already stated that signal carrying same information of data is transmitted simultaneously in different time slots. The uncorrelated signal is received at the receiving end only when the coherence time of the channel is equal or less than the separation in successive time slots. The time separation between replicas of transmitted signals is provided by *time interleaving* to obtain independent fades at the decoder's input. Since time-interleaving results in decoding delays, this type of technique is effective for fast fading environments where the coherence time of the channel is small for slow fading channels, large interleavers are needed and this can lead to a significant processing delay which may be intolerable for applications like voice communications.

2.5.2 Frequency Diversity

When the mobile radio channel is frequency selective then is desirable to use the frequency diversity. In frequency diversity, different frequencies are used to transmit the same information signal to the receiver. The frequencies are required to be sufficiently separate enough to ensure an independent fading associated with each frequency i.e. the separation needs to be greater than coherence bandwidth. The coherence bandwidth is different for different propagation environments. For example, in case of urban or hilly environments, the coherence bandwidth on the average is about 200 kHz and 50 kHz respectively. Therefore frequency diversity will lower the probability of error. In case of sub-urban environments, the coherence bandwidths can be in excess of 1MHz which requires a set of very widely separated carriers to fully exploit the frequency diversity. In that case this may prove to be spectrum inefficient.

2.5.3 Antenna Diversity

This type of diversity is also known as ***Space diversity*** and is implemented using multiple antennas or antenna arrays arranged together in space for transmission or reception [39]. The multiple antennas are separated physically so that signals are uncorrelated. The separation requirement varies with antenna height, propagation environment and frequency. A few

wavelengths separation is enough to obtain uncorrelated signals. The primary aim of MIMO antenna design is to reduce correlated signals by exploiting various forms of diversity that arises due to use of multiple antennas, like space diversity (spacing antennas far apart), using antennas with different or orthogonal radiation patterns. Spatial diversity involves the placing of receive antennas at such a distance from each other that it is statistically unlikely for both antennas to experience the identical channel conditions from the transmitter. The objective is that when one antenna is in a deep fade, the other antenna still has a strong signal. Since spatial diversity can be used at both the transmitter and the receiver, antennas should be spaced by more than one coherence distance apart. The *coherence distance is the minimum spatial separation of antennas for independent fading* and depends on the angular spread of multipath arriving at (or departing from) an antenna array. If antennas are close to each other then there is a high correlation of signals as compared to antennas far apart where correlation is low. Basically the diversity methods are employed to mitigate the effect of multipath fading and improve the performance of the system without extra expenditure of the power or using more of the bandwidth in wireless communication systems [62]. Therefore diversity can be regarded as an important technique to mitigate the effects of deep fading, the main aim of the diversity is that if two or more independent samples are considered in space, these samples will fade in an uncorrelated manner that is some will be severely faded while others are less attenuated. Thus the combination of various spatial samples results in reduced severity of fading. As a result, the reliability of transmission is improved.

In space diversity the signals received by the receiving end are redundant in spatial domain thereby not inducing any loss in the bandwidth efficiency like time and frequency diversity. **Antenna/space diversity** can be achieved by a variety of arrangements as shown in Figure 2.32(a) below.

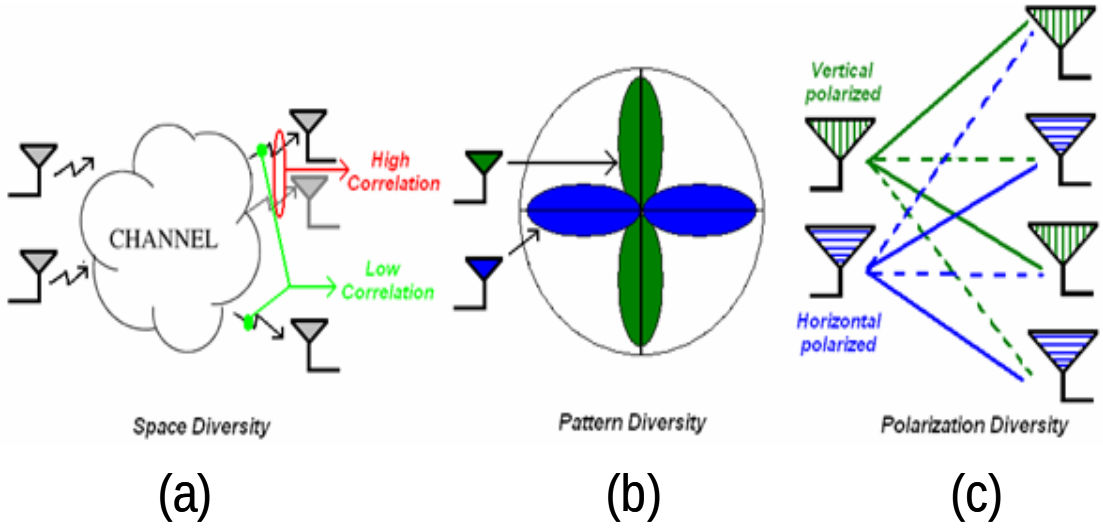

Figure 2.32: Configuration of different antenna diversities

a. Spatial

Space diversity can be classified as *transmit diversity* or *receive diversity or both* depending upon the number of antennas being used for transmission or reception. In ***receive diversity*** multiple antennas are used at receiving end to pick up independent copies of the transmitted signals. The replicas of the transmitted signal are combined to increase the overall received SNR and mitigate the multipath fading. In ***transmit diversity***; multiple antennas are used at the transmitting end. The transmitted signal is processed at the transmitting end and then passed to multiple antennas to be sent to receive antenna [80]. The behaviour of transmit diversity is different from that of receive diversity. Two difficulties with transmit diversity are (i) since the transmitted signals from multiple antennas are mixed spatially before they arrive at the receiver, additional signal processing is required at both transmitter and receiver in order to separate the received signals and exploit the diversity and (ii) the transmitter does not have the information about channel unless the information is fed back from receiver to the transmitter. Transmit/ Receive diversity provides additional diversity by increasing the number of combinations of different paths that the signal can take across the fading channel.

b. Angle

In case of angle diversity as the signals are highly scattered in space, the received signals from different directions are independent of each other. Thus two or more directional antennas can be pointed in different directions at the receiver site to provide uncorrelated replicas of the transmitted signals. Hence, this requires a number of directional antennas to select the waves arriving from narrow angle of arrival in order to achieve independent fading.

c. Polarization

In polarization diversity, horizontal and vertical polarization signals are transmitted by two different polarized antennas and received by two different polarized antennas. Different polarizations ensure that two signals are uncorrelated without placing two antennas far apart. Polarization diversity uses the property that scattering tends to de-polarize the signal and uses vertically and horizontally polarized receive antennas.

2.6 Simulation results for fading channels

2.6.1 Phase estimation of the Rayleigh Channel

In Section 2.2, the performance of a simple digital communication system in additive white Gaussian noise was obtained by computer simulation using Matlab. These results were compared with theoretical models and found to be in close agreement. In this section, computer simulations of a digital communication system are presented for the case of a fading channel. The channel model is implemented digitally using the techniques detailed in previous sections. Initially, results will be presented for a simple flat-fading mobile channel and subsequently results will be presented for the multipath channel.

Figure 2.22 showed the variation of the real and imaginary terms of the channel coefficients of a simulated narrowband channel. Equivalently, this can be expressed in terms of a magnitude and phase variation of the channel coefficient, as shown in Figure 2.33.

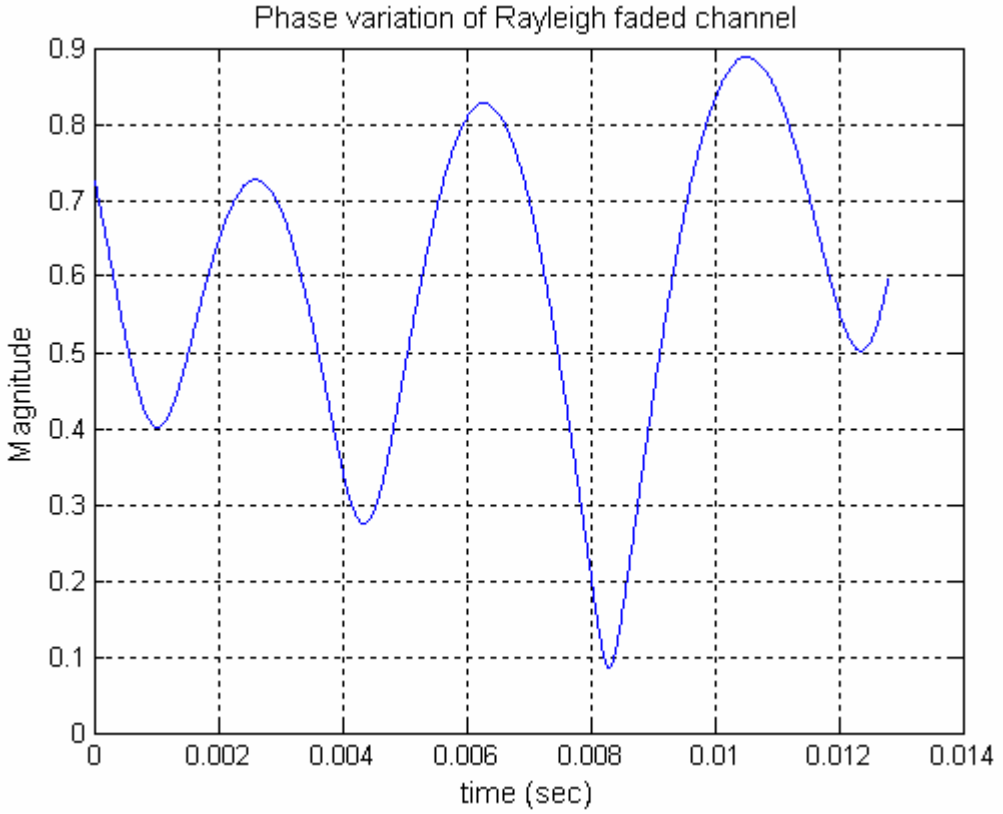

Figure 2.33: Magnitude and phase variation of the Rayleigh faded channel

Because coherent modulation schemes such as PSK and QAM rely on the receiver having perfect knowledge of the carrier phase in order to accurately demap the symbols from the received signals, the phase rotation of the signal as it passes through the channel has an

adverse effect on signal recovery. The phase shift created by the channel is random with a uniform distribution when measured over a long period compared with the channel coherence time and if this phase shift is not corrected in the receiver, it produces an average error rate of 50%. Fortunately, modern digital communication systems operate at a data rate that is considerably higher than the channel coherence time. For example, for a WiMax channel at 2.4GHz communicating with a mobile terminal operating at a speed of 20m/s (72kmph), the maximum Doppler shift is 160Hz giving a channel coherence time of ~1ms. However, for a data rate of 10Mbps, using BPSK modulation, this corresponds to the transmission of about 10,000bits. Consequently, frames of data less than 1ms effectively see a static channel. This provides the opportunity to be able to estimate the channel characteristics, especially the phase induced by the channel, so that the impairment can be corrected prior to sending the frame of data.

In this work, a simple channel estimator is used based on the transmission of a short block of data bits whose pattern is known in the receiver. The length of the block of channel estimation bits is typically one tenth of the coherence time. The sequence of bits is a pseudo random sequence. Each received signal symbol in the block is received and compared with the expected signal symbol if the channel had been perfect and from this, the phase of the channel is estimated for that symbol. This is repeated for all N symbols in the block and the estimate of the phase shift through the channel is simply the average:

$$\phi_{est} = \frac{1}{N}\sum_{i=1}^{N}\tan^{-1}\left(\frac{X_i}{X_{0_i}}\right) \tag{2.46}$$

where X_i is the actual signal sample (complex-valued) and $X_{0\mathrm{i}}$ is the expected signal sample from the *a priori* knowledge of the sequence and ϕ_{est} is the estimate of the phase rotation due to fading. For this phase phase estimator, the length of the preamble, N, determines how much averaging is employed to obtain an accurate estimate of the phase in the presence of the additive noise of the receiver. However, it will be recognised that N cannot be so long that the channel characteristics change during the phase tracking process. This estimate is then used to compensate the remaining blocks of data that are transmitted after the channel estimator block. As the period between channel estimates is allowed to lengthen, the accuracy of the phase estimate deteriorates and the errors obtained for each data block increases. The block size and the number of blocks transmitted between channel estimates were adjusted to match the coherence time of the channel to ensure that this was not a problem.

A model of a Rayleigh faded mobile channel, as described above, was implemented in Matlab that allowed a large block of channel coefficients to ensure that the channel model

could allow a very large number of symbols to be sent over the channel. Different types of channel could be implemented depending on whether flat-fading or frequency-selective channels were modelled. The various multipath channels covered by the COST 207 standard, such as urban and hilly were modelled. In this thesis, only representative results are presented in the interests of space.

Figure 2.34 shows plots of the true wrapped phase of the channel and the tracked phase over approximately 5000 data bits for a flat-fading Matlab Rayleigh channel for a mobile user moving at speed of 1.25m/sec, corresponding to a Doppler shift of 10Hz at a carrier frequency of 2.4GHz. The SNR of the received data bits, used to estimate the channel was set at 1. The data was clocked at a rate of 200kbps. In Figure 2.34(a) the preamble length, N=20 was used, whereas for Figure 2.34(b), the preamble length was 50. In these figures, the blue curve is the true phase and the green curve is the tracked phase. Only preamble blocks are sent so that the tracking of the phase is constantly being obtained. In Figure 2.34(a), the impact of the relatively short preamble length is shown by the phase errors that are immediately apparent. Particularly noticeable in (a) are the apparently random phase wraps which would cause burst errors. In contrast, Figure 2.34(b) shows the impact of using the longer preamble length which results in a higher accuracy.

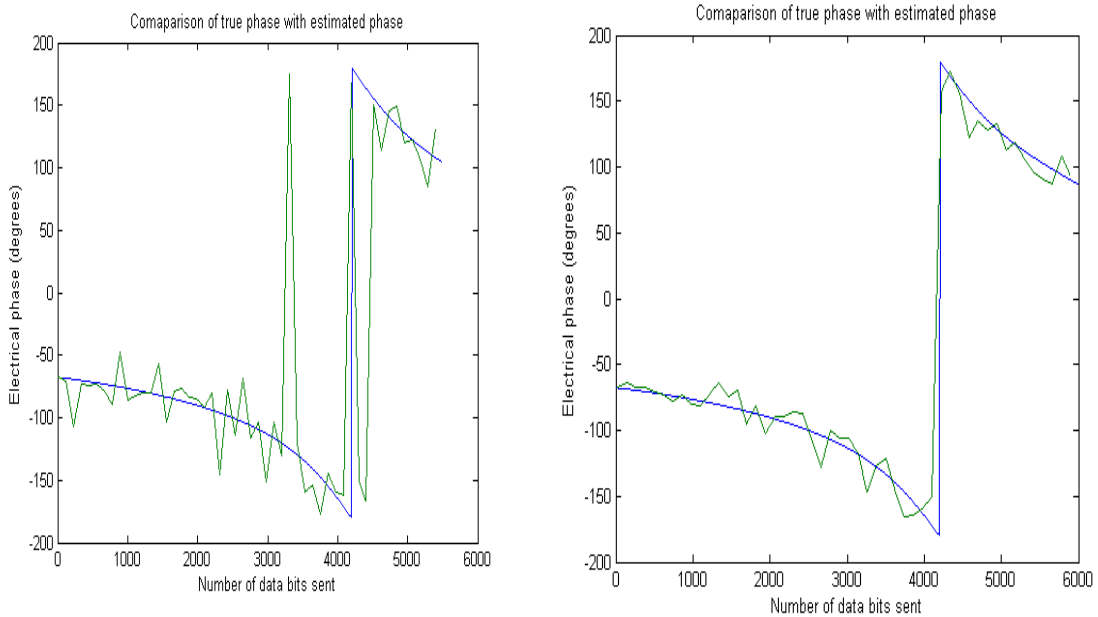

(a) (b)

Figure 2.34: Comparison of true and estimated channel phase of a typical Rayleigh faded channel

2.6.2 Phase compensation

Having estimated the phase shift, ϕ_{est}, provided by the channel it is possible to compensate for this by rotating the phase of each received symbol by $\exp(-j\phi_{est})$, i.e.

$$y_{rec}(n) = y(n)\exp(-j\phi_{est}) \tag{2.47}$$

2.6.3 Zero forcing equalizer

For the case of a multipath faded channel, the multipath echoes can cause inter-symbol interference if the delay spread is of the same duration as the data symbol, or longer. For conventional single carrier systems such as M'PSK or QAM, the usual method of compensating the effect of the delay spread is to use a delay equaliser. Here, a simple two-path equaliser is described as a model for an arbitrary length equaliser for an L-path channel.

The output of the two-path channel where the path echo is delayed by precisely one symbol period, is given by:

$$y(n) = a_1(n)x(n) + a_2(n)x(n-1) \tag{2.48}$$

where $x(n)$ is the nth complex-valued data symbol and $a_{1,2}(n)$ are the complex valued path gains for the two paths at data sample n. Coefficients $a_{1,2}(n)$ are assumed to be drawn from independent Rayleigh distributions, although for some channel models, $a_1(n)$ and $a_2(n)$ may be related. Ignoring the time variation of the path coefficients, for simplicity, from (2.48):

$$y = a_1 x + a_2 x z^{-1} = x\left(a_1 + a_2 z^{-1}\right) \tag{2.49}$$

A zero forcing equaliser, as shown in Figure 2.35, perfectly compensates for the delay distortion produced by the channel.

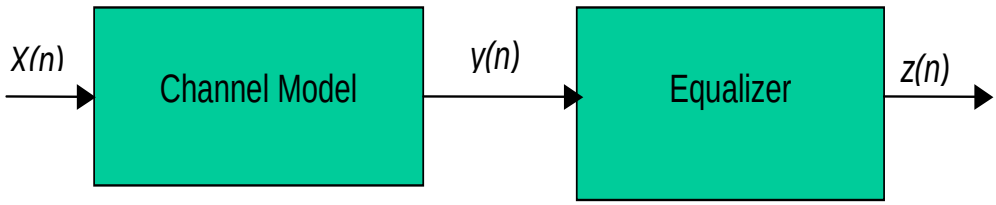

Figure 2.35: Schematic of a zero-forcing equaliser used to compensate the multipath channel

Thus, if the input to the equaliser is y, and the output is Z, an equaliser characteristic that will achieve the required distortionless output $Z = x$ is given by:

$$Z = E(z)y = x \tag{2.50}$$

i.e.

$$E(z) = \frac{Z}{y} = \frac{x}{y} = \frac{1}{\left(a_1 + a_2 z^{-1}\right)} \tag{2.51}$$

This can be implemented using an all-pole filter, in the usual way, as follows:

$$a_1 Z(n) + a_2 Z(n-1) = y(n) \tag{2.52}$$

where $y(n)$ is the current input sample, $Z(n)$ is the current output sample and $Z(n\text{-}1)$ is the previous output. This can be rearranged as:

$$Z(n)=\frac{1}{a_1}\left(y(n)-a_2Z(n-1)\right) \tag{2.53}$$

which represents the IIR digital filter implementation of the equaliser. In the general case of an L tap channel:

$$y=x\left(a_1+a_2z^{-1}+a_3z^{-2}+...+a_Lz^{-L+1}\right) \tag{2.54}$$

and the corresponding zero forcing equaliser is given by:

$$E(z)=\frac{1}{\left(a_1+a_2z^{-1}+a_3z^{-2}+...+a_Lz^{-L+1}\right)} \tag{2.55}$$

and the corresponding IIR filter is given by:

$$Z(n)=\frac{1}{a_1}\left(y(n)-a_2Z(n-1)-a_3Z(n-2)-...-a_LZ(n-L+1)\right) \tag{2.56}$$

In this work, it has been assumed that the path coefficients of the channel are known perfectly and all echo delays are an integral number of symbol periods.

The general equaliser given by (2.56) was implemented in Matlab. When initially starting the simulation, the initial state of the equaliser, [$Z(n\text{-}1)$ to $Z(n\text{-}L\text{+}1)$] = 0, but for all other situations, the state of the equaliser was stored to be used for the next frame of data.

2.6.4 Scenario 1 – Effect of Doppler

Whenever a signal is transmitted across channel it experiences a phase shift which affects the performance of the system. If that phase rotation is not compensated at receiving end then error of about 50% is expected. Therefore in simulations the phase compensation is carried out with the help of zero forcing equaliser explained in above section. In this scenario it is expected that when a user is moving characteristics of channel are changing. As a result there is phase change in the path length difference of RF waves which ultimately affects the performance of the system. For this set of results the parameters used for analysis of Doppler Effect are given in Table 2-2 below. Figure 2.36 shows the impact of the different Doppler frequencies on the BER of the simulated systems using zero forcing equalizer at the receiving end.

Parameters	***Value***	***Parameters***	***Value***
Channel model	Rayleigh	Number of paths	1,2,3,4,5
N_symb (number of payload Symbols)	1000,000	Modulation scheme	PSK
Sampling time (t_s)	0.2E-6	Modulation order (M)	2
Doppler frequency (f_d Hz)	0,10,20,30,40,50		

Table 2-2: Design Parameters for scenario-1

From the simulation result in Figure 2.36, it is seen that the bit error rate is substantially worse than for the AWGN case, as expected due to the deep, finite duration of fades because of doppler described above.

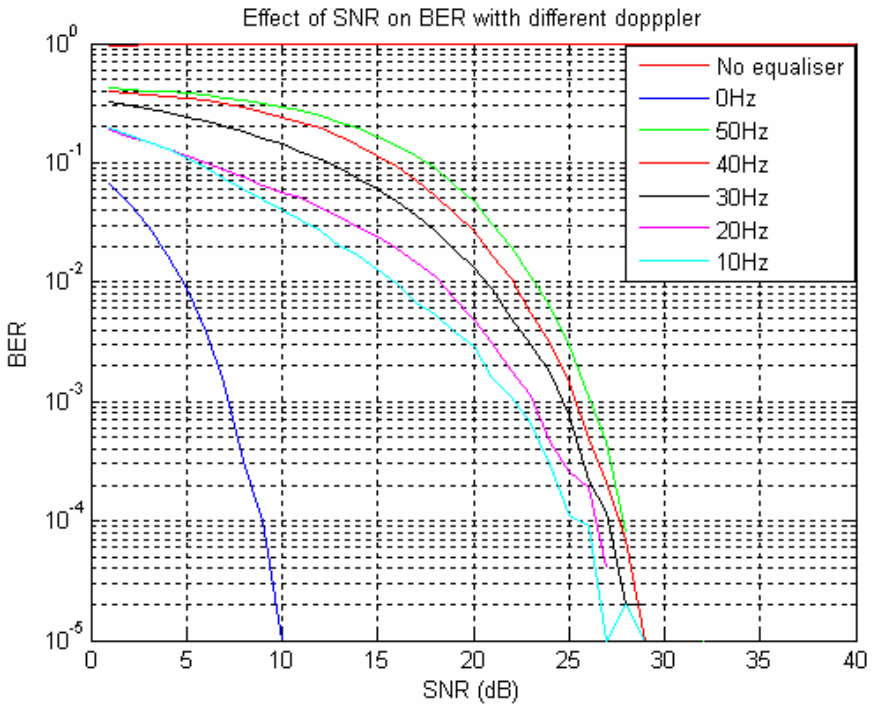

Figure 2.36: Impact of Doppler frequencies

2.6.5 Secenario-2 (Multipath frequency selective Rayleigh Channel)

Here in this case a Matlab Rayleigh channel model is implemented in frequency selective environment to investigate the performance of system in terms of BER with and without equaliser. The design parameters for simulation are given below in Table 2-3. In this case, a two and three path channels are assumed in which the path delay of the echo is considered as one symbol period. In Figure 2.37 the performance of BER for different types of channel are compared. These channels include:

a. AWGN
b. Two/Three paths Rayleigh with f_d = 10Hz, t_s = 0.2E-6, PG = [1 0.1 0.2], with symbol spaced delay but no equalizer.
c. Two/Three paths Rayleigh with f_d = 10Hz, t_s = 0.2E-6, PG = [1 0.1 0.2], with symbol spaced delay and zero forcing equalizer.

Parameters	***Value***	***Parameters***	***Value***
Channel model (frequency selective environment)	Rayleigh +AWGN	Modulation scheme	BPSK
Number of paths	1,2,3	Modulation order (M)	2
N_symb (number of payload Symbols)	40000000	Sampling time (t_s)	0.2E-6
Doppler frequency (f_d Hz)	10	PG (Path gains)	[1 0.1 0.2]
delay	Symbol spaced		

Table 2-3: Design parameters for Scenario-2

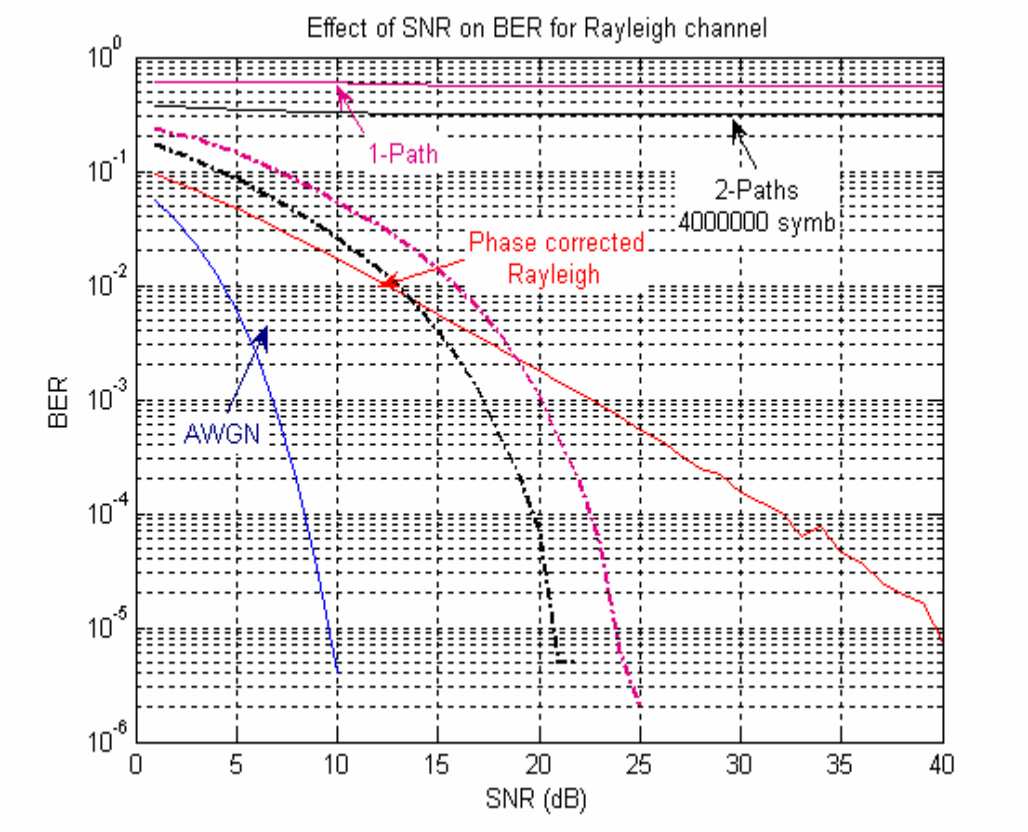

Figure 2.37: BER Probability of Rayleigh Channel with equaliser

2.6.6 Results Analysis

BER probability of binary phase shift keying (BPSK) modulated signal in additive white Gaussian (AWGN) and Rayleigh fading environment is implemented with the help of Matlab. The simulation results of both channel models are shown in Figure 2.37 above.

The graph shows that in case of true Rayleigh channel with phase correction at the receiving end, the curve is as shown in Red colour where BER of 10^{-4} is achieved at SNR of 33dBwhilst in case of an AWGN channel the BER of 10^{-4} is achieved at SNR of 8dB.

Now the comparison is made with Matlab Rayleigh channel using two and three paths. It is observed that if channel distortion is not corrected at the receiving end, then there is an error of about 50% as shown in green curve but using equaliser this error is reduced and BER performance characteristics curve is pulled down from a flat line thereby improving the BER performance significantly closer to an AWGN channel characteristics curve as shown in Figure 2.37above. Here in case of Rayleigh faded channel with two paths the BER of 10^{-4} is achieved at SNR of 10dB with equaliser at the receiving end. All theses results are subject to change every time the simulation is implemented due to random numbers generated every time and characteristics of channel changing everytime because of the doppler effect.

The curves with equaliser shown in dotted pattern as compared to the BER curves with out equaliser in solid lines are giving better performance with symbol spaced delay data

It is worth mentioning that equaliser used works perfectly and BER performance improves significantly by using Zero forcing equaliser at the receiving end.

2.7 Spatial Channel Model (SCM)

In case of the 3rd generation (3G) and beyond wireless communication systems, main emphasis in addition to the quality of the links is on the demand of higher data rate. This forms the basis for analysis of the exploitation of time, frequency, and spacatial domains. Therefore SCM channel model can be configured as MIMO system by using multiple spatially separated antenna elements both at transmitting as well as at the receiving end to improve the performance of the system based on improvement of the link reliability [39]. Foschini showed in [66] that in case of rich scattering environment the MIMO channel capacity grows linearly with the number of antenna elements at transmitting and receiving end.

The spatial channel model (SCM) developed by 3GPP is considered as a standard model and main aim of the model is to implement and evaluate the system and link level simulations for different parameters of the model in spatial domain. This channel model uses number of clusters and every cluster having number of scatterers is linked with one main path. For the purpose of simulations this channel model comprises of six main paths in every environment, where every path further consists of 20 sub-paths as described in [118]. SCM is dedicated to outdoor propagation, and defines three environments such as *suburban macro-cell, urban macro-cell and urban micro-cell.* A simplified 4x4 antenna elements geometrical representation of SCM is given in Figure 2.38. The definitions of parameters used are summarized in Table 2-5.

The SCM is a geometric model based on stochastic modelling of scatterers and is a more realistic channel model [118,119] offering three propagation scenarios such as *suburban macro-cell, urban macro-cell and urban micro-cell*. Urban micro-cellular environment is further differentiated into line of sight (LOS) and non line of sight (NLOS) propagation. SCM (Spatial Channel Model) is an example of physical channel model because physical model uses some crucial physical parameters, such as AoA and AoD to model the channel as shown in the Figure 2.38 below. In this case as the radio propagation takes place in the azimuth plane

containing the transmitter and the receiver so the channel model is regarded as two-dimensional model.

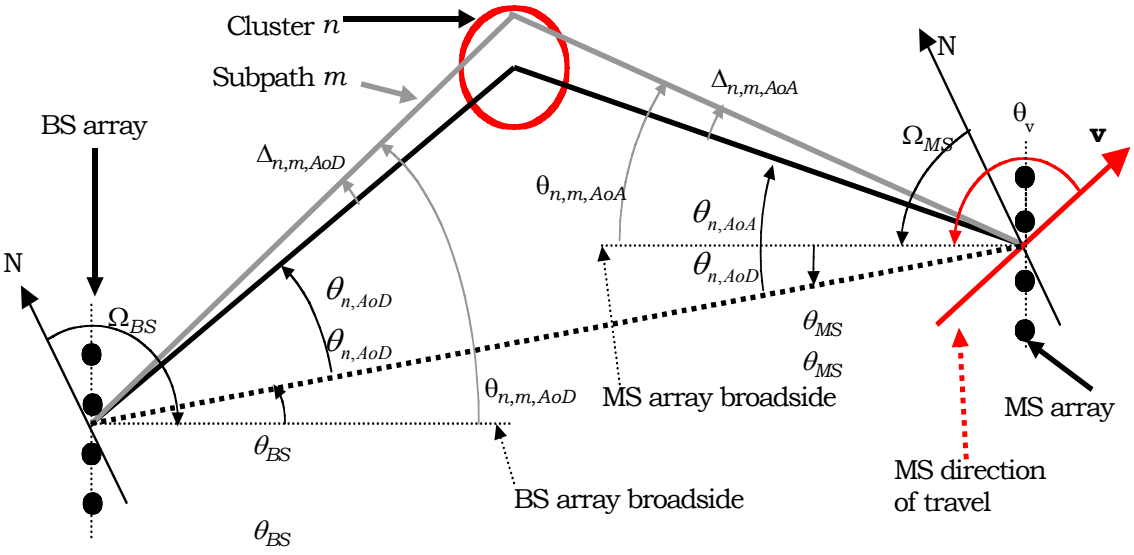

Figure 2.38: Geometric Structure of Spatial Channel Model [118]

The SCM [118] developed by the 3GPP is proposed for simulations of both link and system levels. The generation of channel coefficients involves the complexity due to generation of other parameters like AoA and AoD. In SCM each path consists of a superposition of several sub rays (subpaths) and is formed by summing together a number of rays (called subpaths). The parameters of the sub-rays have been pre-defined to produce the desired angular spread. In the SCM model, 6 paths each with 20 sub-rays are used. The physical interpretation is that each path is the last interaction with a cluster of 20 scatterers. However, it must be noted that while the cluster positions are random, the positions of scatterers within a cluster are fixed; this produces the fixed per-path angle spread (AS). Each cluster has 20 scatterers, which causes the 20 sub rays corresponding to one of the 6 rays. Each sub ray has the same delay and identical power but has different angle of arrivals and departure, which are predefined as a relative offset to the AoA and AoD of the corresponding ray. The sub rays at the MS and BS are then randomly paired.

Hence, 3GPP SCM model is a ray-based (geometry-based) model and **selection criteria** for use of SCM model was based on following:

(i) The availability of a realistic mobile radio channel model that depicts the realistic scenario for MIMO system implementations with different antenna configurations supported.

(ii) The standard SCM model defines the parameters for a wide range of outdoor environments.
(iii) The model has the ability to operate in different cellular environments like urban-micro, suburban-macro and urban-macro.
(iv) The frequency range and bandwidth that is supported by 802.20 systems.
(v) The SCM model supports the mobility factor of mobile user.
(vi) Path loss that occurs because of short-term and long-term fading.
(vii) The model exploits the spatial correlation characteristics.

A realistic mobile radio channel model (SCM) that suits the third generation standards developed by 3GPP is considered for simulation purposes in the outdoor environments like *suburban_macro, urban macro and urban micro*. The channel model is designed for up to 5MHz bandwidth and is suitable for most of the third generation systems. It can always be compared with systems having different bandwidths. The channel model is designed for multiple antenna architectures at BS and MS also. BS antenna elements are placed high above the ground level, which means that there are few or no local objects that can reflect or spread the electromagnetic waves. MS that is on the ground level may have many local objects that can reflect or block the signal between BS and MS. Different electromagnetic waves having different delays in relation to a distance traveled by each wave are generated as a result of reflection and diffraction from the scatterers. At the receiving end these waves are added constructively or destructively to create a received a signal that varies in amplitude and phase depending upon the local scatterers or movement of the MS. This phenomenon is also called the multipath propagation. Due to the different spatial position of antenna elements at transmit and receiving antenna array, different channel characteristics are obtained and hence concept of MIMO system is supported. Complexity of implementation of simulations is quite high because many parameters are required to be generated by the channel model.

The signal received at the BS consists of six time-delayed paths considered to be the main paths of the transmitted signal, where every main path comprises of another twenty subpaths. A main path corresponds to cluster of scatterers and is resolvable but the sub-paths corresponding to every main path are not resolvable. The channel impulse response in this case is given as in [118]

$$h_{u,s}(t,\tau) = \sum_{n=1}^{N} h_{u,s,n}(t)\delta(\tau - \tau_n) \tag{2.57}$$

Where $h_{u,s}$ is regarded as the channel coefficient from antenna element at BS to antenna element at the MS. In case of SCM the electromagnetic waves are transmitted from BS and

since the mobile terminal is moving the received signals frequency is affected due to the Doppler Effect. A plane wave with angle θ incident on MS is received with positive frequency shift (Doppler shift) given by

$$f_d = f\cos\theta \tag{2.58}$$

where, $f = \frac{v}{\lambda}$ and λ is regarded as the carrier wavelength of the signal and v is the velocity of MS. Signals with same angle of arrivals but with opposite moving direction will generate a negative frequency shift of the same size.

2.7.1 Calculation of Path Loss

The following are assumptions made for the *suburban macrocell* and *urban macrocell* environments [118].

a. The macrocell path loss is based on the modified COST231 Hata urban propagation model. "COST" is an abbreviation for European cooperation in the field of scientific and technical research.

$$PL(dB) = (44.9 - 6.55\log_{10}(h_{bs}))\log_{10}\left(\frac{d}{1000}\right) + 45.5 + (35.46 - 1.1h_{ms})\log_{10}(f_c) - 13.82\log_{10}(h_{bs}) + 0.7h_{ms} + C \tag{2.59}$$

Where h_{bs} is the BS antenna height in meters, h_{ms} the MS antenna height in meters, f_c the carrier frequency in MHz, d is the distance between the BS and MS in meters, and C is a constant factor (C = 0dB for suburban macro and C = 3dB for urban macro). Setting these parameters to h_{bs} = 32m, h_{ms} = 1.5m, and f_c =1900MHz, the path losses for suburban and urban macro environments are given as:

$PL = 31.5 + 35\log_{10}(d)$ and $PL = 34.5 + 35\log_{10}(d)$ respectively. The distance d is required to be at least 35m.

b) The microcell NLOS path loss is based on the COST 231 Walfish-Ikegami NLOS model with the following parameters. BS antenna height 12.5m, building height 12m, building to building distance 50m, street width 25m, MS antenna height 1.5m, orientation 30^o for all paths, and selection of metropolitan centre. With these parameters, the equation for microcell NLOS path loss simplifies to

$$PL\ (dB) = -55.9 + 38*\log10\ (d) + (24.5 + 1.5*f_c/925)*\log10\ (f_c) \tag{2.60}$$

The resulting path loss at 1900 MHz is $PL\ (dB) = 34.53 + 38*\log10\ (d)$, where d is in meters. The distance d is at least 20m and a bulk lognormal shadowing applying to all sub-paths has a standard deviation of 10dB.

c) The microcell LOS path loss is based on the COST 231 Walfish-Ikegami street canyon model with the same parameters as in the NLOS case. The path loss is given by following

$$PL\ (dB) = -35.4 + 26*\log10\ (d) + 20*\log10\ (f_c) \quad (2.61)$$

The resulting path loss at 1900 MHz is $PL\ (dB) = 30.18 + 26*\log10\ (d)$, where d is in meters. The distance d is at least 20m and a bulk lognormal shadowing applying to all sub-paths has a standard deviation of 4dB.

2.7.2 Advantages of SCM

a. It models wide-area propagation scenarios such as, suburban macro, urban macro and urban micro scenarios.

b. Both link level and system level channel models are included.

c. The system level channel model is not based on fixed temporal profiles rather statistically changing spatial and temporal domains.

d. The model is an antenna independent channel model and it allows any antenna geometry and patterns in azimuth plane.

e. Generation steps for user parameters are clearly defined.

f. Different parameters of channel model can be redefined in structures.

h. It can meet the requirements of MIMO system model.

i. The channel model can generate the coefficients for frequency selective environment.

2.7.3 Weaknesses of SCM

a. The assumption of all paths arriving/departing from the same angle in the link level channel model is non-physical. This indicates that the scatterers for the different taps are in the same direction.

b. Due to random realizations in spatial and temporal domains, large amount of simulations are needed to get enough and accurate statistics. The complete randomization of the channel modeling makes the generation procedure tedious, thus increasing the computational load tremendously.

c. Number of simulation runs is required to be taken in order to get the optimum solution.

2.7.4 Characteristics of SCM in spatial and temporal domain

The 3GPP SCM [118][120] model is basically developed for simulations and analysis of fading characteristics in three environments considered as suburban macrocell, urban macrocell, and urban microcell. A simple geometry of the model as shown in Figure 2.38 [118] dictates that one cluster comprising of number of scatterers is used for simulation puposes. The model shows different angular parameters with respect to BS and MS broad side and same parameters are given in Table 2-5. From the Figure 2.40 AoAs and AoDs of subpath corresponding to main path are represented as:

$$\theta_{n,m,AoD} = \theta_{BS} + \theta_{n,AoD} + \Delta_{n,m,AoD} \tag{2.62}$$

$$\theta_{n,m,AoA} = \theta_{MS} + \theta_{n,AoA} + \Delta_{n,m,AoA} \tag{2.63}$$

Where,

θ_{BS} is the direct angle between BS and MS.

θ_{MS} is the angle between the BS and MS.

$\theta_{n,AoD}$ is the AoD of the main path.

$\theta_{n,AoA}$ is the AoA for the main path.

$\Delta_{n,m,AoD}$ is the offset for the m^{th} subpath of the n^{th} path with respect to $\theta_{n,AoD}$.

$\Delta_{n,m,AoA}$ is the offset for the m^{th} subpath of the n^{th} path with respect to $\theta_{n,AoA}$.

Equations (2.62) and (2.63) dictate that AoD and AoA are based on three parameters which could be constant or random variables at any instant of time to define the characteristics of the channel with respect to change of the values of these three parameters. Therefore taking into account the properties of these three variable parameters the SCM provides the characteristics in spatial and temporal domains at three levels defined as system, link and cluster levels.

As far as the ***cluster*** **level** is concerned in this case the scatterers within the cluster change their positions while the cluster position remains unchanged, as a result (2.62) and (2.63) dictate that $\theta_{n,m,AoD} = \theta_{BS} + \theta_{n,AoD}$ and $\theta_{n,m,AoA} = \theta_{MS} + \theta_{n,AoA}$ are kept constant, whereas the values of offsets corresponding to scatterers within the cluster $\Delta_{n,m,AoD}$ and $\Delta_{n,m,AoA}$ are subject to distribution of scatterers. Therefore it can be stated that at cluster level the characteristics of channel model are subject to scatterers within the clusters. Different values of the offsets as dictated by 3GPP for all three environments are fixed and given below in Table 2-4 [118].

At ***link*** **level**, it is considered that there exists only one link between BS and MS. From (2.62) and (2.63) it reveals that angle between BS and MS is fixed while clusters may

have their positions changed as result θ_{BS} and θ_{MS} have constant values while $\theta_{n,AoD}$ and $\theta_{n,AoA}$ have random variables subject to position of clusters.

As far as the ***system*** **level** is considered in this case from (2.62) and (2.63) the values of θ_{BS}, θ_{MS}, $\theta_{n,AoD}$, and $\theta_{n,AoA}$ are defined as random variables. Moreover it is also emphasised that the actual values of θ_{BS} and θ_{MS} correspond to the change in positions between MS and BS.

2.7.5 Simulation of SCM

Here ***spatial channel model (SCM)*** is used in uplink case where BS receives the signal from MS and forms broad beam in the direction of wanted user while placing a null in the direction of an interferer. During each simulation run, the channel undergoes fast fading according to motion of MS. The channel state information is fed back from MS to BS and BS uses the schedulers to determine the direction of user where to transmit. The spatial channel model uses ***scm.m*** as the main function for generating channel matrix coefficients. Input structures such as ***scmparset, antparset and linkparset*** are used to define the parameters required for configuration of model are given below.

a. **scmparset**

This is an input structure used to define various parameters and main fields of this structure are as under.

(i) ***NumBsElements***, Number of BS antenna array elements.

(ii) ***NumMsElements,*** Number of MS antenna array elements.

(iii) ***Scenario,*** could be defined as **suburban_macro**, **urban_macro** or **urban_micro**.

(iv) ***Sample density***, defines the number of samples per half wavelength. It is the time sampling interval of channel. Since Doppler analysis is required so sampling density is calculated by the formula as $\left(\frac{\lambda}{2 * t_s MSvel}\right)$ where λ is wavelength in meters, t_s is sampling time and *MSvel* is the velocity of mobile user.

(v) ***BsUrbanMacroAS***, Mean angle spread of BS for urban_macro environment only and possible values considered are 8^0 or 15^0.

(vi) ***Numpaths***, Number of paths, which are changeable as defined by the user.

(vii) ***NumSubPathsPerPath***, Number of sub_paths per path, which are fixed to 20 as, is the only value, which is supported by SCM. The sub_paths offset AoA /AoD are taken from Table 6-5 below.

(viii)***CenterFrequency***, Centre frequency is set to 2.4 GHz, which affects the path loss and time sampling interval.

(ix) ***ScmOptions,*** could be none, polarized, urban_canyon or LOS.

Sub-path # (m)	***Offset for a 2 deg AS at BS (Macrocell)*** $\Delta_{n,m,AoD}$ ***(degrees)***	***Offset for a 5 deg AS at BS (Microcell)*** $\Delta_{n,m,AoD}$ ***(degrees)***	***Offset for a 35 deg AS at MS*** $\Delta_{n,m,AoA}$ ***(degrees)***
1, 2	± 0.0894	± 0.2236	± 1.5649
3, 4	± 0.2826	± 0.7064	± 4.9447
5, 6	± 0.4984	± 1.2461	± 8.7224
7, 8	± 0.7431	± 1.8578	± 13.0045
9, 10	± 1.0257	± 2.5642	± 17.9492
11, 12	± 1.3594	± 3.3986	± 23.7899
13, 14	± 1.7688	± 4.4220	± 30.9538
15, 16	± 2.2961	± 5.7403	± 40.1824
17, 18	± 3.0389	± 7.5974	± 53.1816
19, 20	± 4.3101	± 10.7753	± 75.4274

Table 2-4: Sub-Path AOD and AOA offsets (SCM Model)

b. antparset

This is also an input structure, which defines the antenna's parameters configuration for spatial channel model. In this case only linear arrays are supported and antenna pattern doesn't have to be identical. The main fields of this input structure are

(i) ***BsGainPattern***, which is set to ''1'' assuming that all elements have uniform gain.

(ii) ***BsAnglesAzimuth***, is a vector containing azimuth angles for BS antenna field pattern values. It is given in degrees over the range of –180 to +180 degrees.

(iii) ***BsElementPosition***, distance between antenna elements is set to 0.5.

(iv) ***MsGainPattern***, which is set to ''1'' assuming that all elements have uniform gain.

(v) ***MsAnglesAzimuth***, is a vector containing azimuth angles for MS antenna field pattern values given in degrees over the range of –180 to +180 degrees

(vi) ***MsElementPosition***, Uniform spacing of 0.5 is considered for antenna elements at MS linear array.

c. linkparset.

This is again an input structure where all parameters are vectors of length *'K'* and *K* defines the number of links. The main fields of this input structure are

(i) ***MsBsDistance*** is the distance in meters between MS and BS. Here users are uniformly distributed in a circular cell over a distance of 35 to 500 m.

(ii) ***ThetaBs*** is the angle of arrival of signal in degrees.

(iii) ***ThetaMs*** is the angle of MS in degrees.

(iv) ***MsVelocity*** is the velocity of MS in m/sec.

(v) ***MsDirection*** is the direction of MS with respect to Broadside of MS antenna array.

(vi) ***MsHeight*** is the height of MS set to 1.5 meters.

(vii) ***BsHeight*** is the height of BS set to 32 meters.

(viii)***MsNumber*** indicates the number of MS for each simulated link. It is a vector of 1 to *K*, where *K* is the number of links.

The output argument ''*H*'' is a 5-D array and size (*H)* = [*U S N T K*] where

U = Number of MS antenna elements.

S = Number of BS antenna elements.

N = Number of paths.

T = Number of time samples per path.

K = Number of links or Users.

When all the parameters are defined as stated above then the channel coefficients between MS and BS are generated subject to fading characteristics of the channel that is dictated by the movement of MS

2.7.6 Generation of channel matrix

The aim of the model is to generate channel coefficients between BS and MS derived from summation of directional plane waves impinging on the receive antenna elements. The process of generation of channel coefficients is as defined in [118]:

a. Specify the ***environment*** to be implemented.

b. Obtain the ***parameters*** associated with particular environment.

c. Generate the ***channel coefficients*** based on these parameters.

If there are S elements at BS and U elements at MS then the channel coefficients matrix for one of the six paths is given as $\mathbf{H}_n(t)$, where the channel impulse response between BS and MS for n[th] path as given in [118] is represented as:

$$h_{u,s.n}(t) = \sqrt{\frac{P_n \sigma_{SF}}{M}} \sum_{m=1}^{M} \begin{bmatrix} \sqrt{G_{BS}(\theta_{n,m,AoD})} \exp\left(j\left[kd_s \sin(\theta_{n,m,AoD}) + \phi_{n,m}\right]\right) \times \\ \sqrt{G_{MS}(\theta_{n,m,AoA})} \exp\left(jkd_u \sin(\theta_{n,m,AoA}) \times \right. \\ \left. \exp\left(jk\|v\|\cos(\theta_{n,m,AoA} - \theta_v)t\right)\right. \end{bmatrix} \tag{2.64}$$

Here it is assumed that that the antenna gains of each element of the antenna array is unity and given as $G_{BS}(\theta_{n,m,AOD}) = G_{MS}(\theta_{n,m,AOA}) = 1$.

where,

P_n = Power of n^{th} path.

M = Number of sub_paths per path.

σ_{SF} = log normal shadow fading.

θ_{nmAOD} = Angle of departure for m^{th} subpath of n^{th} path.

θ_{nmAOA} = Angle of arrival for m^{th} subpath of n^{th} path.

$G_{BS}(\theta_{nmAOD})$ = BS antenna gain of each array element

$G_{MS}(\theta_{nmAOA})$ = MS antenna gain of each array element

j = square root of –1

$k = 2\pi / \lambda$, where k is the wave number and λ is the carrier wavelength in meter

d_s = distance of BS antenna element from reference element in meters

d_u = distance of MS antenna element from reference element in meters

ϕ_{nm} = phase of m^{th} subpath of the n^{th} path.

$\|\mathbf{v}\|$ = Magnitude of MS velocity vector

θ_v = Angle of MS velocity vector

Ω_{BS}	BS antenna array orientation
θ_{BS}	LOS angle of departure between BS and MS
$\theta_{n,AoD}$	Angle of departure of n^{th} path corresponding to line of sight
$\Delta_{n,m,AoD}$	Off set for m^{th} sub-path of n^{th} path with respect to $\theta_{n,AoD}$
$\theta_{n,m,AoD}$	Angle of departure of m^{th} sub-path of n^{th}.
Ω_{MS}	MS antenna array orientation
θ_{MS}	Angle between BS and MS
$\theta_{n,AoA}$	Angle of arrival of n^{th} path corresponding to line of sight
$\Delta_{n,m,AoA}$	Off set for m^{th} sub-path of n^{th} path with respect to $\theta_{n,AoA}$
$\theta_{n,m,AoA}$	Angle of arrival of m^{th} sub-path of n^{th} path
v	MS velocity vector
θ_v	Angle of velocity vector

Table 2-5: Angular parameters of SCM

2.7.7 Scenario-1 (SCM implementation)

Here in this scenario SCM is implemeted as per procedure described in above sections and parameters used for simulation are provided in Table 2-6 below. Aim of the simulation is to compare the performance of Matlab Rayleigh and Spatial channel models in frequency selective environment using zero forcing equaliser.

Parameters	***Value***	***Parameters***	***Value***
Channel models	Matlab Rayleigh, SCM and AWGN	Modulation scheme	PSK
Number of paths	1,2,3,4,5	Modulation order (*M*)	2
N_symb (number of payload Symbols)	1000,000	PG (Path gains)	[1 0.2,0.3]
Sampling time (t_s)	0.2E-6	Delay	Symbol spaced
Doppler frequency (f_d Hz)	10		

Table 2-6: Design parameters for comparison of channels (Scenario-1)

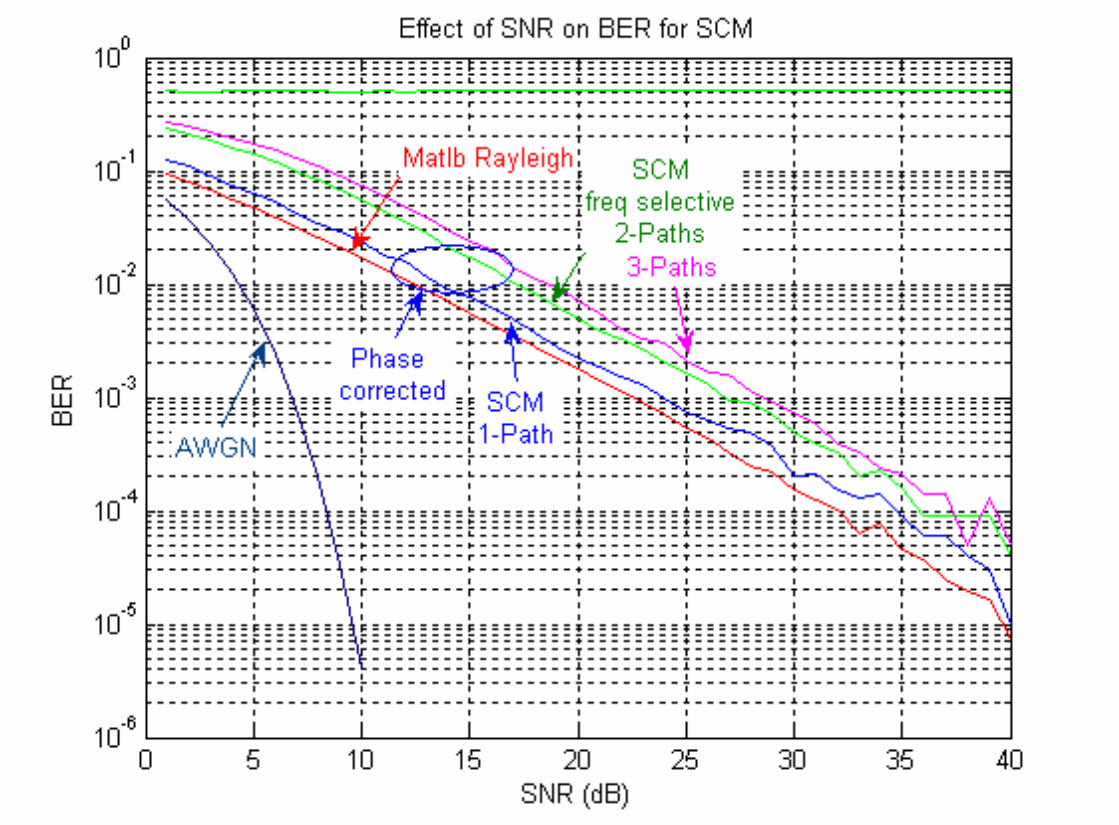

Figure 2.39: Comparison of Matlab Rayleigh and SCM

2.7.8 Results Analysis

BER probability of binary phase shift keying (BPSK) modulated signal in additive white Gaussian (AWGN), Mattlab Rayleigh and Spatial channel models frequency selectve fading environment is demonstrated in Matlab. The simulation results of the channel models are shown in Figure 2.39 above.

It is observed that BER between transmitted and received signal in case of AWGN channel model is around 10^{-4} at SNR of 8dB, whereas in case of Matlab Rayleigh fading channel BER of 10^{-4} at SNR of 33dB with five paths is achieved with zero forcing equaliser at the receiving end that compensates the distortion induced in the channel.

From simulation results it is observed that if channel distortion is not corrected at the receiving end, then there is an error of about 50% but using equaliser this error is reduced and BER performance characteristics curve is pulled down from a flat line thereby improving the performance significantly.

Similarly in case of spatial channel model the BER of 10^{-4} is achieved with one path at SNR of 35dB, while using same channel with two and three paths in frequency selective environment provides BER of 10^{-4} at SNR of 37dB and 40 dB respectively with zero forcing equaliser used at the receiving end. There is some degradation in the BER performance when

more number of paths are considered because of delay spread that induces the inter symbol interference.

This verifies SCM is more frequency selective than Matlab Rayleigh channel and the same is compensated by Zero forcing equaliser that perfectly works well by pulling the characteristic curve from flat line.

2.8 Matlab Rayleigh and SCM channel response

In case of complex scattering environment, signal propagating through a channel is affected by reflection, refraction, diffraction and scattering etc which gives rise to fading and path loss. Here the time variation of the channel in such an environment is quite complicated and time varying impulse response of the channels leading to time varying frequency selective channel response for Rayleigh and SCM channel models, simulated in Matlab are as shown in Figure 2.40 (c) and (d) below respectively. Figure 2.40(a) and (b) represent the channels impulse response in frequency domain with sampling rate of 0.2μsec and mobile user moving with a velocity of about 63.720 km/h corresponding to a Doppler of about 141.6Hz. Both channels implemented with multipath effect of 6 paths per channel each. From the channel response different parameters like path loss, delay spread, Doppler spread and frequency etc can be extracted. The rate of change of channel amplitude is related to time and frequency of the signal for different values of the delay and Doppler spread. From the simulation results it reveals that with increase in Doppler spread the channel characteristics also vary. Therefore in case of mobile radio systems, the received signal amplitude depends on both frequency and location (or time) of a mobile. Moreover from the simulation results it reveals that there is quite randomness observed in Matlab Rayleigh channel as shown in Figure 2.40(c) but in the of Spatial channel model it looks as if the scatterers are located in the same line due to which less scattering in observed.

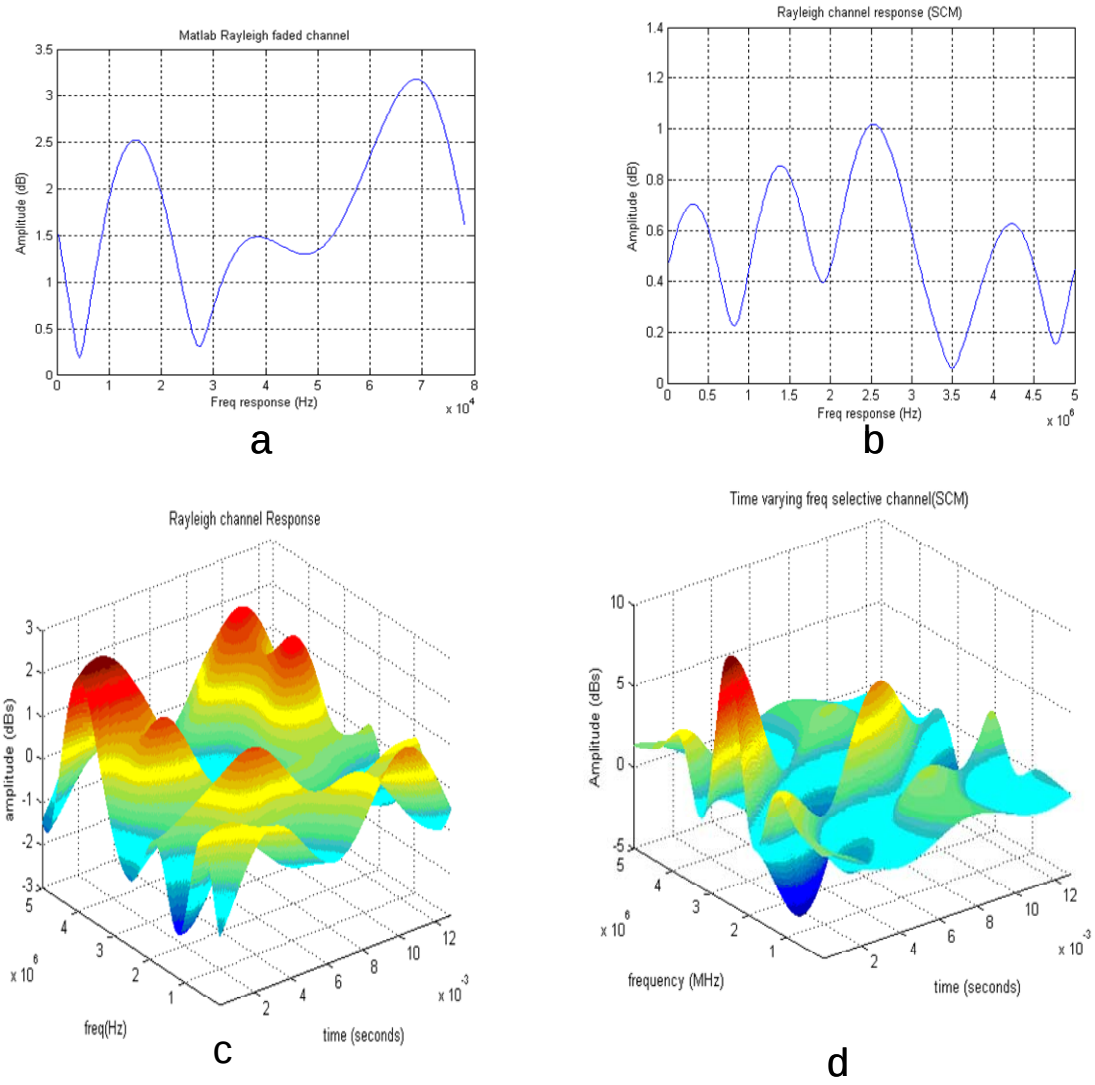

Figure 2.40: Channel response of SCM and Rayleigh channel Models

2.9 Summary

In this chapter the mechanism of transmission through the mobile radio channel, modelling digital communication system, especially the wireless channel and computer simulations of digital communication systems has been described. It was shown with the help of simulations how the multipath phenomenon severely degrades the quality of the transmitted signal and affects the performance of a digital communication link. The worst scenario of a mobile radio channel is when there is no line of sight in which case the channel is considered to be a Rayleigh faded channel. The multipath effect is worsened when the mobile user is in motion due to the Doppler spreading which makes it difficult for the receiver to track the carrier frequency of the transmitted signal. In wideband systems, the phenomenon of multipath gives rise to intersymbol interference and imposes a constraint on the maximum transmission rate thereby reducing the performance of a system in terms of BER. Intersymbol interference can be reduced by the use of channel equalisation and different techniques like error correction coding and interleaving may be used to achieve the acceptable performance of communication link in terms of bit error rate. A deterministic and stochastic model of digital communication system has been described in this chapter. The concept of line of sight and plane earth propagation is also described and path loss variation has been described as to how does it vary with increase in distance between transmitter and receiver. A channel is said to be a narrowband when the bandwidth of the transmitting signal is less than the coherence bandwidth of the channel; otherwise it is referred to as wideband. The signal fading resulting from the distance travelled by the signal and the multipath effect may be divided into two categories, namely, fast fading and slow fading. Fast fading refers to the instantaneous changes in the signal's amplitude and may be approximated to be Rician, if line of sight exists otherwise Rayleigh distributed in case of non line of sight environment. Slow fading, on the other hand, refers to the variations in the average signal's field strength and may be approximated to have a Log normal distribution.

The COST 207 channel's delay profiles for a typical urban and hilly terrain environments have been outlined for a discrete GWSSUS tapped delay line channel model. The time varying properties of the channel is modelled by generating time varying complex multiplicative coefficients. These are produced by using pairs of uncorrelated AWGN generators, where each pair represents the real and imaginary part of one coefficient. The Doppler Effect is simulated by passing the coefficients though a low-pass filter with a frequency response defined by the Doppler spectrum.

A number of techniques like equalisation, convolutional coding, multicarrier modulation and interleaving for combating the channel's imposed limitations have been

briefly reviewed and demonstrated with the help of simulation results that there is significant improvement in performance of a system by using convolutional encoder with different constraint lengths.

Spatial channel model has been described in detail along with factors that form the basis of selection of the channel model. This is the model that is considered as realistic physical channel model as it uses physical channel parameters like AoA, AoD to model the channel. The channel model has the capability of configuring the system with multiple antenna elements at transmitting and receiving end having applicability in different outdoor propagation environments like urban micro, suburban macro and urban macro environments, where urban micro environment is further divided into LOS and NLOS environment. The path loss models used in these environments are based on COST231 Hata urban for urban macro/suburban macro environments while walfisch Ikegami model is used for urban micro (NLOS) environment.

Chapter-3

3 The Use of the Antenna Array in Communications

3.1 Introduction

The basic antenna array comprises of several antenna elements such as dipoles, monopoles or patch antenna elements organized generally in 1D or 2D space with a regular spacing. Very simple examples of phased array antennas are the uniform linear array (ULA) and the uniform circular array (UCA), as shown schematically in Figure 3.1 for the case of vertically polarised dipoles. Often, but not always, these individual elements may be electrically connected together to provide a single output from the entire array. In this case, although each dipole element is *omni-directional* in azimuth, depending upon how the signals received by each antenna element are connected, the antenna array may well be *highly directional* so that signals arriving from one direction are received preferentially to signals arriving from a different direction [30]. It is this directional behaviour of the antenna array that makes them so useful, and this aspect of the antenna array is discussed in this chapter. In other cases, each antenna element in the array may be fed directly to an individual receiver. In this case the array is then said to provide *spatial diversity*. The use of antenna arrays to provide spatial diversity is discussed in Chapter 6. Meanwhile delay spread, which occurs in multipath propagation environments when a desired signal coming from different directions is delayed due to difference in travel distances, can be reduced with an antenna array that is capable of forming beams in certain directions and nulls in other directions thereby canceling some of the delayed arrivals. The most important feature of smart antenna system is its capability to cancel the co-channel interference, which may be caused by radiation from other cells that use the same set of channel frequencies. Hence co-channel interference in the transmitting mode is reduced by focusing the directive beam in the direction of desired user while nulls in the direction of other receivers [1]. In case of receiving mode this co-channel interference is reduced by knowing the direction of source of the signal and utilizing the interference cancellation. The capacity of the system can be improved by reducing the CCI with the help of adaptive nulling. In case of SDMA adaptive nulling is used to isolate the mobile users operating in the same cell at the same time with same frequency and forming one beam in direction of one user while placing a null in the direction of other unwanted users.

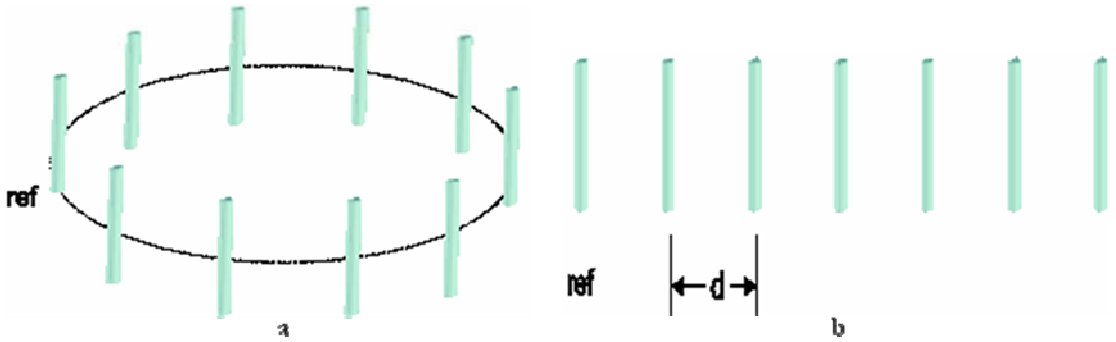

Figure 3.1: Schematic of an antenna array: (a) uniform circular array (b) uniform linear array

3.2 Uniform Linear Array

The directional behaviour of an antenna array arises because each element, relative to the reference element, is shifted in space creating a time-delay relative to the reference element. For narrowband signals [5], this time-delay can be represented as a *phase-shift*. At some points in space, the phase of signals transmitted from element 1 may perfectly reinforce with signals from element 2 (for example), but may destructively interfere at other points in space. Consequently, the received signal when multiple antenna elements are connected is apparently stronger in some directions than others.

Assume that a continuous-time signal, $x_m(t)$, is received at the m^{th} element of a uniform linear array (ULA), for example. Let this signal now be sampled by a digital receiver so that $x_m(n)$ is the discrete-time equivalent of the signal at the m^{th} element and n represents the n^{th} sample of the signal. The discrete-time signals at each element of the entire ULA, may be written as a column vector of the individual element signals [5]:

$$\mathbf{x}(n) = \begin{bmatrix} x_1(n) & x_2(n) & \cdots & x_M(n) \end{bmatrix}^T \tag{3.1}$$

Where, M represents the number of antenna elements in the array and T represents the transposition of the vector. A single observation of this signal vector given by (3.1) is known as an *array snapshot*. It is usually assumed that the signal source, $x(t)$, is a modulated sinusoidal carrier:

$$x(t) = A(t)\cos(2\pi f_c(t) + \alpha(t)) \tag{3.2}$$

where $A(t)$ is the time-varying amplitude, representative of amplitude modulation (AM), amplitude shift keying (ASK) or quadrature amplitude modulation (QAM), $f_c(t)$ is a time-varying carrier frequency representative of frequency modulation (FM) or frequency shift

keying (FSK) and $\alpha(t)$ is a time-varying phase shift representative of phase modulation (PM) or QAM.

3.3 Narrowband assumption

A key assumption, often made when considering the use of antenna arrays for communications use, is that the modulated signal of interest is narrowband where the bandwidth of the signal, in comparison to the carrier frequency, is extremely small[3]. This critical simplifying assumption means that the *time delay*, τ, due to the propagation of the wave between the elements of the array can be represented as a *phase shift*, θ, of the carrier signal:

$$\tau = \frac{\theta}{2\pi f_c} = \frac{\lambda\theta}{2\pi c} \tag{3.3}$$

However, when the antenna array is used for wideband applications, this approximation does not hold and the time delay, τ, must be handled explicitly. This complicates the design of the antenna considerably. In order to simplify the analysis, a narrowband assumption will be made throughout.

3.4 Array snapshot

To illustrate how the array snapshot is arrived at in practice; assume that the signal of interest arrives from a distant single point-source so that it can be assumed that the wavefront from the source is flat. It is also assumed that the overall length of the antenna array (i.e. its *aperture*) is sufficiently small that the propagation loss experienced by the wavefront as it propagates along the length of the array is negligible. The wavefront impinges on the antenna array at an angle of arrival (AoA), ϕ, as shown in Figure 3.2. Because of the inter-element spacing, d, there is a time delay between the arrival of the wavefront at consecutive elements of:

$$\tau(\phi) = \frac{d\sin\phi}{c} \tag{3.4}$$

where c is the velocity of light. By choosing element 1 as the reference element, this delay, relative to element 1, increases as the wavefront moves along the antenna array to element m:

[3] typically less than 1%

$$\tau_m(\phi) = (m-1)\frac{d\sin\phi}{c} \tag{3.5}$$

Using the narrowband assumption, this time-delay can be represented as an equivalent electrical phase shift progression along the array [5]:

$$\theta_m(\phi) = (m-1)\frac{2\pi d\sin\phi}{\lambda} \tag{3.6}$$

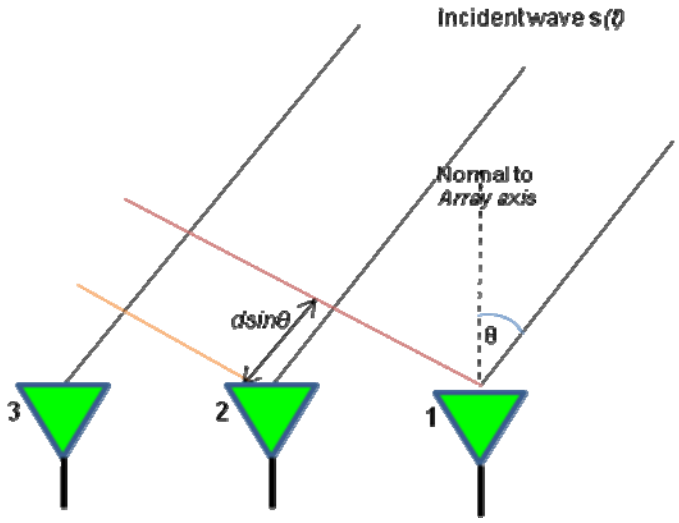

Figure 3.2: Schematic of a plane wave impinging on ULA

As a result, the n^{th} array snapshot can be written as:

$$\begin{aligned}\mathbf{x}(n) &= x_1(n)\left[e^0 \quad e^{-j\theta_2} \quad \cdots \quad e^{-j\theta_M}\right]^T \\ &= x_1(n)\left[1 \quad e^{-j2\pi d\sin\phi/\lambda} \quad \cdots \quad e^{-j2\pi(M-1)d\sin\phi/\lambda}\right]^T\end{aligned} \tag{3.7}$$

where $x_1(n)$ is the n^{th} sample of the received signal at element 1.

It is generally convenient to represent the array snapshot in terms of the signal of interest and an antenna-dependent *space factor*, $\mathbf{v}(\phi)$, that accounts for the time-delay between the signal wavefront and each of the elements at the desired angle of arrival:

$$\mathbf{x}(n) = \sqrt{M}\,\mathbf{v}(\phi)x_1(n) \tag{3.8}$$

where, for the ULA defined above, the space factor is given by [5]:

$$\begin{aligned}\mathbf{v}(\phi) &= \frac{1}{\sqrt{M}}\begin{bmatrix}1 & e^{-j\theta} & \cdots & e^{-j(M-1)\theta}\end{bmatrix}^T \\ &= \frac{1}{\sqrt{M}}\begin{bmatrix}1 & e^{-j2\pi d\sin\phi/\lambda} & \cdots & e^{-j2\pi(M-1)d\sin\phi/\lambda}\end{bmatrix}^T\end{aligned} \tag{3.9}$$

This is also known as the *array response vector*.

The reason why the factor $\sqrt{M}$ appears in (3.8) and is perfectly compensated by the factor $\frac{1}{\sqrt{M}}$ that appears in (3.9) is because it is usual to normalize the array response vector so that it provides the antenna array with unit gain in the wanted direction ϕ (i.e. $\|\mathbf{v}(\phi)\|^2 = \mathbf{v}^H(\phi)\mathbf{v}(\phi) = 1$). Equation 3.8 is a convenient representation because the same basic formulation for the array snapshot holds just as well for any other type of array, including the uniform circular array. This is accommodated by using an array factor appropriate for the circular array given in [18] as:

$$AF\ (\phi,\theta) = \sum_{m=1}^{M} x_m(n) e^{j\alpha_m} e^{j[2\pi d\ \sin\ \cos\ (\theta-\theta_m)/\lambda]} \tag{3.10}$$

Where ϕ is the angle of the distant source to the centreline of the array, $x_m(n)$ is the signal sample of the m^{th} element located at $\theta = \theta_m$ around the circumference of the circle, α_m is the associated phase excitation relative to the array centre located at the coordinate origin, and *d* is the radial distance of each element from the origin. To create the array response vector, (3.10) is evaluated at each array element in turn and the values placed in the array, as for (3.7).

3.5 Spatial Sampling using the Antenna Array

In the previous section the view was taken that the wavefront of the distant source propagated past each antenna element and was otherwise unchanged except for being delayed in time. An alternative (and equivalent) view is that each element of the antenna array *samples* the propagating wave in space and that a ULA provides linear spatial sampling. Consequently, in an equivalent way to considering the sampling frequency, $f_s = 1/T_s$ of a sampled time-varying signal sampled with a period, T_s, we can consider the spatial sampling frequency of a spatially varying signal sampled by an antenna array with an element spacing d to be $U_s = 1/d$. As with temporal signals, the phase progression for uniform spatial sampling is as

a consequence of the frequency of the signal. In the case of a spatially propagating signal, this frequency is given by:

$$U = \frac{\sin\phi}{\lambda} \tag{3.11}$$

which can be thought of as the *spatial frequency*. The *normalized spatial frequency* is then given by:

$$u = \frac{U}{U_s} = \frac{d\sin\phi}{\lambda} \tag{3.12}$$

This means that the array response vector can be written in terms of the normalized spatial (sampling) frequency as:

$$\mathbf{v}(\phi) = \mathbf{v}(u) = \frac{1}{\sqrt{M}}\begin{bmatrix}1 & e^{-j2\pi u} & \cdots & e^{-j2\pi(M-1)u}\end{bmatrix}^T \tag{3.13}$$

There is a particularly interesting reason for drawing this analogy with temporal sampling. It will be remembered from Shannon's Theorem that discrete-time signals can suffer from *aliasing* if the normalized sampling frequency, $F_s = f_s / f_{\max} \geq 2$, where $f_{\max}$ is the maximum frequency component in the signal. This also happens with spatial sampling and to avoid spatial aliasing, $-1/2 \leq u \leq 1/2$ and the full range of possible 'unambiguous' angles from $-90^\circ \leq \phi \leq 90^\circ$ is only possible if the sensor spacing is:

$$d = \frac{\lambda}{2} \tag{3.14}$$

and this sets the requirement for an 'unambiguous' antenna array[4].

3.6 Conventional Spatial Filtering:- Beamforming

In order for the antenna array to provide a directional radiation pattern, it is necessary to vectorially combine the signals at each element in some way. This is achieved in a beamforming network (BFN) [24]. The BFN may simply add the signals together using a summing junction, or it may weight, phase shift or delay each signal prior to summing the

[4] Note that the ULA is always ambiguous with respect to the North and South direction because the path length difference is the same in either case.

signals. Because the BFN can take many different forms, the BFN critically affects the spatial response of the antenna array for the same array response vector. The beamformer produces its output by forming a weighted combination of the array snapshot, given by [17]:

$$y(n) = \sum_{m=1}^{M} w_m^* x_m(n) = \mathbf{w}^H \mathbf{x}(n) \tag{3.15}$$

where,

$$\mathbf{w} = \begin{bmatrix} w_1 & w_2 & \cdots & w_M \end{bmatrix}^T \tag{3.16}$$

is the column vector of the beamforming weights, the operator * represents complex conjugation and the operator H represents the Hermitian operation (i.e. conjugate transpose).

3.7 Beamformer weights – a practical note

The weights of the beamformer are generally complex valued in order to provide the necessary compensating phase shift to match (or at least modify) the phase shift produced by the array response vector. Often, optimum performance of the beamformer relies on these complex valued weights being very accurate. Whilst this is straightforward in computer baseband simulations where complex valued, double precision, numbers are supported, it is less easy in real systems, especially if the antenna array is adaptive and the weights must change automatically in response to the received signal. Ideally, since the purpose of the complex weights in a narrowband beamformer is to create *phase shifts* at the RF frequency, these should be implemented by using phase shifters such as switched-length delay-lines or digital phase shifter. Using switched-length delay-lines and digital phase shifters *discretises* the phase shifts. In the interests of economy, the number of available switched delays may be very limited and the beam response may be compromised as a result.

Switched delay-lines are used for wideband antenna for reasons given earlier.

An alternative method of implementing a phase shift when the beamformer operates directly at the RF carrier frequency is to split the received signal into I (real) and Q (imaginary) channels that are 90° apart in phase using a fixed 90° phase shifter. Having now created I and Q channels, real coefficients are used for each I and Q channel[5]. Also, it is important to realize that in order to remove the need for a bank of 2*M* RF amplifiers, the weight vectors should all

[5] It will be seen that this is identical to using complex numbers

be less than 1 so that they can be implemented using (variable) attenuators. This is actually a very important constraint on the design of an adaptive antenna array. In some circumstances, where it is impossible to provide the necessary beam pattern without using attenuators for the weights, active antenna elements must be used where each radiating element is powered by its own RF source within the beamforming network. Because the signal is assumed to be narrowband, it is relatively straight forward to implement a fixed 90° phase shifter over a narrow range of frequencies using either an RC network or a time delay where the delay $\tau_{delay} = 1/4f_c$. However, it must be remembered that one of these networks must be used for each complex weight. When the signal is wideband it becomes much more difficult to implement a wideband 90° phase shifter.

3.8 Beam response

The performance of a beamformer for a given weight vector **w** is its response as a function of the azimuth angle, ϕ, known as the *beam response*. This angular response is found by applying the beamformer, **w**, to a set of array response vectors from all possible angles in the range $-90^\circ \le \phi \le 90^\circ$ to give:

$$C(\phi) = \mathbf{w}^H \mathbf{v}(\phi) \tag{3.17}$$

The *beampattern* is given by $|C(\phi)|^2$. Alternatively, the beampattern can be computed as a function of the normalized spatial frequency *u*. Whichever method is used, the beampattern is obtained at each *look angle*, ϕ, by evaluating the array response vector in that direction.

It is also worth commenting that as well as the beam response, which is the directional response of the antenna given its array response vector and its BFN weight vector, another common term is the *steered response*. The steered response is the actual response of the array to point-source signals distributed around the array, as the array is steered through all possible angles.

It is clear from (3.17) that the beam response (and hence beampattern) is continuous in azimuth angle. In practice, the beam pattern is only plotted at a finite number of points. Recall from (3.13) the form of $\mathbf{v}(\phi)$. It is clear that this is identical in structure to the discrete-time Fourier transform (DTFT) used in spectrum analysis. The DTFT uses a finite number of discrete time samples of the signal and produces a continuous frequency spectrum. Here, a finite number of spatial samples produce a continuous far-field beampattern. The DTFT is

often approximated by the discrete Fourier transform (DFT) which provides the spectrum (or beampattern) at a finite number of points.

A problem with using the standard DFT is that the number of samples defining the output (i.e. the beampattern) must be the same as the number of samples defining the input (i.e. the number of antenna elements). When the number of elements is very small (say 5 or so) this allows only five look angles to be defined over the range: $-90^\circ \le \phi \le 90^\circ$. Also the DFT algorithm is computationally inefficient and it is generally replaced by the fast Fourier transform (FFT). This is much more computationally efficient[6] but it has the further restriction that the number of points that can be used is limited to $N = 2^p$, where p is an integer.

When the FFT is used in spectral estimation the number of input samples can be made arbitrarily large in order to obtain a sufficiently high resolution in the spectrum, and so the restrictions of the FFT and the DFT are generally not a problem. However, when used to compute the beam pattern of an antenna array, where the number of antenna elements is very low, this is a real problem that must be resolved using the *zero-padded FFT*.

3.9 Use of the zero-padded FFT

For a ULA with $d = \lambda/2$ element spacing, the beampattern as a function of u can be computed quite efficiently using the fast Fourier transform (FFT) in the range $-1/2 \le u \le 1/2$ at N discrete points in spatial frequency, u (or, equivalently, at N different look angles, ϕ). If the approach is taken to obtain the spatial frequency spectrum, this can be converted into the correct azimuth angle using the transformation:

$$\phi = \sin^{-1}\frac{\lambda}{d}u \tag{3.18}$$

over the range of azimuth angles $-90^\circ \le \phi \le 90^\circ$. However, as discussed above, when using the FFT algorithm, the number of look angles N must be the same as the number of elements in the array M; but this would give very poor beampattern resolution. The generally accepted solution to this problem is that the number of array elements is *artificially increased* to be the same as the number of look angles that is desired to give an acceptable beampattern (i.e. N=M) by the artifice of using *zero padding*. By this means, the aperture of the array appears to have been increased by using N elements, hence the improved angular resolution of the array. However, only M elements use finite valued weights which contribute to the output $z(n)$,

[6] the number of operations is reduced from $O(M^2)$ for the DFT to $O(M\log_{10}M)$ for the FFT, where M is the number of array elements

whilst the (*N-M*) `virtual elements' do not contribute to the output since their weights are set to zero, and so the output response is not compromised.

Throughout this work, the beam response and the beam pattern has been obtained using the zero-padded FFT. Typically, a 512 point zero-padded FFT was used to plot the beam pattern irrespective of the actual number of antenna elements.

3.10 Output signal to noise ratio

It is of particular interest to determine the improvement in SNR of the received signal due to the use of an *M* element antenna array in preference to a simple omni-directional antenna. This improvement in SNR is known as the *beamforming gain*. First, assume that the signal of interest is *sampled* in the receiver. Assume that the n^{th} array snapshot is *x(n)*. Signal vector *x(n)* comprises a wanted component, *s(n)* which arrives from an angle ϕ_s and a temporally and spatially uncorrelated noise vector, n*(n)*. The array response vector in the direction of the wanted signal is $\mathbf{v}(\phi_s)$ and $\mathbf{v}(\phi_s)\mathbf{s}(n)$ represents the wanted signal vector at the array elements. Applying a beamformer **w** to the array signal vector, *x* yields an output from the beamformer of [5]:

$$\begin{aligned} y(n) &= \mathbf{w}^H x(n) \\ &= \sqrt{M}\,\mathbf{w}^H \mathbf{v}(\phi_s) s(n) + \mathbf{w}^H \mathbf{n}(n) \\ &= \sqrt{M}\,\mathbf{w}^H \mathbf{v}(\phi_s) s(n) + \overline{\mathbf{n}}(n) \end{aligned} \tag{3.19}$$

where $\overline{\mathbf{n}} = \mathbf{w}^H \mathbf{n}(n)$ is the noise at the beamformer output due to a spatial noise field at the array. The factor $\sqrt{M}$ for the wanted signal term occurs because the wanted signal is spatially coherent, whereas the noise term is not. The beamformer output power is given by:

$$P_y = E\left[\left|y(n)\right|^2\right] = \mathbf{w}^H R_x \mathbf{w} \tag{3.20}$$

where,

$$R_x = E\left[\mathbf{x}(n)\mathbf{x}^H(n)\right] \tag{3.21}$$

is the *correlation matrix* of the array snapshot $\mathbf{x}(n)$. The actual signal at each antenna element of the ULA is given by:

$$x_m(n) = e^{-j2\pi(m-1)u_s} s(n) + n_m(n) \tag{3.22}$$

where u_s is the normalized spatial frequency in the direction of the wanted signal. Consequently, the signal to noise ratio in each element is given by:

$$SNR_{elem} \stackrel{\Delta}{=} \frac{\sigma_s^2}{\sigma_{\mathbf{n}}^2} = \frac{E\left[\left|e^{-j2\pi(m-1)u_s}s(n)\right|^2\right]}{E\left[\left|\mathbf{n}_m(n)\right|^2\right]} \tag{3.23}$$

where $\sigma_s^2 = E\left[\left|s(n)\right|^2\right]$ and $\sigma_{\mathbf{n}}^2 = E\left[\left|\mathbf{n}_m(n)\right|^2\right]$ are the element level signal and noise powers, respectively. It is assumed that the background noise power is the same for all the elements. SNR_{elem} is the element level SNR.

Now, consider the case for the output of the beamformer. In this case, the wanted signal power at the beamformer output is given by:

$$P_s = E\left[\left|\sqrt{M}\mathbf{w}^H\mathbf{v}(\phi_s)s(n)\right|^2\right] = M\sigma_s^2\left|\mathbf{w}^H\mathbf{v}(\phi_s)\right|^2 \tag{3.24}$$

and the noise power is:

$$P_n = E\left[\left|\mathbf{w}^H\mathbf{n}(n)\right|^2\right] = \mathbf{w}^H R_n\mathbf{w} = \left\|\mathbf{w}\right\|^2\sigma_{\mathbf{n}}^2 \tag{3.25}$$

because $R_n = \sigma_{\mathbf{n}}^2\mathbf{I}$,(where $\left\|\mathbf{w}\right\|$ is the norm of **w** and **I** is the identity matrix). Consequently, the SNR at the beamformer output, known as the array SNR, is:

$$SNR_{array} = \frac{P_s}{P_n} = M\frac{\left|\mathbf{w}^H\mathbf{v}(\phi_s)\right|^2}{\left\|\mathbf{w}\right\|^2}\frac{\sigma_s^2}{\sigma_{\mathbf{n}}^2} = M\frac{\left|\mathbf{w}^H\mathbf{v}(\phi_s)\right|^2}{\left\|\mathbf{w}\right\|^2}SNR_{elem} \tag{3.26}$$

which is simply the product of the beamforming gain and the element level SNR. The beamforming gain is thus [5]:

$$G_{bf} = \frac{SNR_{arrar}}{SNR_{elem}} = \frac{\left|\mathbf{w}^H\mathbf{v}(\phi_s)\right|^2}{\left|\mathbf{w}\right|^2}M \tag{3.27}$$

Consequently the beamforming gain is a function of the angle of arrival, ϕ_s , of the desired signal, the beamforming weight vector, **w** , and the number of antenna elements *M*.

3.11 Spatial matched filter

In this section, a special case is considered where the beamformer weight vector is chosen that perfectly *phase aligns* with the signal that is impinging on each of the antenna elements of the ULA at an azimuth angle, ϕ_s . Such a beamformer is referred to as a *spatial matched filter*. To

do this, the weights of the beamformer must be chosen to provide the opposite electrical phase shift to the phase shift that occurs at each element due to the spacing of the antenna elements. For example, for the case of a ULA where:

$$\begin{aligned} x(n) &= \sqrt{M}\,\mathbf{v}(\phi_s)s(n) + \mathbf{n}(n) \\ &= \left[s(n) \quad e^{-j2\pi u_s} s(n) \quad \cdots \quad e^{-j2\pi(M-1)u_s} s(n)\right]^T + \mathbf{n}(n) \end{aligned} \tag{3.28}$$

where $u_s = \dfrac{d}{\lambda}\sin\phi_s$, choosing the weight vector to be:

$$\mathbf{w}_{mf}(\phi_s) = \mathbf{v}(\phi_s) = \left[1 \quad e^{-j2\pi u_s} \quad \cdots \quad e^{-j2\pi(M-1)u_s}\right]^T \tag{3.29}$$

perfectly compensates the phase shift due to the element spacing and the conjugation operation in the expression for the beamformer output, given by $y(n) = \mathbf{w}^H \mathbf{x}(n)$. In this case, the steering vector of the beamformer is matched to the array response of the signals impinging on the array in the *look direction* ϕ_s. It is now possible to obtain the beamforming gain of the spatial matched filter by substituting (3.29) into (3.27).

$$G_{bf} = M \frac{\left|\mathbf{w}^H \mathbf{v}(\phi_s)\right|^2}{\left|\mathbf{w}\right|^2} = M \frac{\mathbf{w}_{mf}^H \mathbf{w}_{mf}}{\left|\mathbf{w}_{mf}\right|} = M \tag{3.30}$$

In other words, the beamformer gain for the spatial matched filter is numerically equal to the number of elements in the array.

For the case of *spatially white noise*, the spatial matched filter is optimum in the sense of maximizing the SNR at the output of the beamformer. However, it must be remembered that for the case where the noise or interference is not spatially uncorrelated, this beamformer is no longer optimum. For such situations, the optimum beamformer will attempt to maximize the signal-to-noise-plus-interference ratio (SINR) rather than the SNR.

3.12 A geometrical interpretation of the spatial matched filter

The beamforming gain of the spatial matched filter is known as the *array gain* because it is the maximum possible gain of a signal with respect to the sensor thermal noise for a given array. Clearly from this perspective, the more elements in the array, the greater the beamforming gain. However, physical reality places limitations on the number of elements that can be used. The spatial matched filter maximizes the SNR because the individual sensor signals are coherently aligned prior to their combination. The beampattern of the spatial matched filter

can serve to illustrate several key performance metrics of an array. A sample beampattern of a spatial matched filter is shown in Figure 3.3 for $\phi_s = 0^\circ$. The first and most obvious attribute is the large lobe centered on ϕ_s known as the mainlobe or *mainbeam*, and the remaining, smaller peaks are known as *sidelobes*. The value of the beampattern at the desired angle $\phi = \phi_s$ is equal to 1 (i.e. 0 dB) due to the normalization used in the computation of the beampattern. A response of less than 1 in the look direction corresponds to a direct loss in desired signal power at the beamformer output. The sidelobe levels determine the rejection of the beamformer to signals or noise not arriving from the look direction. The second attribute is the beamwidth, which is the angular span of the mainbeam. The resolution of the beamformer is determined by this mainlobe width, with smaller beamwidths resulting in better angular resolution. The beamwidth is commonly measured from the half-power (-3dB) points $\Delta\phi_{3dB}$ or from null to null of the mainlobe $\Delta\phi_{nn}$.

Using the beampattern, we next set out to examine the effects of the number of elements and their spacing on the array performance in the context of the spatial matched filter. However, in the following example, we first illustrate the use of a spatial matched filter to extract a signal from noise.

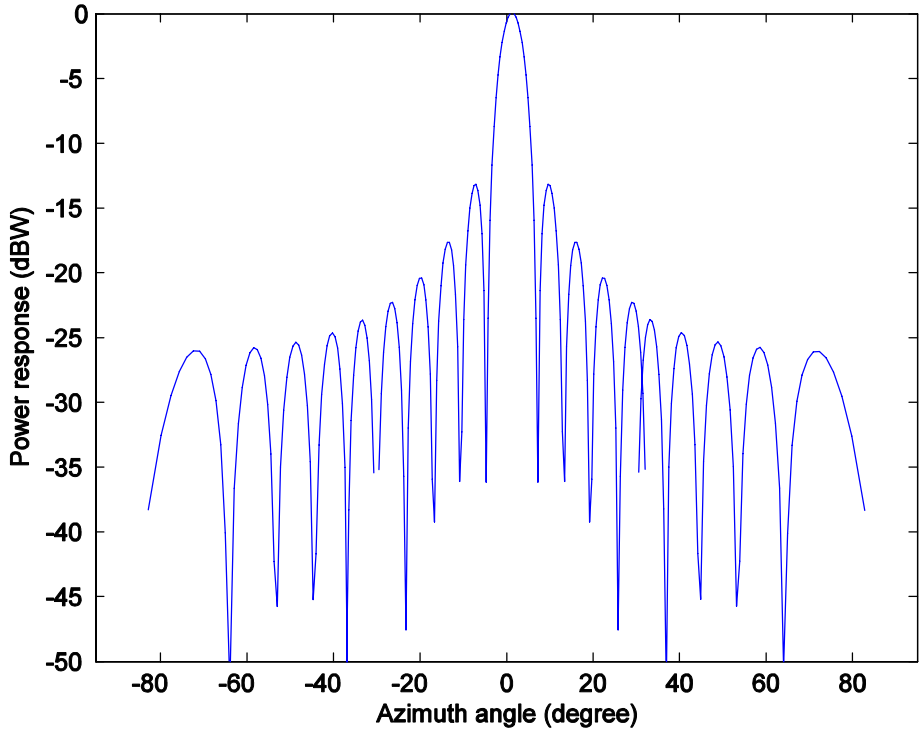

Figure 3.3: Beampattern of ULA implementing spatial matched filter steered to $\phi = 0^\circ$

3.13 Simulation of spatial matched filter

3.13.1 Example-1

A signal at a carrier frequency of 1.8GHz is received by a ULA with $M = 20$ elements and λ/2 spacing. It contains both a signal of interest at $\phi_s = 20^\circ$ with an array SNR of 20dB and thermal sensor noise with unit power ($\sigma_w^2 = 1$). The signal of interest is an impulse that is present only in the l00th sample. The aim of this example is to show how using a spatial matched filter centered on the known angle of arrival can significantly improve the response. The following figures show the implementation of the spatial matched filter with the design parameters as given below in Table 3-1:

Parameter	***value***	***Parameter***	***value***
SNR(dB)	20	antenna spacing (*d*)	λ/2
Antenna elements (*M*)	20	AoA (ϕ_s)	20^o
Sample Points (N)	200	C (m/s)	3.0E8
f_c*(Hz)*	1.8E9	λ	c/f_c

Table 3-1: Spatial matched filter parameters

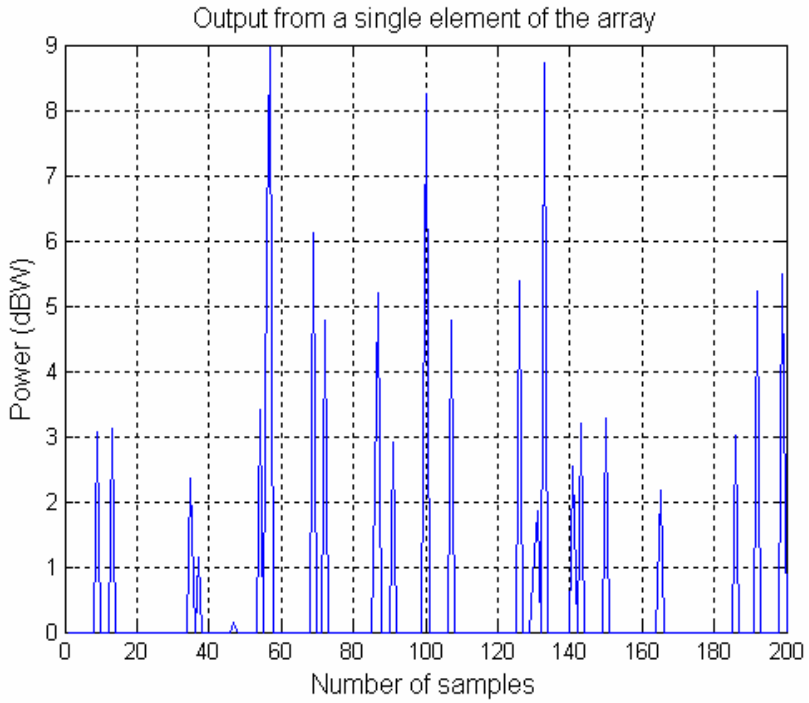

Figure 3.4:Power at one of the antenna elements

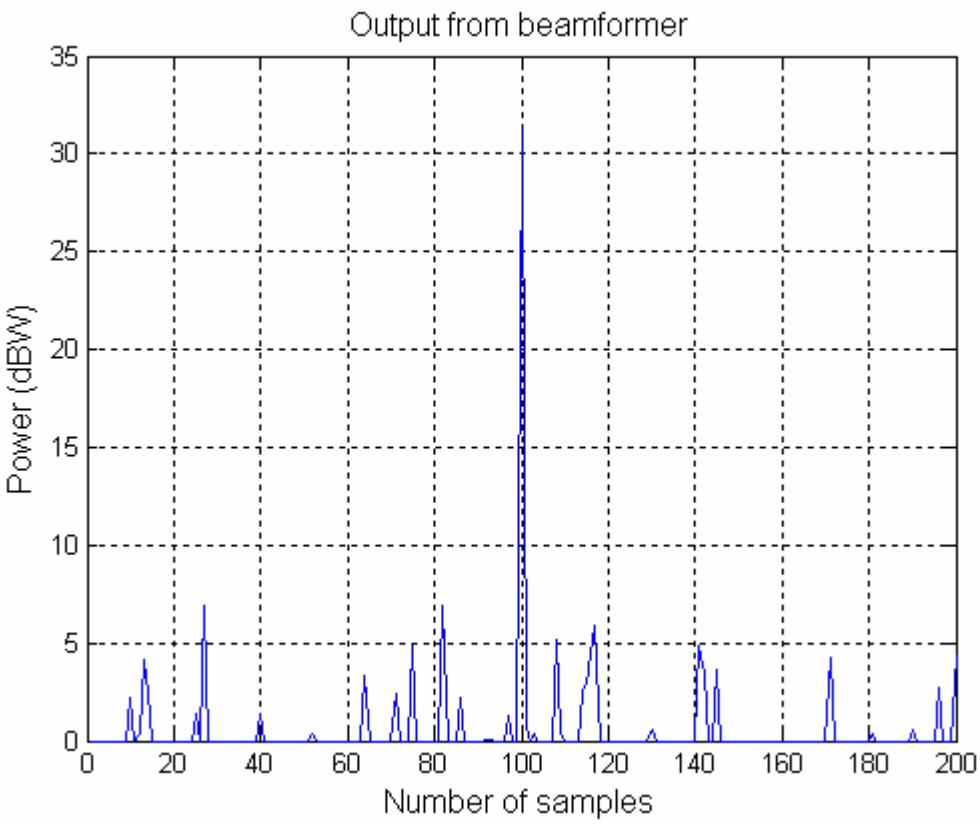

Figure 3.5: Power at output of the spatial matched filter beamformer

3.13.1.1 Result Analysis

Figure 3.4 shows the instantaneous power (dBW) of all 200 samples from antenna element 10 (arbitrarily chosen), whereas Figure 3.5 shows the power (dBW) at the output of the spatial matched filter beamformer, with the weights set up as a spatial matched filter looking in the wanted direction of the user.

From the simulation results above it is apparent that although the wanted signal impulse is not observable when viewed at any of the array elements as in Figure 3.4 (since the SNR at each element is 20dB - $10\log_{10}M$= 7dB), it is clearly observable when viewed at the output of the spatial matched filter beamformer as in Figure 3.5, since the array SNR is 20dB (i.e. 7dB original power level + $10\log_{10}M$ array gain). Therefore, the array SNR needs to be at least 10 to 12dB to clearly observe the signal.

3.13.2 Example-2

Here we consider two co-channel mobile users communicating with common BS using an 8 element array as given in the design parameters from two different locations such that the wanted user is operating from an angle of 40^0 while the interferer operates at an angle of -20^0

relative to the array broadside. We consider an array of antenna elements spaced at a distance of half wavelength relative to carrier frequency together with a spatial matched filter beam former centred on the wanted user. Figure 3.6 shows the beam pattern for this situation indicating the maximum in the direction of the wanted user. In this case the unwanted user is well outside the main lobe of the spatial matched filter and its contribution to the received signal at the output of the beamformer is reduced because the signal is received in the antenna sidelobes. In this example, the direction of the interferer (-20^0) is close to one of the nulls defining the sidelobes structure and is suppressed in the output. However, this is entirely fortuitous. If, for example, the interfering signal had been at 80^0, the steered response for this case of unwanted user would have been x1.8 (and not null in that direction) compared with wanted signal response of x8. The design parameters for implementation of the spatial matched filter for this scenario are given in the Table 3-2 below:

Parameters	***Values***	***Parameters***	***Values***
Number of samples (M)	400	Sampling period (t_s)	1.0E-10
Number of antenna elements	8	Frequency (f_c)	2.0GHz
AoA of wanted User (θ_w)	40^o -40^o 10^o	Wavelength (λ)	C/f_c
AoA of Jammer (θ_j)	-20^o	Velocity of light (c)	3.0E8 m/sec

Table 3-2: Design parameters for Example-2

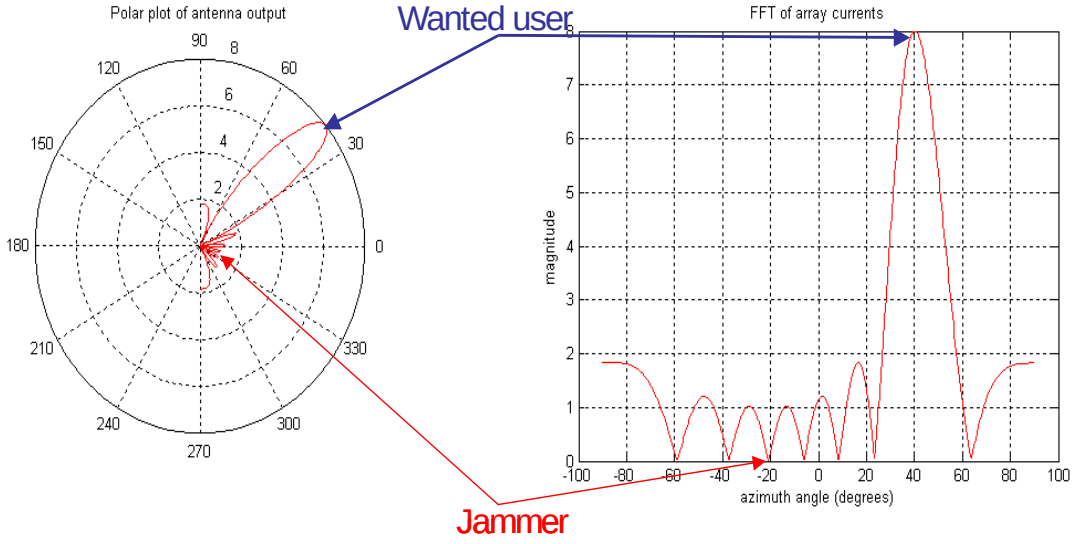

Figure 3.6: Spatial Matched Filter

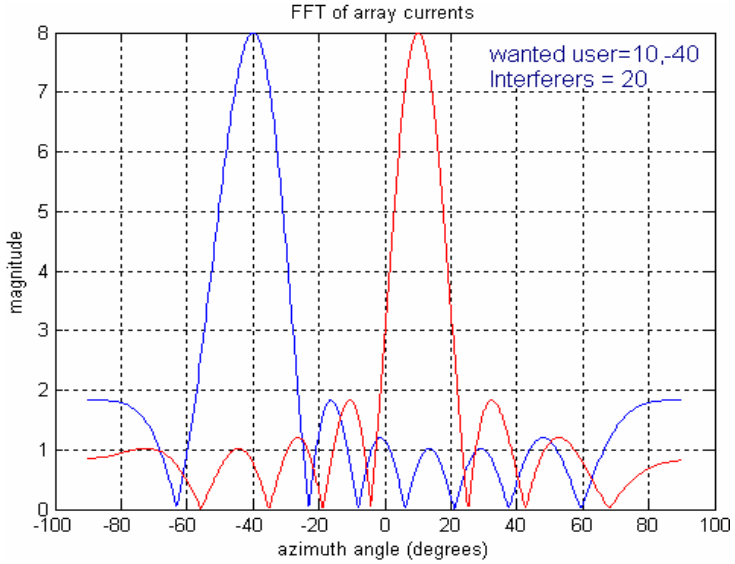

Figure 3.7: Isolation of wanted user from interferer

3.13.2.1 Results Analysis

From simulation results of spatial matched filter beamformer shown in Figure 3.6 and Figure 3.7 it is observed that two cases were considered. In the first case the unwanted user is well outside the main lobe of the spatial matched filter and its contribution to the received signal at the output of the beamformer is reduced because the signal is received in the antenna sidelobes. In this example, the direction of the interferer (-20^0) is close to one of the nulls defining the sidelobes structure and is suppressed in the output. However, this is entirely fortuitous. Whereas when the wanted user is operating at an angle of (10^0) and interferer is at (20^0) then the interferer is not nulled out as shown with red colour beamforming pattern in Figure 3.7 above.

It is important to recognise that the spatial matched filter makes no attempt to null out the interfering signal, only to maximise the gain in the wanted direction. However, a number of beamforming networks are specifically designed to null out interferers and these are described in the next sections.

3.13.3 Null-formation

In contrast with steering beams towards mobiles, as described above for the case of the spatial matched filter, it is also possible to adjust the antenna pattern such that it forms *nulls* in the directions of interference sources. Formation of nulls in the antenna patterns towards co-channel interference in mobiles helps to reduce the co-channel interference in two ways [24][25]. In transmit mode, less energy is transmitted from the BS towards these mobile users,

reducing the interference from BS to those users, whereas in receiving mode, this helps to reduce the contribution from these mobile users at the BS.

A null in an antenna pattern denotes zero beam response, achievable by choosing weights that create zero response in the direction of that interferer (or multiple interferers). In practice, however, this is seldom achievable because the antenna has the additional constraint of requiring some level of gain in the wanted user direction. The need for some gain in the wanted user direction compromises the depth of the null in the directions of the unwanted users.

3.13.4 Null-Steering Beam former

This type of beamformer is said to be a beamforming network that forms a null in the radiation pattern after cancelling a plane wave that impinges on the array of antenna elements from known direction [25]. The conventional beamformer is used to steer in the direction of known signal to estimate the signal and then subtracting the same estimated signal from each antenna element. The signal is estimated with the help of shift registers that provide the necessary delay at each antenna element and summing network, the ultimate signal received is in phase. These waveforms are summed with the help of summing network with equal weighting and then subtracted from every antenna element after desired delay. A strong interference can be cancelled with this process of forming null in the known direction. Figure 3.8 shows a schematic diagram of the null-steering beamformer.

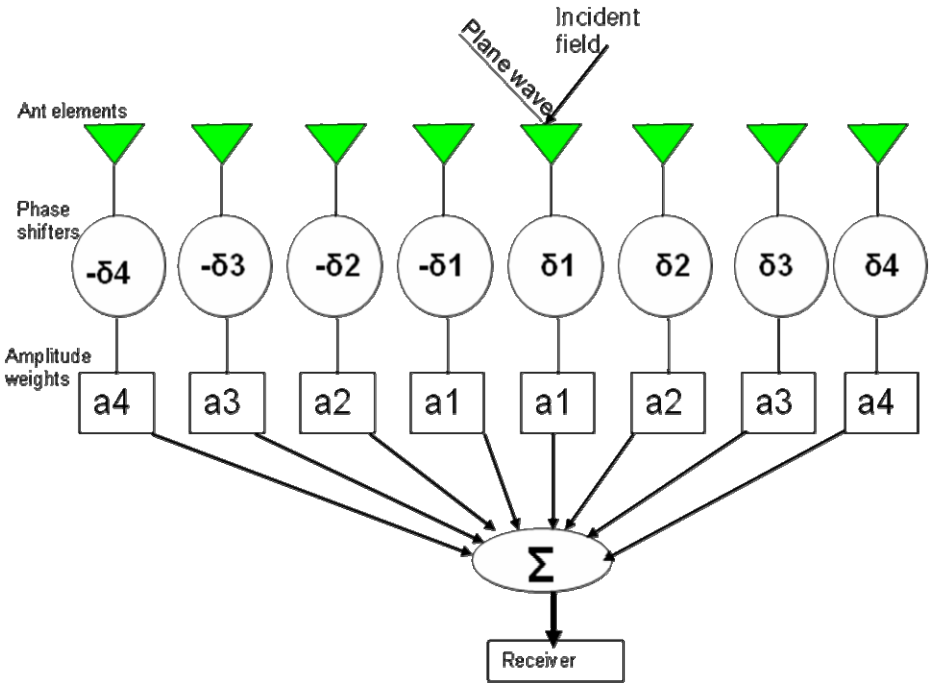

Figure 3.8: Schematic diagram of the null-steering beam former

3.14 Optimum Array Processing

When all the elements in an array are uniformly weighted, maximum SNR is obtained if the noise contributions from various elements have equal power and are uncorrelated [27]. This is achieved by the spatial matched filter. When there is directional interference, however, the noise from various element channels will be correlated. Consequently, the problem of selecting an optimum set of beamformer weights may be regarded as a problem of attempting to cancel out correlated noise components. Signal environment descriptions in terms of correlation matrices therefore play a fundamental role in determining the optimum solution for the complex weight vector. Different performance measures can be adopted to govern the operation of the adaptive processor that adjusts the weighting for each of the sensor elements.

An optimum signal processor is one whose output approximates the desired response that is almost compatible to the input signal [5]. Weiner developed the theory of optimum filters in the continuous signal domain and Kolmogorov in [121] did much the same for signals that were discrete in time. When the characteristics of the input data are same as that of the information known *a-priori* then the filter is said to be an optimum filter. In contrast if the *a-priori* information and the input data are not same, then the designed filter may not be an optimum filter. In that situation, one possible approach is to estimate the statistical parameters of the relevant signal using an adaptive filter approach because adaptive filter is based on the process of recursive algorithm which makes it possible to give satisfactory performance in an environment where the knowledge about the behaviour of the signal characteristics does not exist. For the case of a stationary environment, after successive iterations of the adaptive algorithm it converges to an Optimum Weiner solution in some statistical sense.

The aim of this section is to derive the theory which provides the optimum weights. Once this theory has been developed, it is then applied in Chapter 4 to the case of the Adaptive Antenna. Here it is shown how *a priori* knowledge of the statistics of the received signal (including interference and noise) can be used to obtain beamformer weights that optimize the detection of the wanted part of the received signal. As is often the case, the statistical parameters on which the optimum beamformer weights depend are found in the *correlation matrix* computed from the array snapshots. Correlation is defined as the average product of two signals and tells how much two signals or waveforms are similar to each other [4].

A major practical problem with this approach is that the true statistics of neither the received signal nor the interference are known in advance and it is necessary to *estimate* these parameters from the received signal itself. Since the optimum beamformer performance can be critically dependent on this estimate, estimation errors can have a significant impact on overall antenna performance, as will be shown.

Consider an array signal that consists of the desired signal, $\mathbf{s}(n)$, an interference signal $\mathbf{i}(n)$, along with spatial thermal noise field $\mathbf{n}(n)$, that is:

$$\mathbf{x}(n) = \mathbf{s}(n) + \mathbf{i}(n) + \mathbf{n}(n) = \sqrt{M}\,\mathbf{v}(\phi_s)s(n) + \mathbf{i}(n) + \mathbf{n}(n) \tag{3.31}$$

where $s(n)$ is a signal with a statistically defined power in terms of its variance, σ_s^2 and uniformly distributed random phase. The interference-plus-noise component of the array signal is:

$$\mathbf{x}_{i+n}(n) = \mathbf{i}(n) + \mathbf{n}(n) \tag{3.32}$$

which are both modeled as zero mean stochastic processes. The interference has spatial correlation according to the angles of arrivals of the contributing interferers, while the thermal noise is spatially uncorrelated. The sensor thermal noise is assumed to be temporally uncorrelated with power $\sigma_{\mathbf{n}}^2$. The assumption is made that all three components are mutually uncorrelated. As a result, the array correlation matrix is:

$$\mathbf{R}_x = E\left[\mathbf{x}(n)\mathbf{x}^H(n)\right] = M\sigma_s^2\mathbf{v}(\phi_s)\mathbf{v}^H(\phi_s) + \mathbf{R}_i + \mathbf{R}_n \tag{3.33}$$

where σ_s^2 is the power of the signal of interest and $\mathbf{R}_i$ and $\mathbf{R}_n$ are the interference and noise correlation matrices, respectively. The interference-plus-noise correlation matrix is the sum of these latter two matrices:

$$\mathbf{R}_{i+n} = \mathbf{R}_i + \mathbf{R}_n = \mathbf{R}_i + \sigma_{\mathbf{n}}^2\mathbf{I} \tag{3.34}$$

since the sensor thermal noise is spatially uncorrelated.

3.15 Optimum Beamforming

The ultimate goal of the prospective adaptive beamformer is to combine the sensor signals in such a way that the interference signal is reduced to the level of the thermal noise while the desired signal is preserved (i.e. maximizing the ratio of the signal power to the interference plus noise (SINR)) [30]. Maximizing the SINR is the optimal criterion for most detection and estimation problems. This criterion should not be confused with maximizing the SNR (spatial matched filter) in the absence of interference. At the input of the array, the SINR for each individual sensor is given by:

$$SINR_{elem} = \frac{\sigma_s^2}{\sigma_i^2 + \sigma_{\mathbf{n}}^2} \tag{3.35}$$

where σ_s^2, σ_i^2 and $\sigma_{\mathbf{n}}^2$ are the signal, interference and thermal noise powers in each individual element. The SINR at the beamformer output, following the application of the beamforming weight vector, **w** is:

$$SINR_{out} = \frac{\left|\mathbf{w}^H \mathbf{s}(n)\right|^2}{E\left[\left|\mathbf{w}^H \mathbf{x}_{i+n}(n)\right|^2\right]} = \frac{M\sigma_s^2 \left|\mathbf{w}^H \mathbf{v}(\phi_s)\right|^2}{\mathbf{w}^H \mathbf{R}_{i+n} \mathbf{w}} \tag{3.36}$$

After some manipulation [5] the optimum weight vector is given by:

$$\mathbf{w}_o = \alpha \mathbf{R}_{i+n}^{-1} \mathbf{v}(\phi_s) \tag{3.37}$$

where α is an arbitrary constant. Thus, the optimum beamforming weights are proportional to $\mathbf{R}_{i+n}^{-1} \mathbf{v}(\phi_s)$.

The proportionality constant α can be set in a variety of ways dependent on the normalizations (or *constraints*) placed upon the array weights. For example, a common constraint placed on the beamformer is that there should be unity gain in the desired look direction (i.e. the output signal is kept constant in the direction of desired user whilst the SINR is maximized). This is called the minimum variance distortionless response (MVDR) [34]. An alternative constraint is that the weight be chosen to normalize the spatial noise field to unity or that the interference plus noise is normalized to 1. Table 3-3 gives various formulations of the optimum beamformer and the corresponding normalization for α that are needed to provide optimum performance.

The method used to obtain the optimum beamformer weights from these normalizations is illustrated here for the case of the MVDR normalization. Constraining the beamformer to have unity gain in the wanted signal look direction, is given by $\mathbf{w}_o^H \mathbf{v}(\phi_s) = 1$

$$\mathbf{w}_o^H \mathbf{v}(\phi_s) = \alpha \left[\mathbf{R}_{i+n}^{-1} \mathbf{v}(\phi_s)\right]^H \mathbf{v}(\phi_s) = 1 \tag{3.38}$$

and the resulting optimum beamformer is given by:

$$\mathbf{w}_o = \frac{\mathbf{R}_{i+n}^{-1} \mathbf{v}(\phi_s)}{\mathbf{v}^H(\phi_s) \mathbf{R}_{i+n}^{-1} \mathbf{v}(\phi_s)} \tag{3.39}$$

Note that the weight of the optimum beamformer (and hence the array response) are dependent upon the correlation matrix of the interference plus noise, $\mathbf{R}_{i+n}^{-1}$. This is not surprising. This correlation matrix provides all the information about the spatial distribution of the interfering signals and noise so it can be used 'in reverse' to nullify the effect of these

interfering sources. Effectively, the $\mathbf{R}_{i+n}^{-1}$ term is being used as a decorrelator of the interference signal.

The major problem to obtain the optimum beamformer weights is that: (a) the direction, ϕ_s, of the wanted signal must be known and (b) the correlation matrix of the interference plus noise (only) must be known or estimated. In practice, the received signal will comprise not only the interference and noise signals but the wanted signal as well. This means that when the weights of the optimum array are being computed, the wanted signal must be temporarily stopped so that the adaptive antenna can receive only the interference plus noise to be able to compute $\mathbf{R}_{i+n}^{-1}$. The weights are then computed and the wanted signal can then be reapplied. The essential feature of an optimum beamformer is that wanted signal and interference signal must be decorrelated.

Constraint	***Mathematical formulation***	***Optimum beamformer Normalization***
Unit gain in look direction	$\mathbf{W}_o^H \mathbf{V}(\phi_s) = 1$	$\alpha = \left[\mathbf{V}^H(\phi_s)\mathbf{R}_{i+n}^{-1}\mathbf{V}(\phi_s)\right]^{-1}$
Unit noise gain	$\mathbf{W}_o^H \mathbf{W}_o = 1$	$\alpha = \left[\mathbf{V}^H(\phi_s)\mathbf{R}_{i+n}^{-2}\mathbf{V}(\phi_s)\right]^{-1/2}$
Unit gain on interference-plus-noise	$\mathbf{W}_o^H \mathbf{R}_{i+n} \mathbf{W}_o = 1$	$\alpha = \left[\mathbf{V}^H(\phi_s)\mathbf{R}_{i+n}^{-1}\mathbf{V}(\phi_s)\right]^{-1/2}$

Table 3-3 Normalization constraints

3.16 Interference cancellation performance

The interference cancellation performance of the optimum beamformer can be determined by examining the beam response at the angles of arrivals of the interferers. The beam response at these angles indicates the depth of the null that the optimum beamformer places on the interferer. Using the MVDR optimum beamformer (3.39), the response in the direction of the p^{th} interferer at ϕ_p for an optimum beamformer steered in the direction of ϕ_s is:

$$C_\circ(\phi_p) = \mathbf{w}_o^H \mathbf{v}(\phi_p) = \alpha \mathbf{v}^H(\phi_s)\mathbf{R}_{i+n}^{-1}\mathbf{v}(\phi_p)$$

Where, from Table 3-3,

$$\alpha = \left[\mathbf{v}^H(\phi_s)\mathbf{R}_{i+n}^{-1}\mathbf{v}(\phi_s)\right]^{-1}$$

3.17 Simulation of optimum beamformer

3.17.1 Example-1

Here we consider that three co-channel mobile users are communicating with common BS using an 8 element array as given in the design parameters Table 3-4 below from three different locations such that the wanted user is operating from an angle of 20^o while two interferers from -20^o and 40^o relative to the array broadside. The correlation matrix $\mathbf{R}_{i+n}^{-1}$ was estimated from 400 snapshots to calculate the weight of the optimum beamformer and the thermal noise has unit variance $\sigma_{\mathbf{n}}^2 = 1$. We consider the ULA with $d = \lambda/2$ relative to the carrier frequency together with an optimum beamformer is centred at the interferer. The design parameters for implementation are given below in the Table 3-4.

Figure 3.9 shows this situation indicating a null in the direction of interferers. In this case the wanted user is well away from interferers and main beam is also formed in the direction of wanted user in addition to nulling of the interferers. However, this is entirely fortuitous. Whereas when the wanted user is operating from closer angle with respect to interferer then the interferer is nulled out but main beam is not directed in the direction of wanted user. This scenario is depicted in example-2 in the next section.

Parameters	***Values***	***Parameters***	***Values***
Number of samples (M)	400	Sampling period (t_s)	1.0E-10
Number of antenna elements	8	frequency (f_c)	2.0GHz
AoA of wanted User (θ_w)	20^o, -30^o, -25^o, 40^o	wavelength (λ)	C/f_c
AoA of Jammers (θ_j)	-20^o, 40^o	velocity of light (c)	3.0E8 m/sec

Table 3-4: Design parameters for optimum beamformer

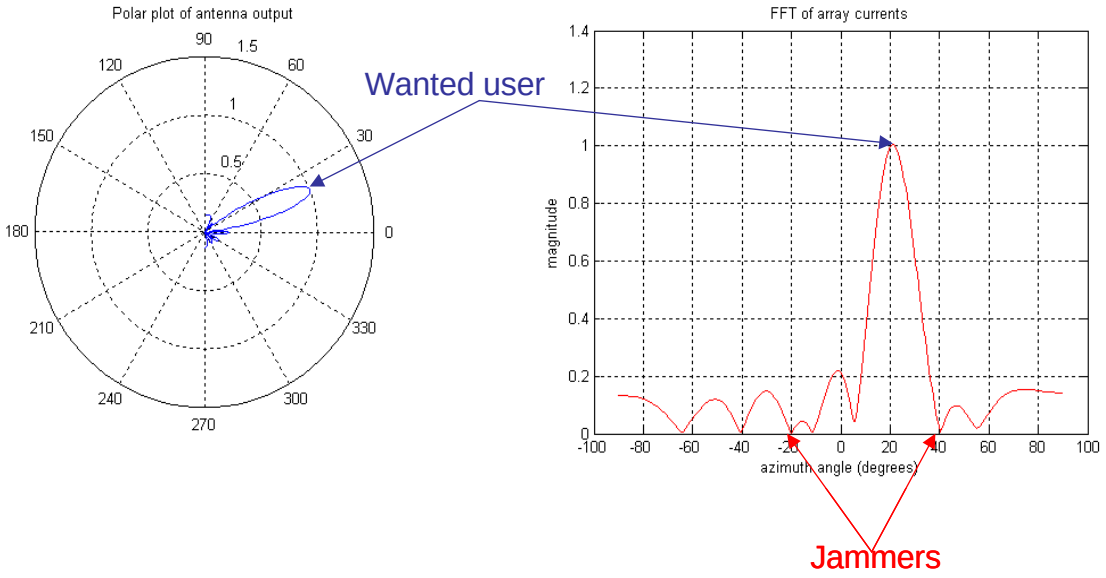

Figure 3.9: Optimum beamformer

3.17.2 Example-2

Here we consider that two co-channel mobile users communicating with common BS using an 8 element array as given in the design parameter table above in example-1 from two different locations, such that the interferer is always operating from an angle of -20^o while the wanted user is operating from different angles $-10^\circ, -25^\circ, -30^\circ$ and 40° relative to the array broadside. We consider an array of antenna elements spaced at a distance of half wavelength relative to carrier frequency. The design parameters considered are same as given in design parameters Table 3-4 above for Example-1 except that the angle of wanted user is changed. The resultant output of an optimum beamformer with interferer -20° is plotted as shown in Figure 3.10 below. From simulation of an optimum beamformer it is seen that the interferer has always been fully nulled out and maximum in case of wanted user is not achieved at exact wanted angles which is shifted due to the effect of sidelobes.

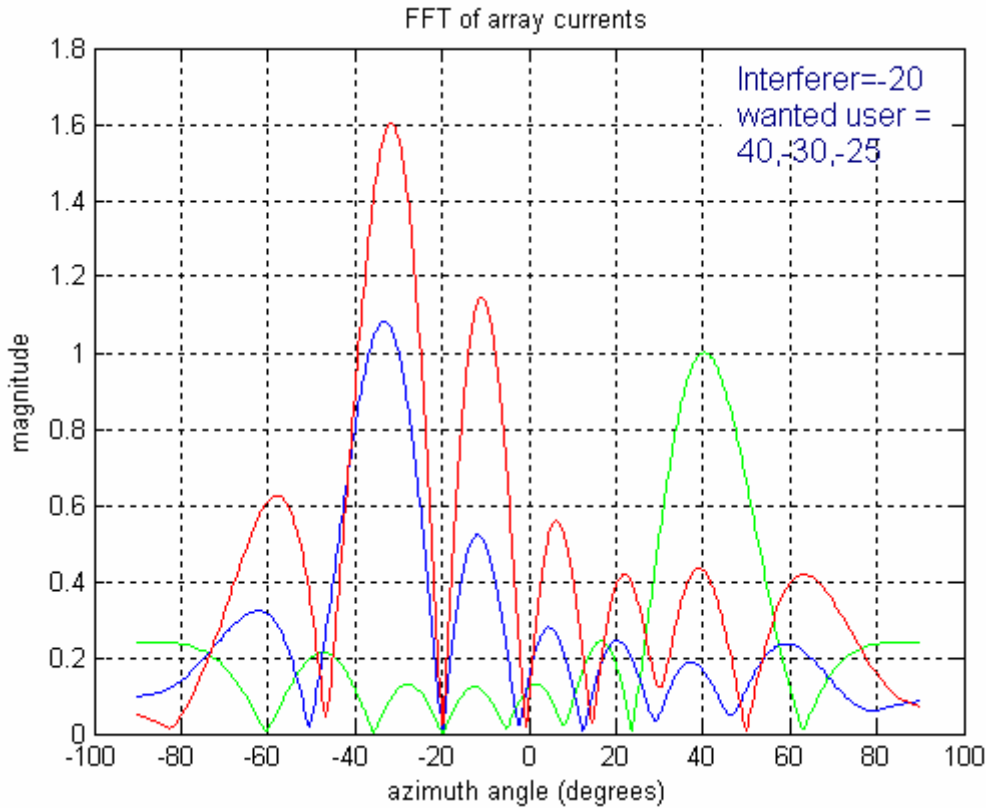

Figure 3.10: Cancellation of interferer by optimum beamformer

3.17.2.1 Results Analysis

From simulation results shown in Figure 3.9 and Figure 3.10 it is observed that two cases were considered. When the wanted user and interferers are operating from angular position farther apart the interferers are nulled out properly along with forming main beam by maximising the gain in the direction of wanted users.

In example-2 when the wanted user and interferers are operating from closer angular position then although null is formed in the direction of interferer but at the same time main beam is not directed towards wanted user and is shifted in direction other than that of wanted user's direction as shown in Figure 3.10 above.

It is important to recognise that the optimum beamformer makes no attempt to form main beam by maximising the gain in the wanted direction, only to null out the interfering signals.

3.18 Summary

This chapter covered the topics for conventional beamforming with the help of array processing starting with fundamentals of antenna elements and covering the description of spatial matched filter and optimum beamformer. In this chapter throughout the use of ULA is considered and model for spatial signal received by ULA is presented with simulations. The concept of beamforming with the help of spatial matched filter, which maximises the gain in the direction of wanted user, is discussed along with simulation results presented. It is observed that spatial matched filter is only used to form main beam in the direction of a wanted user by increasing the gain and makes no attempt to not null out the interferer at all. At times when the wanted user and an interferer are ooperating from angles away from each other then there is a chance that in addition to forming main beam towards wanted user, a null is also formed towards an interferer but this is fortuitous as the contribution of interferer towards wanted user is very less and null is formed due to the effect of sidelobes. It has also been shown with the help of simulations that when wanted user and an interferer are operating from closer angles then main beam is directed towards wanted user but null is not formed towards an interferer. However, for the case of *spatially white noise*, the spatial matched filter is optimum in the sense of maximizing the SNR at the output of the beamformer. However, it must be remembered that for the case where the noise or interference is not spatially uncorrelated, this beamformer is no longer optimum. For such situations, the optimum beamformer will attempt to maximize the signal-to-noise-plus-interference ratio (SINR) rather than the SNR.

In addition to that of spatial matched filter an optimum beamforming technique is also discussed that cancels the interferer by placing a null in the direction of an interferer and does not cater for the main beam to be directed towards the wanted user. The method for optimisation of weights for spatial matched filter and optimum beamformer is also presented in this chapter. Difference between spatial matched filter and an optimum beamformer has been shown with help of simulation results that give the graphs of isolation of wanted user from interferers operating from closer and farther angular positions. The simulation results verify that the optimum beamformer makes no attempt to form main beam by maximising the gain in the wanted direction, only nulls out the interfering signals. In addition to that for the case of an optimum beamformer it is necessary that wanted user and an interferer must be spatially uncorrelated otherwise wanted signal and unwanted signal can not be isolated.

Chapter 4:

4 Adaptive Beamforming

4.1 Introduction

The previous chapter has examined the use of the beamforming network as a means of optimising the signal to interference ratio of signal arriving from an angle θ when corrupted by a spatially random field and/or coherent interference signals at specific angles of arrivals θ_i.

This approach is appropriate when the signal source and the interference sources are stationary, but it is not optimised when either the wanted signal or the coherent interference are moving. It is, of course, possible to treat each change of position of the signals as quasi-static sources in which the sources are assumed to be stationary over a given period where the angles of arrivals are being estimated prior to some form of optimal beam forming. This is acceptable if the sources move slowly, compared with time taken to estimate the angle of arrivals, but the method begins to fail as the rate of change of direction of the signal sources increases. The reason for this is that the adaptive beamformer utilizes the optimum beamformer and this requires that the correlation matrix of the interference-plus-noise is known. Since this is generally not available *a priori*, it must be estimated from the received signals [5]. The accuracy of the estimate of the correlation matrix is dependent on array snapshots needed to obtain the expectation of (3.33). If the spatial noise field is large, the number of snapshots needed for an acceptable estimate may exceed the period for which the signal sources may be considered to be wide sense stationary (WSS). In this case, a number of adaptive algorithms have been developed that allow the antenna beam pattern to respond dynamically, to the changes in the position of the wanted and interference signal sources. This aspect of antenna arrays is considered in this chapter.

4.2 Adaptive Beamforming Network

A uniform linear array, with adjustable element weights is shown in Figure 4.1 below. The weighted sum of the received signals is represented as the estimated output of the array $\mathbf{y}(n)$ and $\mathbf{n}(n)$ is the receiver thermal noise. Here in this beamforming network $\mathbf{s}_1(n)$ is considered as the desired signal, and remaining $M-1$ signals are considered as the interferers. In one type of adaptive system, the weight vector $\mathbf{w}$ is determined on the basis of the estimated output $\mathbf{y}(n)$, a reference signal $\mathbf{d}(n)$ that uniquely identifies the desired signal, and an array of previous weights. In practice the training sequence is used to determine the reference signal, $r(n)$, that is almost the same as that of desired signal.

The estimated array output is given by

$$\mathbf{y}(n) = \mathbf{w}^H \mathbf{x}(n) \tag{4.1}$$

Where $\mathbf{w}^H$ is the hermitian transpose i.e. the complex conjugate transposes of the weight vector, and $\mathbf{x}(n)$ is the array snapshot of the received signals plus noise.

An error signal is generated, by subtracting the estimated reference signal at the output of the beamformer from the true reference signal, which is subsequently used to adjust the weights optimally. It is these set of optimum weights which control the behaviour of the antenna output completely by maximising either the SNR or the SIR. The optimum output is achieved when this error signal calculated by subtracting estimated output from reference signal approaches to zero [30].

Different adaptive algorithms such as the LMS, NLMS and RLS algorithms have been implemented to get the optimum output by forming main beam pattern in wanted direction while nulling out the interferers. The result of the convergence of the algorithm is also shown when the optimum output is achieved.

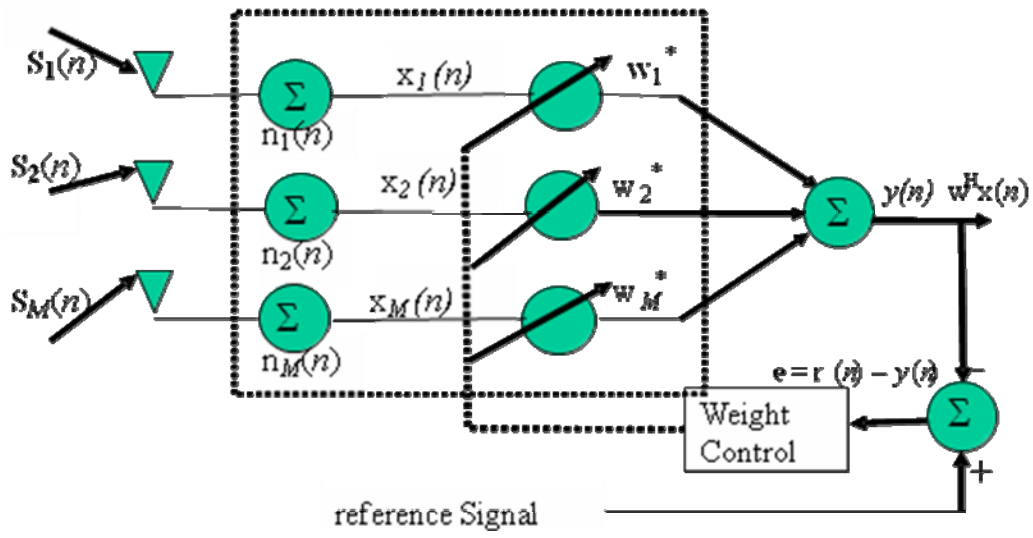

Figure 4.1: Adaptive Beamforming Network

4.3 Adaptive algorithms

4.3.1 SMI algorithm (Sample Matrix Inversion)

The SMI algorithm can be viewed as a block adaptive method and this relies on the signals remaining statistically stationary for the block duration. In the SMI method, the interference-plus-noise correlation matrix is estimated from the received signal in the absence of the wanted signal (sometimes called a *training set)*. The estimate of the correlation matrix is obtained by taking, *K,* array snapshots and performing the following operation [5]:

$$\hat{\mathbf{R}}_{i+n} = \frac{1}{K}\sum_{k=1}^{K}\mathbf{x}_{i+n}(n_k)\mathbf{x}_{i+n}^{H}(n_k) \tag{4.2}$$

where n_k represents the n_k^{th} snapshot within the training set. The size of K is referred to as the sample support. It will be clear that the larger the value of K, the more accurate the estimate of the correlation matrix and the maximum likelihood estimate of the correlation matrix occurs when $K \to \infty$ and $\hat{\mathbf{R}}_{i+n} \to \mathbf{R}_{i+n}$. However, in this case, the training set is infinitely large and no actual data is sent! Consequently, the performance of the beamformer is a compromise between obtaining an 'adequately' accurate estimate of the correlation matrix and reducing the training overhead. This is particularly important if the interference statistics are not stationary, as discussed next.

In practice, the data will be sent as *frames* of data, as shown in Figure 4.2 with periods of signal-quiet prior to the transmission of the wanted data so that the interference-plus-noise correlation matrix can be periodically re-estimated. In this way, as the statistics of the interference and noise change (e.g. the angle of arrival of the interferer changes, or its power changes), this can be re-estimated at the start of each frame of data and new nulls in the direction of the interferer and at an appropriate depth can be created. From this, it will be seen that reducing K allows the frame repetition period to be reduced (for a given payload/support ratio) and this allows the antenna to respond more quickly to changes in the interference signal (i.e. to adapt dynamically to the signal).

For spatially dynamic interferers, the ability of the block adaptive algorithm to respond quickly might be more important than absolute optimum performance in the wanted direction or its sidelobe performance. Also note that Figure 4.2 also includes a second training period after the period of radio quiet. During this period, a *known signal* is transmitted that is as orthogonal to the interferer as possible. For example, the transmitted signal might be a unique data sequence with excellent correlation properties. The receiver uses this training sequence to extract the wanted signal from the interference using correlation and from the array response of the wanted signal, obtains the estimated angle of arrival, ϕ_s. There are a number of different methods to estimate the angle of arrival of the wanted signal. One method is based on

the beam response and is obtained directly from the zero-padded FFT, discussed in Chapter 1. However, other methods exist, including: MUSIC [29] [94], ESPRIT [95][97] and SAGE [98], among many others. Once ϕ_s has been estimated, then the optimum beamformer weights can be found from equation (3.39) using ϕ_s together with the estimated correlation matrix obtained from (4.2):

$$\mathbf{w}_{smi} = \frac{\hat{\mathbf{R}}_{i+n}^{-1}\mathbf{v}(\phi_s)}{\mathbf{v}^H(\phi_s)\hat{\mathbf{R}}_{i+n}^{-1}\mathbf{v}(\phi_s)} \tag{4.3}$$

The number of samples needed to obtain the correlation matrix, (i.e. the sample support) is very important. When fewer samples are used, the estimate of $\mathbf{R}_{i+n}$ becomes progressively poorer and this impacts on the computation of the optimum weight vector. The sidelobe structure becomes increasingly random and the depth of the null in the direction of the interferer also becomes much reduced. Clearly, the number of samples needed to obtain a reliable estimate of $\mathbf{R}_{i+n}$ depends on the level of the uncorrelated spatial noise compared with the correlated interference. It should be noted that this method fails if there is no uncorrelated thermal noise present as the correlation matrix becomes increasingly singular as the interference-to-noise-ratio (INR) diminishes.

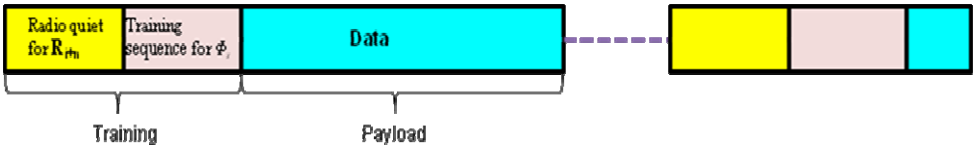

Figure 4.2: Transmission of data

4.3.2 Sample-by-Sample methods

The SMI adaptive beamformer is a least squares block adaptive method. However, optimum beamforming can also be carried out using methods that compute the beamforming weights on a sample-by-sample basis. These methods are referred to as sample-by-sample adaptive. There are two broad classes of sample-by-sample adaptive algorithm: the least mean squares algorithm (LMS) and the recursive least mean squares (RLS) algorithm.

At first sight it might appear that a sample-by-sample adaptive method will provide a continuously varying optimum beam that is better able to cope with dynamic interferers, compared with a block adaptive system. For the block adaptive system, the performance of the adaptive beamformer is set by the support *K* (i.e. the number of samples used to form the data

matrix *X*) which sets the shortest period over which the interferer can be considered to be stationary. However, the sample-by-sample methods take a finite time to *converge* and during this convergence time, the beamforming performance of the array is far from optimum. For example, if the interferer suddenly switches on, the sample-by-sample methods will take the convergence time to adapt to the new interferer. However, if the interferer then slowly moves in space at a rate at which the algorithm can *track* the movement, the performance of the antenna array remains close to optimum as the interferer moves. However, this presupposes that the algorithm actually converges. This is not always the case and considerable fine tuning has often to be carried out to ensure convergence at a fast rate and with low steady-state error.

The sample-by-sample methods trade-off, the speed of convergence against the steady-state error in the weights, relative to their optimum value obtained by the SMI method. A number of variations on the LMS and RLS methods have been developed which attempt to maximize convergence speed and yet retain a small steady-state error.

A major difficulty with the sample-by-sample methods is that it is pointless to permanently remain quiet and so the interference plus noise correlation matrix $\mathbf{R}_{i+n}$ cannot be used and must be replaced by the correlation matrix of the total signal, $\mathbf{R}_x$. This has a profound effect on the performance of the resulting beamformer.

4.3.3 LMS algorithm (Least Mean Square)

Here in case of LMS algorithm the reference or the desired signal $\mathbf{d}(n)$ generated at the receiver is completely known having same directional and spectral characteristics and is usually assumed to have similar properties as that of transmitted signal $\mathbf{s}_w$. This reference signal may not be the exact replica of the desired wanted signal but must be at least highly correlated to the desired signal and uncorrelated with the interference signal components that appear at the output of an antenna array. This algorithm requires that an error signal is generated by subtracting the estimated signal received at the output of the BFN from desired signal. Consequently the same error signal is then used to update the weight vector as given below [5]:

$$\mathbf{w}(n+1) = \mathbf{w}(n) + \mu\mathbf{x}(n)\mathbf{e}^*(n) \tag{4.4}$$

Where μ is the forgetting factor that determines the convergence characteristics of the algorithm as and when the estimated weights are equal to the optimal weights $\mathbf{w}_{MSE}$. This algorithm can be regarded as constrained or unconstrained LMS algorithm provided the weights are subject to constrained or unconstrained at every iteration of update of the weight vector [23][25]. The optimum output is achieved when the mean squared error between

reference signal and estimated output approaches to zero. The LMS algorithm can be summarised as:

a. First of all the estimated output is obtained at the output of BFN.
b. This estimated output is then subtracted from the actual desired signal to find the error signal.
c. This error signal is then used in (4.4) to update the weight vector that is required for optimisation of beampattern.

4.3.3.1 Simulation of LMS algorithm

Here we consider uniform linear array of 8 antenna elements spaced at a distance of λ/2 relative to the carrier frequency f_c. The uniform linear array of antenna elements receives different signals from different directions in space. In this case the wanted user is operating from angle of 40°, whilst the interferer is operating from angle of -20°. The aim of implementation of LMS algorithm is to estimate the output response at the BFN to calculate the error by subtracting the estimated signal from desired signal. When this error signal approaches to zero the output obtained is considered to be an optimum output where the convergence of the algorithm takes place. The design parameters for simulation of the problem are given in the Table 4-1 below.

Parameters	***Values***	***Parameters***	***Values***
Number of samples (M)	400	Sampling period (t_s)	1.0E-10
Number of antenna elements	8	Frequency (f_c)	3.0GHz
AoA of wanted User (θ_w)	40°	Wavelength (λ)	C/f_c
AoA of Jammers (θ_j)	-20°	Velocity of light (c)	3.0E8 m/sec
μ	0.005		

Table 4-1: Design Parameters for LMS algorithm

Initialization of parameters

Initialize the weight vector w at time $n = 0$, $\mathbf{w}(0) = 0$

Calculate the estimated output response at the BFN using (4.1) as under:

$$y(n) = \mathbf{w}^H(n)\mathbf{x}(n)$$

Where,

$y(n)$ = Estimated output response at time n

$\mathbf{w}(n)$ = Weight vector at time n

$\mathbf{x}(n)$ = Signal vector received at the antenna array at time n represented as:

$$\mathbf{x}(n) = \mathbf{s}(n) + \mathbf{i}(n) + \mathbf{n}_n(n) \tag{4.5}$$

This received signal is the composite signal of wanted user, interferer and Gaussian noise.

Error signal is computed as difference between desired signal and the estimated output signal as under:

$$\mathbf{e}(n) = \mathbf{d}(n) - y(n) \tag{4.6}$$

Update the weight vector '$\mathbf{w}$' for 'M' number of iterations using (4.4)

$$\mathbf{w}(n+1) = \mathbf{w}(n) + \mu\mathbf{x}(n)\mathbf{e}^*(n)$$

The simulation result of LMS algorithm is shown in Figure 4.3 below indicating the mean squared error and the number of iterations it takes for convergence in order to achieve the optimum solution.

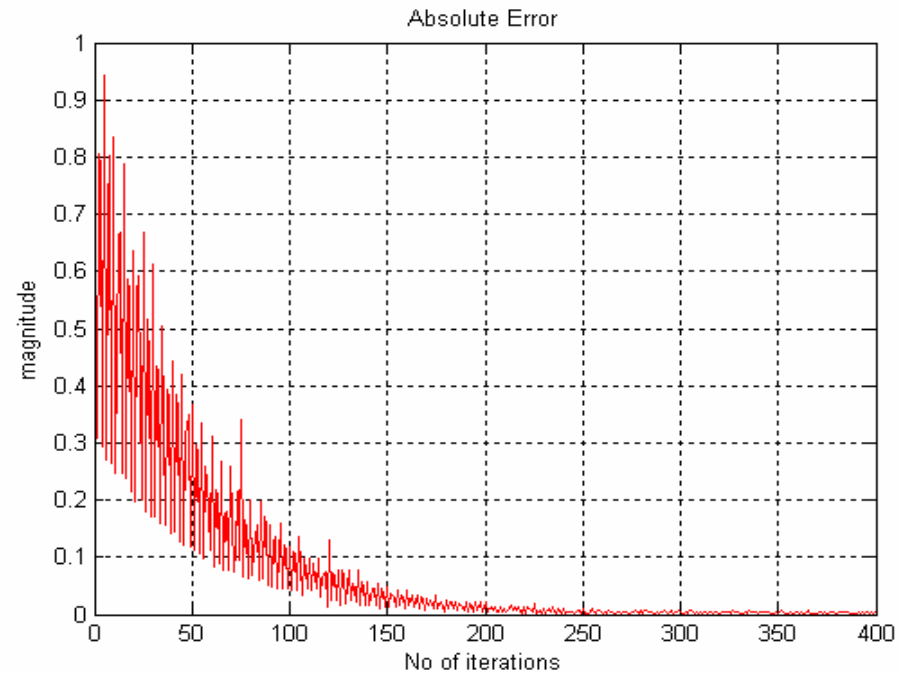

Figure 4.3: Convergence of LMS algorithm

4.3.4 NLMS algorithm (Normalised LMS)

The NLMS algorithm is faster compared with the LMS algorithm where the weight vector is updated in the same way as it is done for the LMS algorithm described above. In case of the

NLMS algorithm, when the value of the input vector is small, numerical difficulties are likely to arise and in order to counter that we have to divide a small value a(t) with squared norm $||x(n)||^2$ [25]. To overcome this problem the equation for update of weight vector is slightly updated and normalised. Having all the design parameters same as defined in case of LMS algorithm except the value of forgetting factor μ=0.0996 is used in case of NLMS implementation, the simulation graph showing the mean squared error and the number of iterations it takes to converge in order to achieve the optimum solution is as shown in Figure 4.4 below which indicates that in this case the convergence is quite faster as compared to LMS and the algorithm tends to converge after about 45 iterations.

4.3.4.1 Simulation of NLMS algorithm

The design parameters for the simulation of the NLMS algorithm are the same as those considered for the LMS algorithm given in Table 4-1 above, except that the value of forgetting factor, which determines the rate of convergence is different than that of LMS algorithm. In this case μ = 0.0996 is considered in the simulation.

Initialization of parameters

Initialize the weight vector $\mathbf{w}$ at time $n = 0$, $\mathbf{w}(0) = 0$

Calculate the estimated output response at the BFN using (4.1):

$$y(n) = \mathbf{w}^H(n)\mathbf{x}(n)$$

Where,

$y(n)$ = Estimated output response at time *n*

$\mathbf{w}(n)$ = Weight vector at time *n*

$\mathbf{x}(n)$ = Signal vector received at the antenna array at time *n* represented as:

$$\mathbf{x}(n) = \mathbf{s}(n) + \mathbf{i}(n) + \mathbf{n}_n(n)$$

This received signal is the composite signal of wanted user, interferer and Gaussian noise.

Error signal is computed as difference between desired signal and the estimated output signal calculated as:

$$\mathbf{e}(n) = \mathbf{d}(n) - y(n)$$

Subsequently this error signal computed is used to update the weight vector and update of the weight vector $\mathbf{w}$ for 'M' number of iterations is computed by [5][7]:

$$\mathbf{w}(n+1) = \mathbf{w}(n) + \left[\mu \Big/ a + \|\mathbf{x}(n)\|^2 \right] \mathbf{x}(n)\mathbf{e}^*(n) \tag{4.7}$$

Where,

$\mathbf{w}(n)$ = Weight vector at time n

$\mathbf{x}(n)$ = Input data vector at time n

a = positive constant i.e. (a > 0)

μ = 0.0996

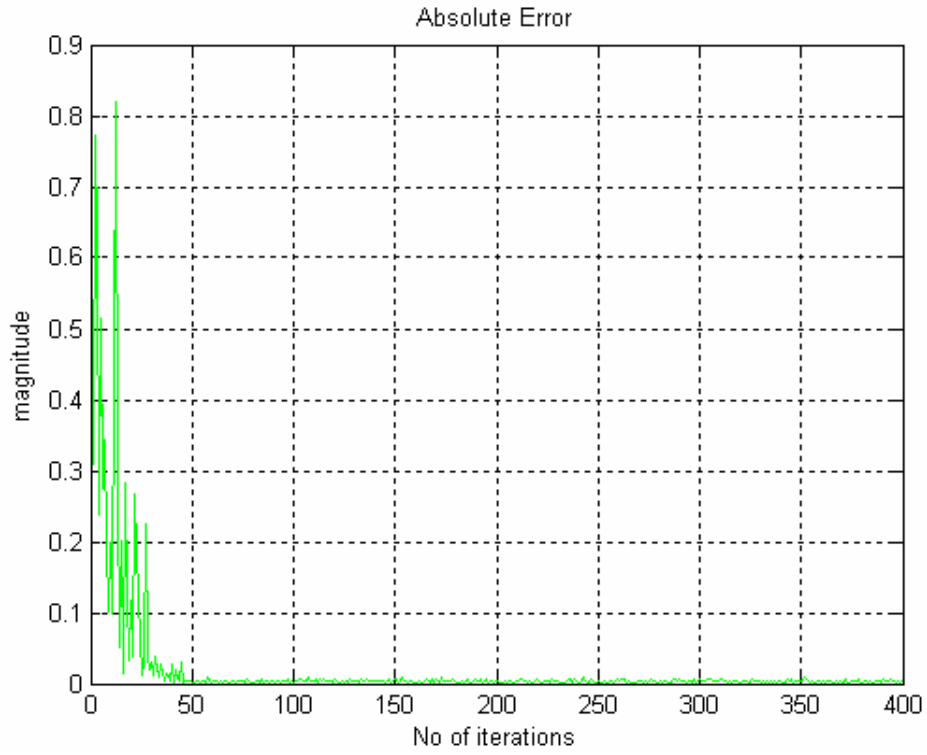

Figure 4.4: Convergence of NLMS algorithm

4.3.5 RLS algorithm (Recursive Least Square)

In the previous sections LMS and NLMS algorithms have been implemented and is observed from the simulation results that convergence of the algorithms is highly dependent on the values of forgetting factor. In order to resolve the problem of slow convergence, RLS algorithm that uses the information of the input data signal is used in [5], where is observed that rate of convergence of the system is faster than the LMS algorithm. In this case the performance of the system is improved at the expense of involvement of more computational complexity [5][25]. It requires a reference signal and also correlation matrix information due to which it is quite complex because at each iteration along with the weight vector $\mathbf{W}$, $\mathbf{R}^{-1}$ is also updated but it is almost ten times faster than the LMS algorithm. In the case of the RLS algorithm μ is replaced by $\mathbf{R}^{-1}(n)$ at the n^{th} iteration producing a weight update given by [5]:

$$\mathbf{w}(n) = \mathbf{w}(n-1) - \mathbf{R}^{-1}(n)\mathbf{x}(n)\mathbf{e}^{*}\mathbf{w}(n-1) \tag{4.8}$$

Where,

$\mathbf{R}(n) = \delta_0 \mathbf{R}(n-1) + \mathbf{x}(n)\mathbf{x}^H(n)$ and in this case (forgetting factor) $\delta_o \leq 1$

4.3.5.1 Matlab routine of RLS algorithm

$\mathbf{x}(n) = \mathbf{s}(n) + \mathbf{i}(n) + \mathbf{n}_n(n)$	Received signal constitutes components of desired signal, interference and receiver thermal noise
$\mathbf{R}(:,:) = (1/\delta)*I(8,8)$	Correlation matrix of input signal
$\delta = 0.1$	
$\mathbf{R} = \mathbf{R}(:,:)$	Correlation Matrix $\mathbf{R}^{-1}$
$\mathbf{v} = \mathbf{R}^* \mathbf{x}(n)$	Intermediate vector
$\mathbf{v}1 = 1/\lambda * (\mathbf{x}(n) * \mathbf{v})$	Intermediate vector
$\lambda = 0.999$	forgetting factor
$\mathbf{y} = \mathbf{a} + \mathbf{v}\mathbf{1}$, (a=1)	To keep parameters in range
$\mathbf{y}1 = 1/\lambda * (\mathbf{y} * \mathbf{v})$	Intermediate vector
$\mathbf{w}(0) = 0$	Initialize the weight vector
$\mathbf{e}(n) = \mathbf{r}(n) - \mathbf{w}^H \mathbf{x}(n)$	Calculation of error on each iteration (describes filtering of algorithm)
$\mathbf{w}(n+1,:) = \mathbf{w}(n) + \mathbf{e}(n) * \mathbf{y}1'$	Update weight vector on each iteration (adaptive operation of algorithm)
$\mathbf{w} = \mathbf{w}(n+1,:)$	Updated weight vector used for processing the signal
$\mathbf{R} = 1/\lambda * (\mathbf{R} - \mathbf{y}1 * (\mathbf{x}(n) * \mathbf{R}))$	Update of R^{-1} at each iteration

Having all the parameters same as used in case of ***LMS*** and ***NLMS*** algorithms except forgetting factor = 0.999, the simulation graph showing the mean squared error and the number of iterations it takes to converge in order to achieve the optimum solution is as shown in Figure 4.5 below which indicates that in this case the ***convergence is even faster than LMS and NLMS*** algorithms. Here as seen from simulation results below the RLS algorithm tends to converge after about ten iterations.

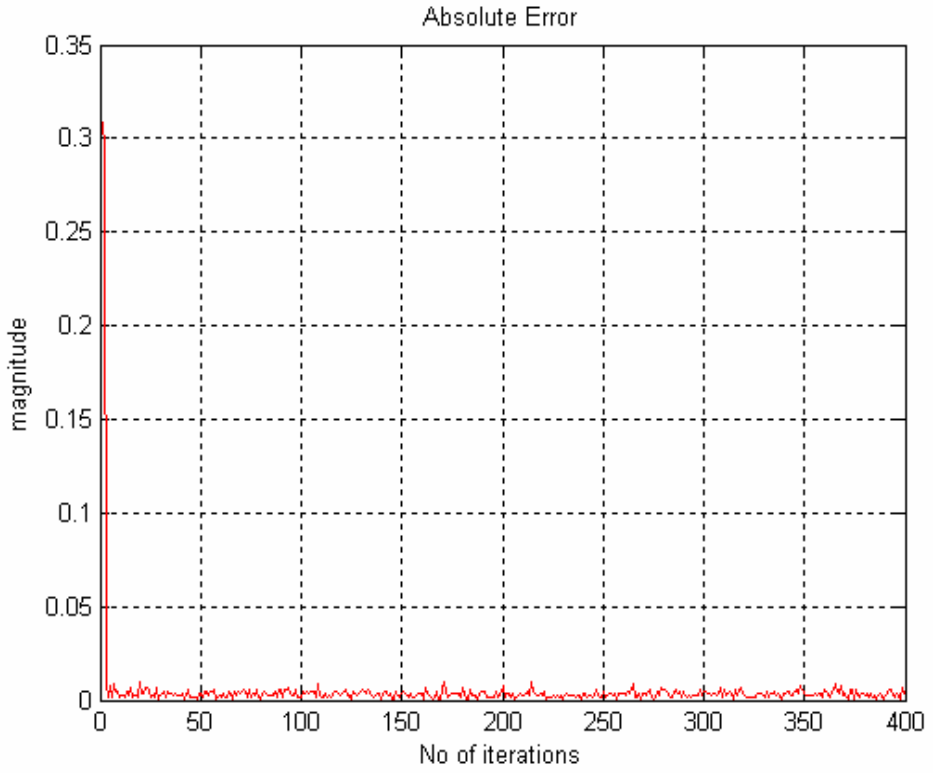

Figure 4.5: Convergence of RLS algorithm

4.4 Comparison of implemented adaptive Algorithms

Comparison of different adaptive algorithms in terms of convergence has been carried out and a result analysis is described below.

4.4.1 Result Analysis

(a) **LMS**. The rate of convergence for the case of the LMS algorithm is highly dependent on the step size parameter 'μ' which, if reduced, increases the rate of convergence of the LMS algorithm. On the other hand when the value of 'μ' is large, the rate of convergence is slowed down.

The weights are updated after every iteration for calculation of optimum output. The updated weight vector reached the optimum weight vector in about 150-200 iterations.

(b) **NLMS**. It is convergent in the mean square if value of 'μ' satisfies the condition i.e.$0<\mu<2$. If a small value is assigned to 'μ' then the adaptation will be slow which is equivalent to LMS algorithm.

Weight is updated but with slight modification than that of LMS. The updated weight vector reached the optimum weight vector in about 45 iterations.

(c) **RLS**. Rate of convergence is even faster than NLMS, almost ten times faster. This fast convergence rate is achieved because of the computational complexity involved in the computation of correlation matrix. Here along-with update of weight vector w, the fundamental difference between LMS and RLS is that step-size parameter μ is replaced by $\mathbf{R}^{-1}$ (inverse Correlation matrix) of received signal which is also updated at each iteration This has profound impact on convergence behaviour of RLS algorithm for stationary environment. Updated weight vector is used for calculation of an estimated output and from simulation graph it is seen that the updated weight vector reached the optimum weight vector in about 10 iterations. Mean squared error of RLS algorithm converges to zero as number of iterations approaches to ∞.

Algorithm	*Design Parameters*	*Forgetting factor (μ)*	*# of Iterations*	*Convergence Rate*
LMS	Number of iterations = 400 antenna elements = 8 $\mathbf{x}(n) = \mathbf{s}(n) + \mathbf{i}(n) + \mathbf{n}(n)$	$0 < \mu < 1$	200	Slow
NLMS	Same as in LMS	$0 < \mu < 2$	45	Faster than LMS
RLS	Same as in LMS	$\mathbf{R}^{-1}$ is used instead of μ	less than 10	Even Faster

Table 4-2 Comparison for rate of convergence of Adaptive algorithms

4.5 Simulations of adaptive algorithms for isolation of users

4.5.1 Statement of the Problem

Here we consider uniform linear array of 8 antenna elements spaced at a distance of half wavelength relative to the carrier frequency. The uniform linear array of antenna elements receives different signals from different directions in space. In this case the wanted user is operating from angle of 40^o, whilst the interferer is located at angle of -20^o. The aim of implementation of adaptive algorithms is to optimize the antenna array pattern in such a way that maximum possible gain is directed in the direction of a wanted user while placing a null in the direction of an interferer. In addition to that weight vector is also updated using equation (4.4) to calculate the error by subtracting the estimated signal from desired signal. When this

error signal approaches to zero the output obtained is considered to be an optimum output where the convergence of the algorithm takes place.

4.5.1.1 Implementation of algorithms

Let the desired signal of a wanted user denoted by $\mathbf{s}_w$ is arriving at 8 element antenna array spaced at distance of λ/2 from angle θ_w in degrees and interfering signals denoted by $\mathbf{s}_i$ are arriving at the antenna elements from angle of incidences θ_j respectively. It is also assumed here that the adaptive processor has a-priori knowledge of the direction of arrivals (DoAs) of both the desired and interfering signals. Each of the elements in the ULA is scaled by corresponding weights and summed to form the output signal. The weights are then controlled by an adaptive algorithm weight control, which operates on the received estimated signal and the desired signal from the direction of wanted user. The antenna array beamforming network configuration used for simulation is shown in Figure 4.1.

In case of ULA, the array steering vector is given by [5]

$$a = \left[1 \exp(-j\phi) \exp(-j2\phi) ..... \exp(-j(M-1)\phi)\right] \tag{4.9}$$

The estimated output of the adaptive processor $y(n)$ using (4.1) is as under:

$$y(n) = \mathbf{w}^H \mathbf{x}(n)$$

Where,

$\mathbf{w}$ = M -element weight vector

x(n) = The signal received at the antenna array given as:

$$\mathbf{x}(n) = \mathbf{s}(n) + \mathbf{i}(n) + \mathbf{n}_n(n)$$

This received signal is the composite signal of wanted user, interferer and Gaussian noise.

$\phi = 2\pi d \sin\theta / \lambda$

θ = Angle of arrival in degrees

d = inter antenna element spacing

λ = Wavelength in meters

$\lambda = c / f_c$

c = $3*10^8$ i.e. velocity of light

f_c = carrier frequency

The mean squared error (MSE) criterion is used for optimization. The aim is to develop a general framework for the simulation of the *LMS, NLMS and RLS* algorithms and to simulate their performance for various configurations of the antenna array and the number of interferers. The design parameters used for implementation of the algorithms are given as in the Table 4-3 below.

Parameters	***Values***	***Parameters***	***Values***
Number of samples (M)	400	Sampling period (t_s)	1.0E-10
Number of antenna elements	8	Frequency (f_c)	2.0GHz
AoA of wanted User (θ_w)	40^0	Wavelength (λ)	C/f_c C=3.0E8 m/sec
AoA of Jammer (θ_j)	-20^0	forgetting factor (μ)	0.0999(NLMS) 0.005(LMS)

Table 4-3: Design Parameters for LMS/NLMS and RLS adaptive algorithms

The simulation results for identifying AoAs and convergence of *LMS, NLMS* and *RLS* algorithms obtained are shown below in Figure 4.6, Figure 4.7 and Figure 4.8 respectively.

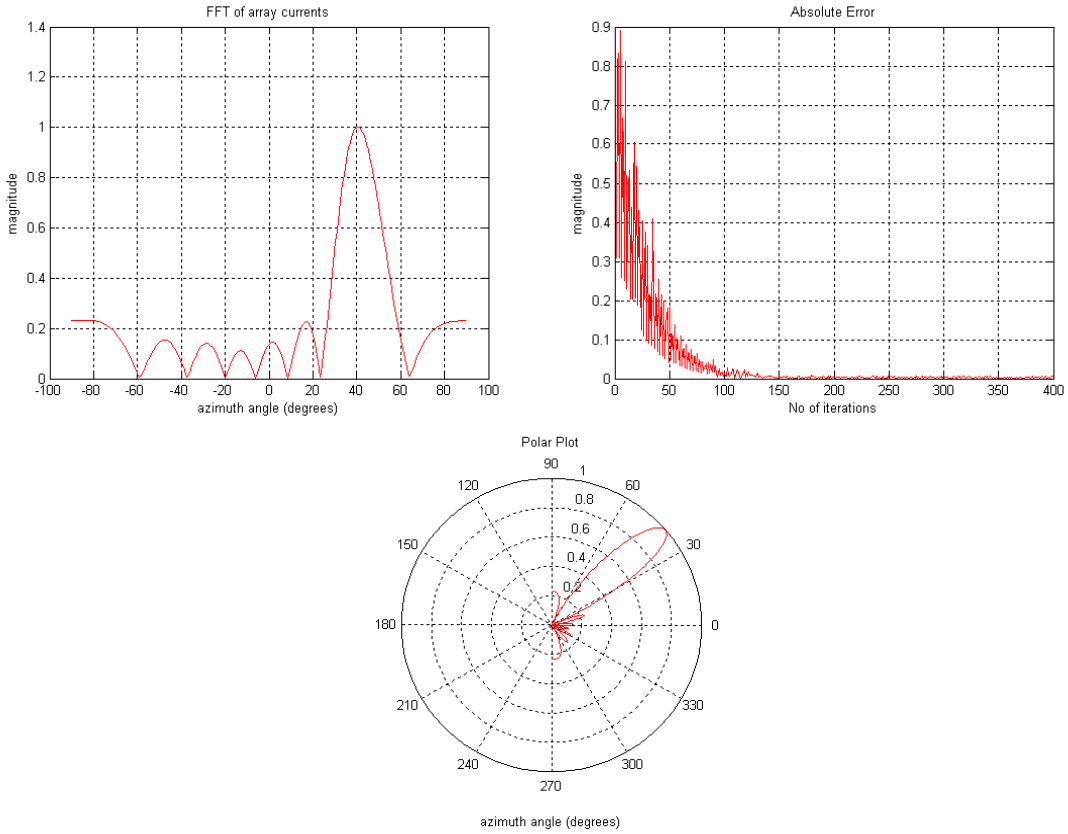

Figure 4.6: (2-D, Polar and MSE) Plots of LMS algorithm

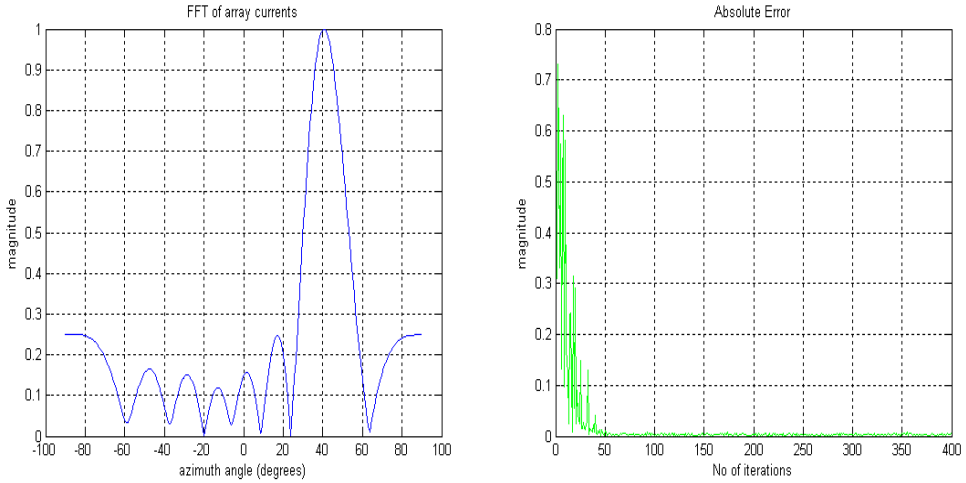

Figure 4.7: (2-D and MSE) Plots of NLMS algorithm

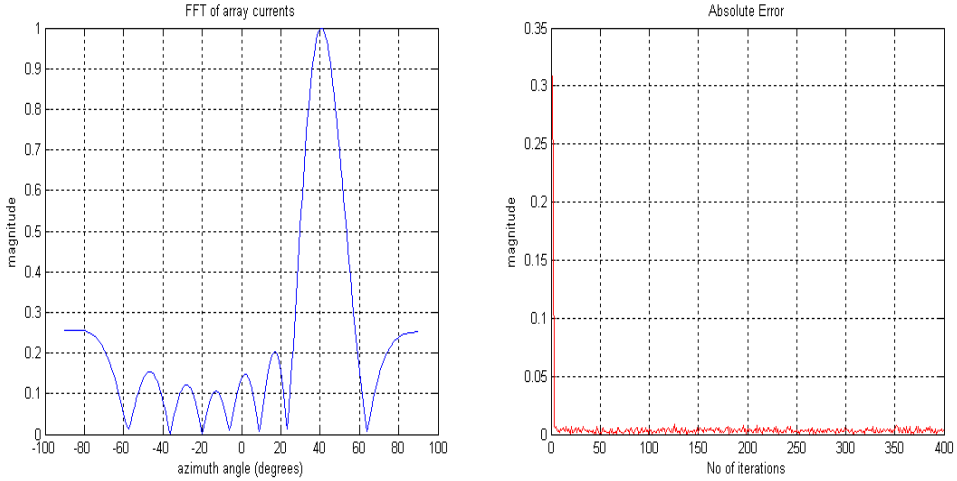

Figure 4.8: (2-D and MSE) Plots of RLS algorithm

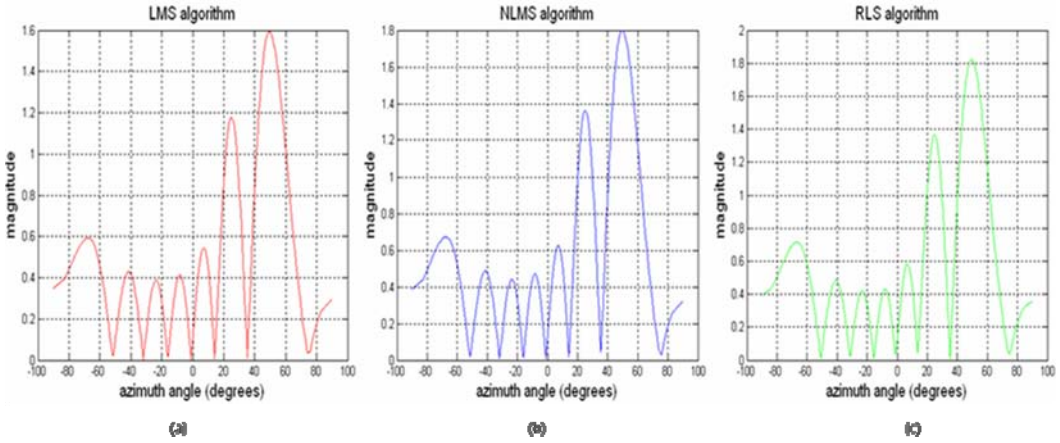

Figure 4.9: Nulling of interferer at closer angular positions (40^o, 35^o)

4.5.2 Results Analysis

From the simulation graphs of adaptive algorithms in Figure 4.6, Figure 4.7 and Figure 4.8 it is observed that convergence time of all the algorithms is dependent on forgetting factor. The values of forgetting factor chosen for simulation of all the adaptive algorithms have been given in the design parameters Table 4-3 above. In case of RLS algorithm the convergence rate is faster than other two algorithms. This fast convergence rate is achieved because of the computational complexity involved in the computation of correlation matrix. The simulation results for convergence of adaptive algorithms are quite close to theoretical results in [5].

For isolation of an interferer from a wanted user the simulation graph of Figure 4.9 shows that in all the algorithms once interferer is operating from a position closer to the wanted user (in this case the interferer is at 35^o and wanted user is operating from an angle of 40^o).It is observed that from closer angles although null is formed in the direction of an interferer but the main beam is not directed towards wanted user rather is shifted due to the effect of sidelobes of the interferer.

4.6 Genetic Algorithms

4.6.1 Introduction

In the previous sections of chapter-3 and chapter-4 classical methods of LMS, NLMS and RLS adaptive algorithms have been discussed and is observed from the simulations of the adaptive algorithms that the convergence time in order to find the optimum output is very fast in case of RLS adaptive algorithm, where the algorithm converges in first 4-5 iterations but on the other hand it is also observed that if wanted user and an interferer are operating with common BS from close angular positions may be about 5-10 degrees apart, a null as compared to conventional method of nulling an interferer by an optimum beamformer is formed in the

direction of an interferer but still the interferer is not nulled out properly by forming deep null, in addition to that main beam is also not directed towards a wanted user because of the effects of side-lobes. In the second case when two users are farther apart by about more than 15-20 degrees, then wanted user is isolated from interferer by forming main beam in the direction of wanted user but still the interferer is not nulled out properly.

There are many ways to improve the beamformer but in order to isolate the wanted user from an interferer by always forming a deep null in the direction of an interferer irrespective of the fact that they are operating from closer angular positions or far apart a novel method of optimising the weights with the help of Genetic algorithm and then using in the RLS adaptive algorithm is used.

The first time research on GA was conducted by John Holland and his colleagues at the University of Michigan [19]. The aim of GA is to find the approximate solutions to the problems that are difficult to be solved by application of the principles of evolutionary biology to computer science. The techniques used by GA to find the solution of a particular problem are based on natural selection, crossover and mutation. These algorithms are regarded as a particular class of evolutionary algorithms where the individuals are randomly generated and the process of evolution starts on these randomly generated population and goes to generations. The fitness of the whole population is evaluated in every generation and base on the fitness different individuals are selected from the current population before going through the process of mutation or crossover to create a new population that then becomes the current population for the next iteration.

Genetic algorithms represent a highly idealized model of natural process that are loosely based on Darwinian principles of biological evolution. Biological strategies are used to enhance the probability of survival and propagation during their evolution [26][35]. Genetic algorithms are very useful in solving complicated problems. A genetic algorithm is an efficient method to perform a search of a very large, discrete space of phase settings for the minimum output power of the array. It randomly generates a set of possible solutions to the problem, which is being investigated and is termed as initial generation. While developing a genetic algorithm, strings and characters are used in order to simulate chromosomes and genes corresponding to natural genetic system.

4.6.2 Strengths of GAs

As most of the other algorithms are serial and have the capability to find out the solution of particular problem by one method only and in case the solution is not correct the process starts over from the beginning. However, as the GA have the capability of performing task in

parallel, they can find out the solution of a particular problem in parallel at once. If the solution is not found in one task then that task is left out and parallel processing is continued until an optimum solution is achieved.

The important field of the application of GA is in case of discontinuous functions having complex fitness value or the problem defining many local optimum solutions. In that case the gradient based methods do not find the exact solution by getting stuck to the local optimum solutions but GA has the capability to search over the entire area starting from bottom and reach to an optimum solution.

4.6.3 Limitations of GAs

Although GAs have the capability of solving the problem very efficiently but these algorithms have some of the limitations.

The first and most important consideration in creating a genetic algorithm is defining a representation for the problem. The problem can be defined in away that the individuals are represented by numbers such as binary-valued, integer-valued, or real-valued. In case of binary values the strings are regarded as 0 or 1.

There is another problem of defining the fitness function that needs to be carefully defined so that fitness value of higher degree is achieved that is closer to an optimum solution of the given problem. If the fitness function is not defined properly, the optimum solution of a problem will not be found by the genetic algorithm.

4.6.4 Characteristics of GAs

Some of the fundamental differences between GA and traditional optimization routines are as under [21,22]

a. The method of optimisation is quite different from classical optimization algorithms.
b. Genetic algorithms work with a coding of parameter set and not the parameters themselves.
c. Genetic algorithms search from a population of points and not a single point.
d. Genetic algorithms use the objective function information and not the derivatives or the auxiliary knowledge.
e. Genetic algorithms are original systems based on the supposed functioning of the living natural things.
f. Genetic algorithms use probabilistic transition rules and not the deterministic rules.

4.6.5 Working of a simple genetic algorithm

A flow chart of a simple genetic algorithm is given in Figure 4.10 below. Here in this case population of individuals is generated randomly, where theses randomly generated individuals are decoded and evaluated on the basis of the value defined in the fitness or cost function [21]. These individuals are ranked based on the value of fitness. In the next step the individuals with high fitness value are selected for generation of new population of individuals. After the *ranking* procedure the bottom 50% of the members are discarded and then the *Crossover* is performed on remaining 50% by forming pairs of these genes and then selecting a crossover point for each pair of genes. Two new and slightly different ''*children*'' are formed from this cross over point. The next generation again consists of top 50% of previous generation and other 50% is the result of this crossover operation on these parents. At last *mutation* is performed which randomly selects and changes 1's to 0's and vice versa. This random mutation helps to keep the system from settling into local minimum [22].

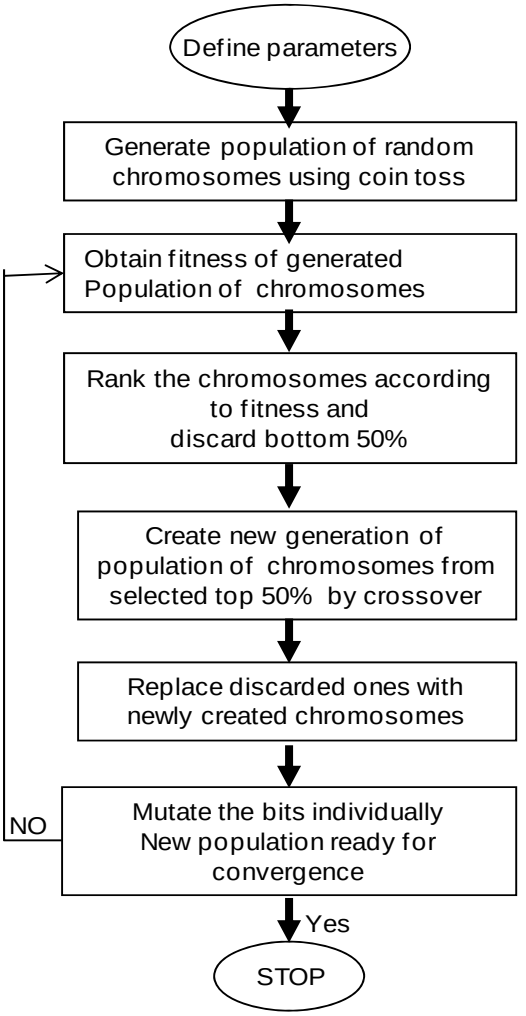

Figure 4.10: Flow Chart of simple genetic algorithm

4.6.6 Operators of Genetic Algorithms

4.6.6.1 Selection

The method of selection [21] used is based on ‘‘roulette wheel’’ technique to select the individuals based on some performance. The schematic of roulette wheel selection is shown in Figure 4.11. In this method the chromosomes are selected from population of chromosomes generated randomly by coin toss on the basis of fitness value. In this process there is no surety that a chromosome with high value of fitness will be selected for next generation. The working mechanism of is such that entire wheel represents the total fitness value of the population. The roulette wheel is divided into different sections and one section of the wheel is allocated to each chromosome of the population. Every section of the wheel is according to the fitness value i.e. if the value of fitness is more then size of that section of the wheel will be large as compared to other sections having less fitness value. In this case as shown in Figure 4.11 chromosomes 5 and 7 have more fitness value, they are allocated larger part of the wheel whereas chromosomes 4 and 8 are the least fit and have correspondingly smaller part of the roulette wheel. This operator selects the chromosomes from existing generation that are regarded as parents for next generation. The probability of selection of each chromosome is given as:

$$F\left(x_i\right) = \frac{f\left(x_i\right)}{\sum_{i=1}^{N_{pop}} f\left(x_i\right)}$$

Where $f(x_i)$ is the fitness value for each chromosome N_{pop} is the total size of the population. This fitness assignment ensures that each individual has a probability of reproducing according to its relative value of fitness. Parents are selected in pairs, when one chromosome is selected the probabilities are renormalised without selected chromosomes, so that spouse is selected from remaining chromosomes. Thus each pair is composed of two different chromosomes and is even possible for a chromosome to be in more than one pair.

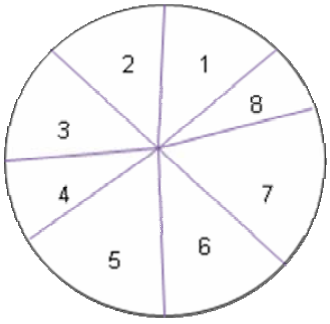

Figure 4.11: Roulette wheel selection technique

4.6.6.2 Crossover

The crossover is simply a chance that two chromosomes will swap their genes/bits. A good value of crossover may be defined to have a value of 0.7 to 0.8. In case of this crossover process a point is randomly selected in the chromosomes and all genes after that point are swapped. The same can be represented by example where two chromosomes are given as:

Chromosome-1 = 10001001

Chromosome-2 = 01011110

Here a random bit at point 4 is chosen in the chromosomes and then all the bits after that point are swapped. The new chromosomes would then be as under:

Chromosome-1new = 10001110

Chromosome-2new = 01011001

4.6.6.3 Mutation

In GA mutation is a process where a point is chosen randomly along the length of chromosome and a bit is inverted at that chosen point. The main aim of mutation process is to stop the GA from stucking to a local minimum. For example a binary digit '1' will be changed to a binary digit '0' and digit '0' will be changed to digit '1'.

4.6.6.4 Example for implementing a GA

This example demonstrates the implementation of a genetic algorithm, where four individuals defined as 'A', 'B' ,'C' and D form a population. Theses indivuals are considered as binary strings (genes) having a length of 8 bits in every string. The value of the fitness is based on the number of '1's in the binary encoded string, with the probability of crossover such as $p_{cross}=0.8$, and probability of mutation considered as $p_{mut}=0.001$. Here the definition of fitness function is very simple and does not involve any complexity in terms of decoding. The initial (randomly generated) population is given in Figure 4.12 below:

Individuals	***Genes***	***Fitness Value***
A	00000111	3
B	11101111	7
C	01100000	2
D	01110100	4

Figure 4.12: Initial population of Chromosomes

Taking into account the fitness value defined above as the selection criteria we have to choose 4 individuals defining two sets of parents. Let the two sets of parents like {B,D} and {B,C} are chosen according to the probabilistic procedure of selection. After this selection procedure of the parents, the process of Crossover is performed with probability of crossover (p_{cross}) thereby producing two off-springs. There is also a possibility that exact copies of parents are obtained as off-springs in case crossover is not performed. In the example stated above, crossover takes place between parents B and D at the (randomly chosen) first bit position thereby creating offsprings denoted as E=11110100 and F=01101111, whereas no crossover is performed on parents B and C, thereby creating the offsprings that are exact copies of B and C. After crossover operation now the process of mutation takes place with probability of mutation as (p_{mut}) per bit. For example, if offspring 'E' is mutated at the sixth position then we get E'=11110000, offspring B is mutated at the first bit position to form B'=01101111, there is not any mutation that takes place on offsprings F and C. The next generation of population of chromosomes, after going through the cycle of operations like selection, crossover, and mutation is therefore as shown in Figure 4.13 below:

Label	*Genes*	*Fitness*
E'	11110000	4
F	01101111	6
C	01100000	2
B'	01101111	6

Figure 4.13: New generation of population

In this new generation, although there is not any individual that has fitness value of 7 as shown in Figure 4.12 above, but now the overall value of fitness is increased to 18 as compared to a value of 16. If this procedure is performed consecutively the GA will eventually find an individual with fitness value of '8' i.e. all the bits in a string of that individual will be '1's to give a fitness value of '8'.

4.6.7 Characteristics of an adaptive algorithm [22]

(a) It places deep nulls in the direction of interference sources.

(b) It rejects the interference over bandwidth of antenna.

(c) It places nulls very quickly.

(d) It minimizes the pattern perturbations

Although an adaptive algorithm possesses some of these characteristics, but no adaptive algorithm meets all of these characteristics. Hence selection of an adaptive algorithm depends

upon the antenna, the cost, performance and the interference requirements. A phased array has many advantages over other antennas, including higher gain than a single element, electronic beam steering and control over the antenna pattern. Changing the weights of elements changes the antenna pattern with lower side-lobes and nulls in the direction of interferers.

4.6.8 Simulation of RLS adaptive algorithm based on GA

Here GA is used for optimisation of beam pattern thereby having a capability of forming deep null in the direction of interferers by minimising the total output power of the array. A uniform linear phased antenna array considered is a group of 8 antenna elements equally spaced at a distance of $\lambda/2$ whose outputs are added together to provide a single output. The architecture of phased antenna array is such that half of the antenna elements in the array are operating as conjugate of the other half antenna elements. The schematic diagram of phased antenna array comprising of 8-elements equally spaced called as linear phased antenna array beamforming network configuration is given in Figure 4.14 below. Aim is to cancel an interferer adaptively with the help of phase-nulling antenna array using a technique of adaptive RLS based genetic algorithm, which uses a limited number of bits of the digital phase shifters. In this case the phase shifter settings evolve until the antenna pattern has nulls in the direction of interferers. The genetic algorithm begins with the population of 8 chromosomes through 50 iterations to create a new generation after going through all the processes of selection, crossover and mutation. This new population created is then used to find the phase angle after decoding and ultimately weight vector $\mathbf{'w'}$ is calculated from vector containing these nulling bits. Weight vector update is obtained by adaptive method used for RLS algorithm. This process is repeated for 200 iterations to get the optimum solution of weight vector that is then used to form a deep null in the direction of jammers operating from different angles.

Here two cases are considered in the simulation for the purpose of analysing the difference in results if the interferers are operating from closer angular distance or they are away from each other. In first case it is assumed that two interferers are operating from 50^o and 70^o angles respectively and simulation results of Figure 4.16 indicate that deep null is formed in the direction of both interferers with the help of RLS based GA. In the second case now the interferers are operating from closer angles such as 20^o and 30^o then even closer angles of 10^o and 15^o. The simulation result of Figure 4.16 shows the radiation pattern, where deep nulls are formed in the direction of all the interferers operating from closer angular distances. A genetic algorithm finds an optimum solution by simulating evolution in nature. The number of chromosomes, number of bits per chromosome and the number of iterations

are defined in the beginning of the program. The design parameters for simulation of algorithm are given in the Table 4-4 below:

Parameter	***Value***
Number of iterations	200
Number of ant elements (2*M*)	8
Angle of interferer-1 θ_{j1}	$50^0, 20^0, 10^0$
Angle of interferer-2 θ_{j2}	$70^0, 30^0, 15^0$
Carrier frequency (f_c)	2.0GHz
Sampling time (t_s)	1.0E-10
Inter element distance (d)	$\lambda/2$
wave length (λ)	C/f_c
Probability of mutation (*rho*)	0.001
Probablity of crossover (crossprob)	0.8

Table 4-4: Design parameters for RLS based GA

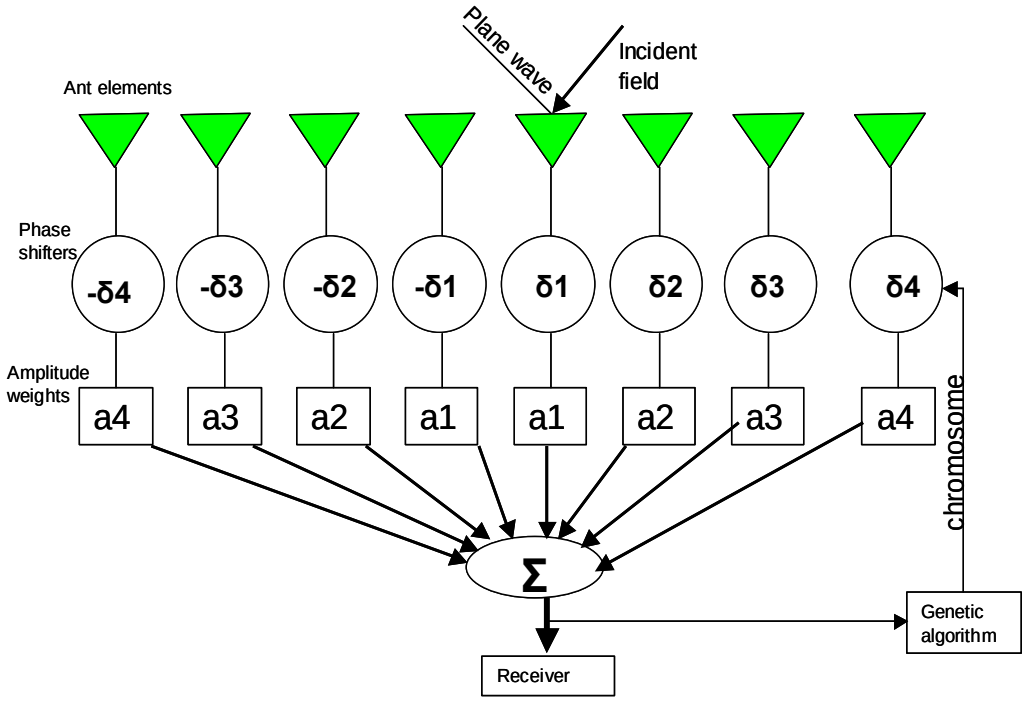

Figure 4.14: Phased Antenna Array[93]

The array far field pattern is given by [91]

$$AF = \frac{\sin(\phi)}{2M} \sum_{m=1}^{2M} \mathbf{w}_m e^{j(m-M-0.5)\psi} \tag{4.10}$$

Where,

$2M$ = number of elements in the array

$\mathbf{w}_m = a_m e^{j\delta m}$ Complex array weight at element m

$$\psi = kdu$$

$$k = 2\pi / \lambda$$

λ = wave length in meters

d = inter element spacing

$u = cos(\phi)$

ϕ = Angle of incidence of electromagnetic plane wave

a_m = Amplitude of the weights

δ_m = Phase shifters

The amplitude weights are fixed and digital phase shifters have 'B' bits. The 'B' needs to be as small as possible to reduce the cost of the phase shifters but must be large enough to maintain low sidelobes over the scan angles of array. The nulling phase δ_m is given by

$$\delta_m = 2\pi \sum_{p=1}^{P} B_p 2^{-p} \tag{4.11}$$

where,

B = total number of bits in the phase shifters

P = number of phase bits used for nulling

$\delta_m = [b_1\ b_2\ \ldots\ldots\ldots b_p]$, vector containing nulling bits

The parameters and cost functions must be specified for optimization of an antenna array. The cost function used for optimization is given by

$$Y = 24 * x - 3 * x^2 \tag{4.12}$$

Here x is the population of chromosomes used for the generation of population. The cost function is used to ensure that deep null is directed towards an interferer which is achieved as and when the value of (4.12) is zero and contribution of interferers is cancelled as a result a deep null is formed in the direction of interferers. This nulling of interferers is alos dependent upon the best set of population achieved after specified number of iterations.

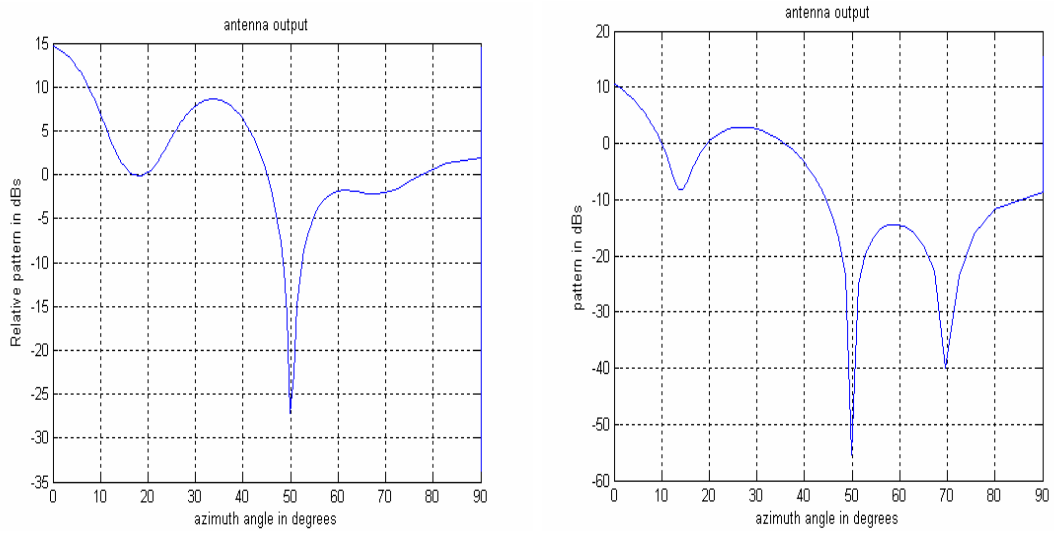

Figure 4.15: Radiation pattern with nulls in the direction of Interferers at 50 and 70 degrees

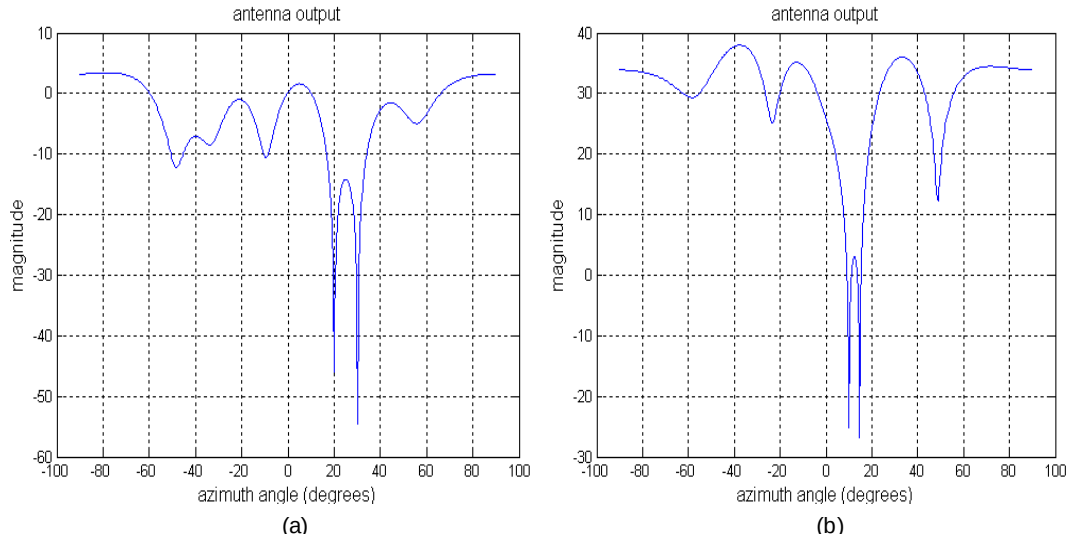

Figure 4.16: Radiation pattern with nulls in the direction of interferers at 20,30,10 and 15 degrees

4.6.8.1 Results Analysis

From the simulation results shown in Figure 4.15 and Figure 4.16, it is observed that when interferers are operating from angles wider apart or closer to each other, a deep null is formed towards each interferer. This is achieved due to optimization of weights with the help of genetic algorithm and then updating with RLS adaptive algorithm. The nulling of interferers is dependent upon the best set of population achieved after specified number of iterations.

Here the advantage of using GA with RLS adaptive algorithm is that interferers are nulled out properly even if they are operating from closer positions which can not be achieved with traditional gradient based search algorithms. Traditional methods search for the best solutions depending upon the gradient and/or random guesses. In case of gradient methods

they converge to a minimum once an algorithm is close to that minimum, therefore have the disadvantage of getting stuck to that local minimum. On the other hand random search methods tend to get slow and getting stuck to local minimum.

Here in this case RLS based GA has proved to be successful, where the algorithm places deep nulls very quickly by minimising the output power to reject the interferers.

If the algorithm is not converging then to sort out the problem of convergence the number of chromosomes may be increased.

4.7 Summary

In this chapter different adaptive algorithms such as LMS, NLMS and RLS algorithms have been implemented to get the optimum output by forming main beam pattern in wanted direction while nulling out the interferers. The results of the convergence of the algorithms are also shown when the optimum output is achieved by comparing the reference signal with estimated output. A comparison and result analysis of all the algorithms is also described after the simulation of these algorithms to observe the efficiency and performance of each algorithm. It is observed that rate of convergence of each adaptive algorithm is dependent on the definition of forgetting factor which needs to have a small value may be i.e. $0 < \mu \leq 1$. The convergence of RLS algorithm is quite fast compared to LMS and NLMS algorithm because of the involvement of computational complexity of correlation matrix **R** of input data.

In this chapter it is also highlighted that while implementing block adaptive method (SMI), the number of samples needed to obtain the correlation matrix, (i.e. the array support) is very important. When fewer samples are used, the estimate of $\mathbf{R}_{i+n}$ becomes progressively poorer and this impacts on the computation of the optimum weight vector. The sidelobe structure becomes increasingly random and the depth of the null in the direction of the interferer also becomes much reduced.

In addition to above some basics required for implementation of genetic algorithm are also discussed before implementation of GA alongwith some strengths and weaknesses of the GA. Finally novel method of RLS based GA is implemented to show the simulation results for forming deep nulls in the direction of interferers operating from closer angular distances about 5^o apart from each other, which can not be achieved with traditional gradient based search algorithms. Traditional methods search for the best solutions depending upon the gradient and/or random guesses. In case of gradient methods they converge to a local minimum or local maximum once an algorithm is close to that minimum or maximum, therefore have the disadvantage of getting stuck to that local minimum or local maximum. Therefore in ordre to avoid this problem the method of GA is used that searches over population of points and finds the maximum or minimum over range of populations.

Here RLS based GA has proved to be successful, where the algorithm places deep nulls very quickly by minimising the output power to reject the interferers.

Chapter -5:

5 Opportunistic Communication System

5.1 Introduction

The previous chapter has examined the use of the number of adaptive algorithms that allow the antenna beam pattern to respond dynamically, to the changes in the position of the wanted and interference signal sources and isolating the wanted user and an interferer with the help of an antenna array.

In this chapter, the opportunistic communication system is implemented that uses a novel network protocol, that only transmits to a user when the channel conditions to that particular user are good, whereas in case of traditional communications systems the resources are allocated according to the demands of user without considering the quality of a channel as a result channel capacity is lost when the channels get faded. Different cooperation protocols like amplify-and-forward and decode-and-forward [106][107] have been introduced for wireless networks. In most of the existing cooperative communication in wireless systems the communication is based on the multi-hop systems, where the information from source is carried to the destination through other mobiles that act as the relays. This relaying operation overcomes the problem of path-loss that occurs because of large distances. This relay channel was introduced by Van der Meulen [108] and then investigated by Cover and El Gammal [109]. The research work carried out the analysis of three nodes such as source, relay and destination. As in case of mobile channel the fading is considered to be a source of unreliability that needs to be mitigated at all cost and communication is considered to be a source of mitigating the fading in wireless networks by achieving spatial diversity. Relays are used to help the source by transferring the information to the destination but source needs to decide when to cooperate by taking the ratio between source-destination channel and source-relay channel conditions [110]. The concept of multiuser diversity is exploited by opportunistic communication, where multiple users are communicating with common BS in the time varying fading channels while remaining in the same cell. It is assumed that channel state information is tracked at the receivers and fed back to the transmitters and scheduling in this case is done on the basis that a user with good channel conditions is only allowed to transmit to the BS. Here the diversity gain is achieved in a sense, that since many users are communicating with common BS via an independent varying channel so there are all the chances that a user may get a channel at an instant when the channel is at its peak. Traditionally the fading in a channel is considered to be a source of unreliability which must be mitigated. When multiple users are communicating simultaneously then transmission is

scheduled by allocating a channel to users only when their channels are at peaks [112]. Therefore an opportunistic communication may be used to exploit the channel fluctuation where transmission only takes place when the channel is at its peak. So the performance of the system is then related to a channel condition when it is at peak rather than average conditions of the channel. From Figure 5.1 below it is seen that opportunistic communication systems allocate bandwidth dynamically based on the condition of the channel to individual users and all users with good channel conditions are dynamically allocated lots of bandwidth while users in deep fades are allocated little bandwidth. Since the fading is random so all users get their fair share of the bandwidth, hence the opportunistic communication systems can provide more capacity in fading channels as compared to traditional approach.

In this case, a number of algorithms in various fading environments using Rayleigh and spatial channel models using omni directional and adaptive antenna at the BS have been developed that allow the users to communicate with common BS, depending upon the condition of the channel of that particular user. This aspect of opportunistic communication is considered in this chapter.

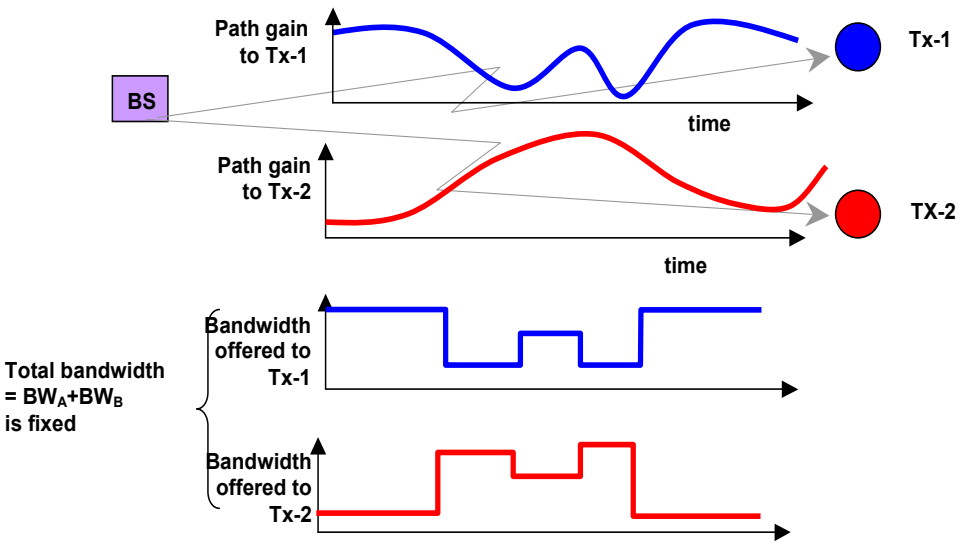

Figure 5.1: Fair allocation of Bandwidth

5.2 Channel allocation based on quality

In this case a communication system is considered where multiple users equipped with single antenna are communicating with common BS that is equipped with uniform linear array of antenna elements. The opportunistic communication system provides the idea of Multiuser

diversity in the sense that in this system different users are operating over an independently fading channel, there is a chance that one of the users is likely to have very good channel condition at the instant of time. Whenever a particular user with good channel condition has been allocated a channel for the duration it remains at its peak, then that user has a chance of transmitting the maximum data to the BS. The resultant SNR of that particular user at the instant of time when the data is transferred can be written as:

$$SNR(t) = \max |h_k(t)|^2 \tag{5.1}$$

Where, $k = 1 \ldots\ldots K$ i.e. the total number of users in a system

The resultant output of the system can be expressed as

$$y(t) = \sum_{k=1}^{K} h_k(t) x_k(t) + \mathbf{w}(t) \tag{5.2}$$

Where, $h_k, x_k, \mathbf{w}$ are the channel gain, data transmitted and the additive white Gaussian noise respectively.

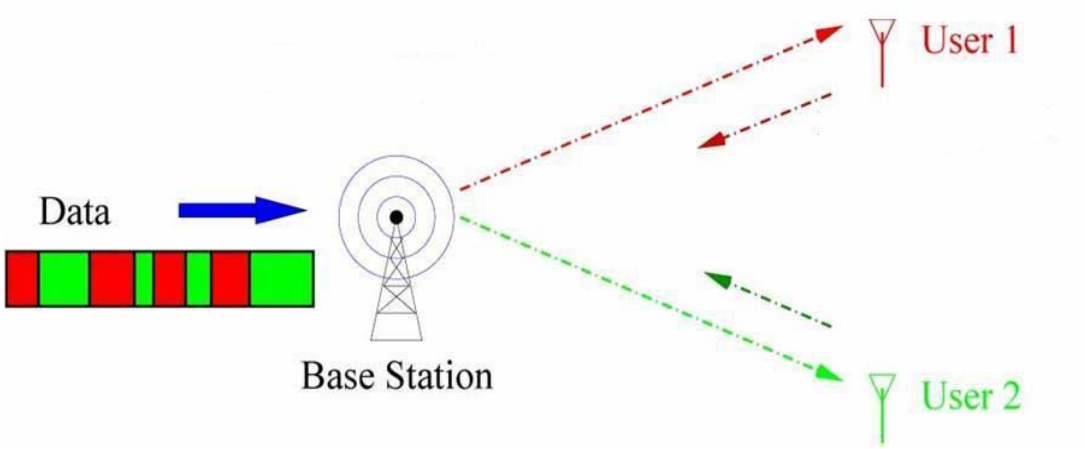

Figure 5.2: Channel allocation based on quality

Here in this Figure 5.2 it is seen that both the users are placing a request to the BS for fair scheduling of resources depending on the Bandwidth and allocation of channel. So in this case the channel quality of the user k at the instant of time based on the requested data rate is represented as $R_k(t)$. This is the data rate that a user can support at the instant of time. The scheduling algorithm works on the principle that it keeps track of the average throughput denoted as $T_k(t)$ of every user in the previous interval of time t. In time slot t, the scheduling algorithm transmits with highest ratio of request to the throughput represented as:

$\frac{R_k(t)}{T_k(t)}$, where R_k is the request of the user placed to the Bs while T_k is the throughput transferred to BS. This scheduling of the users is done on the basis that whichever user has

good channel conditions is allowed to transmit to the BS. The total throughput increases with the number of users in both the fixed and mobile environments. As the channel fades in both cases, the rate of variation is more in case of mobile channel as compared to fixed channel as a result the peaks are going to be higher in case of mobile channel environment, which determine the scheduling of the users. It can be stated that Multiuser diversity is variable in case of mobile channel as compared to fixed channel where it is limited. The amount of Multiuser diversity depends on the dynamic change in the fluctuation of channel characteristics.

Consider a system having *N* transmit antennas at the BS and let $h_{n,k}(t)$ is the gain from antenna *n* to the user *k* at the instant of time *t*. The block of symbols *x(t)* is transmitted in the time slot *t*. Then the signal received by the k^{th} user during the time slot *t* is given by

$$y_k(t) = \sum_{n=1}^{N} \sqrt{\alpha_n(t)} e^{j\theta_n(t)} h_{n,k}(t) * x(t) \tag{5.3}$$

Where $n = 1 \cdots\cdots N$ is the number of transmit antennas, and overall channel gain seen by the receiver *k* is given by

$$h_k(t) = \sum_{n=1}^{N} \sqrt{\alpha_n(t)} e^{j\theta_n(t)} h_{n,k}(t) \tag{5.4}$$

Where, $\alpha_n(t)$ is the power allocated to each of the transmit antenna and $\theta_n(t)$ is the phase shift applied to the signal at each antenna. The fluctuation in the channel is achieved by varying these quantities ($\alpha_n(t)$ from 0 to 1 and $\theta_n(t)$ from 0 to 2π) over a time period *t*.

In case of single transmit antenna system, every receiver *k* feeds back the overall SNR i.e. $|h_k(t)|^2$ of its own channel to the BS and accordingly BS schedules the transmission to all users depending upon the quality of channel of a particular user. There could always be a possibility that the channels are symmetric having same quality with equal SNRs or asymmetric with different properties. The analysis for both types is carried out with the help of simulations to see the effect on BER performance in section 5.14 below.

5.3 Rayleigh channel model

Different scenarios like flat fading and multipath frequency selective fading of Matlab Rayleigh channel model using omni-directional antenna at BS are implemented in the subsequent sections to see the BER performance characteristic curves of different co-channel users communicating with common BS.

5.4 Scenario-1 (flat fading)

Here the scenario is that two Mobile users MS-1(user 1) and MS-2(user 2) moving at a speed of 1.25m/s corresponding to a doppler of 10Hz and carrier frequency of 2.4GHz are communicating with a common BS, each mobile user is operating at independent path with BS. Two Rayleigh dice are rolled that determine which channel should transmit. When the channel is allocated to one transmitter it is allowed to send across the data in frames depending upon the condition as to when the channel is allocated to that particular user and AWGN is added to it. Here phase estimation is done at receiving end to compensate the phase distortion in the channel.

5.4.1 Methodology implemented

a. Generate two data streams of random integer numbers for Mobile_1 and Mobile_2 and then split this stream of data into blocks of data.
b. Modulate the two data streams using appropriate phase shift keying modulator.
a. Generate two Rayleigh channels (single path) with 10Hz doppler for both links.
d. These two channels are monitored regularly at every block of data and at the instant of time when the link_1 is better than link_2 the entire block of data from Mobile_1 is sent to Base Station, Where it is equalised, demodulated and then checked for errors.
e. At the end of each block the channel is checked again and block of data is sent from Mobile_1 or Mobile_2 depending upon the condition of channel whichever is in better state/condition.

The schematic diagram of two users communicating with common BS is shown in Figure 5.3 below, whilst the design parameters for implementation of the scenario are given in Table 5-1 below.

Parameters	***Values***	***Parameters***	***Values***
Channel Rayleigh	flat fading	Sampling time	100μsec
Number of Paths	1	Doppler (f_d Hz)	10
Number of Users	2	Modulation Scheme	PSK
Number of frames	20,000	Modulation order (M)	2
Bits/frame	10		

Table 5-1: Rayleigh flat fading Parameters (2-Users opportunistic)

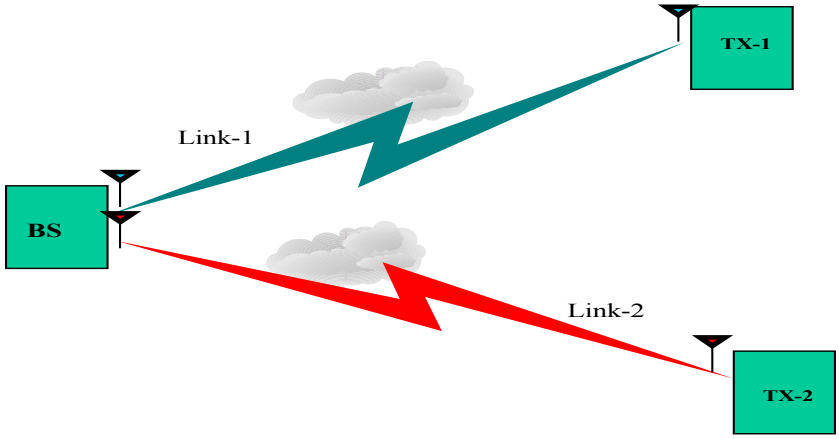

Figure 5.3: Two Users communicating with common BS

5.4.2 Description of Simulation

In this case channel coefficients are generated for both users operating between BS with independent paths. A channel selection criterion is made on the basis of magnitude^2 of the channel coefficients in order to determine as to when the Mobile_1 or Mobile-2 should communicate with the BS depending upon the quality of channel. Once the channel has been allocated to a particular user depending upon the quality of the channel a frame of random binary data bits is generated and converted into symbols. This data comprising of stream of symbols is modulated with the help of phase shift keying modulator and then sent across the channel. At the receiving end the received signal is corrupted with additive white Gaussian noise and then demodulated with the help of an appropriate demodulator taking into account the phase estimator to compensate the phase error. Finally the received stream of symbols is converted back to binary data bits and stored in the buffer. The same procedure is repeated for other user when the channel is allocated to that user as opportunistic method of transmission is used to explore the quality of the system. At the end the data bits stored in the buffer are compared with the original randomly generated binary data bits and BER performance is computed and plotted as shown in the graphs of Figure 5.4. The simulation result is also plotted for the case when there is no cooperation between both users and the channel is used by both users simultaneously.

5.4.3 Simulation result

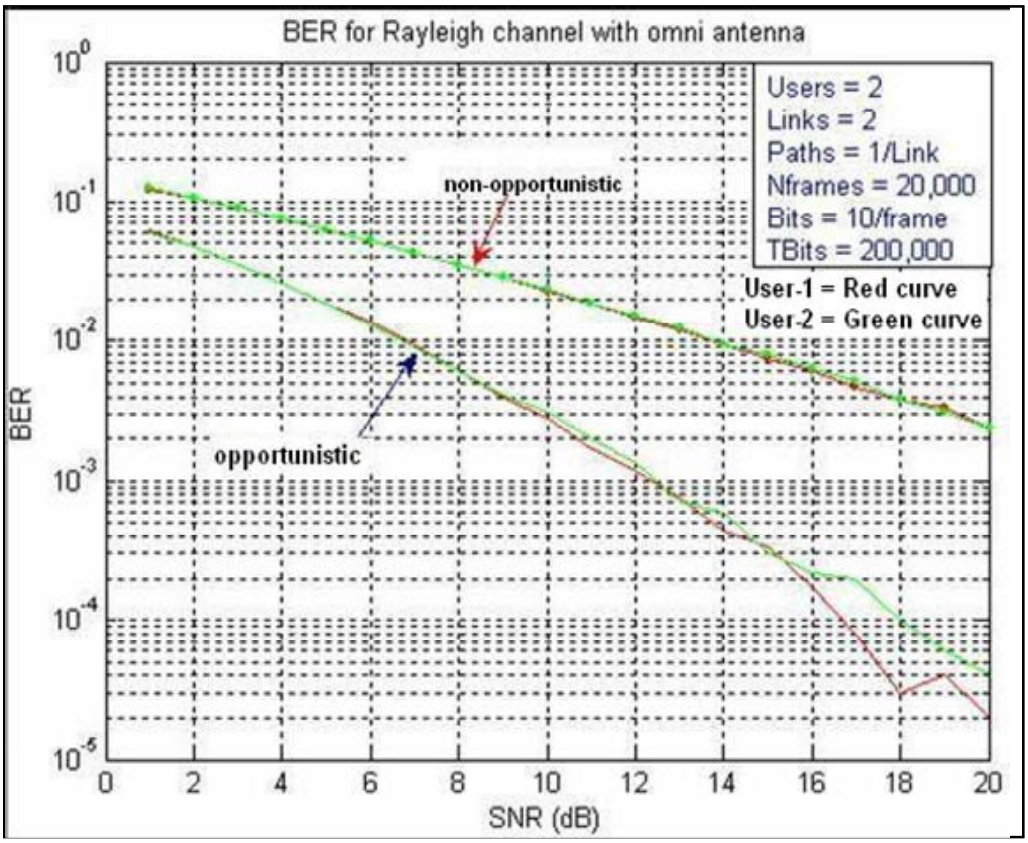

Figure 5.4: BER with opportunistic communication in Rayleigh Channel

5.4.4 Results Analysis

a. Characteristics of the channel coefficients remain constant while frame of data is being transmitted and channel coefficients are generated on the basis of frame and time period is also defined per frame basis.

b. From Figure 5.4 it is observed that the curves of opportunistic communication system using flat fading Rayleigh channel model have better BER performance as compared to the case of non-opportunistic communication system. Hence the users communicating under the environment of an opportunistic communication system get fair share of bandwidth allocation.

c. The BER performance of an opportunistic communication system (Cooperation) is measured depending upon the condition of channel as to when the channel is given to Tx-1 or to Tx-2. The simulation results shown above dictate that if a data of about 0.2 Million bits is sent across Rayleigh channel, BER of 10^{-2} at SNR of 7dB in case of opportunistic communication system as compared to non opportunistic

system where BER of 10^{-2} at SNR of about 14dB is achieved. So there is a difference of 7dB having same BER rate.

d. The BER performance is very poor when no channel selection is made and there is no cooperation amongst users.

5.5 Scenario-2 (frequency selective fading)

Here in this case two Mobile users MS-1 (user 1) and MS-2(user 2) moving at a speed of 1.25m/s corresponding to a doppler of 10Hz and carrier frequency of 2.4GHz are communicating with a common BS, each mobile user is operating at independent link but having two paths/link with BS. Two Rayleigh dice are rolled that determine which channel should transmit. When the channel is allocated to one transmitter it is allowed to send across the data in frames depending upon the condition as to when the channel is allocated to that particular user and AWGN is added to it. Here an equaliser at receiving end is used to compensate for the phase distortion in the channel.

5.5.1 Methodology of implementation in Matlab

The following steps are taken to implement a simulation in Matlab and graph of BER performance is plotted to compare the performance under the conditions of cooperation and when there is no cooperation in an environment of multipath frequency selective Rayleigh fading channel.

a. Generate two data streams of random integer numbers for Mobile_1 and Mobile_2, then split this stream of data into blocks of data.

b. Modulate the two data streams using appropriate phase shift keying modulator.

c. Generate two Rayleigh channel coefficients (2-paths) each symbol spaced delayed with 10Hz doppler for both links.

d. At the end of each block the channel is checked again and block of data is sent from Mobile_1 or Mobile_2 depending upon the condition of channel whichever is in better state/condition.

e. These two channels are monitored regularly at every block of data and at the instant of time, when the link_1 is better than link_2 the entire block of data from Mobile_1 is sent to BS, Where an equaliser at receiving end is used to compensate for the phase error, the received signal is then demodulated using an appropriate demodulator and compared with original randomly generated stream of data to compute the errors. The characteristic curve for BER is plotted against signal to noise ratio as shown in Figure 5.5.

The schematic diagram of two users communicating with common BS in frequency selective environment is shown in Figure 5.5 below, whilst the design parameters for implementation of the above mentioned scenario are given in the Table 5-2.

Parameters	***Values***	***Parameters***	***Values***
Channel Rayleigh	freq selective	Sampling time (t_s)	3.75msec
Number of Paths	2	Doppler (f_d Hz)	10
Number of Users	2	Modulation Scheme	PSK
Number of frames	20,000	Modulation order (M)	2
Bits/frame	10	Path gains	[1 0.2]

Table 5-2: Rayleigh freq selective fading Parameters (2-Users opportunistic)

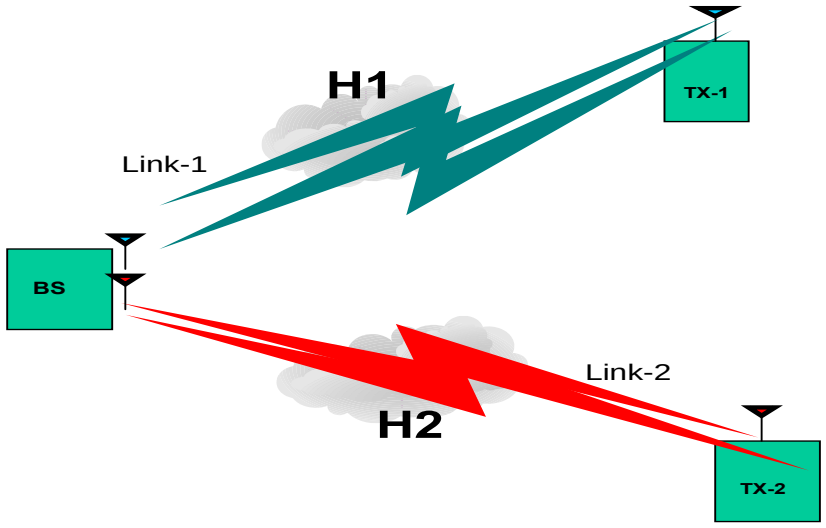

Figure 5.5: 2xUsers communicating with common BS in Multipath environment

5.5.2 Description of Simulation

Here in case of frequency selective multi-path Rayleigh faded channel a random stream of data is generated and sent across the channel by each user depending upon the quality of channel whenever it is allocated to user-1 or user-2. The stream of data sent across the channel is symbol spaced delayed. Channel coefficients are generated for both users operating between base-station in multi-path environment. The path gain of path-1 for both users is set to unity while the path gain of path-2 for both users is set to 0.2. A channel selection criterion is made on the basis of magnitude^2 of the channel coefficients in order to determine as to when the user-1 or user-2 should communicate with the BS depending upon the quality of channel. Once the channel has been allocated to a particular user depending upon the quality of the

channel a frame of random binary data bits is generated and converted into symbols. This data comprising of stream of symbols is modulated with the help of phase shift keying modulator and then sent across the channel with symbol spaced delay from both the paths. At the receiving end the received signal is corrupted with additive white Gaussian noise and an equalizer is used to compensate for the phase error in the distorted signal due to channel and then demodulated with the help of an appropriate demodulator. Finally the received stream of symbols is converted back to binary data bits and stored in the buffer. The same procedure is repeated for other user when the channel is allocated to user-2 as opportunistic method of transmission is used to explore the quality of the system. At the end the data bits stored in the buffer are compared with the original randomly generated binary data bits and BER performance is computed and plotted as shown in Figure 5.6. The graph is also plotted for the case when there is no opportunism between both users and both users use the channel simultaneously.

5.5.3 Simulation result

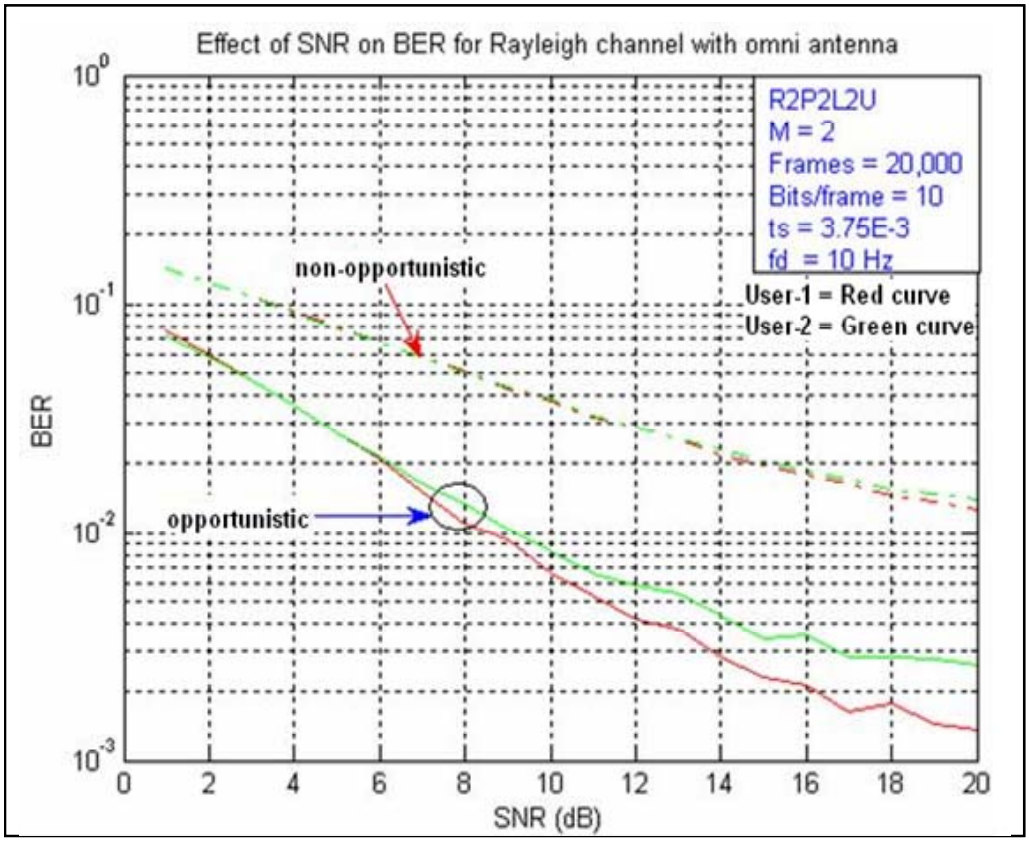

Figure 5.6: BER of 2xUsers in frequency selective environment

5.5.4 Results Analysis

a. Characteristics of the channel coefficients are assumed to be constant while frame of data is being transmitted.
b. In the curves of opportunistic communication system are compared with non-opportunistic case using frequency selective Rayleigh fading channel model.
c. The BER performance of an opportunistic communication system (Cooperation) is measured depending upon the condition of channel as to when the channel is given to Mobile user-1 or to Mobile user-2. The simulation results shown in the above dictate that if a data of about 0.2 Million bits is sent across multi-path Rayleigh channel, BER of 10^{-2} is achieved at SNR of 9 dB in case of opportunistic communication system as compared to non-opportunistic system where BER is 10^{-2} at SNR of about 23 dB. So there is a difference of 14 dB having same BER rate under non- opportunistic environment.
d. The BER performance is very poor when no channel selection is made and there is no cooperation between both users.
e. Here BER performance is degraded due to intersymbol interference that occurs because of multipath effect.

5.6 Scenario-3(frequency selective fading)

Here in this case three Mobile users MS-1 (user 1), MS-2(user 2) and MS-3(user 3) moving with doppler of 10Hz are communicating with a common BS, each mobile user is operating at independent link but having two paths/link with BS. Three Rayleigh dice are rolled that determine which channel should transmit. When the channel is allocated to a transmitter it is allowed to send across the data in frames depending upon the condition as to when the channel is allocated to that particular user and AWGN is added to it. Here an equaliser is used at receiving end to compensate for the phase distortion in the channel.

The following steps are taken to implement a simulation in Matlab and graph of BER performance is plotted to compare the BER performance under the conditions of cooperation and when there is no cooperation in an environment of multipath frequency selective Rayleigh faded channel.

5.6.1 Methodology of implementation in Matlab

a. Generate three data streams of random integer numbers for Mobile_1, Mobile_2 and Mobile_3, then split this stream of data into blocks of data.
b. Modulate the data streams using appropriate phase shift keying modulator.

c. Generate three Rayleigh channels coefficients for (2-paths) each symbol spaced delayed with 10 Hz doppler for all three links.
d. At the end of each block the channel is checked again and block of data is sent from Mobile_1/Mobile_2 or Mobile_3 depending upon the condition of channel whichever is in better state/condition.
e. These three channels are monitored regularly at every block of data and at the instant of time when the link_1 is better than link_2/3 the entire block of data from Mobile_1 is sent to Base Station, Where an equaliser at receiving end is used to compensate for the phase error, the received signal is then demodulated using an appropriate demodulator and compared with original randomly generated stream of data to compute the errors. Then the BER is plotted against signal to noise ratio as shown in Figure 5.8.

The schematic diagram of three users communicating with common BS is shown in Figure 5.7 below, whilst the design parameters for implementation of the above mentioned scenario are given in the Table 5-3 below.

Parameters	***Values***	***Parameters***	***Values***
Channel Rayleigh	freq selective	Sampling time (t_s)	3.75msec
Number of Paths	2	Doppler (f_d Hz)	10
Number of Users	3	Modulation Scheme	PSK
Number of frames	20,000	Modulation order (M)	2
Bits/frame	10	Path gains	[1 0.2]

Table 5-3: Rayleigh freq selective fading Parameters (3-Users)

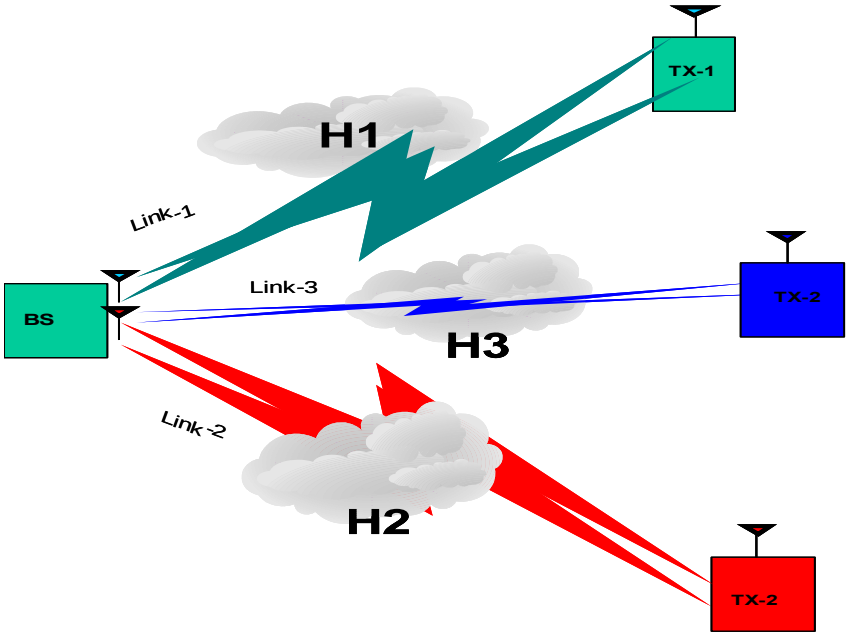

Figure 5.7: 3xUsers communicating with common BS in Multipath environment

5.6.2 Description of Simulation

Here in case of frequency selective multi-path Rayleigh faded channel a random stream of data is generated and sent across the channel by each user depending upon the quality of channel when is it allocated to user-1, 2 or user-3. The stream of data sent across the channel is symbol spaced delayed. Channel coefficients are generated for all three users operating between base-station in multipath environment. The path gain of path-1 for all three users is set to unity while the path gain of path-2 for all the users is set to 0.2. A channel selection criterion is made on the basis of magnitude$^{\wedge 2}$ of the channel coefficients in order to determine as to when the user-1/2 or user-3 should communicate with the BS depending upon the quality of channel. The same is done with the help of a matrix comprising of all paths of coefficients generated for all links. Then a vector is formed representing the indices of maximum of all the coefficients from matrix defined above. This vector representing the indices is used for selection criterion of channel as to when should that be allocated to User-1/2 or to User-3 depending upon the quality of channel. Once the channel has been allocated to a particular user depending upon the quality of the channel, frame of random binary data bits is generated and converted into symbols. This data comprising of stream of symbols is modulated with the help of phase shift keying modulator and then sent across the channel with symbol spaced delay from both the paths. At the receiving end the received distorted signal is corrupted with additive white Gaussian noise and an equalizer is used to compensate for the phase error in the distorted signal due to channel and then demodulated with the help of an appropriate

demodulator. Finally the received stream of symbols is converted back to binary data bits and stored in the Buffer. The same procedure is repeated for other users when the channel is allocated to user-2 or to user-3 as method of transmission is used to explore the quality of the system. At the end the data bits stored in the buffer are compared with the original randomly generated binary data bits and bit error rate (BER) performance is computed and plotted as shown in the graphs of Figure 5.8. The graph is also plotted for the case when there is no cooperation amongst all three users, and all users use the channel simultaneously.

5.6.3 Simulation result

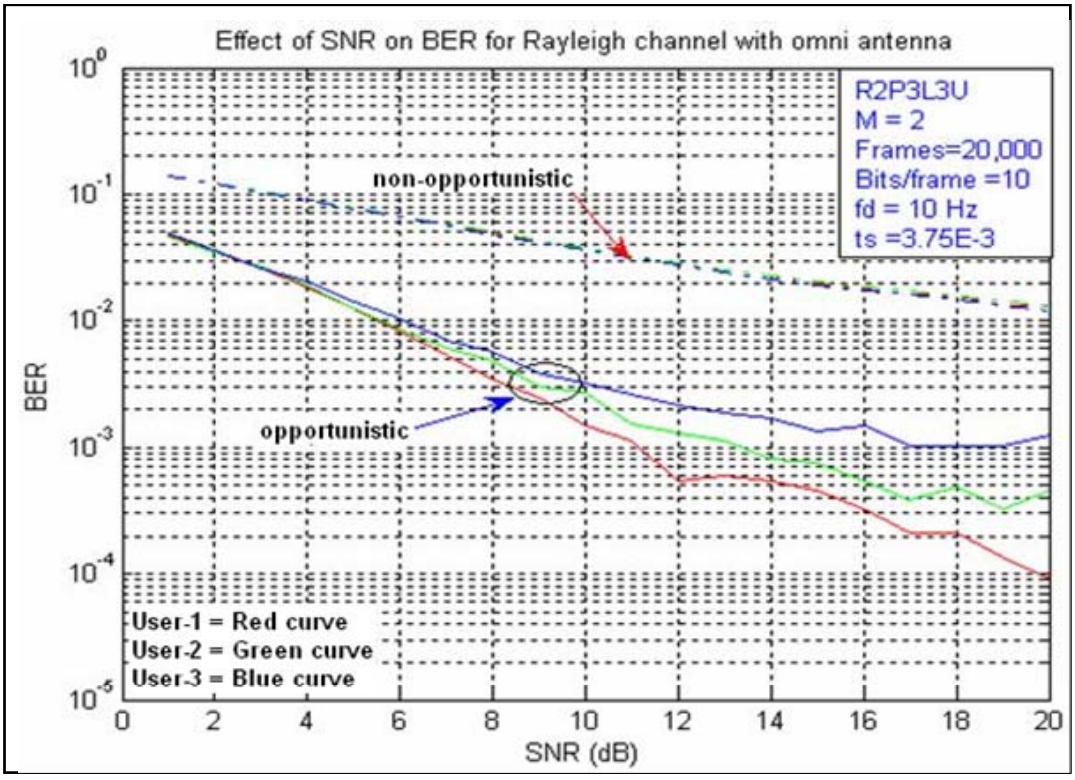

Figure 5.8: BER of 3xUsers in frequency selective environment

5.6.4 Results Analysis

a. Characteristics of the channel coefficients are assumed to be constant while frame of data is being transmitted every time.

b. In Figure 5.8 the curves of opportunistic communication system using frequency selective Rayleigh fading channel model are compared with curves of non-opportunistic communication system.

c. The BER performance of an opportunistic communication system (cooperation) is measured depending upon the condition of channel as to when the channel is given to Tx-1/Tx-2 or to Tx-3. The simulation results in the graph above dictate that if a

data of about 0.2 Million bits is sent across multi-path Rayleigh faded channel, at SNR of 6 dB the BER is 10^{-2} in case of opportunistic communication system as compared to non-opportunistic communication system where BER is 10^{-2} at SNR of about 23 dB. So there is difference of 17 dB having same BER performance because of conditions.

d. The BER performance of opportunistic communication system is made depending upon the condition of channel as to when the channel is given to Tx-1/Tx-2 or to Tx-3 and is far better than under non-opportunistic communication case.
e. As channel-1 remains in better state for long duration of time so the BER performance of Tx-1 is even far better than Tx-2 and Tx-3.

5.7 Simulation of Spatial Channel Model

Here spatial channel model (SCM) is used in uplink case where a signal transmitted from MS is received by the BS that forms beam in the direction of user thereby indicating the angle of arrival of that signal coming from MS. During each simulation run the fast fading of the channel is dictated by the movement of the MS. The information regarding state of the channel is given to BS from MS and then BS uses the schedulers to determine the direction of user where to transmit. The detailed description of spatial channel model is given in section 2.7 of chapter 2.

5.8 Scenario-1 (flat fading environment)

Here the scenario is defined such that two Mobile users MS-1(user 1) and MS-2(user 2) moving at a speed of 1.25m/s corresponding to a doppler of 10Hz and carrier frequency of 2.4GHz are communicating with a common BS; each mobile user is operating at independent path with BS. Two dice are rolled that determine which channel should transmit. When the channel is allocated to one transmitter it is allowed to send across the data in frames depending upon the condition as and when the channel is allocated to that particular user and then AWGN is added to it. Here phase estimation is done at receiving end to compensate the phase distortion in the channel.

5.8.1 Methodology implemented

a. Generate two data streams of random integer numbers for Mobile_1 and Mobile_2. Then split this stream of data into blocks of data.
b. Modulate the two data streams using appropriate PSK modulator.

c. Generate channel coefficients for each link.
d. These two channel links are monitored regularly during transmission of every block of data and at the instant of time when the link_1 is better than link_2 the entire block of data from Mobile_1 is sent to BS, Where it is equalised, demodulated and then checked for errors.
e. At the end of each block the channel is checked again and block of data is sent from Mobile_1 or Mobile_2 depending upon the condition of channel link whichever is in better state/condition.

The design parameters for simulation of above scenario-1 are given in Table 5-4 below.

Parameters	***Value***	***Parameters***	***Value***
Number of frames sent	20,000	sampling time (t_s)	3.75E-3
Number of bits/frame	10	Modulation order (*M*)	2
Total bits sent	200,000	Number of Paths	1
Modulation scheme	PSK	Number of Users	2
Doppler frequency (f_d (Hz))	10	Carrier frequency *(f_c)*	2.4GHz

Table 5-4: SCM flat fading Parameters (2-Users)

5.8.2 Description of Simulation

In this case channel coefficients are generated for both users operating between base-station with independent paths. A channel selection criterion is made on the basis of magnitude^2 of the channel coefficients in order to determine as to when the user-1 or user-2 should communicate with the base-station depending upon the quality of channel. Once the channel has been allocated to a particular user depending upon the quality of the channel a frame of random binary data bits is generated and converted into symbols. This data comprising of stream of symbols is modulated with the help of PSK modulator and then sent across the channel. At the receiving end the received signal is corrupted with additive white Gaussian noise and then demodulated with the help of an appropriate demodulator taking into account the phase estimator to compensate the phase error. Finally the received stream of symbols is converted back to binary data bits and stored in the buffer. The same procedure is repeated for other user when the channel is allocated to that user as opportunistic method of transmission is used to explore the quality of the system. At the end the data bits stored in the buffer are compared with the original randomly generated binary data bits and BER performance is computed and plotted as shown in the graphs of Figure 5.9. The graph is also plotted for the case when there is no cooperation between both users, and both users use channel simultaneously.

5.8.3 Simulation result

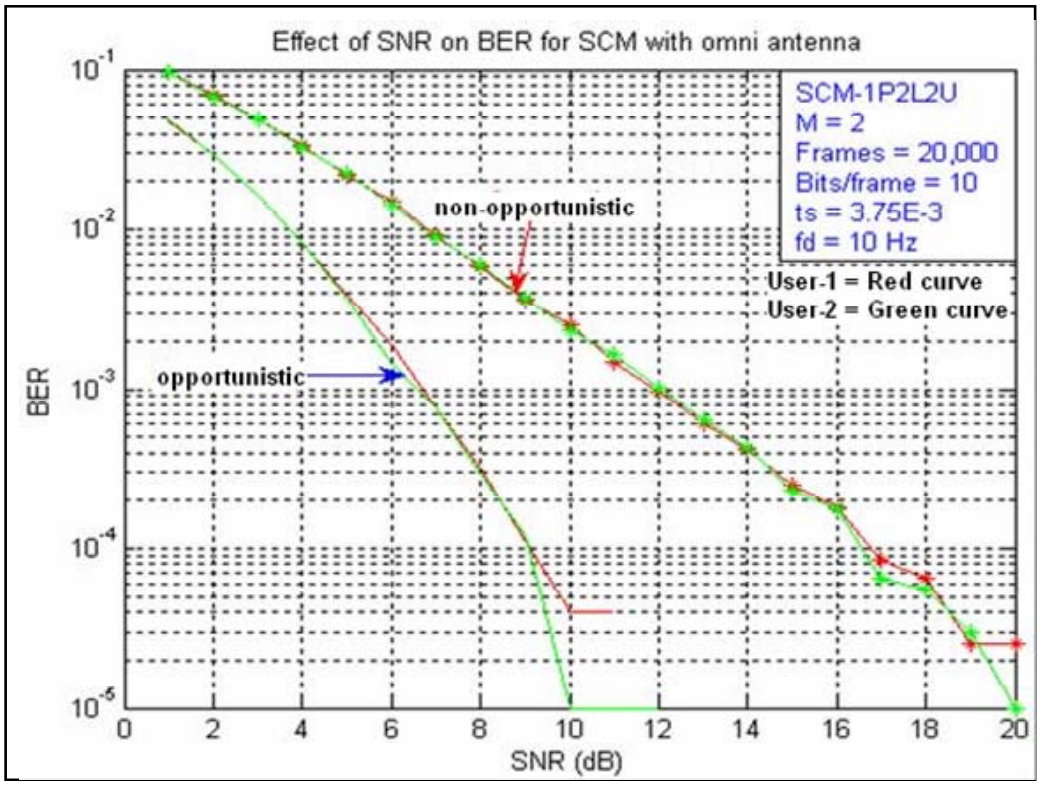

Figure 5.9: BER of 2xUsers with opportunistic communication using SCM

5.8.4 Results Analysis

a. Characteristics of the channel coefficients are assumed to be constant while transmission of every frame.

b. In Figure 5.9 the curves of opportunistic communication system are compared with curves of non-opportunistic communication system.

c. The BER performance of an opportunistic communication system (Cooperation) is measured depending upon the condition of channel as to when the channel is given to Tx-1 or to Tx-2. The simulation result above dictates that if a data of about 0.2 Million bits is sent across Spatial Channel model, at SNR of 9 dB the BER is 10^{-4} in case of opportunistic communication system is achieved as compared to non-opportunistic system where BER 10^{-4} at SNR of about 17dB is achieved. So there is an improvement of 8dB with opportunistic system having same BER rate.

d. The BER performance of opportunistic communication system is made depending upon the condition of channel as to when the channel is given to Tx-1 or to Tx-2 and is far better than that of non- opportunistic case as is obvious from simulation results shown in Figure 5.9 above.

e. Compared with Rayleigh channel results in Figure 5.4, The BER performance of SCM systems is much better, where BER of 10^{-3} is achieved at SNR of 12dB in Rayleigh channel whilst in case of SCM channel same BER of 10^{-3} is achieved at 7dB, so there is a difference of about 5dB in both channels.

5.9 Scenario-2 (Multi-path frequency selective environment)

Here in this scenario three Mobile users MS-1(user 1), MS-2(user 2) and MS-3(user 3) moving at a speed of 1.25m/s corresponding to a doppler of 10Hz and carrier frequency of 2.4GHz are communicating with a common BS, each mobile user is operating at independent link with symbol spaced delayed two paths/link with BS. Three dice are rolled that determine which channel should transmit. When the channel is allocated to one transmitter it is allowed to send across the data in frames depending upon the condition as to when the channel is allocated to that particular user and AWGN is added to it. Here equalizer is used at receiving end to compensate the phase distortion in the channel.

5.9.1 Methodology for implementation of scenario

a. Generate three data streams of random integer numbers for Mobile_1, Mobile_2 and Mobile_3. Then split this stream of data into blocks of data using frequency selective spatial channel model for 2-paths each with symbol spaced delay for each user/Link.
b. Modulate the three data streams using appropriate phase shift keying modulator.
c. Generate channel coefficients for three channels (2-path) symbol spaced delayed for each link.
d. These three channels are monitored regularly at every block of data and at the instant of time when the link_1 is better than link_2/ link_3 the entire block of data from Mobile_1is sent to BS, Where it is equalised, demodulated and then checked for errors.
e. At the end of each block the channel is checked again and block of data is sent from Mobile_1, Mobile_2 or Mobile_2 depending upon the condition of channel link whichever is in better state/condition.

The design parameters for simulation of above scenario are given in the Table 5-5 below.

Parameters	***Value***	***Parameters***	***Value***
Number of frames sent	20,000	Number of Paths	2
Number of bits/frame	10	Number of Users	3
Total bits sent	200,000	Modulation scheme	PSK
Sampling time (t_s)	3.75E-3	Modulation order (*M*)	2
Doppler frequency (f_d Hz)	10	Carrier frequency (f_c)	2.4GHz

Table 5-5: SCM frequency selective fading Parameters (2-Users)

5.9.2 Description of Simulation

In this case channel coefficients are generated for three users operating between base-station in multi-path environments with 2 paths each delayed with symbol space. A channel selection criterion is made on the basis of magnitude^2 of the channel coefficients in order to determine as to when the user-1, user-2 or user-3 should communicate with the base-station depending upon the quality of channel. Once the channel has been allocated to a particular user depending upon the quality of the channel, a frame of random binary data bits is generated and converted into symbols. This data comprising of stream of symbols is modulated with the help of phase shift keying modulator and then sent across the channel. At the receiving end the received distorted signal due to the effect of channel is corrupted with additive white Gaussian noise and Zero forcing equalizer is used to compensate for the phase error in the distorted signal due to channel and then demodulated with the help of an appropriate demodulator. Finally the received stream of symbols is converted back to binary data bits and stored in the buffer. The same procedure is repeated for User-2 and User-3 when the channel is allocated to user-2/3 as opportunistic method of transmission is used to explore the quality of the system. At the end the data bits stored in the buffer are compared with the original randomly generated binary data bits and BER performance is computed and plotted as shown in the graphs of Figure 5.10. The graph is also plotted for the case when there is no cooperation between three users.

5.9.3 Simulation result

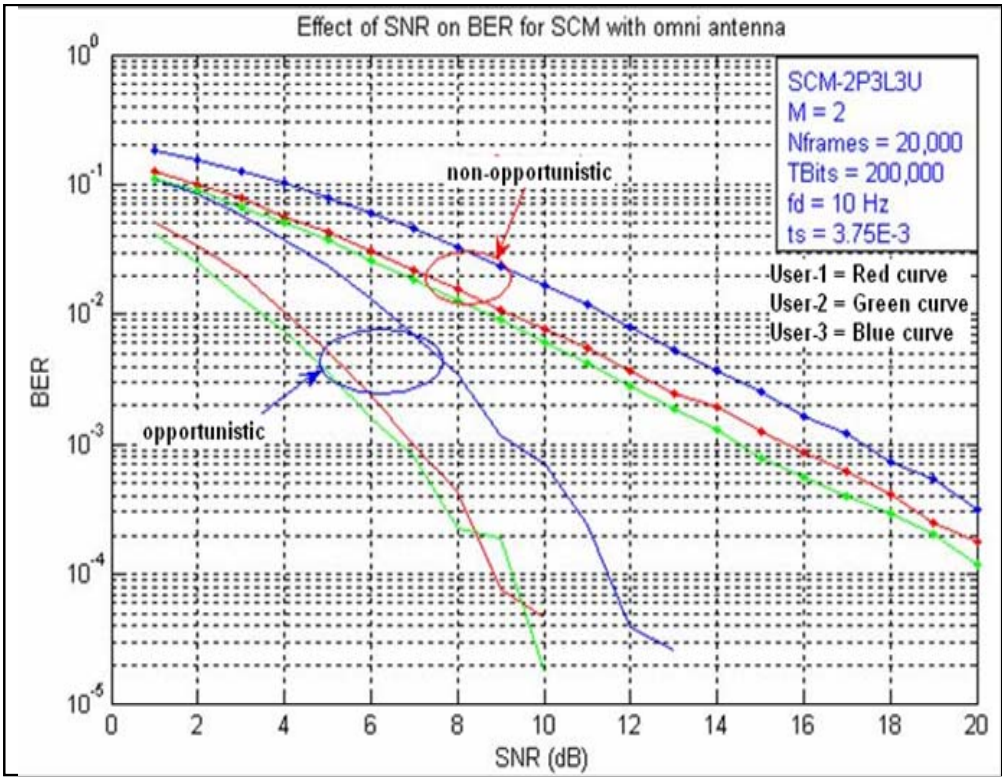

Figure 5.10: BER of 3xUsers using SCM

5.9.4 Results Analysis

a. From Figure 5.10 above it is observed that BER characteristics curves of all three users are better in opportunistic case than that of non- opportunistic environment as all users get the fair share of channel bandwidth.

b. Amongst three users the BER performance of user-2 in green curve is better than user-1 and user-3 below 8dB SNR, but after that BER performance of user-1 in red curve is better because of good channel conditions. The user-3 in blue curve does not get the good channel conditions, so its performance in terms of BER is poor as compared to other two users.

c. From the simulation graph it is seen that with opportunistic conditions the user 2 has BER of 10^{-3} at SNR of 7dB as compared to non opportunistic case where same user has BER of 10^{-3} at SNR of 15dB. So there is an improvement of 8dB with opportunistic system.

d. Comparing the reults of Rayleigh channel in Figure 5.7, where BER of 10^{-2} is achieved at 6dB while using SCM channel same BER of 10^{-2} is achieved at 3/4/6

dB for user-1, user-2 and user-3 respectively. So there is adifferenec of 2-3 dB for two users.

5.10 Implementation of an adaptive antenna at BS

In the previous sections different scenarios using Matlab Rayleigh channel and spatial channel model (SCM) have been implemented considering omni-directional antenna to evaluate the BER performance of all the system models.

In the next sections different scenarios will be implemented using an adaptive antenna at the BS. In this case it is assumed that there is one jammer whose direction is known in advance. It uses the known direction of the jammer to calculate the interference plus noise correlation matrix $\mathbf{R}_{i+n}$ so that it can place a null in the direction of jammer. When user-1 is communicating with the BS a composite signal is received using the optimal beamformer that forms main beam towards user-1, while placing a null towards user-2 considering it as a jammer. The interference plus noise correlation matrix $\mathbf{R}_{i+n}$ is used to find the weight of an optimal beamformer using (3.39) from chapter 3.

5.11 Matlab Rayleigh Channel model simulations

Different scenarios like flat fading and frequency selective fading for implementation of Rayleigh channel model with adaptive antenna at BS are implemented as under.

5.11.1 Scenario-1(flat fading)

In this scenario we consider that two Mobile stations MS-1(user-1) and MS-2(user-2) are communicating from different angles of -20^o and 40^o, with a common BS using an 8 antenna element array using concept of SDMA and two optimal beamformers to obtain the isolation between the two users. Beamformer-1 looks at user-1 and rejects user-2, while beamformer-2 looks at user-2 and rejects user-1. ULA with $d = \lambda/2$ relative to the carrier frequency f_c is used.

The design parameters for implementation of the scenario are given in Table 5-6 below.

Parameters	***Value***	***Parameters***	***Value***
Antenna elements	8	Carrier frequency (f_c)	2.4GHz
Number of frames sent	20,000	λ	c/ f_c
Number of bits/frame	10	C (m/sec)	3.0E8
Total bits sent	200,000	FFT resolution points	2048
Modulation scheme	PSK	A0A user 1	40^o
Modulation order (M)	2	A0A user 2	-20^o
Sampling time/frame (t_s)	3.75msec	Number of Paths	1
		Number of Users	2

Table 5-6: Rayleigh flat fading Parameters using adaptive antenna on BS

The methodology of simulation is same as given in section 5.4 above for omni-directional antenna and the simulation results for omnidirectional are given in (a), whereas simulation results for an adaptive antenna with help of an optimal beamformer to isolate the two users and plotting BER performance, AoA simulation results are also shown in (b)&(c) respectively.

5.11.2 Simulation results

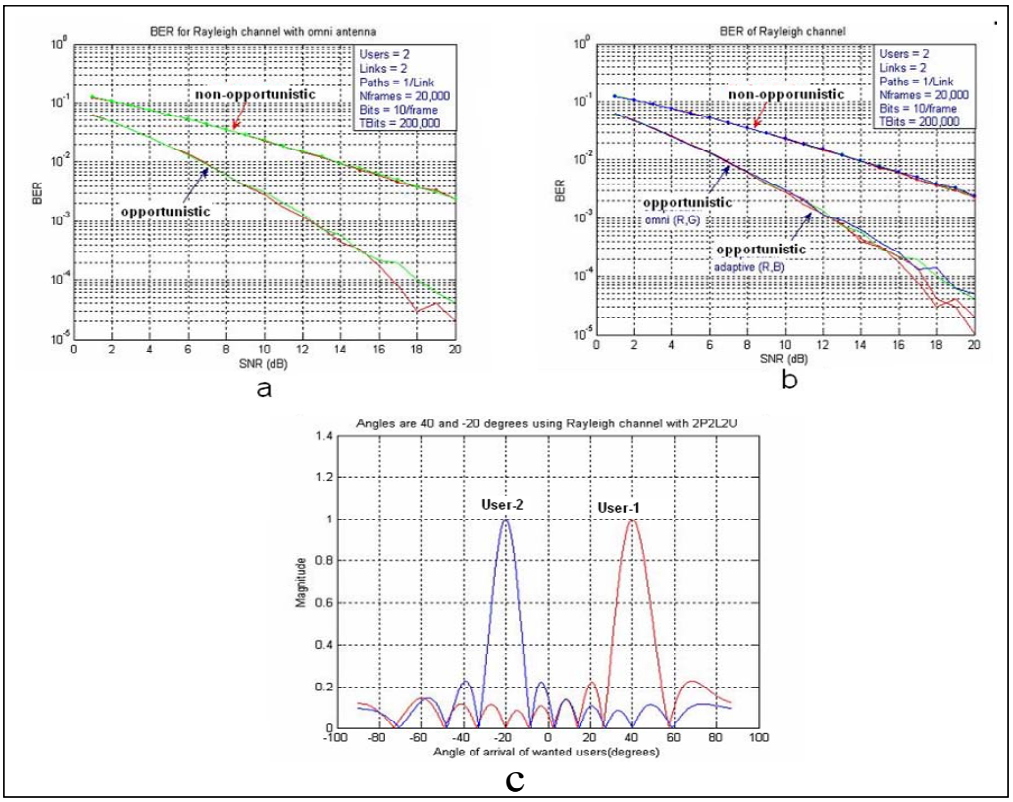

Figure 5.11: 2xUsers with dedicated links

5.11.3 Results Analysis

a. Here two users are communicating with common BS having a dedicated link and one path/link depicting a scenario of flat fading environment.
b. From (a) simulation results it is seen that BER performance is better in opportunistic mode when omni-directional antenna is used, where BER of 10^{-3} at SNR of 11dB is achieved as compared to non-opportunistic system, where same BER performance is achieved above 20dB. There is significant improvement with opportunistic communication system.
c. Here as is a case of flat fading environment so comparison of BER performance using omni-directional and an adaptive antenna is shown in (b). It is observed that when two users have got a dedicated link, the BER performance is same whether using omni-directional antenna or an adaptive antenna under opportunistic and non-opportunistic environments where the curves in both cases are overlapped. Both antennas have same BER performance till 12.5dB SNR but above that one of the users has better performance then the other because of allocation of channel for longer duration of a time.
d. AoAs of two users operating from different angles are plotted in (c) with the help of an optimal beam-former to isolate each user by forming main beam towards a wanted user communicating with BS at the time of transmission.
e. A phase estimator is used at the receiving end to compensate for the phase error.

5.11.4 Scenario-2(Multipath frequency selective fading)

In this scenario we consider that two Mobile stations MS-1(user-1) and MS-2(user-2) are communicating from different angles of -20^{o} and 40^{o}, with a common BS using an 8 antenna element array using concept of SDMA and two optimal beamformers to obtain the isolation between the two users. Beamformer-1 looks at user-1 and rejects user-2, while beamformer 2 looks at user-2 and rejects user-1. ULA with $d = \lambda / 2$ relative to the carrier frequency f_c is used.

In this case two users communicating with common BS have a dedicated link but operating in Multi-path fading (freq selective) environment. Here two paths/link with symbol spaced delay data, model is used. At the receiving end zero forcing equalizer is used to compensate for the phase error due to delay of multipath frequency selective environmrnt.

The design parameters for implementation of the scenario are given below in Table 5-7 below.

Parameters	***Value***	***Parameters***	***Value***
Antenna elements	8	Carrier frequency (f_c)	2.4GHz
Number of frames sent	20,000	λ	c/ f_c
Number of bits/frame	10	C (m/sec)	3.0E8
Total bits sent	200,000	FFT resolution points	2048
Modulation scheme	PSK	A0A user 1	40^o
Modulation order (M)	2	A0A user 2	-20^o
Sampling time/frame (t_s)	3.75msec	Number of Paths	2/link
Doppler (f_d)	10 Hz	Number of Users	2

Table 5-7: Rayleigh frequency selective fading Parameters (adaptive antenna)

The methodology of simulation is same as described in section 5.5 above for omni-directional antenna and the simulation results for omnidirectional are given in Figure 5.12(a), For implementation of adaptive calculation of $\mathbf{R}_{i+n}$ and optimum weight vector procedure described in section 5.10 is used. The simulation results for adaptive antenna with help of an optimal beamformer to isolate the two users and plotting BER performance, AoA simulation results are also shown in Figure 5.12 (b)&(c) respectively.

5.11.5 Simulation result

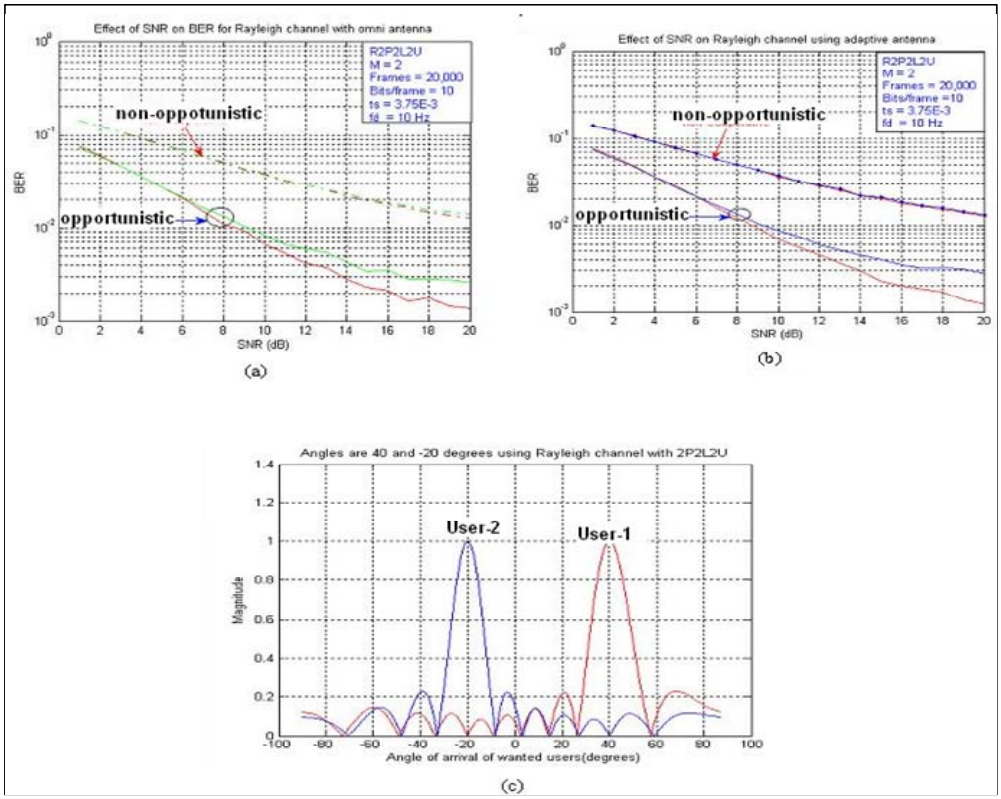

Figure 5.12: 2xUsers with dedicated links in multipath environment

5.11.6 Results Analysis

a. Here a scenario of two users operating in frequency selective environment is depicted in Figure 5.12(a). Although both users have got a dedicated link but due to frequency selective environment BER performance is poor as compared to case of flat fading environment discussed earlier. From simulation results it is seen that BER performance with opportunistic is better that non- opportunistic case and is almost same irrespective of an omni-directional antenna or adaptive antenna being used as shown in Figure 5.12(a) &(b). It is seen that BER of 10^{-2} at SNR of 9dB is achieved with opportunistic system as compared to non-opportunistic system where same BER is achieved above 20dB. There is significant improvement in SNR when using opportunistic communication system.

b. It is also noted that in opportunistic system one of the users has better BER performance compared to other due to better channel characteristics. This is true in both cases whether omni-directional or an adaptive antenna is used at the BS.

c. AoAs of two users operating from different angles are plotted in Figure 5.12 (c) with the help of an optimal beam-former by forming main beam towards each user.

5.11.7 Scenario-3 (Multipath frequency selective fading)

In this scenario we consider that three Mobile stations MS-1(user-1), MS-2(user-2) and MS-3(user-3) are communicating from different angles of -20^{o}, $+20^{o}$ and 40^{o}, with a common BS using an 8 antenna element array exploiting the concept of SDMA, where three optimal beamformers obtain the isolation between the three users. Beamformer-1 looks at user-1 and rejects user-2 and user-3, while beamformer-2 looks at user-2 and rejects user-1 and user-3 and beamformer-3 looks at user-3 and rejects user-1 and user-2. A ULA with $d = \lambda/2$ relative to the carrier frequency f_c is used.

In this case three users communicating with common BS have a dedicated link but operating in multi-path fading (freq selective) environment. Here two paths/link with symbol spaced delay data, model is used. At the receiving end zero forcing equalizer is used to compensate for the phase error that occurs due to multipath delays.

The design parameters for implementation of the scenario are given below in Table 5-8.

Parameters	***Value***	***Parameters***	***Value***
Antenna elements	8	Carrier frequency (f_c)	2.4GHz
Number of frames sent	20,000	λ	c/ f_c
Number of bits/frame	10	C (m/sec)	3.0E8
Total bits sent	200,000	FFT resolution points	2048
Modulation scheme	PSK	A0A user 1	40^o
Modulation order (M)	2	A0A user 2	-20^o
Sampling time/frame (t_s)	3.75msec	A0A user 3	$+20^o$
Number of Paths	2/link	Number of Users	2

Table 5-8: Rayleigh flat fading Parameters using adaptive antenna on BS-3 Users

The methodology of simulation is same as given in section 5.5 above for omni-directional antenna and the simulation results for omnidirectional are given in Figure 5.13(a), For implementation of adaptive antenna calculation of $\mathbf{R}_{i+n}$ and optimum weight vector procedure described in section 5.10 is used. The simulation results for an adaptive antenna with help of an optimal beamformer to isolate the two users and plotting BER performance, AoA simulation results are also shown in Figure 5.13 (b)&(c) respectively.

5.11.8 Simulation results

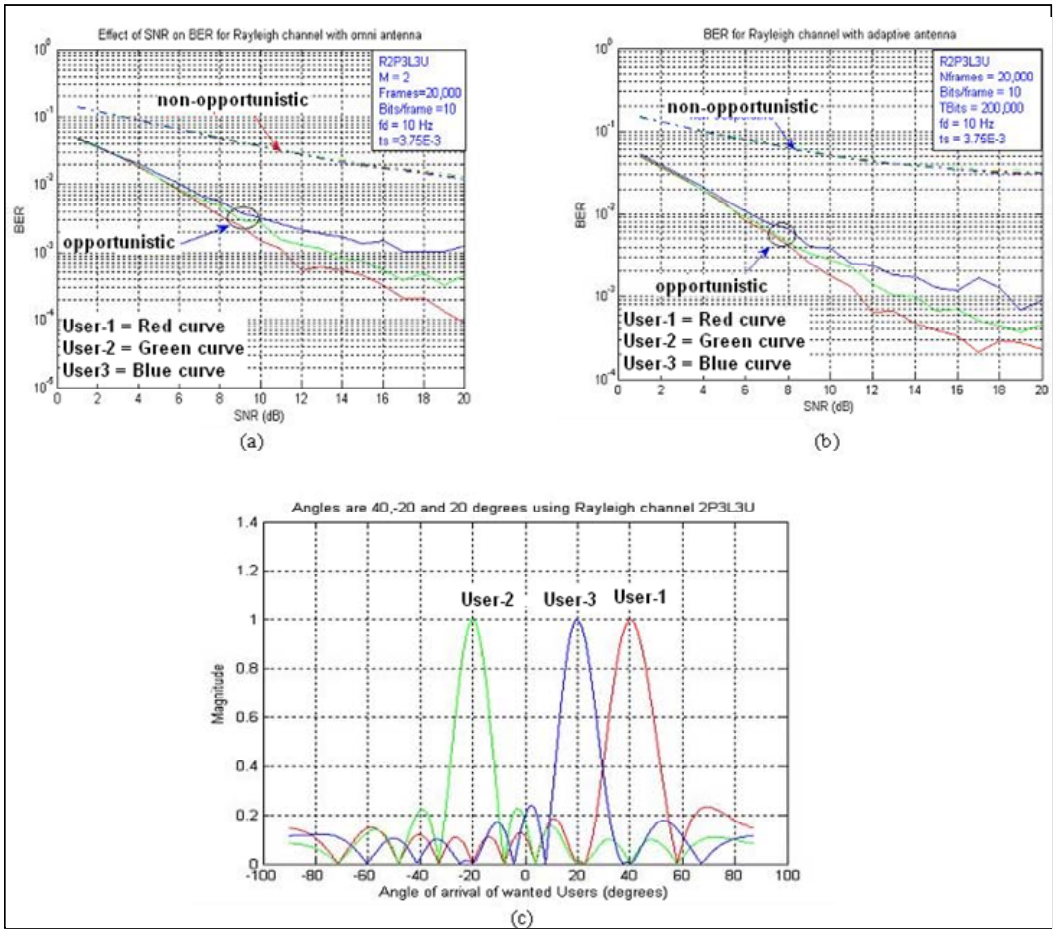

Figure 5.13: 3xUsers with dedicated Links in Multipath environment

5.11.9 Results Analysis

a. Here a scenario of three users operating in frequency selective Rayleigh fading environment is depicted in Figure 5.13(a). All three users are communicating with common BS via dedicated link having two paths with symbol space delayed data /link. From simulation results it is seen that BER performance with opportunistic is better than non-opportunistic case irrespective of an omni-directional antenna or adaptive antenna being used at BS as shown in Figure 5.13(a) & (b).

b. It is observed that BER performance is much better with opportunistic system, where BER of 10^{-3} at SNR of 11dB is achieved by one of the users as compared to non-opportunistic system where all users have poor BER performance and irreducible error floor is achieved at 10^{-2} after 20dB SNR in case of omni-

directional and an adaptive antenna at the BS as shown in the results in Figure 5.13 (a) & (b).

c. AoAs of three users operating from different angles are plotted in Figure 5.13(c) with the help of an optimal beam-former by forming main beam towards each user.

5.12 Spatial Channel Model

Different scenarios like flat fading and frequency selective fading for implementation of spatial channel model with adaptive antenna at BS are described as under.

5.12.1 Scenario-1 (flat fading)

In this scenario we consider that two Mobile stations MS-1(user-1) and MS-2(user-2) are communicating from different angles of -20^o and 40^o, with a common BS using an 8 antenna element array using concept of SDMA and two optimal beamformers to obtain the isolation between the two users. Beamformer-1 looks at user-1 and rejects user-2, while beamformer-2 looks at user-2 and rejects user-1. ULA with $d = \lambda/2$ relative to the carrier frequency f_c is used.

The design parameters for implementation of the scenario are given below in Table 5-9 below.

Parameters	***Value***	***Parameters***	***Value***
Antenna elements	8	Carrier frequency (f_c)	2.0GHz
Number of frames sent	20,000	λ	c/ f_c
Number of bits/frame	10	C (m/sec)	3.0E8
Total bits sent	200,000	FFT resolution points	2048
Modulation scheme	PSK	A0A user 1	40^o
Modulation order (*M*)	2	A0A user 2	-20^o
Sampling time/frame (t_s)	3.75msec	Number of Paths	1
Doppler (f_d)	10 Hz	Number of Users	2

Table 5-9: SCM flat fading Parameters using adaptive antenna on BS

The methodology of simulation is same as given in section 5.8 above for omni-directional antenna and the simulation results for omnidirectional are given in Figure 5.14(a), whereas simulation results for an adaptive antenna with help of an optimal beamformer to isolate the two users and plotting BER performance, AoAs simulation results are also shown in Figure 5.14(b)&(c) respectively.

5.12.2 Simulation Results

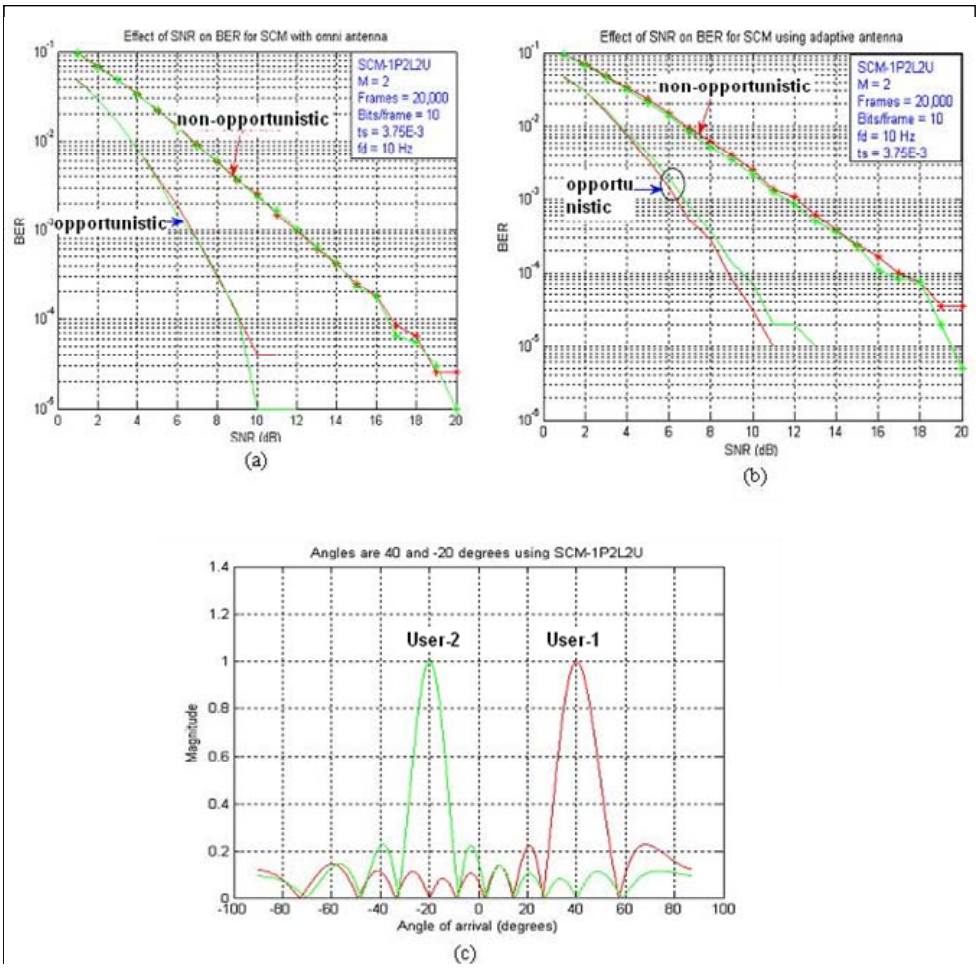

Figure 5.14: 2xUsers with dedicated Links using SCM

5.12.3 Results Analysis

a. Here two users are communicating with common BS each having a dedicated link with one path per link thereby depicting a scenario of flat fading environment of spatial channel model.

b. The Simulation results using omni-directional antenna and an adaptive antenna at BS are given in Figure 5.14 (a) & (b) respectively. From simulation results it reveals that BER performance in both cases is almost same because of dedicated link. But BER performance with opportunistic system is better than non-opportunistic system due to fair share of resources allocated to both users. In this case BER of 10^{-3} is achieved at SNR of 6.5dB in opportunistic case, whilst same BER 10^{-3} is achieved at SNR of 12dB in case of non-opportunistic system, so there is an improvement of 5.5dB.

c. From Simulation results shown in Figure 5.14 (a) it is seen that the result of BER for SCM case with opportunistic environment is much better than that of Matlab Rayleigh channel with flat fading shown in Figure 5.11(a), where BER of 10^{-3} is achieved at SNR of 12.5dB but here in this case BER of 10^{-3} is achieved at SNR of 6.5dB so there is an improvement of 6dB in case of SCM channel.

d. AoAs of two users operating from different angular positions are also plotted with the help of an optimal beam-former as shown in Figure 5.14 (c).

5.12.4 Scenario-2 (Multipath frequency selective fading)

In this scenario we consider that three Mobile stations MS-1(user-1), MS-2(user-2) and MS-3(user-3) are communicating from different angles of -10^o, 30^o and 40^o, with a common BS using an 8 antenna element array exploiting the concept of SDMA and three optimal beamformers to obtain the isolation between the three users. Beamformer-1 looks at user-1 and rejects user-2 and user-3, while beamformer-2 looks at user-2 and rejects user-1 and user-3 and beamformer-3 looks at user-3 and rejects user-1 and user-2. ULA with $d = \lambda/2$ relative to the carrier frequency f_c is used.

The design parameters for implementation of the scenario are given below in Table 5-10.

Parameters	***Value***	***Parameters***	***Value***
Antenna elements	8	Carrier frequency (f_c)	2.0GHz
Number of frames sent	20,000	λ	c/ f_c
Number of bits/frame	10	C (m/sec)	3.0E8
Total bits sent	200,000	FFT resolution points	2048
Modulation scheme	PSK	A0A user 1	-10^o
Modulation order (M)	2	A0A user 2	30^o
Sampling time/frame (t_s)	3.75msec	A0A user 3	40^o
Number of Paths	1/link	Number of Users	2

Table 5-10: SCM freq selective fading Parameters (adaptive antenna on BS)

The methodology of simulation is same as described in section 5.9 above for omni-directional antenna and the simulation results for omnidirectional are given in Figure 5.15(a), whereas simulation results for an adaptive antenna with help of an optimal beamformer to isolate the three users and plotting BER performance, AoA simulation results are also shown in Figure 5.15(b)&(c) respectively.

5.12.5 Simulation results

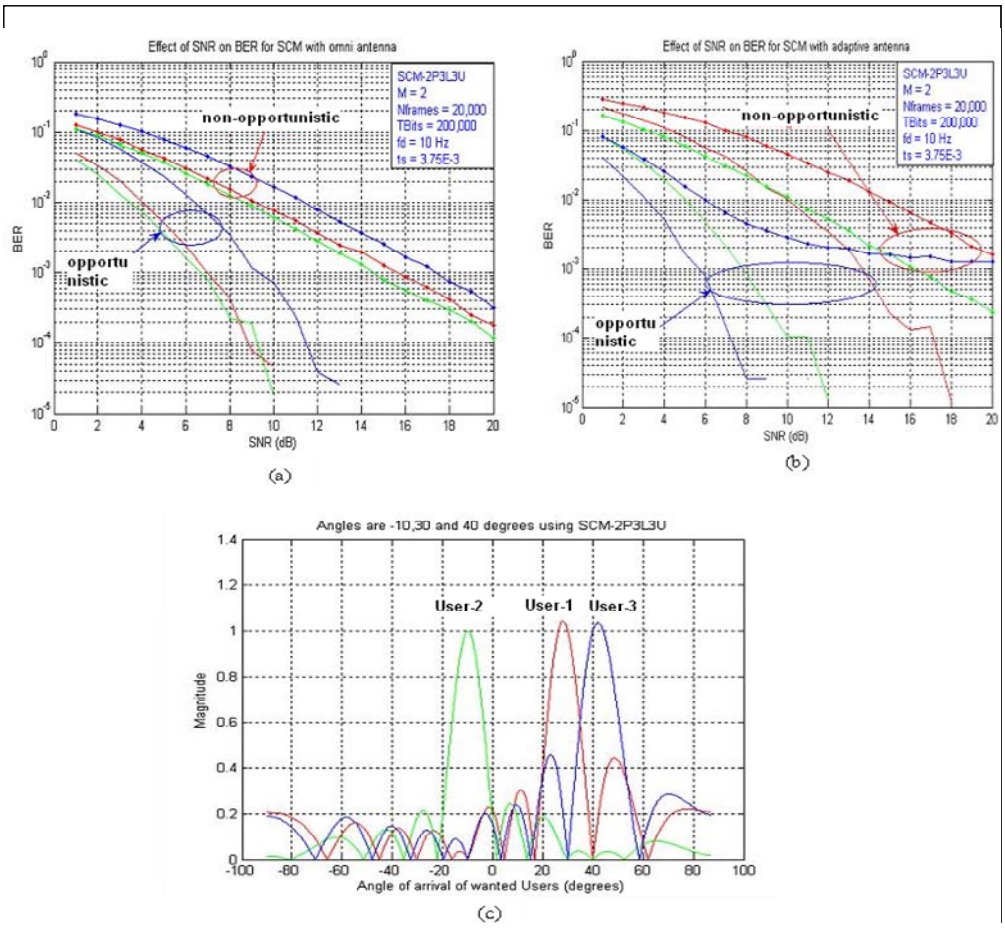

Figure 5.15: 3xUsers with dedicated Links in frequency selective environment

5.12.6 Results Analysis

a. Here the scenario of frequency selective fading environment using SCM is implemented with omni-directional and an adaptive antenna at the BS. The results of omni-directional antenna and an adaptive antenna at BS are given Figure 5.15 (a) & (b) respectively. From simulation results in Figure 5.15 (a) & (b) it is seen that BER performance with opportunistic system is better than non-opportunistic system.

b. In case of omnidirectional antenna at BS, one of the users has BER of 10^{-3} at 7dB SNR with opportunistic system as compared to non-opportunistic system, where same BER is achieved at 14.5dB SNR. There is an improvement of 7.5dB with opportunistic system than non-opportunistic communication system.

c. When an adaptive antenna is used at BS one of the users has BER of 10^{-3} at 5dB SNR with opportunistic system as compared to omni-directional antenna where

same BER is achieved at 7dB. There is an improvement of 2dB with adaptive antenna at BS in opportunistic communication system.

b. AoAs of three users operating from different angles are also plotted with the help of an optimal beam-former as shown in Figure 5.15(c).

5.13 Statistical analysis of Simulations

In case of opportunistic communication simulations the data for different users is generated randomly everytime it goes through a loop. In order to find out the fact that data is generated randonmly and and has not come from same population it is necessary to perform some statistical analysis, where it could be analysed that if the null hypothesis is not rejected at defined sigficant level then the data generated has been drawn from same population while in other case if the null hypothsis is rejected then the data is drawn from different population. In order to perform theses tests to see that everytime data generated is different for different users, following statistical analysis tests are performed.

5.13.1 Kolmogorov-Smirnov test

Kolmogorov-Smirnov test is one of the non parametric methods used for comparing two samples in order to find out whether the samples are drawn from same distribution of population or otherwise [61]. In above simulations Kolmogorov-Smirnov test is performed to compare the distribution of two BERs drawn from generating two random integer samples and it compares the values of two data vectors d1 and d2 of length n1 and n2 respectively, representing random samples from some distributions having a normal distribution (i.e. having mean 0 and variance 1).

5.13.2 Null Hypothesis

The null hypothesis (H=0) for the Kolmogorov-Smirnov test states that two data numbers d1 and d2 generated randomly are drawn from the same continuous distribution, hence null hypothesis is not rejected at tested significance level. The alternative hypothesis (H=1) states that they are drawn from different continuous distributions and null hypothesis is rejected at tested significance level.

Following command performs this test in Matlab

[H P K] = kstest2 (d1 d2 ‘alpha’), where alpha is the defined significance level (0.05 considered here).

where,

H is the null hypothesis defining, whether median is equal (H=0) or not (H=1).

P is the probability of observing the result.

K is the value of maximum difference between two empirical cdfs.

The result of this test performed on data distribution of two users is as shown below.

Statistical analysis of Kolmogorov smirnov Test								
Modulation Order	No of Frames	SNR (dB)						
2	500	BER1	Sample nos	1	2	3	4	5
			1	0.08986	0.0594	0.0594	0.03478	0.0203
			2	0.07681	0.058	0.0507	0.03623	0.0217
			3	0.06667	0.0696	0.0478	0.03044	0.0188
			4	0.07101	0.0594	0.0551	0.02754	0.0159
			5	0.07101	0.0536	0.0435	0.02609	0.00435
		BER2	1	0.37419	0.3129	0.3387	0.25484	0.3065
			2	0.34839	0.3129	0.3387	0.3129	0.2677
			3	0.3129	0.3654	0.271	0.30323	0.3161
			4	0.32258	0.3355	0.2903	0.27419	0.2774
			5	0.32258	0.3548	0.3032	0.26452	0.2839
		Kolmogorov smirnov Test	Null Hypothesis					
				1	1	1	1	1

Table 5-11: Statistical analysis of Kolmogorov Smirnov test

From the results above it is observed that BER at different values of SNR for two users is different thereby resulting into null hypothesis values of '1' indicating that the data of both the users is drawn from different populations.

5.13.3 Wilcoxon rank sum test

This test is another non-parametric significance test that was proposed by Mann and Whitney (1947) and Wilcoxon (1945), therefore this test is also called as Mann-Whitney-Wilcoxon (MWW) test or the Wilcoxon rank-sum test [61]. In statistics this test is performed to determine the statistic significance of in the difference of medians between observations of two data samples. This test is also performed in order to see the result of null Hypothesis test that is performed at desired significance levels.

5.13.4 Null Hypothesis

If *H=0* that means medians (estimate of centers of sample data) of two data sets are equal and two data sets are drawn from continuous distributions that are identical hence, null hypothesis can not be rejected at tested significance level.

Whereas If *H=1* that means medians of two data sets are not equal and two data sets are drawn from different continuous distributions that are not identical *and null hypothesis can be rejected* at tested significance level.

Following command performs this test in Matlab

[P H] = ranksum(x y 'alpha'),

where alpha is the defined significance level (0.05 considered here).

P is the probability of observing the result.

5.14 Effect of Correlation on BER Performance

The BER performance is monitored using different values of correlation factor while implementing SCM channel model in Matlab. The two channels defined as **'Chan-1'** and **'Chan-2'** are given as under.

$$\mathbf{Chan-1} = \alpha\mathbf{x} + (1-\alpha)\mathbf{y} \tag{5.5}$$

$$\mathbf{Chan-2} = (1-\alpha)\mathbf{x} + \alpha\mathbf{y} \tag{5.6}$$

From above equations it is seen that when value of α considered as correlation factor is 0.5, then equation (5.5) and (5.6) have the same values thereby indicating that both channels **'Chan-1'** and **'Chan-2'** are correlated.

In simulations the correlation factor is chosen to vary from 0 to 0.5, where the channels are fully uncorrelated at 0 and fully correlated when the value of correlation factor is 0.5. The same has been implemented in Matlab by sending data of 0.1 Million bits and observing BER performance while the channels get fully correlated by selecting different correlation factor. The simulation results for SNR vs BER of Rayleigh channel are shown in Figure 5.16 (a) to (f).

The design parameters for simulation of two correlated Rayleigh channels are given below in Table 5-12.

Parameters	***values***	***Parameters***	***values***
No of frames sent	10000	Bits/frame	64
Sampling time (t_s)	100μsec	Number of Users	2
Correlation factor (α)	[0:0.1:0.5]	Doppler (f_d) Hz	10
Number of Links	2	Paths/link	1
Carrier frequency(f_c)	2.4 GHz	λ	c/f_c

Table 5-12: Correlated channel Parameters

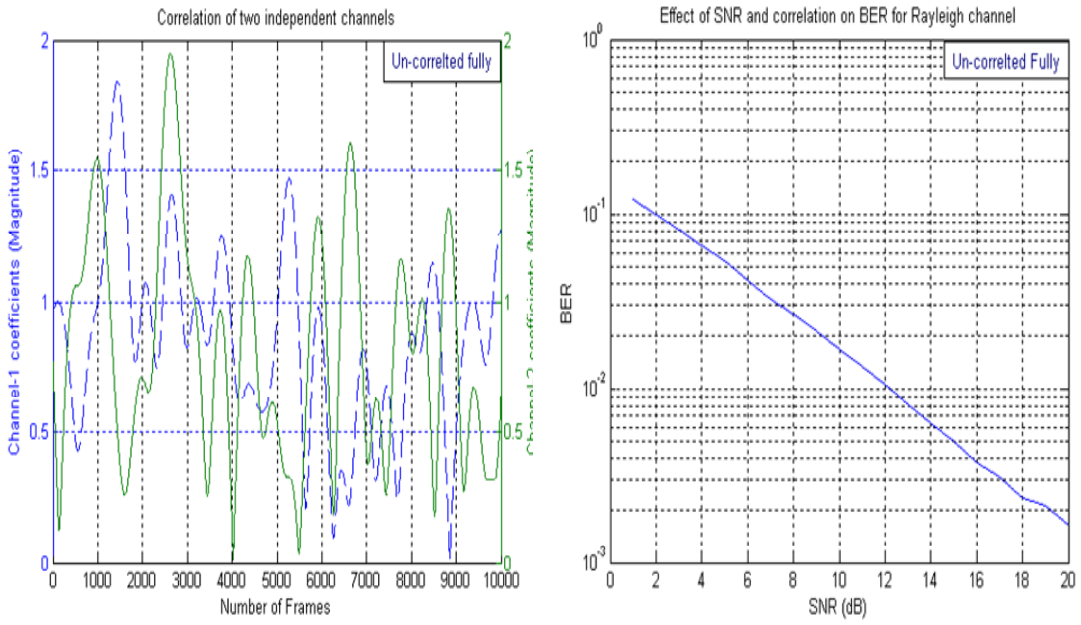

(a)

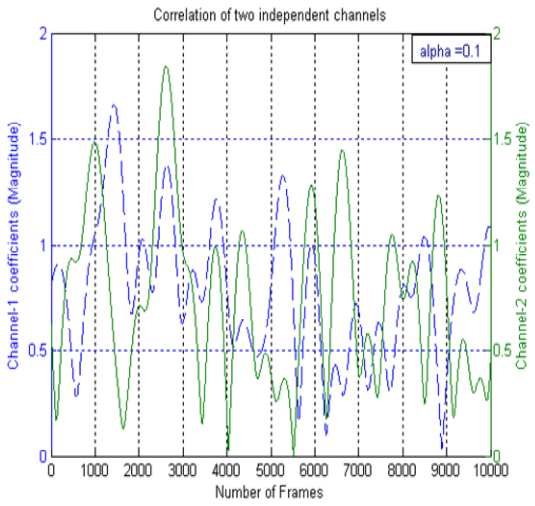
Correlation of two independent channels
alpha =0.1
Channel-1 coefficients (Magnitude)
Channel-2 coefficients (Magnitude)
Number of Frames

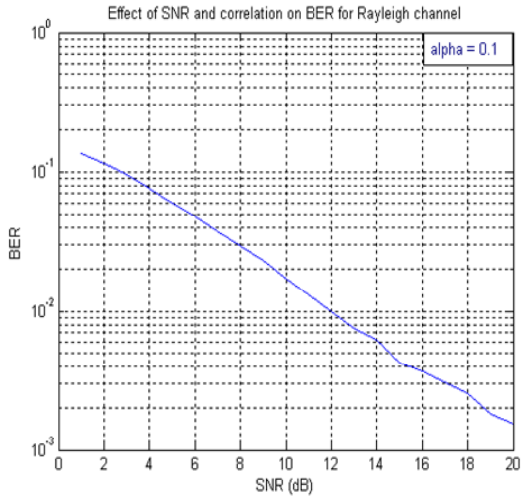
Effect of SNR and correlation on BER for Rayleigh channel
alpha = 0.1
BER
SNR (dB)

(b)

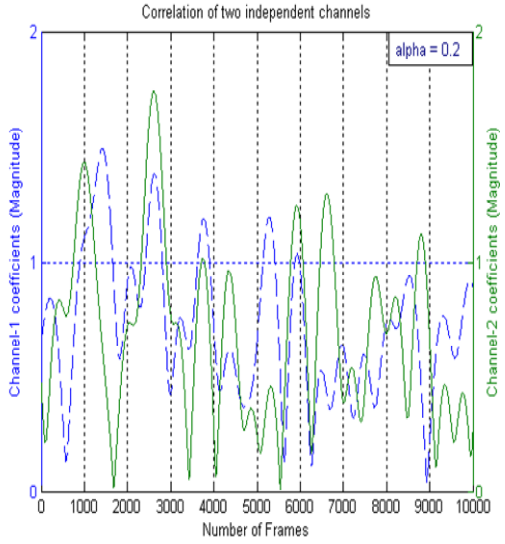
Correlation of two independent channels
alpha = 0.2
Channel-1 coefficients (Magnitude)
Channel-2 coefficients (Magnitude)
Number of Frames

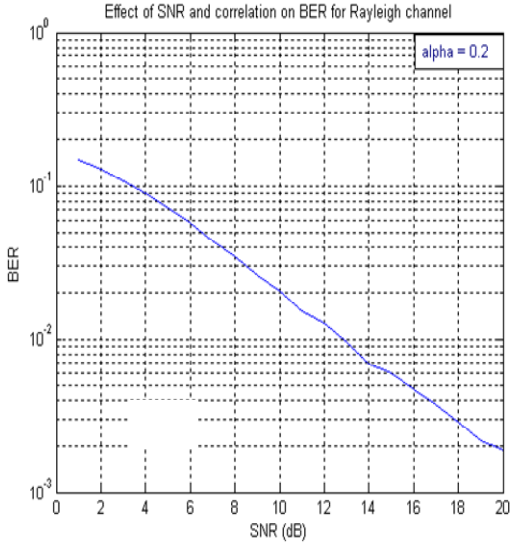
Effect of SNR and correlation on BER for Rayleigh channel
alpha = 0.2
BER
SNR (dB)

(c)

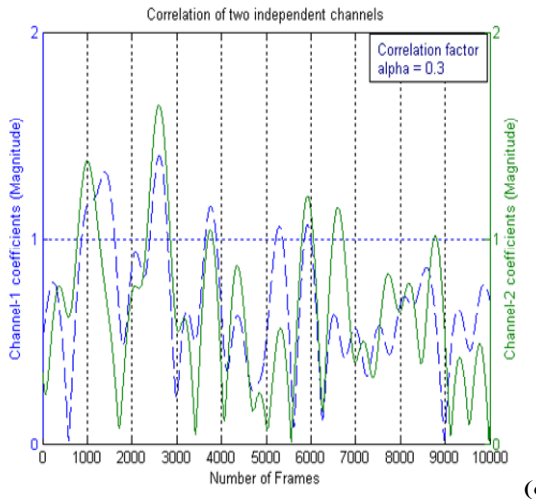
Correlation of two independent channels
Correlation factor
alpha = 0.3
Channel-1 coefficients (Magnitude)
Channel-2 coefficients (Magnitude)
Number of Frames

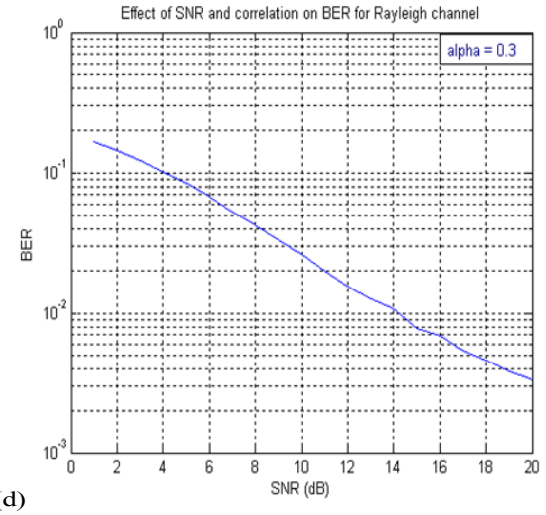
Effect of SNR and correlation on BER for Rayleigh channel
alpha = 0.3
BER
SNR (dB)

(d)

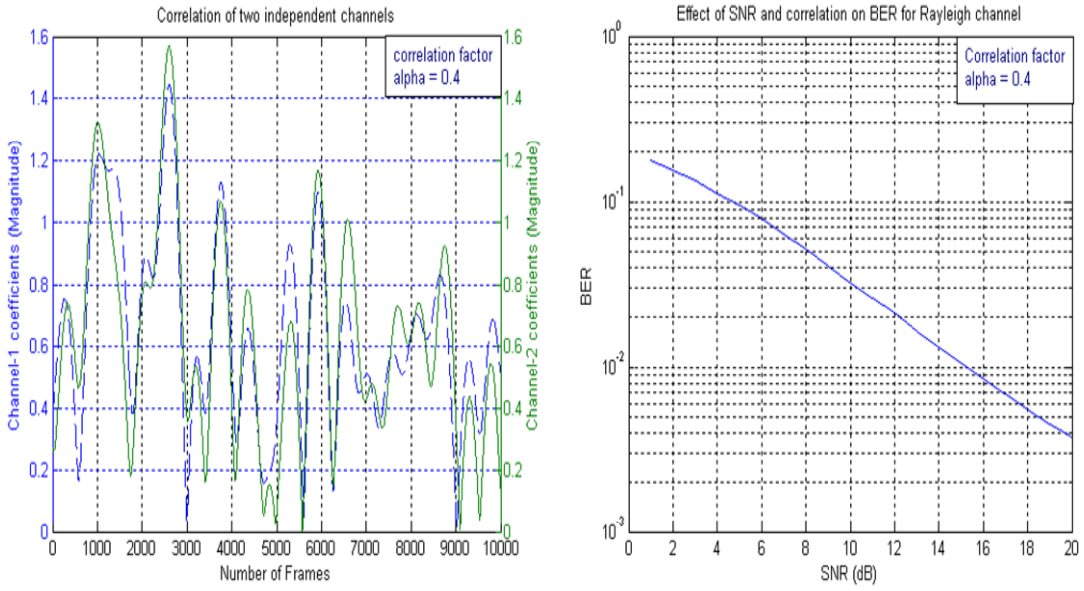

(e)

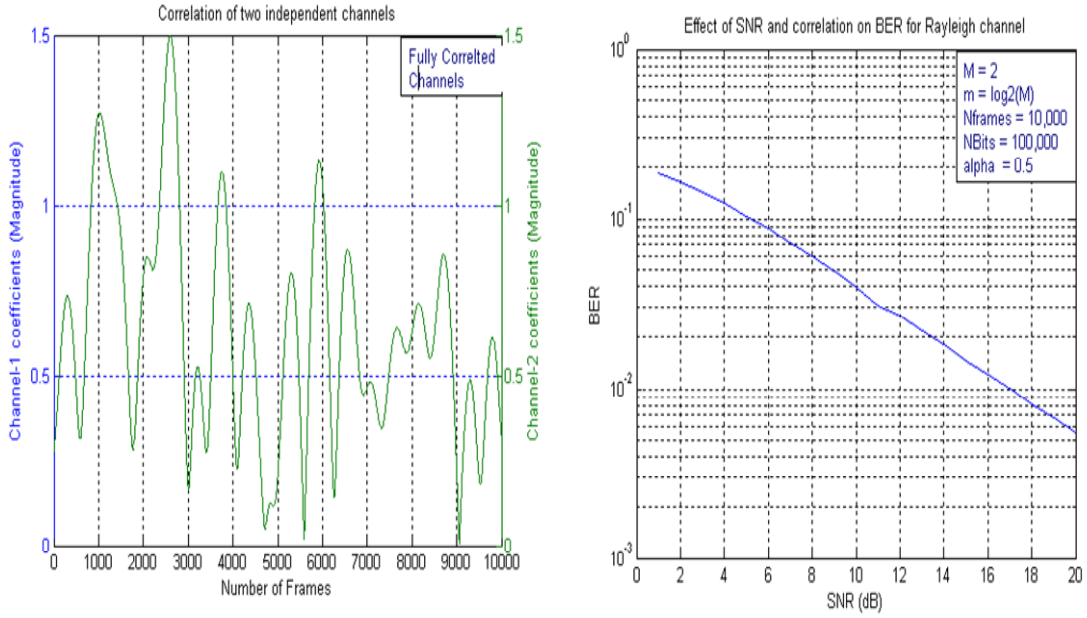

(f)

Figure 5.16: Effect of Correlation on BER

5.14.1 Results analysis

From above simulations it is observed that when the correlation factor varies from 0 to 0.5 the channels are fully correlated and BER performance is degraded. When the correlation factor is 0 at that time the channels are fully uncorrelated and BER performance is 10^{-2} at 12 dB SNR as shown above inFigure 5.16 (a)

When the correlation factor is 0.2 the channels are slightly correlated and BER performance gets slightly worse that is 10^{-2} at 13 dB SNR and even degrades to 14 dB SNR having same BER but with correlation factor of 0.3 as shown above in Figure 5.16 (c) and (d) respectively.

When the channels are fully correlated at correlation factor of 0.5 the BER performance is even degraded that is 10^{-2} at 17 dB SNR given above in Figure 5.16 (f). Hence the degradation in terms of SNR is about 5dB when the channels get fully correlated from un-correlation.

5.15 Summary

This chapter describes the use of opportunistic communication systems, where resources are allocated to the users depending upon the condition of channel in contrast to a traditional communication system, where resources are allocated as per demand of the user. In that case of traditional communication system when one of the users gets into deep fades then the channel quality is lost. Different scenarios of opportunistic communication systems have been implemented; where common and dedicated links in flat-fading and multipath fading environments using omni-directional and adaptive antennas are implemented in order to see the effect of BER performance with different antenna design. The optimal beam-former is used to identify the wanted user from an interferer by forming directional beam towards the wanted user while rejecting other users by forming nulls in those directions. As a result when the channel is allocated to wanted user, that user is able to transmit the data while making use of all the resources allocated to him at the instant of time.

The simulations are implemented using Matlab Rayleigh and spatial channel models to compare the BER performance of both channels. It is observed that under all circumstances opportunistic systems have better BER performance than non-opportunistic communication systems because of the fair scheduling of the resources and in some cases the performance of an adaptive antenna is better than omnidirectional antenna when used in multipath frequency selective environment with three co-channel users are communicating with common BS. This is because of the fact that optimal beam former is used to null out the unwanted users while forming a main beam in the direction of wanted users.

As far as the performance of the two channels is concerned it is observed that the performance of spatial channel model is better than matlab Rayleigh channel model because of the spatial and temporal parameters provided by the characteristics of spatial channel model. In addaition to that it is also observed that spatial channel has the capability of using number of scatterers to provide the multipath effect for different users communicating with common BS in various environments such as urban-macro, suburban macro and urban micro. Fair scheduling of resources was done on the basis of allocation of channel to different users and since the data and channel generation was random so it was observed that the channel was changing dynamically because of the randomness. There could always be an occasion that one of the channels goes into deep fades for a long time and user does not get enough time to send the data. In that case a switch can be used to switch off the user having good channel for long time so that the other user gets chance to send his data for the time channel is allocated to him.

Here while performing simulations although the data for different users is generated randomly everytime it goes through a loop but in order to find out the fact that data is

generated randonmly and has not come from same population some statistical analysis test was required to be performed. In order to be positive that everytime data is generated, it is different and not from same population of generations, two statistical analysis tests such as Kolmogorov and Wilcoxon ranksum tests were performed to investigate that data was generated from different populations.

In addition to that since there are chances that two users communicating have same channel characteristics as a result the correlation takes place and performance of the system in terms of BER is deterrioted since both users are likely to see the same channel. The simulation rseults for correlated channels have also been implemented to see the effect on BER performance of the systems and is observed that if the channels are correlated there is degradation in the BER performance of the system as compared to the result of uncorrelated channels where the BER performance of the system is quite good.

Chapter-6

6 MIMO System Model

6.1 Introduction

As is mostly realised that there is too much of attenuation observed in the slow fading channel as and when the channel goes into deep fade and the system is not considered to be reliable. Therefore in order to improve the capacity of the channel in rich scattering environment it is necessary to use multiple antennas at transmitting as well as at the receiving end. In case of multiple antennas being used at both ends the spectral efficiency of the system is quite high because all the transmitting antennas are using the same frequency band. Therefore this type of multiple antenna system is known as Multiple Input Multiple Output (MIMO) system that is used in in wireless local area networks (WLAN) and cellular micro-cells. Therefore a rich scattering environment exists when **WLANs** and other short range wireless systems are operating in an indoor environment.

Hence if multiple antenna elements are used at the transmitting as well as receiving end then the system configured is said to be a MIMO system. The main aim of the MIMO system is that signals at transmitting as well as receiving end are combined in such a way that the quality of the every user in a system in terms of data rate (bits/sec) is improved. Therefore this technique of configuring multiple antenna elements at both ends is considered to be a significant technique that is used to improve the performance a communication system [64].In most of the research papers it has been highlighted that using MIMO technology provides tremendous improvement in the context of throughput and range of the communication system [69],[124],[126],[128]. The history of MIMO in radio communication shows that Jack Winter at Bell Laboratories filed a patent on wireless communications using multiple antennas in 1984, where he used multiple antennas to investigate the effect of adaptive system. Then a paper giving the results in terms of the capacity gains of MIMO system was also published by Winter [127]. Jack Salz [130] from Bell Laboratories based on Winter's research also published a paper on MIMO in 1985. In 1996, Gerard J. Foschini [66] and Greg Rayleigh [131] investigated new approaches to MIMO that increased its efficiency. It has even been shown by Telatar [128,129] by increasing the number of antennas at transmitting and receiving end increases the capacity of the channel for MIMO system. At the same time another practical transmitter/receiver algorithm called the ''BLAST'' algorithm used in MIMO technique was also developed by the Foschini [134]. In this chapter different configurations of the MIMO systems have been used to analyse the performance in terms of BER of the system under various channel conditions using Matlab Rayleigh and spatial

channel models. All the simulations for different system have been run in Matlab in order to carry out the comparative analysis of BLAST and STBC MIMO systems. Simulation results are implemented alongwith the result analysis giving the advantage of use of antenna diversity.

6.2 Types of MIMO Systems

MIMO systems can be categorised as space time and spatial multiplexing systems.

6.2.1 Spatial Multiplexing System

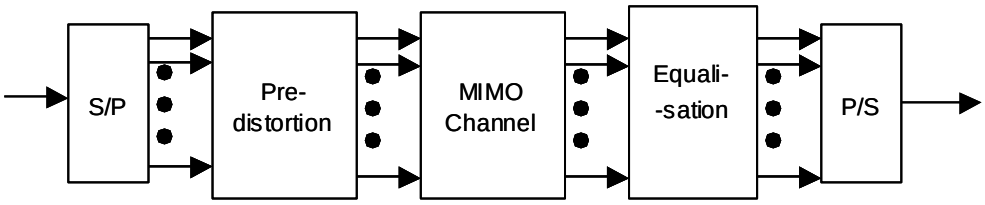

Figure 6.1: Block diagram of Spatial Multiplexing System

As spatial multiplexing is a MIMO technique and in case of rich scattering environment when this scheme is used it is possible for the receiver to de-scramble the signals that are transmitted simultaneously from different antennas. At the receiving end independent parallel data streams are received as a result an increase in the transmission rate is achieved without an extra use of power for the same bandwidth. The objective of spatial multiplexing is to maximize the transmission rate. The data throughput in this case increases almost linearly with $\min(M_T, N_R)$ as indicated by [124], where M_T and N_R are the number of transmit and receive antennas. This phenomenon of increase in the transmission rate is known as multiplexing gain. In addition to that in order to improve the quality of the system it is also recommended that some equaliser such as Zero forcing or MMSE may also be used to improve the quality of system in terms of BER, which gives better performance.

Several encoding options such as Horizontal Encoding (H-BLAST), Vertical Encoding (V-BLAST) or combination of both (D-BLAST) may be used in conjunction with spatial multiplexing.

6.2.2 Space-Time System

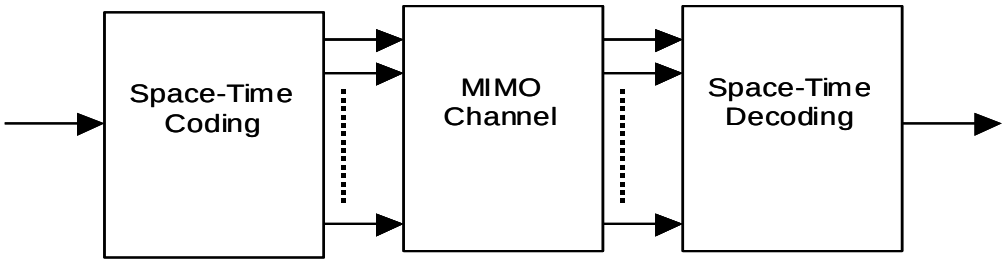

Figure 6.2: Block diagram of Space-Time System

Space-time coding is also another MIMO technique, where the streams of data are transmitted from different antennas in an appropriate manner to obtain spatial diversity. Overall, the system can achieve high throughput and reliable communication via diversity and coding gain. Space-time systems [62] have received much interest for MIMO wireless systems due to vast improvement in capacity. The same is achieved by exploiting the multipath diversity within the rich scattering channel that exists between multiple antennas at both transmitting as well as at the receiving end [43],[87]. Here in case of space-time coding the data is distributed in space by using multiple antennas and time in the form of different symbols. Different approaches in space-time coding such as space-time block codes (STBC), space-time trellis codes (STTC), space-time turbo-trellis codes (STTTC) and layered space-time codes (LST) are used [62,132]. The key feature of all these coding techniques is the exploitation of multipath effects to be able to achieve the higher performance gains. For space-time receivers to be effective to recover the transmitted signal, they rely on accurate channel state information for both narrowband and wideband systems.

6.3 Performance of MIMO Systems

MIMO systems have all the characteristics of the conventional system such as SIMO/MISO systems referred to as smart antennas employing the technique of signal processing that uses the data that has been received by multiple antenna elements at one end. In case of conventional systems if the response of each antenna element has been estimated is same as that of a desired signal, then the elements can be combined with the weights optimally. The average combined signal level can then be maximised and other components such as noise/interference can be minimised. Moreover in the case of multipath fading, since the antenna elements are fading independently so the chance of losing the signal is also vanishes exponentially. In such type of a system, the Shannon capacity of SIMO/MIMO link grows with the log of the number of the antenna elements being used [66]. Therefore the separation

of the MIMO channel is dependent on the existence of rich multipath, which is required for the channel to be spatially selective. Therefore it can be stated that MIMO system is basically meant to exploit the multipath environment, and the performance of the system in multipath environment using MIMO technology is better. In contrast, the beam forming and interference rejection antenna array systems will perform better in LOS environment because the optimisation criteria, in that case is dependent upon AoA and AoD.

6.4 MIMO Channel Model

MIMO channel models can be categorized in different ways and can be divided into wideband and narrowband based on the system's bandwidth because the characteristics of the models are affected by both the carrier frequency and bandwidth of the system. In case of wideband channel models, the bandwidth of the system is more than the coherence bandwidth of the channel so different frequencies of the channel have different channel responses. In contrast, since the bandwidth of the narrowband channel is less than the coherence bandwidth of the channel so the frequencies of the channel have same response over the bandwidth of the system. Therefore by analyzing the characteristics of the channel parameters, the MIMO channel models can be divided into physical models and non-physical channel models [45]. Therefore non-physical models are the ones which use non-physical channel parameters based on the channel's statistical characteristics, whereas the physical models use some crucial physical parameters, such as AoA, AoD and ToA to model the channel. SCM channel model is an example of physical channel model.

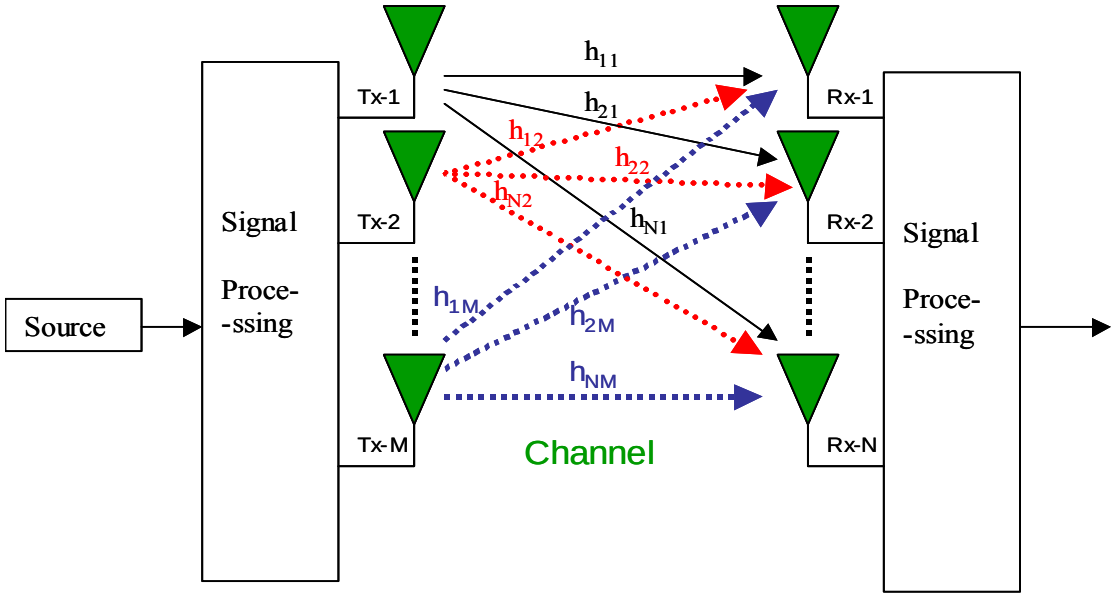

Figure 6.3: Block diagram of MIMO System

Figure 6.3 shows the block diagram of MIMO system with multiple antennas (M) at transmitter and (N) at receiver respectively. The channel matrix is denoted as $\mathbf{H} = [h_{NM}]$, where, h_{NM} are the coefficients from M^{th} transmit antenna to N^{th} receive antenna. If vector $\mathbf{x} = [x_1 \ldots\ldots\ldots\ldots x_M]^{\mathrm{T}}$ is transmitted then the received signal vector **y** is given by

$$\mathbf{y} = \mathbf{H}\mathbf{x} + \mathbf{n} \tag{6.1}$$

$$\mathbf{H} = \begin{bmatrix} h_{11} & \cdots & h_{1M} \\ \vdots & \ddots & \vdots \\ h_{N1} & \cdots & h_{NM} \end{bmatrix}$$

Where,

H is the $N \times M$ matrix of channel coefficients, **x** is a vector of transmitted signals and **n** is a vector of additive noise components.

6.5 Space-Time Coding

In order to achieve the capacity of MIMO communication systems, space-time coding is used. Here in this technique coding is done in such a way that correlation of signals transmitted at different time periods from different antenna elements is achieved in spatial and temporal domains [62]. The basic aim of spatial and temporal correlation is exploit the fading that exists in the MIMO channel thereby reducing the rate of transmission errors at the receiving end. The coding structures can be categorized into various approaches like, space-time block codes (STBC), space-time trellis codes (STTC), space-time turbo trellis codes and layered space-time (LST) codes. All these coding schemes are used to exploit the effects of the multipaths and achieving high performance of the system based on improved throughput. For the purpose of thesis STBC and LST are implemented in different environments having different antenna configurations at transmitting and receiving end using Matlab Rayleigh and spatial channel model to investigate the performance of MIMO systems in terms of bit error probability.

6.5.1 Space-Time Block Code

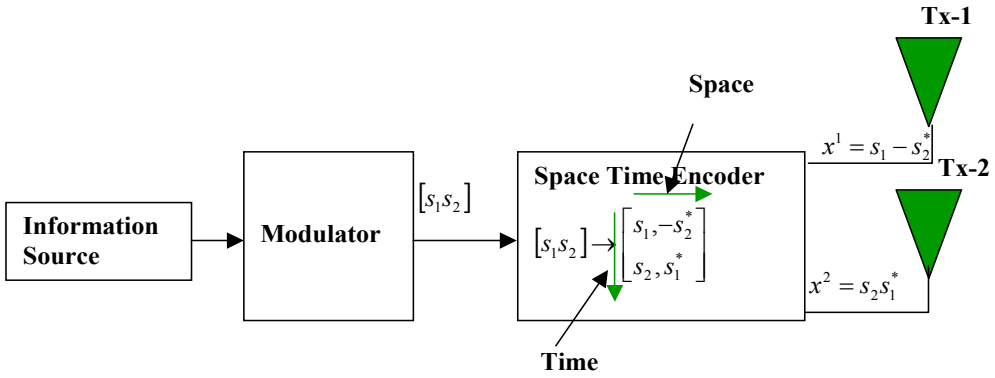

Figure 6.4: Space-Time Block Encoder

The space time block coding introduced by Alamouti is referred to as Alamouti STBC scheme [40][62][132]. The aim of the scheme is to provide diversity by processing across two transmit antennas and improving the quality of the signal at the receiving end. Therefore this scheme can be generalized to two antennas at the transmitting end and M number of antennas at the receiving end in order to provide a diversity order of $2M$. This transmit diversity scheme can improve performance of the system in terms of error rate, data rate and capacity of wireless communication system. *The essential feature of the scheme is that the sequences of data bits being generated from two transmit antennas is orthogonal to each other.* The STBC can achieve full transmit diversity specified by transmit antennas with maximum likelihood decoding algorithm. In case of Alamouti scheme, space-time encoder used is as shown in Figure 6.4 which is used to modulate each group of m information bits, where $m = \log 2(M)$ and M is the modulation order. Here in this case as shown in the Figure 6.4 above the two modulated symbols s_1 and s_2 are fed to the encoder in every encoding operation, which are then mapped to two antennas at the transmitting end as per the coding matrix given as:

$$\mathbf{X} = \begin{bmatrix} s_1 & -s_2^* \\ s_2 & s_1^* \end{bmatrix} \tag{6.2}$$

The output of the encoder is transmitted in two consecutive transmission periods from two transmitting antennas. During the first transmission period, two signals such as s_1 and s_2 are transmitted from transmitting antenna[1] and transmitting antenna[2] respectively. In the second transmission period signals such as $-s_2^*$ and s_1^* are transmitted from transmitting antenna[1] and antenna[2] respectively. s_1^* is the complex conjugate of s_1 .

It is necessary to note that in this case encoding is done in special and temporal domains, However sequence of transmission from antenna[1] and antenna[2] denoted by x^1 and x^2 respectively is given by.

$$x^1 = \left[s_1, -s_2^*\right] \tag{6.3}$$

$$x^2 = \left[s_2, s_1^*\right] \tag{6.4}$$

As already stated that the essential feature of the Alamouti scheme is that the sequence of transmission from two transmitting antennas is orthogonal, Therefore the inner product of the sequences x^1 and x^2 is zero, i.e.

$$x^1.x^2 = s_1 s_2^* - s_2^* s_1 = 0 \tag{6.5}$$

If two antennas at transmitting end and one antenna at the receiver are used, then the block diagram for implementation of Alamouti scheme is as shown in Figure 6.5

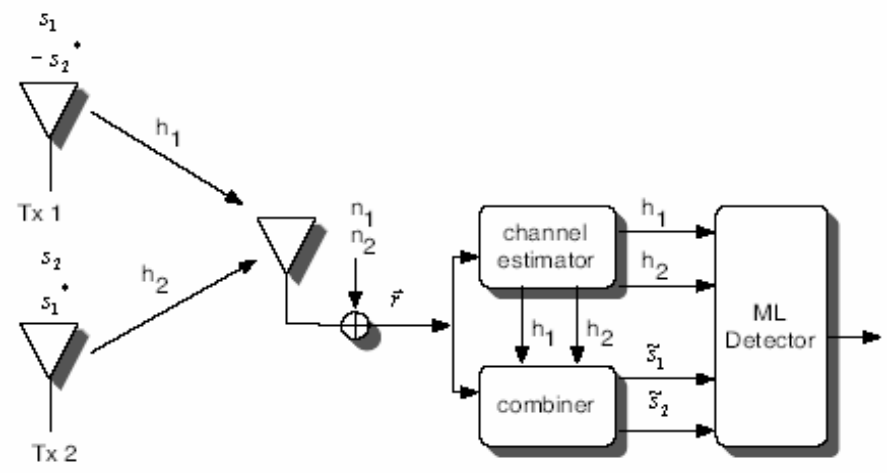

Figure 6.5: Alamouti Scheme Receiver

The channel coefficients from Tx-antenna[1] and Tx-antenna[2] at time '*t*' denoted as $h_1(t)$ and $h_2(t)$ respectively, assumed to be known in the receiver. At the receiving end the signals received over two consecutive symbol periods denoted as r_1 and r_2 are given as:

1_{st} symbol period $\qquad r_1 = h_1 s_1 + h_2 s_2 + n_1$ (6.6)

2_{nd} symbol period $\qquad r_2 = -h_1 s_2^* + h_2 s_1^* + n_2$ (6.7)

Where n_1 and n_2 are independent complex variables representing additive white Gaussian noise samples.

6.5.1.1 Detection and signal combining at Receiver

In order to be effective in recovering the received symbols the space–time receiver relies upon perfect channel estimation for both narrowband and broadband cases. In this case also it is assumed that the state of the behaviour of the channel characteristics is known a priori. An antenna array for diversity combining technique is used to de-correlate the signals at the receiving end. Therefore when the signal at any of the antenna elements is going through a deep fade, it is very rare that the signals at the other antenna elements are also in deep fade at that time; hence reception of signal on one of the antenna elements is always good. Therefore combining the signals from various elements will increase the fidelity of the received signal.
The output of the combiner in Figure 6.5 is given as [132]:

$$\tilde{\mathbf{s}}_1 = h_1^* r_1 + h_2 r_2^* \tag{6.8}$$

$$\tilde{s}_2 = h_2^* r_1 - h_1 r_2^* \tag{6.9}$$

The output of the combiner is then sent to ML detector where for every transmitted signals s_1 and s_2 decision rule of finding the minimum distance of desired point with respect to ideal constellation points is used, Here ML detection is done in two steps, First all possible combinations are generated which gets the constellation points then minimum distance from ideal points is calculated to get the optimum choice of transmitted bits. This phenomenon of maximum likelihood detector is already explained in chapter 2.

6.5.2 Diversity with '*M*' receivers

In order to achieve higher order diversity multiple antennas (M) may be used at the receiving end. Then diversity of the order of $2M$ may be achieved with two transmit antennas and M receive antennas using same STBC technique. If two antenna elements are used at the receiving end then the symbols received would be as under:

1st symbol period $\quad r_1 = h_1 s_1 + h_2 s_2 + n_1$ (6.10)

2nd symbol period $\quad r_2 = -h_1 s_2^* + h_2 s_1^* + n_2$ (6.11)

3rd symbol period $\quad r_3 = h_3 s_1 + h_4 s_2 + n_3$ (6.12)

4th symbol period $\quad r_4 = -h_3 s_2^* + h_4 s_1^* + n_4$ (6.13)

The output of combiner to be sent to ML detector in this case would be

$$\tilde{s}_1 = h_1^* r_1 + h_2 r_2^* + h_3^* r_3 + h_4 r_4^* \tag{6.14}$$

$$\tilde{s}_2 = h_2^* r_1 - h_1 r_2^* + h_3^* r_3 - h_3 r_4^* \tag{6.15}$$

6.6 Simulation of Space-Time Block Code

There are so many space time systems proposed in the recent years, but the performance of all these systems is dependent on the configuration of antenna elements at transmit and receive end in addition to existence of the spatial correlation in the channel. STBC system developed by Alamouti is one of the space time systems that can be used in different configurations. The important feature of STBC is that data transmitted from the antenna elements is orthogonal to each other as is shown in the code matrix (6.2) above.

6.6.1 Scenario-1

In this scenario Alamouti space-time block code is implemented with two systems (2Tx,1Rx) and (2Tx,2Rx) in flat fading Rayleigh channel model. The systems implemented and related block diagrams have been explained in section 6.5 above. In this case two antenna elements are used at transmitting end and initially one ant element at receiving end and then two antenna elements are used at the receiver. Different configurations of antenna elements at receiving end are used to explore the concept of receive diversity. The implementation is based to compare the results as shown in book written by Vucetic and Yuan [62]. Due to the essential feature of orthogonality in the sequence of data bits being generated from two antennas at the transmitting end, the Alamouti scheme has the capability of achieving full transmit diversity of the order of $n_T = 2$.

The method implemented assumes that the path coefficients remain constant during period of one block of data. In the simulation of this scenario it is assumed that fading from every transmitting antenna to every receiving antenna is mutually independent and that the perfect knowledge of the channel coefficients is known to receiver a priori. It is also assumed that total transmitting power is equally divided between two antennas at the transmitting end. The design parameters for simulation of these two systems are given in Table 6-1 below.

Parameters	***Values***	***Parameters***	***Values***
Sampling time (t_s)	100μsec	Modulation scheme	PSK
Doppler (f_d)	10 Hz	Modulation order (M)	2
Symbols sent (Nsymb)	200000/400000	m	$\log_2(M)$
Total bits sent	Nsymb *m	Tx antenna elements	2
		Rx antenna elements	1/2

Table 6-1: STBC (2x1) and (2x2) systems Parameters

6.6.1.1 Simulation result

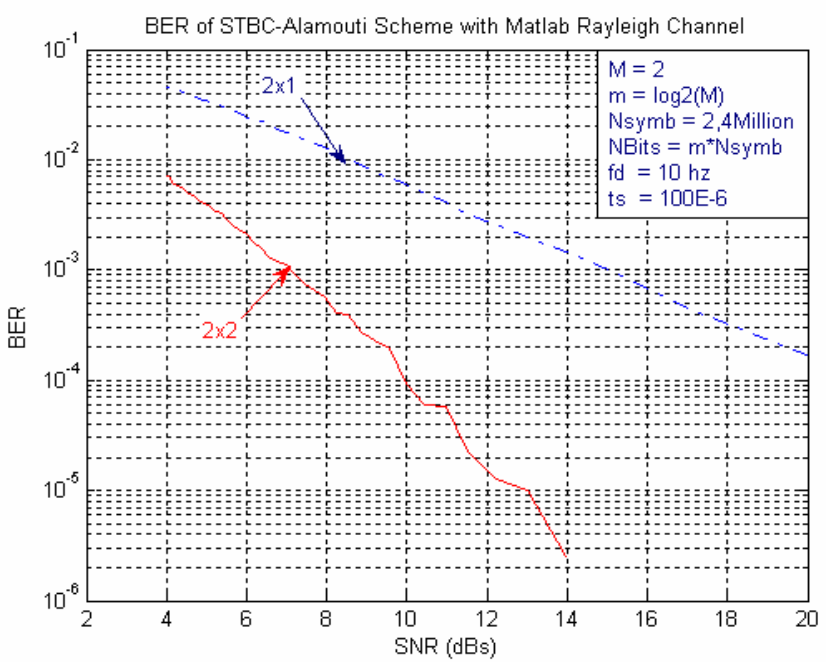

Figure 6.6: BER performance using Alamouti Scheme in Rayleigh faded Channel

6.6.1.2 Results Analysis

The BER performance of Alamouti scheme with two systems is implemented as shown in Figure 6.6 above. From the BER vs SNR relationship in the simulation results it is observed that the BER performance with two receive antennas is improved as compared to one antenna at receiving end, that is due to exploitation of spatial diversity at receiving end by increasing number of antenna elements at the receiving end.

It is observed from the simulation results shown in Figure 6.6 that BER using (2x1) system is 10^{-3} at SNR of 15dB as compared to (2x2) system having same BER performance at SNR of 7dB. So there is an improvement of about 8dB using 2x2 Alamouti scheme thereby confirming the advantage of exploiting spatial diversity at the receiving end.

6.6.2 Scenario-2

In this scenario Alamouti space-time block code is implemented with two systems (2Tx,1Rx) and (2Tx,2Rx) but with different modulation orders in flat fading Rayleigh channel model. The description and related block diagrams of the implemented systems are same as used in scenario-1 above, except that here comparison with different modulation orders is derived. In this case two antenna elements are used at transmitting end and initially one ant element at

receiving end and then two antenna elements are used at the receiver. Different configurations of antenna elements at receiving end are used to explore the concept of receive diversity. The implementation is based to compare the results as shown in book written by Vucetic and Yuan [62]. Due to the essential feature of orthogonality in the sequence of data bits being generated from two antennas at the transmitting end, the Alamouti scheme has the capability of achieving full transmit diversity of the order of $n_T = 2$. Here two systems are implemented with different modulation orders to see the effect on BER performance.

The method implemented assumes that the path coefficients remain constant during period of one block of data. In the simulation of this scenario it is assumed that fading from every transmitting antenna to every receiving antenna is mutually independent and that the perfect knowledge of the channel coefficients is known to receiver a priori. It is also assumed that total transmitting power is equally divided between two antennas at the transmitting end. The design parameters for simulation of these two systems are given in Table 6-2 below.

Parameters	***Values***	***Parameters***	***Values***
Sampling time (t_s)	100μsec	Modulation scheme	PSK
Doppler (f_d)	10 Hz	Modulation order (M)	2/4
Symbols sent (Nsymb)	25000/50000	m	$\log_2$(M)
Total bits sent	Nsymb *m	Tx antenna elements	2
		Rx antenna elements	1/2

Table 6-2: Design parameters for STBC (2x1) and (2x2) systems

6.6.2.1 Simulation result

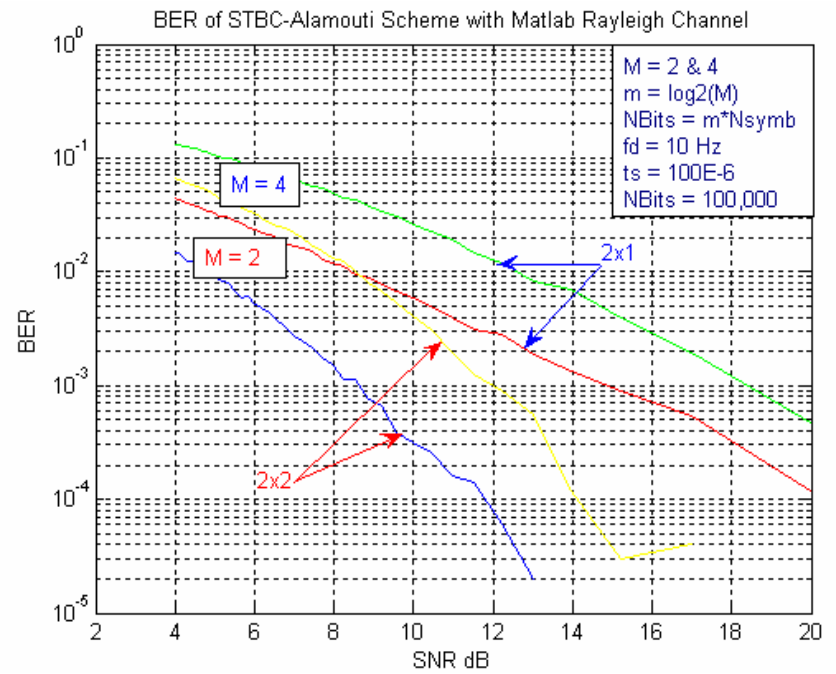

Figure 6.7: BER performance with different Modulation orders

6.6.2.2 Results Analysis

The BER performance of Alamouti scheme with two systems is implemented and BER vs SNR is plotted as shown in Figure 6.7 above.

The comparison using modulation order $M = 2,4$ is made to analyse the difference in BER performance of the system. From the results in Figure 6.7 above it is observed that BER performance with M =2 is better than M=4 modulation order. BER performance using 2x1 Alamouti scheme with M=2 modulation order is 10^{-3} at SNR of 15dB as compared to the result with modulation order of M=4 having same BER performance but at SNR of 18.5dB. There is an improvement of 3.5dB SNR with modulation order M=2.

In both cases it seen that BER performance of 2x2 system is better than 2x1 system because of the exploitation of antenna diversity at the receiving end.

Similarly BER performance using 2x2 Alamouti scheme with M=2 modulation order is 10^{-3} at SNR of 9dB as compared to result of M=4 modulation order having same BER performance but at SNR of 12dB. There is a performance degradation of 3dB SNR with modulation order M=4 due to the fact that number of bits per symbol are more as aresult the data is susceptible to noise.

6.7 Layered Space Time Architecture

6.7.1 Introduction

BLAST (Bell labs layered space time) is a system that uses number of antenna elements at transmitting as well as at the receiving end in order to transmit and receive the independent co-channel stream of data symbols by exploiting the spatial domain [68]. The essential feature of his system is that it exploits the multipath effects so that high spectral efficiency (bits/sec/Hz) of the system could be achieved. Whenever there is a rich scattering offered by multipath channel, that could be exploited by some processing architecture in order to achieve the higher capacities in terms of transmission of data rate of a wireless communication systems. The BLAST system can be categorized as D-BLAST or the V-BLAST. Foschini in [43] proposed the D-BLAST as space time approach that uses multiple antenna elements at transmitting and receiving end using diagonal architecture of the coding blocks. Because of some of the complexities that occurred in the initial implementation of D-BLAST it could not be implemented and was replaced by vertical BLAST (V-BLAST) that was implemented in real time in the laboratory as given in [69]. The D-BLAST and V-BLAST differ only in process of encoding. In D-BLAST the code blocks are organized diagonally in space-time so that high spectral efficiency is achieved for specific number of transmitting and receiving antenna elements. In contrast, for implementation of V-BLAST the vector encoding process involves the process of de-multiplexing followed by bit-to-symbol mapping of each substream independently.

6.7.2 Bell Labs Layered Space Time Architecture

Bell Labs layered space-time architecture (BLAST) was proposed by Foschini in [66] that is used to achieve the higher capacities with the help of MIMO techniques. As stated in the above section that initially D-BLAST with diagonal coding structure was used but due to involvement of some technical complexities it was modified to a new version called (VBLAST) was then proposed and prototyped in the laboratory stated in [67]. The block diagram of the VBLAST system is as shown below in Figure 6.8. From the block diagram it is clear that single stream of information signal is demultiplexed into multiple different substreams, where every substream is of information signal is then mapped to symbols by an appropriate modulator and sent to corresponding transmitting antenna element. The encoding process in this case involves the mapping of every bit to a symbol constellation for every substream, where as seen from block diagram all the substreams are mapped independently. The point to note is that the transmitting power dedicated to all the transmitters is divided equally. Similarly at the receiving end demodulators are operating independently while

remaining in the same frequency band. The signal from every transmitter is transmitted and received by every receiver. Here in this case it is assumed that cahnnel matrix H does not vary over transmission of single block of data and remains constant.

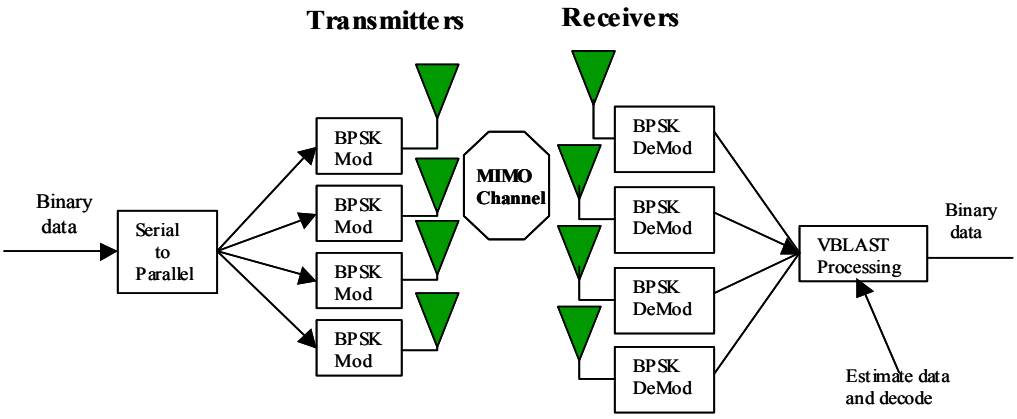

Figure 6.8: V-BLAST Architecture

AS V-BLAST is a single user system, which uses multiple transmitter elements shown in Figure 6.8. In this case all transmitter elements have been driven by information data of one user which is divided into substreams. In this case unlike TDMA all the time, all the transmitting antenna elements are using the whole bandwidth of a system and unlike FDMA whole bandwidth is occupied by every signal that is transmitted. The important and the key feature of the BLAST system is that there is not any orthogonality that is imposed or achieved between transmitting sequences. In this case the environment that exhibits multipath scattering is exploited in order to achieve decorrelation and separate the co-channel signals. The signals transmitted from all the transmitting antenna elements are received by all the receiving antenna elements. The matrix channel function is given by $\mathbf{H}^{NxM}$, where M is number of *transmit antennas* and N *is* the number of *receive antennas*. Moreover h_{ij} is the (complex) transfer function from transmitter j to receiver i. As seen from Figure 6.8 the input signal is divided into M number of substreams and every substream is then modulated with the help of an appropriate modulator and then mapped data is then sent to all the transmitters. The signal processing chain related to every substream is known as a layer. The mapped symbols are arranged into a transmission matrix denoted by $\mathbf{X}$. Where $\mathbf{X}$ is MxL matrix denoting M as number of rows and L as number of columns indicating the length of transmission block. If $\mathbf{x}_t$ is considered as the t^{th} column of a matrix, then it comprises of $x_t^1, x_t^2 \ldots\ldots x_t^M$ as modulated symbols from all the transmitters, where $t = 1,2\ldots\ldots L$. At a given time t, the t^{th}

column is sent by all the transmitters sending one symbol from each antenna. The transmission matrix $\mathbf{X}$ for *Horizontal layered space time* (HLST) architecture system having three transmit antennas is represented as:

$$\mathbf{X} = \begin{bmatrix} x_1^1 & x_2^1 & x_3^1 & x_4^1 & .... \\ x_1^2 & x_2^2 & x_3^2 & x_4^2 & .... \\ x_1^3 & x_2^3 & x_3^3 & x_4^3 & .... \end{bmatrix} \tag{6.16}$$

From transmission matrix X it is seen that sequence $x_1^1, x_2^1, x_3^1, x_4^1$..... is transmitted from antenna-1, the sequence $x_1^2, x_2^2, x_3^2, x_4^2$ from antenna-2 and sequence $x_1^3, x_2^3, x_3^3, x_4^3$ from antenna-3.

A *diagonal layered space time* (DLST) architecture can give better performance [62], where a modulated codeword of each encoder is distributed among M number of transmit antennas along the diagonal of the transmission array. The transmission matrix for three transmit antennas in case of DLST architecture is given by delaying i^{th} row entries by $(i-1)$ time units, so that the first non zero entries lie on a diagonal in transmission matrix $\mathbf{X}$. The entries below the diagonal are padded by zeroes, the first diagonal from transmission matrix given under is transmitted from first antenna, the second diagonal from second antenna and third diagonal from third antenna and then fourth diagonal from first antenna again. Transmission matrix X is given by

$$\mathbf{X} = \begin{bmatrix} x_1^1 & x_1^2 & x_1^3 & x_4^1 & x_4^2 & x_4^3 & .... \\ 0 & x_2^1 & x_2^2 & x_2^3 & x_5^1 & x_5^2 & .... \\ 0 & 0 & x_3^1 & x_3^2 & x_3^3 & x_6^1 & .... \end{bmatrix} \tag{6.17}$$

The diagonal layering introduces space diversity and thus achieves a better performance than the horizontal layering system. From (6.17) because of zero padding in diagonal architecture it is observed that there is a spectral efficiency loss in DLST.

The transmit diversity introduces spatial interference as the signals transmitted are transmitted from all the transmitting antenna elements independently and mix up in the space causing interference at the receiving end. This interference can be represented as

$$\mathbf{r}_t = \mathbf{H}\mathbf{x}_t + \mathbf{n}_t \tag{6.18}$$

Where, $\mathbf{r}_t$ is M element column vector of received signals across N number of receiving antennas, $\mathbf{x}_t$ is the t^{th} column in transmission matrix $\mathbf{X}$ and $\mathbf{n}_t$ is the M element column vector of the AWGN noise signals from the antenna elements at the receiving end.

As the vertical layered space time (VLST) receiver is based on the process of interference suppression and cancellation, therefore in this case every transmitted substream in turn is treated as desired symbol while remainder are considered to be the interfering symbols.

6.7.3 Interference Suppression Combined with Interference Cancellation

In Minimum Mean Square Error (MMSE) detection algorithm given in [62], the mean square error between transmitted vector $\mathbf{x}$ and the received vector $\mathbf{w}^H\mathbf{r}$ is minimized and given as:

$$\min E\left\{\left(\mathbf{x}-\mathbf{w}^H\mathbf{r}\right)\right\} \tag{6.19}$$

Where $\mathbf{W}$ considered as a matrix of coefficients is represented as

$$\mathbf{w}^H = \left[\mathbf{H}^H\mathbf{H}+\sigma^2\mathbf{I}_M\right]^{-1}\mathbf{H}^H \tag{6.20}$$

σ^2 is the noise variance and $\mathbf{I}_M$ is the MXM identity matrix. The decision statistics for the symbol that is sent from antenna i at time t is obtained as

$$\mathbf{y}_t^i = \mathbf{w}_i^H\mathbf{r} \tag{6.21}$$

The estimate of the symbol sent by antenna i, denoted by $\hat{x}_t^i$, is obtained by making hard decision on $\mathbf{y}_t^i$. Here $q(.)$ is the slicing function that makes the hard decision.

$$\hat{x}_t^i = q\left(\mathbf{y}_t^i\right) \tag{6.22}$$

In the process of interference suppression and cancellation the estimated signal is computed using (6.21) and (6.22) from receiving antenna element M. At this stage the strongest signal received based on the more S/N ratio is denoted by $\mathbf{r}^M$. Now in order to calculate the signal received at next antenna $(M-1)$, the interference of the hard estimate $\hat{x}_t^M$ is subtracted from the received signal $\mathbf{r}^M$ of previous step and this new version of the received signal represented as $\mathbf{r}^{M-1}$ is then used in calculating the decision statistics for antenna $(M-1)$ in (6.21) above and its hard estimate from (6.22). In the next stage, in order to receive the signal at antenna $(M-2)$, the interference from ($M-1$) is subtracted from the received signal $\mathbf{r}^{M-1}$ which is then used to calculate the decision statistics in (6.21) for antenna $(M-2)$. This process continues until the first antenna.

After detection of level i, the hard estimate $\hat{x}_t^i$ is subtracted from the received signal inorder to remove the interference contributed and providing a signal for level $i-1$

$$\mathbf{r}^{i-1} = \mathbf{r}^i - \hat{x}_t^i\mathbf{h}_i \tag{6.23}$$

Where $\mathbf{h}_i$ is the i^{th} column in the channel matrix $\mathbf{H}$.

6.7.4 Interpretation of successive interference cancellation algorithm

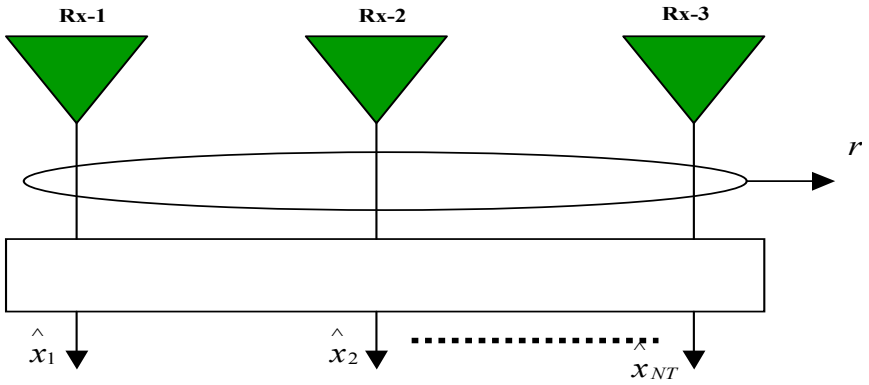

Figure 6.9: Successive interference Cancellation

In Figure 6.9 above there are three receivers and r is the original output signal at the receiving end.

Step-1 This output r is taken and used with $\mathbf{W}_{NT}^{H}$ from (6.20) above to obtain noisy signal

$\mathbf{y}_{NT} = \mathbf{w}_{NT}^{H}\mathbf{r}$ and then using (6.22) we get

$$\hat{x}_{NT} = q(\mathbf{y}_{NT}) \tag{6.24}$$

Step-2 This $\hat{x}_{NT}$ is remodulated with channel coefficients $h_{1NT}h_{2NT}h_{3NT}$..... and then subtracted from original received signal $\mathbf{r}$ i.e.

$$\mathbf{r}' = \mathbf{r} - \hat{x}_{NT}\begin{bmatrix} h_{1\,NT} \\ h_{2\,NT} \\ h_{3\,NT} \end{bmatrix} \tag{6.25}$$

This removes the effect of noisy output $\hat{x}_{NT}$ from signal $\mathbf{r}$.

Step-3 Using this output $\mathbf{r}'$ from (6.25) we obtain a new noisy output for $\mathbf{y}_{NT-1}$ i.e.

$$\mathbf{y}_{NT-1} = \mathbf{w}_{NT-1}^{H}\mathbf{r}' \tag{6.26}$$

Using (6.22) we get

$$\hat{x}_{NT-1} = q(\mathbf{y}_{NT-1}) \tag{6.27}$$

Step-4 This $\hat{x}_{NT-1}$ is remodulated with channel coefficients $h_{1NT-1}h_{2NT-1}h_{3NT-1}$..... and subtracted from received signal in step-2 above $\mathbf{r}'$ i.e.

$$\mathbf{r}'' = \mathbf{r}' - \hat{x}_{NT-1}\begin{bmatrix} h_{1\,NT-1} \\ h_{2\,NT-1} \\ h_{3\,NT-1} \end{bmatrix} \tag{6.28}$$

This removes the effect of $\hat{x}_{NT-1}$ from signal $\mathbf{r}'$.

Step-5 Using this output $\mathbf{r}''$ we obtain a new noisy output for $\mathbf{y}_{NT-2}$ i.e.

$$\mathbf{y}_{NT-2} = \mathbf{w}_{NT-2}^{H} r'' \tag{6.29}$$

Using (6.22) we get

$$\hat{x}_{NT-2} = q\left(\mathbf{y}_{NT-2}\right) \tag{6.30}$$

This process is repeated until first antenna and cancellation of all the interference signals from all transmit antennas. Here in this method ranking of the signals is done on the basis of SNR. The signal with strong SNR is at the top and subsequent signals with interference are ranked and subtracted from previous signals with strong SNR.

6.7.5 Simulation of LST System

LST systems with different configurations are implemented using Matlab and spatial channel models in the next sections in order to see the BER performance of systems with different configuration of antennas at transmit and receive end to exploit the concept of space diversity offered by the channel.

6.7.6 Matlab Rayleigh Channel model

6.7.7 MODEL-1

A simple (2x2) and (3x2) layered space-time systems from [62] have been implemented using Matlab *Rayleigh channel model*. Here the nomenclature used is (Rx,Tx), so (2,2) is considered as two Receive and two Transmit antennas system whereas (3x2) is regarded as three Receive and two transmit antennas system. The block diagrams of 2x2 and 3x2 LST systems are shown in Figure 6.10 and Figure 6.11 respectively.

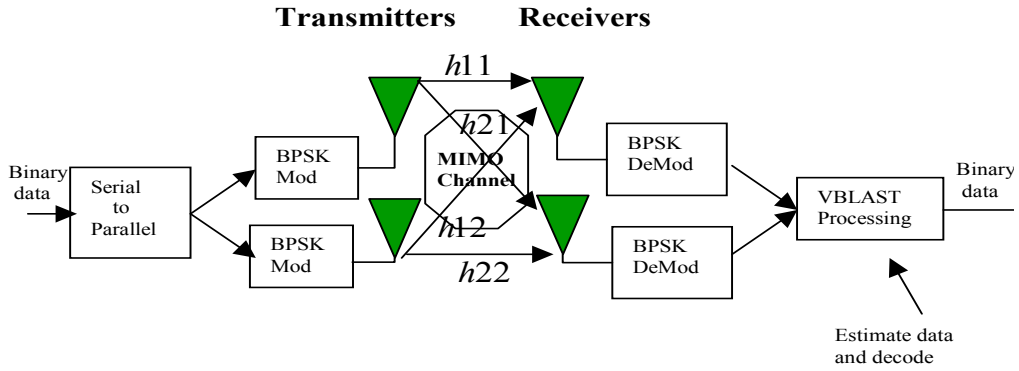

Figure 6.10: LST Architecture for 2x2 antennas

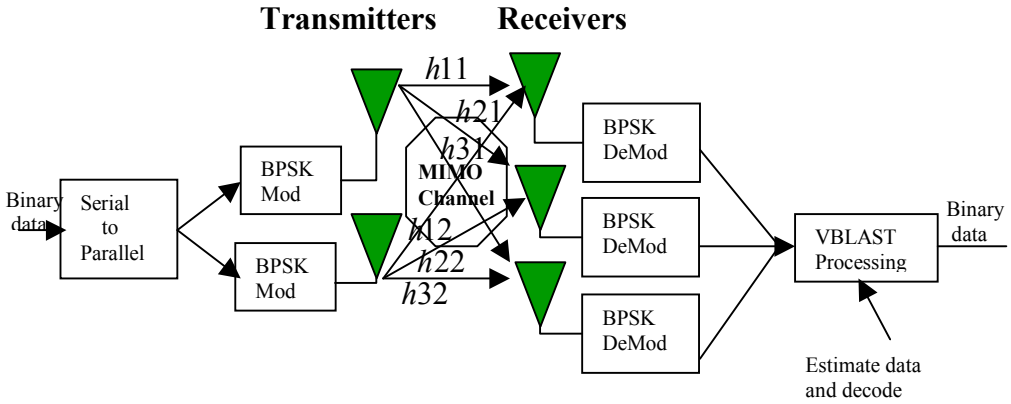

Figure 6.11: LST Architecture for 3x2 antennas

The design parameters used for simulation of both the systems are given in Table 6-3 below.

Parameters	***Values***	***Parameters***	***Values***
Sampling time (t_s)	100µsec	Modulation scheme	PSK
Doppler (f_d)	10 Hz	Modulation order (M)	2
Symbols sent (Nsymb)	100000	m	$\log_2(M)$
Total bits sent	Nsymb *m	Tx antenna elements	2
		Rx antenna elements	2/3

Table 6-3: LST (2x2) and (3x2) systems Parameters

6.7.7.1 Simulation results

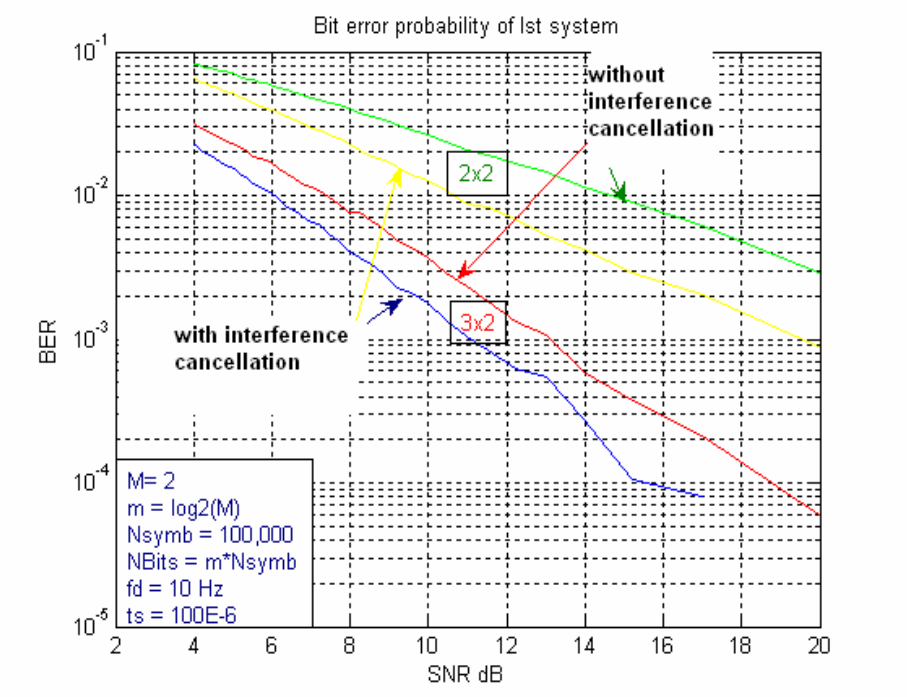

Figure 6.12: BER of LST with 3x2 antennas

6.7.7.2 Results Analysis

The simulation results for 2x2 and 3x2 simulation are shown in Figure 6.12 above. An algorithm for interference suppression and successive interference cancellation is implemented and results for both are presented in the graph.

From the simulations it is observed that overall BER performance of (3x2) system with interference suppression or interference suppression and successive cancellation is better than (2x2) system because of receive diversity in case of (3x2) LST system, where more number of antennas are used at the receiving end.

In case of (3x2) system, BER performance of 10^{-2} is achieved at SNR of 7.5dB with interference suppression only, while in case of (2x2) system same BER of 10^{-2} is achieved at 15dB SNR. Therefore a difference of about 7.5dB achieved is due to antenna diversity at receiving end.

For (2x2) system the BER performance with interference suppression only is 10^{-2} at SNR of about 15dB (green line), while with interference suppression and successive cancellation technique same BER of 10^{-2} at SNR of about 11dB (yellow line) is achieved. There is an improvement of 4dB with interference suppression and successive cancellation technique that is used to cancel the co-channel effect from the transmit antennas.

For (3x2) system, it is seen that the results with interference suppression and successive cancellation are better than interference suppression only, where BER performance of 10^{-3} is achieved at SNR of 11dB, while with interference suppression only same BER of 10^{-3} is achieved at SNR of 13dB. There is an improvement of 2dB with interference suppression and successive cancellation technique.

Similarly with interference suppression and successive interference cancellation in case of (2x2) LST system, the BER is 10^{-2} at SNR of 11dB as compared to (3x2) LST system, having same BER performance but at SNR of 6dB, again there is a difference of 5dB with same BER performance.

6.7.8 MODEL-2

Here in this case three layered space-time systems such as (2x2), (3x3) and (4x4) with a Matlab Rayleigh channel model are implemented. In this case the data rate is doubled because of the multiplexing of data across two transmitters. The aim of the simulation is to see the difference in BER performance using same number of antennas at receiving end as well as on the transmitting end.

The design parameters for the simulation are given in the table Table 6-4 below.

Parameters	***Values***	***Parameters***	***Values***
Sampling time (t_s)	100μsec	Modulation scheme	PSK
Doppler (f_d)	10 Hz	Modulation order (M)	2
Symbols sent (Nsymb)	100000	m	$\log_2(M)$
Total bits sent	Nsymb *m	Tx antenna elements	2/3/4
		Rx antenna elements	2/3/4

Table 6-4: LST (2x2), (3x3) and (4x4) systems Parameters

6.7.8.1 Simulation result

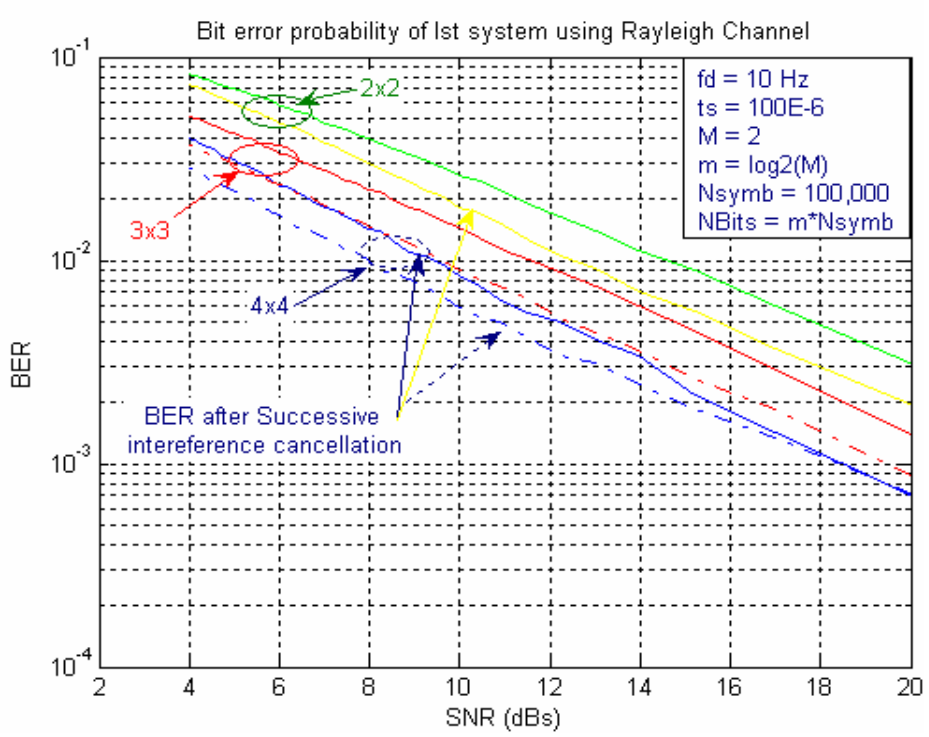

Figure 6.13: BER performance of MIMO LST Systems (Rayleigh channel model)

6.7.8.2 Results Analysis

Here three LST systems (2x2), (3x3) and (4x4) are implemented and simulation results are shown in Figure 6.13 above. An algorithm for interference suppression and successive interference cancellation is implemented to cancel the co-channel interference due to transmit antennas. The results for interference suppression only and interference suppression and successive cancellation are presented in the graph above.

From the simulations it is observed that overall BER performance of 4x4 with interference suppression or interference suppression and successive cancellation is better than 3x3 and 2x2 because of more number of antennas used thereby exploiting the antenna diversity.

For (2x2) system, with interference suppression only BER of 10^{-2} at SNR of 15dB is achieved as compared to (3x3) and (4x4) LST systems having same BER performance but at SNR of 11.5dB and 9.5dB respectively. There is an improvement in BER performance by using more number of antennas at transmit as well as at receive end also.

In case of comparison of BER performance after successive interference cancellation it is observed from simulation result that BER with (2x2) LST system is 10^{-2} at SNR of 12.5dB as compared to (3x3) and (4x4) LST systems, where same BER performance is

achieved at SNR of 9.5dB and 8dB respectively. Hence there is an improvement in BER performance while using more antennas at transmitting as well as at receiving end also.

From the simulation results shown in Figure 6.13 above it is observed that when (4x4) LST system having doppler effect is compared with simulation of (4x4) LST system in [62], It is observed that BER performance in case of [62] is 10^{-3} at SNR of 21dB as compared to simulation result of Figure 6.20 above where same BER performance is achieved at SNR of 18.5dB. So there is an improvement of 2.5dB using Rayleigh channel with 10Hz Doppler Effect also.

6.7.9 MIMO System BER performance using SCM

Here SCM is used to analyse the BER performance of a MIMO systems. For detailed description and geometry of the spatial channel model please refer to section 2.7 of chapter 2.The specific aim is to determine and compare the SCM BER performance with Matlab Rayleigh Channel Model. The MIMO system BER results using SCM and Matlab Rayleigh Channel models are implemented in Matlab.

SCM offers three simulation environments such as *suburban macro-cell, urban macro-cell and urban micro-cell.* The default parameters [118] for these environments are summarized below in Table 6-5 and simulation parameters are presented in Table 6-6 to investigate the MIMO system BER as a function of SNR.

Channel Scenario	***Suburban Macro***	***Urban Macro***	***Urban Micro***
Number of Paths (clusters)	1:6	1:6	1:6
Number of sub-paths/path	20	20	20
Mean angle spread at BS	5^0	8^0,5^0	NLOS:19^0
Per path angle spread at BS (Fixed)	2^0	2^0	NLOS and LOS 5^0
Mean angle spread at MS	68^0	68^0	68^0
Per path angle spread at MS (Fixed)	35^0	35^0	35^0

Table 6-5: Environmental Parameters of SCM

Parameter	*Value*
Center frequency *(f_c)*	2.4 GHz
Bandwidth	5 MHz
Antenna spacing	0.5m
SNR	1: 40 dB
fd	10 Hz
ts	0.2E-6 sec
Modulation scheme	PSK/QAM
Modulation Order (M)	2/4
N_symbols	0.1 Million

Table 6-6 Simulation Parameters of SCM

6.7.10 Model-1

Here in this case two (3x2) and (4x2) LST systems are implemented using spatial channel model to see the difference of BER performance of both the systems. The schematic block diagrams and description of the implemented systems is same as described in 6.7.2 above except that in this case spatial channel model is considered for simulation.

The design parameters for implementation of both the models are given in Table 6-7.

Parameter	*Value*	*Parameter*	*Value*
Center frequency *(f_c)*	2.4 GHz	*ts*	3.75msec
Bandwidth	5 MHz	Modulation scheme	PSK
Antenna spacing	0.5	Modulation Order (M)	2
SNR	1: 20 dB	N_symbols	0.1 Million
Tx antennas	2	*fd*	10 Hz
Rx antennas	3/4		

Table 6-7: LST (3x2) and (4x2) systems Parameters (SCM)

6.7.10.1 Simulation result

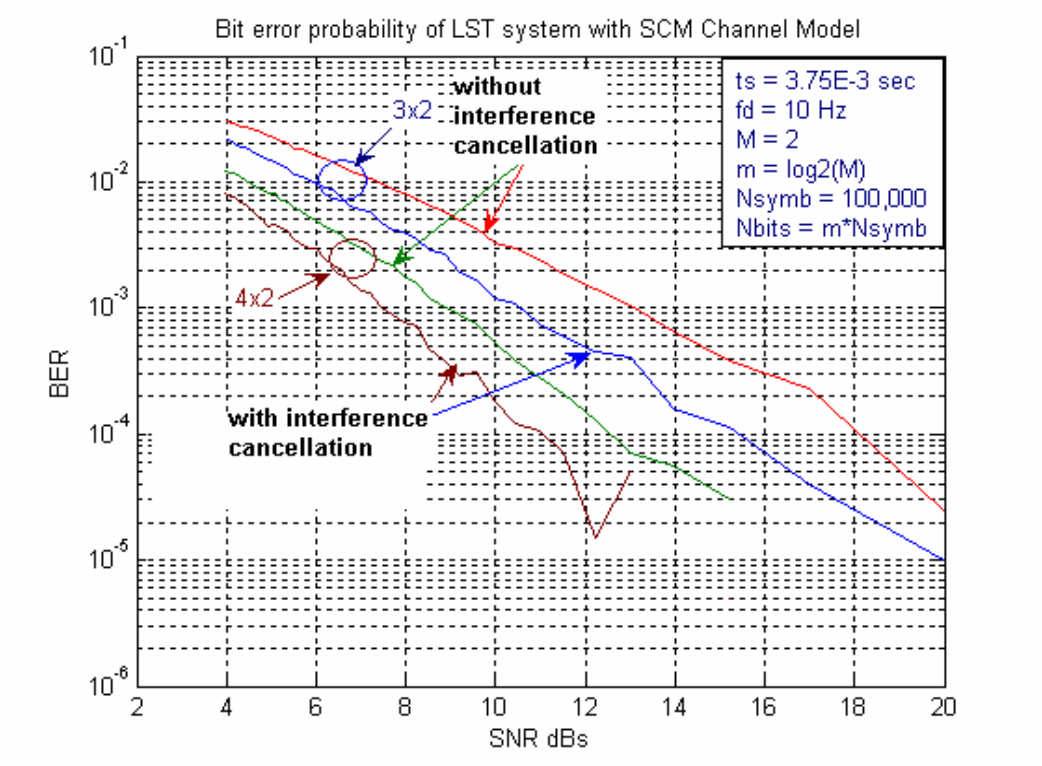

Figure 6.14: BER Performance of 3x2 and 4x2 with SCM

6.7.10.2 Results Analysis

Here in this case two (3x2) and (4x2) LST systems using spatial channel model (SCM) are implemented and simulation results are shown in Figure 6.14. Here in these two systems 2-Tx antennas are used while at receiving end 3 and 4 antennas are used.

From the results it is seen that overall both the systems performance is better when using interference suppression plus successive cancellation technique as compared to a case when only interference suppression technique is used then BER performance is even worse in both the systems. In case of (4x2) system the BER of 10^{-4} at 11dB SNR is achieved with successive cancellation, while same BER 10^{-4} at 13dB is achieved with interference suppression only. There is an improvement if 2dB with successive cancellation technique.

From simulation results it is observed that by increasing number of antennas at receiving end BER performance using 4xreceive antennas is 10^{-4} at SNR of 11 dB as compared to a system with 3xreceive antennas, where same BER performance is achieved at SNR of 15dB. So there is an improvement of 4 dB using 4xreceive antenna elements

employing interference suppression and successive cancellation technique. This is achieved because of additional diversity offered by using more number of antennas at the receiving end.

6.7.11 Model-2

Here in this case three (2x2), (3x3) and (4x2) LST systems are implemented using spatial channel model to see the difference of BER performance of all three systems.

The design parameters for implementation of the systems are same as given above for Model-1 except the number of antenna elements at receiving end are changed to 2, 3 and 4.

6.7.11.1 Simulation result

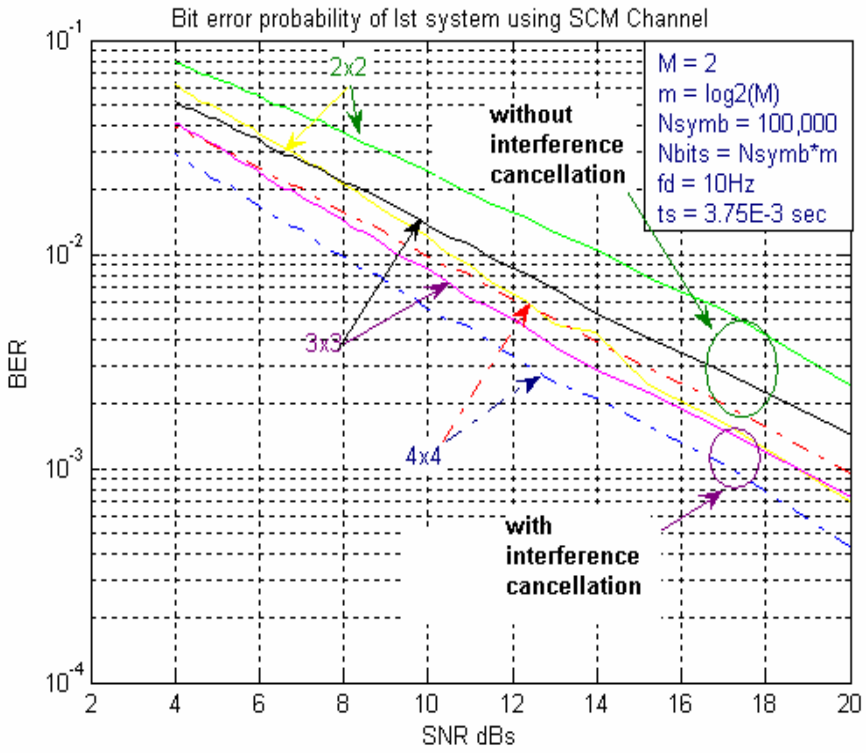

Figure 6.15: BER Performance of MIMO LST

6.7.11.2 Results Analysis

In this case three LST systems with same number of antenna elements are implemented to see the effect on BER performance of the systems with increasing the antenna elements

From the results of Figure 6.15 it is observed that the BER performance of (4x4) system is improved with more number of antennas as compared to (2x2) and (3x3) systems.

If the results are compared with the results in Figure 6.14 it is observed that performance of (2x4) system is better than (4x4) system, where BER of 10^{-4} at SNR of 11dB

is achieved as compared to (4x4) system where same performance is achieved above 20dB SNR.

It is important to note that in case of LST systems the data rate is improved with more number of antenna elements but BER performance is not improved because in this case the diversity is not exploited by using equal number of antennas at both ends.

6.7.12 Model-3

Here in this case one (2x2) LST system is implemented using spatial channel and Matlab Rayleigh models to see the difference of BER performance in both channels.

The design parameters for implementation of the systems are same as given in Table 6-4 and Table 6-8 above for Rayleigh and spatial channel models respectively.

6.7.12.1 Simulation result

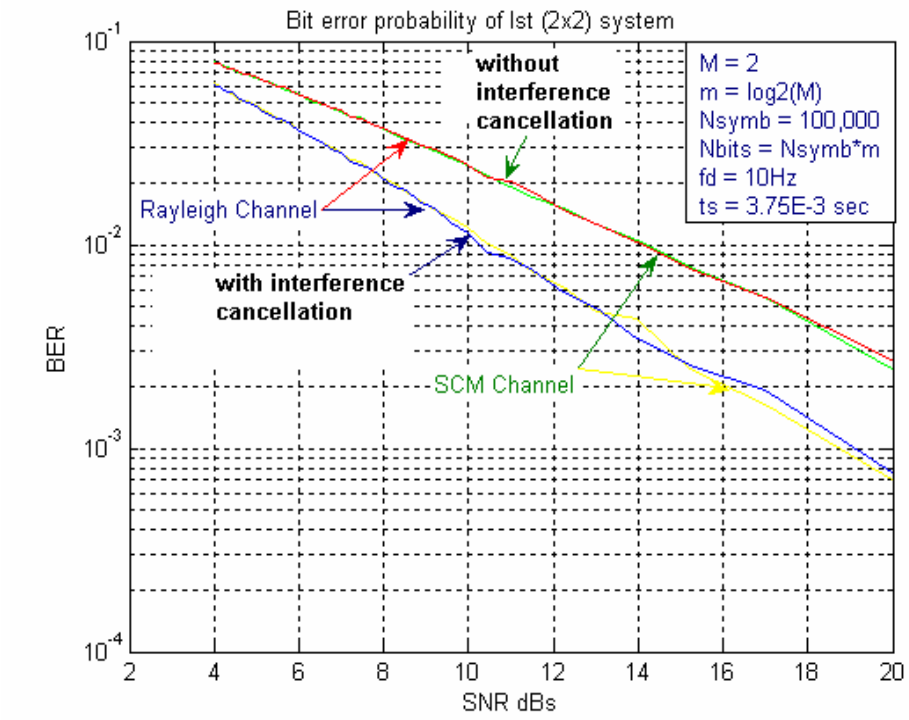

Figure 6.16 : Comparison of SCM and Rayleigh Channel Models in LST Architecture

6.7.12.2 Results Analysis

In this case same (2x2) system model is implemented in Matlab Rayleigh channel and spatial channel model.

In Figure 6.16 comparison of 2x2 antennas using SCM and Rayleigh channel model is simulated with same parameters for both the channels.

It is observed that BER performance in both cases using Matlab Rayleigh channel model or spatial channel model is almost same, where BER performance of 10^{-3} is achieved at SNR of 19dB when implemented with interference suppression and successive cancellation technique.

It is important to note that BER performance with interference suppression and successive technique is better than interference suppression only.

6.8 Summary

This chapter covers the types MIMO systems and then implementation of different configuration of MIMO architecturs with the help of space time block code system and Layered space time architecture. The LST system has different flavours like vertical layered space time system (VLST), diagonal layered space time system (DLST) and horizontal layered space time system (HLST). For the purpose of implementation only VLST system is implemented to compare the BER performance with STBC system.

Simulations of Matlab Rayleigh and spatial channel models using MIMO systems have been implemented using MIMO system configurations to show the BER vs SNR performance of the systems. From simulation results it is observed that BER performance is significantly improved with MIMO systems as more antennas are used to exploit the effect of spatial diversity in the system. In case of STBC system both space and time domains are exploited at transmitting end and is observed that the essential feature of STBC system is that signals at transmitting antenna are orthogonal to each other.

At the same it is also observed that using layered space time architecture the BER performance with MIMO systems is not improved as much as compared to the case of STBC system but data rate in this case is doubled due to multiplexing of data at the transmitting end.

It is also seen from the simulations that overall LST systems using successive interference cancellation technique that cancels the effect of co-channel interference because of transmit antennas have better BER performance than systems where interference cancellation is not carried out. For the purpose of interference cancellation the ranking of received signal is done based on the value of SNR. A signal with highest SNR is at highest priority as compared to other having lower SNR. Then interference cancellation is carried out by subtracting the strongest interference from highest SNR signal.

It is worth to note that STBC systems are better if BER performance improvement is required for fixed data rate, while LST systems are better for improvement of data rate depending on the number of transmit antennas as the data on all the transmitters is multiplexed.

Chapter-7

7 Orthogonal Frequency Division Multiplexing

7.1 Introduction

In a realistic environment the channel is time varying as a result mostly there is not a direct link between transmitter and receiver as the communication channel exhibits strong amplitude and phase distortions and the phenomenon of reflection, refraction, diffraction and scattering etc cause the temporal and spatial frequency dependent fluctuations in the received signals. As a result of all these factors the receiver receives multiple delayed copies of the transmitted signal and this received signal appears to be a distorted version of the transmitted one. In addition to static obstacles there are moving obstacles also and is possible that when the transmitter or the receiver is moving a Doppler shift occurs in the receiver as a result of which the inter carrier interference (ICI) takes place. Because of the multipath effect the signal level at receiving end is not constant and received signal is fluctuated randomly. Hence in order to avoid this problem of distortion orthogonal frequency division multiplexing (OFDM) is used which is a multi-carrier modulation technique where the carrier spacing is selected in such a way that every sub-carrier is orthogonal to the other sub-carriers [8]. In such type of techniques given spectrum is divided into several overlapping sub-bands thereby converting highly frequency selective channel into many flat-fading sub-channels. Moreover it is worth mentioning that correlation technique is used to separate these orthogonal signals at the receiving end in order to remove the ISI amongst channels. In addition to that the ISI can also be removed by proper selection of parameters like number of tones and spacing between tones.

7.2 Concept of FDM and OFDM

Frequency Division Multiplexing (FDM), as shown in Figure 7.1(a) has been extensively used in frequency selective channels, where the data rate is higher than the coherence bandwidth of the channel. FDM divides the bandwidth of the channel into sub-channels, where each sub-channel is served by its own carrier frequency, and stream of data is multiplexed into parallel data streams of lower rate which are then modulated on to these separate carriers. To facilitate demodulation of these parallel signals at the receiving end, the carrier frequencies are at a sufficient distance from each other to avoid the overlapping. The main feature of the FDM method is that the bandwidth of every sub-carrier is less than the coherence bandwidth so that each data stream can be considered to suffer from flat fading rather than frequency selective fading. FDM is difficult to implement because it requires

multiple carriers to be generated in the receiver and multiple local oscillators in the receiver. In addition, it is not spectrally efficient because each sub-carrier must be separated by a frequency guard-band that is sufficiently wide to allow each sub-carrier to be demodulated without causing adjacent channel interference. In order to solve both the bandwidth efficiency problem and the generation of sub-carriers, orthogonal frequency division multiplexing (OFDM) was proposed in [141] using *orthogonal* tones for modulation of the parallel data streams. The spacing between the tones is equal to the duration of symbol rate so that they can be separated at the receiving end using coherent techniques, even though the spectra of each of the sub-carriers fully overlap. This carrier spacing provides optimum spectral efficiency [143]. This is the advantage of OFDM over FDM. If each symbol stream has a bandwidth of *2B*, the FDM system will require a bandwidth of 2*L(B*+GB), (where GB is the frequency guardband) while OFDM will only require a bandwidth of *LB*. This property stems from the fact that symbols are orthogonal over time rather than frequency. Hence in the case of orthogonal frequency division multiplexing, as shown in Figure 7.1(b), minimum frequency space between carriers is set without having inter-carrier interference (ICI). Although OFDM is robust to ISI, it is not immune to the effects of flat fading, which can cause unacceptable performance degradation– indeed OFDM converts frequency selective fading to flat-fading.

Today, OFDM is widely used in a number of important wireless systems. It is used in the WiFi wireless LAN system (802.11) as well as the new WiMAX wireless MAN system 802.16. It is also incorporated into the standard for the WiBro (802.20) mobile wireless MAN standard. In addition it is also proposed for 4G wireless applications [143].

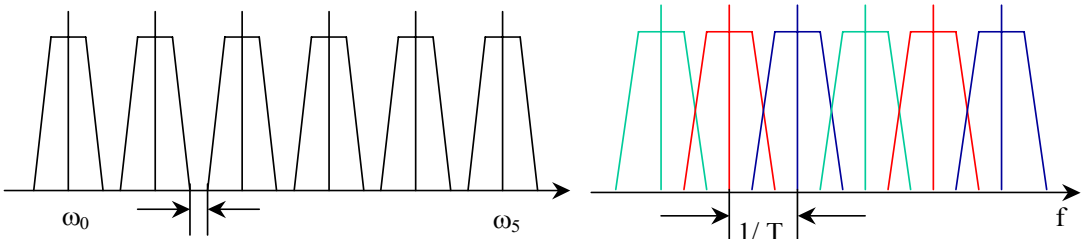

Figure 7.1 (a) Conventional FDM **(b) OFDM**

In case of an OFDM system if is assumed that the data at the k^{th} symbol to be transmitted is encoded into complex symbols given as:

$$d(k) = a(k) + jb(k) \tag{7.1}$$

The signal at the output of the transmitter can be represented as [140]:

$$\begin{aligned}\mathbf{x}(t) &= \sum_{k=0}^{K-1} a(k)\cos(\omega_k t) + b(k)\sin(\omega_k t) \\ &= \Re\left\{\sum_{k=0}^{K-1}\left(a_k + jb_k\right)e^{(j\omega_k t)}\right\} \\ &= \Re\left\{\sum_{k=0}^{k-1} d_k e^{(jw_k t)}\right\}\end{aligned} \tag{7.2}$$

Where *a(k)* is represented as in-phase component and *b(k)* is the quadrature component and $\omega_k = 2\pi f_k$ represents the sub-carrier frequency.

Using the complex conjugate of (7.2) the $\Re$ part can be calculated:

$$\begin{aligned}\mathbf{x}(t) &= \sum_{k=0}^{K-1}\frac{1}{2}\left\{d_k e^{(j2\pi f_{ok}t)} + d_k^* e^{(-j2\pi f_{ok}t)}\right\} \\ &= \sum_{k=-(K-1)}^{K-1}\frac{1}{2} d_k e^{(j2\pi f_{ok}t)}\end{aligned} \tag{7.3}$$

Where $k = 0\ldots\ldots K-1$

$d_{-k} = d_k^*,\ d_0 = 0,\ f_{o(-k)} = -f_{ok},\ f_{oo} = 0,$

$f_k = k\Delta f$, where Δf is the carrier spacing

By introducing the Fourier coefficient F_k (7.3) can be formalized as [140]:

$$F_k = \begin{Bmatrix}\frac{1}{2}d_n & if & 1 \le k \le K-1 \\ \frac{1}{2}d_n^* & if & -(k-1) \le k \le -1 \\ 0 & if & k = 0\end{Bmatrix} \tag{7.4}$$

The Fourier coefficients of a real signal are conjugate complex symmetric, so (7.3) can be written in a form that is very close to DFT as:

$$\mathbf{x}(t) = \sum_{k=-(K-1)}^{K-1} F_k . e^{j2\pi f_{ok}t} \tag{7.5}$$

Assuming that sub-channel carriers take the values of $f_{ok} = kf_o$, where $k = 0\ldots\ldots K-1$ and $f_o = 1/T$ represents the sub-carrier spacing considered as reciprocal of the sub-channel signal interval, The total one sided bandwidth $B=(K-1)f_o$.

Now using the discretised time $t = i\Delta t$, where $\Delta t = 1/f_s$ is the reciprocal of the sampling frequency f_s (7.5) can be written as:

$$\mathbf{x}(i\Delta t) = \sum_{k=-(K-1)}^{K-1} F_k . e^{j2\pi f_{ok} i\Delta t} \tag{7.6}$$

The Nyquist criterion is met if $f_s = 2(K-1)f_o$ and the sampling frequency f_s is an integer multiple of sub-carrier spacing f_o represented as $f_s = Mf_o$. So the spectrum of a sampled signal repeats itself at multiples of the sampling frequency f_s with a periodicity of $M = f_s / f_o$ samples. By exploiting the conjugate complex symmetry of the spectrum, for the Fourier coefficients F_k, we get:

$$F_k = \begin{cases} F_{k-M} = F^*_{M-k} & if \quad \left(\frac{M}{2}+1\right) \le k \le M-1 \\ 0 & if \quad K-1 \le k \le \frac{M}{2} \end{cases} \tag{7.7}$$

Here the frequency region $(K-1)f_o \le f_k \le \frac{M}{2} f_o$ represents the unused band of the communication channel, where amplitude and delay distortion is significant. By exploiting the conjugate complex symmetry from (7.5) the real modulated signal can be written as:

$$\mathbf{x}(i\Delta t) = \sum_{k=0}^{M-1} F_k . e^{j\frac{2\pi}{M}ki}, i = 0 \cdots M-1 \tag{7.8}$$

This is the standard IDFT that can be computed by IFFT if the transform length M is the integer power of 2.

After having achieved the modulation of all the sub-carriers using IFFT at the transmitting end it is assumed that the input signal is periodic in both time and frequency domain with a periodicity of M samples. If the modulated sample sequence of (7.8) is periodically repeated and transmitted via low pass filter (LPF) preceeding the channel, the channel is excited with a continuous, periodic signal. Assuming a LPF with a cutt-off frequency of $f_c = 1/2\Delta t = f_s/2$ and transmitting only one period of $x(i\Delta t)$, the cahnnel's input signal becomes:

$$\begin{aligned} x_{0,LPF}(t) &= x(i\Delta t) * \frac{1}{\Delta t} \frac{\sin\left(\pi t / \Delta t\right)}{\pi t / \Delta t} \\ &= x(i\Delta t) * \frac{1}{\Delta t} \sin c \frac{\pi t}{\Delta t} \end{aligned} \tag{7.9}$$

Where the LPF's impulse response is given by *sinc* function and hence $X_{0,LPF}(i\Delta t)$, is given by

$$x(i\Delta t) = x_{0,p}(i\Delta t)\,rect\frac{t}{T} \tag{7.10}$$

The convolution in (7.9) can be written as:

$$x_{0,LPF}(t) = \sum_{i=1}^{M-1} x_0(i\Delta t)\frac{1}{\Delta t}\sin c\frac{\pi(t-i\Delta t)}{\Delta t} \tag{7.11}$$

In spectral domain (7.11) can be written as

$$\mathbf{X}_{0,LPF}(f) = M_0(f)\,rect\frac{f}{f_c} \tag{7.12}$$

Where, $\mathbf{X}_0(f) = FFT\{x_{0,p}(i\Delta t)\}$ and $H_{LPF}(f) = rect\frac{f}{f_c}$ is the LPF's frequency domain transfer function. Transforming (7.10) into frequency domain we get:

$$\begin{aligned}\mathbf{X}_0(f) &= FFT\left\{x_{0,p}(i\Delta t)\,rect\frac{t}{T}\right\} \\ &= \mathbf{X}_{0,p}(f) * \frac{1}{f_0}\sin c\frac{\pi f}{f_0}\end{aligned} \tag{7.13}$$

Where, $X_{0,p}(f)$ is the frequency domain representation of $x_{0,p}(i\Delta t)$, which is convolved with the Fourier transform of the $rect\frac{t}{T}$ function. Now $X_0(f)$ of equation (7.13) is lowpass filtered according to (7.12), giving:

$$\begin{aligned}X_{0,LPF}(f) &= X_0(f)\,rect\frac{f}{f_c} \\ &= \left[X_{0,p}(f) * \frac{1}{f_0}\sin c\frac{\pi f}{f_0}\right] rect\frac{f}{f_c}\end{aligned} \tag{7.14}$$

So the effect of the time domain truncation of the periodic modulated signal $x_{0,p}(i\Delta t)$, to a single period as in (7.10) manifests itself in the frequency domain as the convolution of (7.13), generating the infinite bandwidth signal $X_0(f)$. When $X_0(f)$ is low pass filtered according to (7.14), it becomes bandlimited to f_c and its Fourier transform pair $x_{0,LPF}(t)$ in (7.9) has an infinite time domain support due to the convolution with $\sin c(\pi t/\Delta t)$. This phenomenon results in interference due to time domain overlapping between consecutive transmission blocks, which can be mitigated by quasi-periodically extending $x_0(i\Delta t)$, for the duration of the memeory of the channel before transmission. At the receiver only unimpaired central section is used for signal detection.

7.3 OFDM Implementation

The block diagram of an OFDM system is shown below in Figure 7.3. Basically OFDM is the combination of modulation and multiplexing, where multiplexing represents the splitting of the single data stream into the parallel lower-rate streams (equivalently splitting the available bandwidth into the parallel sub-channels) and modulation is the mapping of the data symbols (information) as complex-valued signal samples on each of these sub-carriers. The main advantage of OFDM is that it mitigates the effect of frequency-selective fading as well as the equally important problem of Inter-Symbol Interference (ISI), which is common in high-speed wireless communication.

In conventional single carrier systems, the usual method of mitigating ISI due to channel delay spread is to use a delay equaliser, and this approach was covered in Chapter 2, where results were presented to show how the equaliser improved the BER performance in multipath fading. A major problem is the need to use an adaptive delay equaliser because of the changing channel conditions as the handset moves. This can take a long time for the adaptive equaliser to converge and this impacts on the quality of the received data. For the case of OFDM, ISI is mitigated in a different way to the single carrier approach and this has significant improvements in implementing a high-rate communication scheme.

In OFDM [143], ISI is removed by inserting a timeguard-band between each transmitted OFDM symbol equal or longer than the duration of the channel delay spread, T_{ds}. This ensures that any multipath interference that corrupts one symbol is confined to that symbol, thereby removing ISI. In single carrier systems, such an approach is impractical because it naturally limits the data rate to approximately $1/(2T_{ds})$ where T_{ds} is the delay spread. For example, if the delay spread of a typical channel is 5□s, then if the data period is also 5□s, the period between data bits is 10□s and the data rate is 100kb/s. Substantially shortening the data bit period reduces the energy per bit (and hence BER) and this is not effective because of the guard interval between bits.

In the case of OFDM, if the data is split into M parallel streams, the data rate on each stream is reduced by the factor M and the nominal duration of each OFDM symbol is lengthened to MT_s, where T_s is the symbol duration of the original data stream for the chosen modulation scheme. If M is large, such that $MT_s >> T_{ds}$ then the loss in efficiency of using a guard interval is considerably smaller than for the single carrier case. The high data rate of the OFDM system is achieved because M OFDM symbols are transmitted, synchronously in parallel. In a practical system, the guard interval is achieved by adding $T_{ds} = T_g = T_s$GI symbols to the end of each OFDM symbol, where T_s is the symbol duration of the input data stream and GI is the number of symbols used in the Guard band. In practice, the guardband is not

represented by a null signal because, this causes unacceptable inter carrier interference. In practice, the guard interval is a *cyclic extension* of the OFDM frame to ensure that the orthogonality between the sub-carriers is not lost.

The ideal OFDM system does not have any performance degradation in white noise, compared with a single carrier system, as long as no guard interval is used. If a guard interval is used, the bit error performance of the system is reduced because energy has to be wasted sending the cyclic prefix which is then discarded in the receiver. In case of Rayleigh fading channel when used with Doppler, it suffers from inter symbol interference (ISI). In order to solve the problem of ISI the length of an OFDM block has to be equal to or greater than delay spread as shown below.

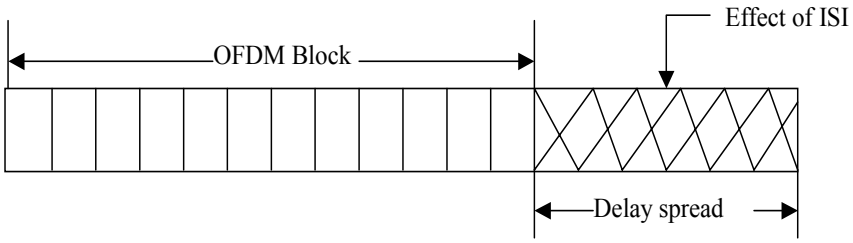

The maximum time delay that occurs is called delay spread of the signal in that particular environment. The delay spread can be large or shorter than the symbol time and in both cases different type of degradation occurs to the signal, as a result the delay spread changes with the change of an environment. It is not wrong to say that when the delay spread is less than one symbol period is considered to be a case of flat fading whereas if the delay spread is larger than one symbol period, the phenomenon is called frequency selective fading. Usually an OFDM system created works as is shown below in Figure 7.2.

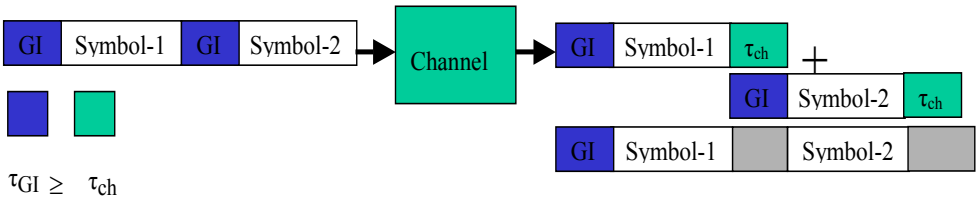

Figure 7.2: Implementation of an OFDM system

7.4 Methodology for implementation of an OFDM system

An OFDM system delivers information in parallel over *M* sub-carriers and *M* is the size of FFT bins. As indicated in Figure 7.3 from block diagram of an OFDM system, the operation of an OFDM system can be described as under:

1. A block of random data bits is generated and then converted to a multi-level symbol according to an appropriate modulation scheme used.
2. The multi-level symbol signal is then mapped to a complex-valued signal using an appropriate modulator (e.g. M'PSK or QAM as used here).
3. This signal mapper is used to set the amplitude and phase of each sub-channel in the form of complex values represented in the shape of constellation.
4. The serial stream of complex-valued signals is converted to *M* lower-rate parallel streams and then an IFFT operation is performed on these M complex samples to convert the frequency domain phase and amplitude data for each sub-channel into block of time domain samples.
5. These parallel samples are then converted to a serial stream of data and cyclic prefix is then added to each OFDM symbol by copying the first GI samples at the IFFT output and adding these to the end of the IFFT output, so that there are now *M*+GI samples in the output stream. These M+GI signal samples are then clocked out (at a higher rate than the original data stream to account for the extra GI prefix samples) to form the transmitted signal.
6. These samples are sent across the Rayleigh faded multipath channel.
7. At the receiving end the guard interval or cyclic prefix is removed and this serial stream of data is converted to parallel stream.
8. FFT operation is performed to extract the phase and amplitude of each received sub-channel from block of received samples and converts the data back to frequency domain.
9. After FFT operation the data is converted to serial stream and then is demodulated using an appropriate demodulator.
10. These received demodulated symbols are then converted to binary form and BER is detected by comparing the input and received output data bits.

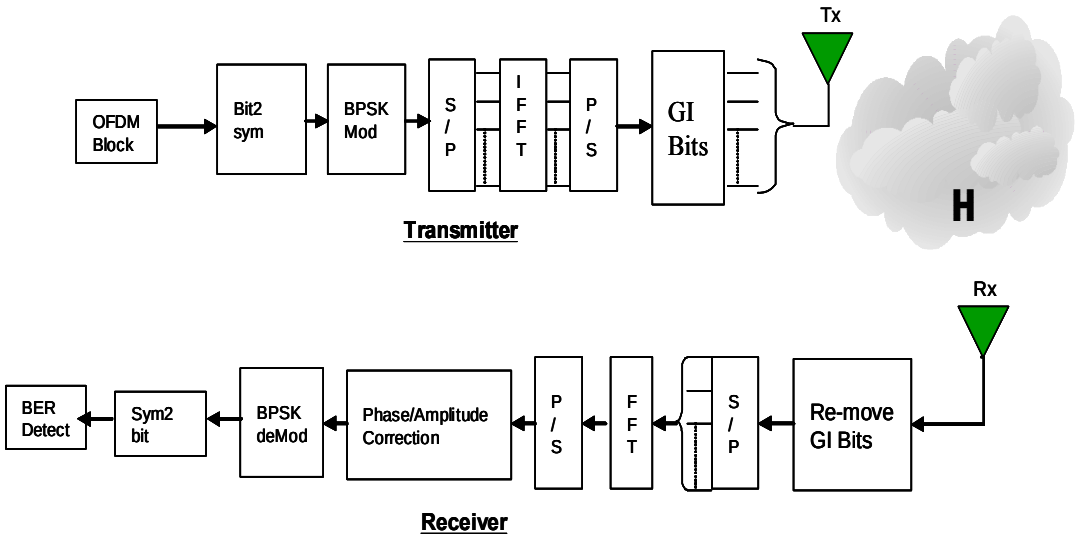

Figure 7.3: Block diagram of an OFDM system

7.5 Key Components of an OFDM system

7.5.1 FFT and IFFT

The FFT at the receiving end and the IFFT at the transmitting end are considered to be the main components of an OFDM system due to their computational efficiency. These operations (IFFT and FFT) perform reversible mapping operations between M complex data symbols and M complex OFDM symbols. In this case an M-point FFT is needed to have an order of $M\log M$ multiplications rather than M^2 operations that are required by a discrete Fourier transform [140]. Consequently, it is usual to always use $M=2^m$ sub-carriers, where m is an integer, wherever possible. This is certainly true of most OFDM systems, such as 802.11 WiFi, but it is equally true that not all $M=2^m$ carriers need to be used.

7.5.2 Cyclic Prefix

The cyclic prefix (as explained in previous section) is appended at rear of every OFDM symbol to maintain and ensure the orthogonality between sub-channels and to combat the effect of multipath. The cyclic prefix is a copy of the first part of an OFDM symbol which is of a length that is equal to or greater than maximum delay spread of the channel. Although the insertion of cyclic prefix imposes a penalty in terms of the transmitted power and the bandwidth, it is still a good compromise between performance and efficiency in the presence of ISI, compared with other modulation schemes. This cyclic prefix allows the delay-spread interference on this symbol to die out, before the next OFDM symbol is received.

7.5.3 Channel Estimation for OFDM Systems

Orthogonal Frequency-Division Multiplexing (OFDM) is regarded as an alternative to the single carrier modulation techniques for communication systems requiring transmission at high data rate. However, even for OFDM, it is still necessary to provide accurate and computationally efficient channel state information when coherent detection is involved. There are many ways in which the channel state information can be provided. Some of the various methods of channel estimation that have been considered by various researchers are described below. From the literature it is revealed that, typically, channel estimation is performed using one of three methods or a combination of these methods. The trade-offs between complexity and performance dictates the choice of algorithm [158].

•***Data Aided Channel Estimation****:* Also known as the pilot symbol method [151]. In this method, a known sequence of symbols is transmitted. At the receiver, the channel estimation algorithm operates on the received signal along with the known stored symbols to generate an estimate of the transmission channel using deconvolution of the actual data symbols with the expected symbols. This is a convenient method but it has the disadvantage that it reduces the amount of payload that can be carried because the pilot bits periodically replace payload bits. This method relies on the channel remaining stationary after channel estimation has taken place. Statistically this is true until the coherence time of the channel has elapsed. It is usual for the pilot symbols to be periodically retransmitted with a period less than the coherence time. There are a number of pilot symbol methods that exist which try and optimise channel estimation by inserting pilot bits within the payload bits [147][150]. However, the operating principle of these different methods is broadly similar.

•***Decision-Directed Channel Estimation*** [152][140]: A rough estimate of the channel is obtained using a suitable estimation method such as a short pilot sequence. Then this estimate is used to make symbol decisions. The channel estimate is further improved using the resulting detected symbols as "pilot symbols." This type of estimation contains some inherent delay because the symbol decisions occur before the final channel estimate can be made. Also, there may be error propagation because any errors in the symbol decisions affect the final estimate. The main benefit of this method is that it delays the need for pilot symbol block transmission, thereby improving end-to-end data throughput. However, the method only works well when the signal level is sufficiently high that the bit error probability is so low as not to cause error propagation.

•***Blind Channel Estimation*** [153]: This estimation process relies not on pilot symbols or symbol decisions but rather on certain characteristics of the modulated signal. For example, the constant modulo algorithm (CMA) uses the amplitude of the signal as the criterion for

estimating the channel. In constant energy modulation schemes such as Quadrature Phase Shift Keying (QPSK), the knowledge that all signals are transmitted with equal energy is used as the basis for obtaining the channel estimate. This type of algorithm typically requires a longer convergence time and usually has a higher mean square error (MSE) than the other two schemes [149].

In the simulations that follow in the next section, it was decided to use the data-aided channel estimation method because it is a relatively simple method with well-known channel estimation error characteristics. Furthermore, it forms the basis of a much more sophisticated channel estimator used for the MIMO-OFDM system provided in a later section of this chapter.

7.6 Interleaving for OFDM systems

In the case of OFDM systems, the sub-carriers have different amplitudes and phases because of frequency selective fading. At times, deep fades in the channel causes the bit errors to occur in bursts rather than being randomly scattered. However, FEC codes such as convolutional codes are extremely poor at correcting burst errors. In this case interleaving [117] is applied to the signal prior to transmission in order to randomise the occurrence of errors before decoding at the receiving end. The interleaver actually modifies the order of transmission of symbols so that if a burst error occurs, the de-interleaver in the receiver (which performs the inverse of interleaving) reorders the received bit into the original correct order, whilst simultaneously randomising the bits that were in the burst error.

In an OFDM system, the signal can be subject to frequency non-selective (flat) fading as well as frequency selective fading. Both forms of fading can be compensated for in the OFDM system by interleaving in the time and frequency domains to provide both time and frequency diversity. This is achieved in practice by first using time-domain interleaving immediately after the viterbi decoder, to break up consecutive errors due to frequency non-selective fades. Then the order of the samples at the IFFT input are randomised to ensure that adjacent symbols in the time domain do not occur in adjacent frequency slots (i.e. adjacent symbols are separated by the interleaver to a frequency separation that is wider than the coherence bandwidth, to ensure that adjacent symbols suffer uncorrelated fades.

In the presence of dominantly frequency selective channels, time interleaving is less effective and should be avoided. In such type of environment frequency interleaving is essential as it averages the impact of the nulls in frequency response of the channel over many bits making it easier for the decoder at receiver to recover the transmitted data. So it can be

said that multipath is an advantage for an OFDM system as it makes the channel frequency selective and hence brings in frequency diversity.

7.7 OFDM Simulations

In the simulations below two different channel models such as AWGN and Matlab Rayleigh channel models are implemented. The description of simulations is described in the next sections and design parameters for the systems implemented are given below in Table 7-1.

Parameters	***Values***	***Parameters***	***Values***
Channel	AWGN/Rayleigh	Sampling period (*ts*)	0.2μsec
Modulation Scheme	PSK/QAM	Symbols/block	64
Modulation order (M)	2,4,16	Doppler (*fd* (Hz))	10
Coding rate	½ Rate convolutional	GI	10
Interleavers	Time, Freq	Paths	2/5
FFT bins	64		

Table 7-1: Design parameters for OFDM systems

7.7.1 CASE-1

In this case, a normal flat fading channel with the impairment of additive white Gaussian noise (AWGN) is implemented using an OFDM system described in section 7.3 above. The design parameters for simulation are given in Table 7-1.

7.7.1.1 Description of Simulation

For this case of AWGN channel implementation, a stream of random data bits is generated and converted into symbols, modulated with the help of an appropriate PSK/QAM modulator and sent across the channel as an OFDM signal. At the receiving end the received symbols are OFDM demodulated before conversion into bits for comparison with input random generated stream of data. The error rate is calculated by a comparison of the input and received data bits and plotted for different modulation orders of M=2, 4, and 16.The number of FFT bins used are 64 and length of symbols sent per block is also 64. Total numbers of symbols sent are 5 to 7 million. The results of this simulation are shown in Figure 7.4 below.

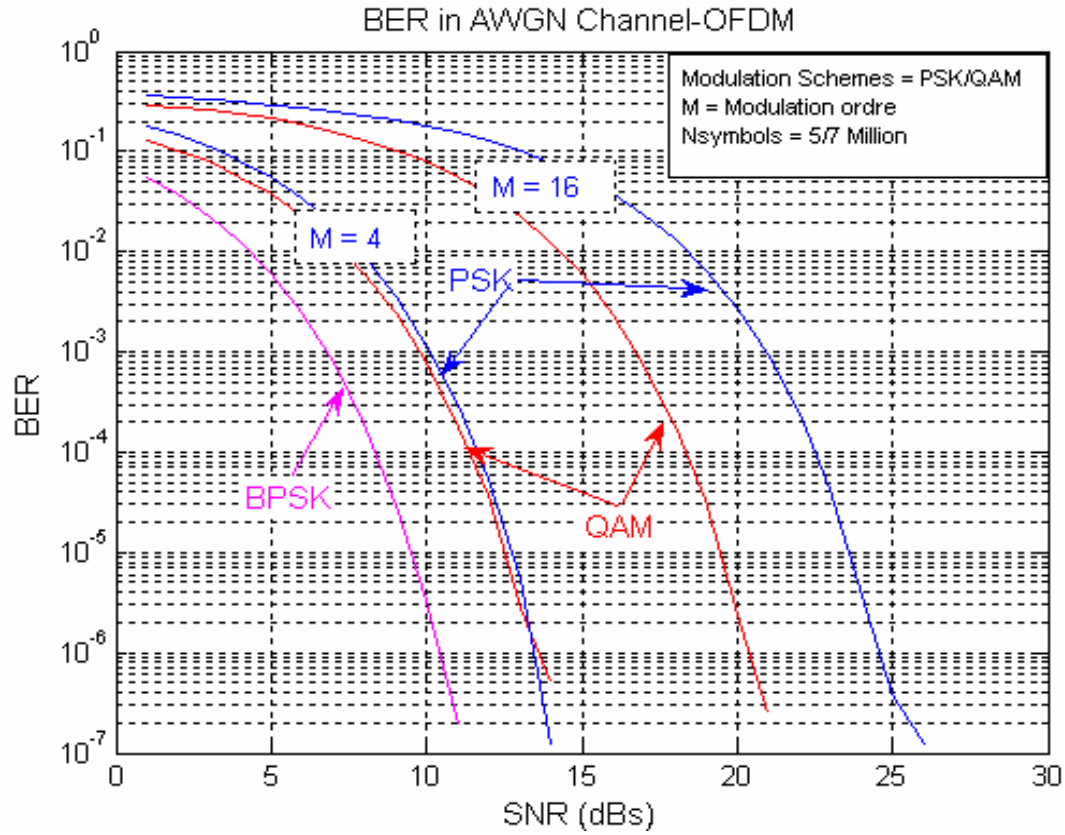

Figure 7.4: BER vs SNR over AWGN channel

From the results of this simulation, it is seen that in case of normal noisy channel the BER performance of an OFDM system is exactly the same as for a single carrier system modeled in Chapter 2. The performance of this simulated system is entirely as expected from a theoretical analysis of the problem, provided in Chapter 2. This figure is used to provide a measure of confidence in the model used to simulate the OFDM system. Indeed, the performance of this system matches the performance of single carrier systems and the theoretical analysis for the different modulation orders for both M'PSK and QAM, provided in Table 7-1.

7.7.2 CASE-2

In this case, an OFDM system is simulated for the case of a time varying multipath Rayleigh channel model. In this case, the implementation of the Rayleigh channel model is provided by the Matlab toolbox. The implementation procedure adopted for the model is described in section 7.4 above. The design parameters of OFDM system implemented with Matlab Rayleigh channel model are given in Table 7-1. The aim of the implementation of this system is to examine the impact of the multipath channel and, in particular to show how the use of interleavers and a Viterbi convolutional coder provides the necessary time and frequency diversity to yield significant improvements in the BER performance of the system. The BER

versus SNR simulation results implemented in Matlab for multipath Rayleigh faded channel are shown in Figure 7.5 to Figure 7.7.

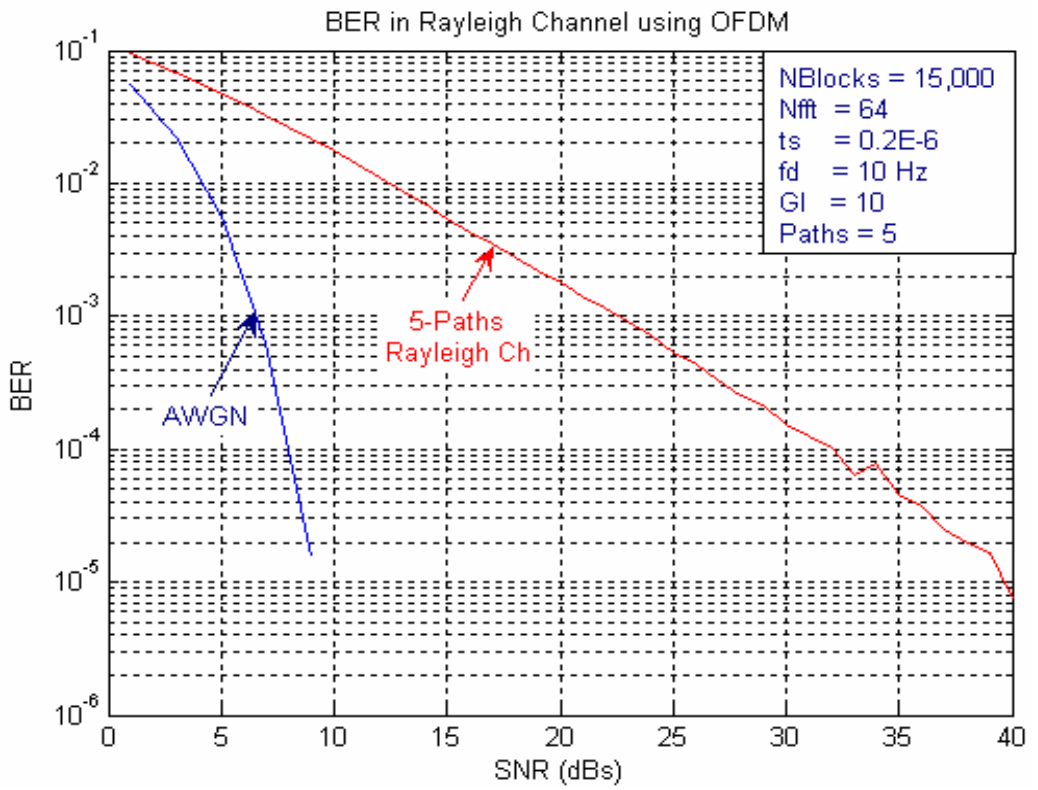

Figure 7.5: BER vs SNR over Rayleigh fading Channel

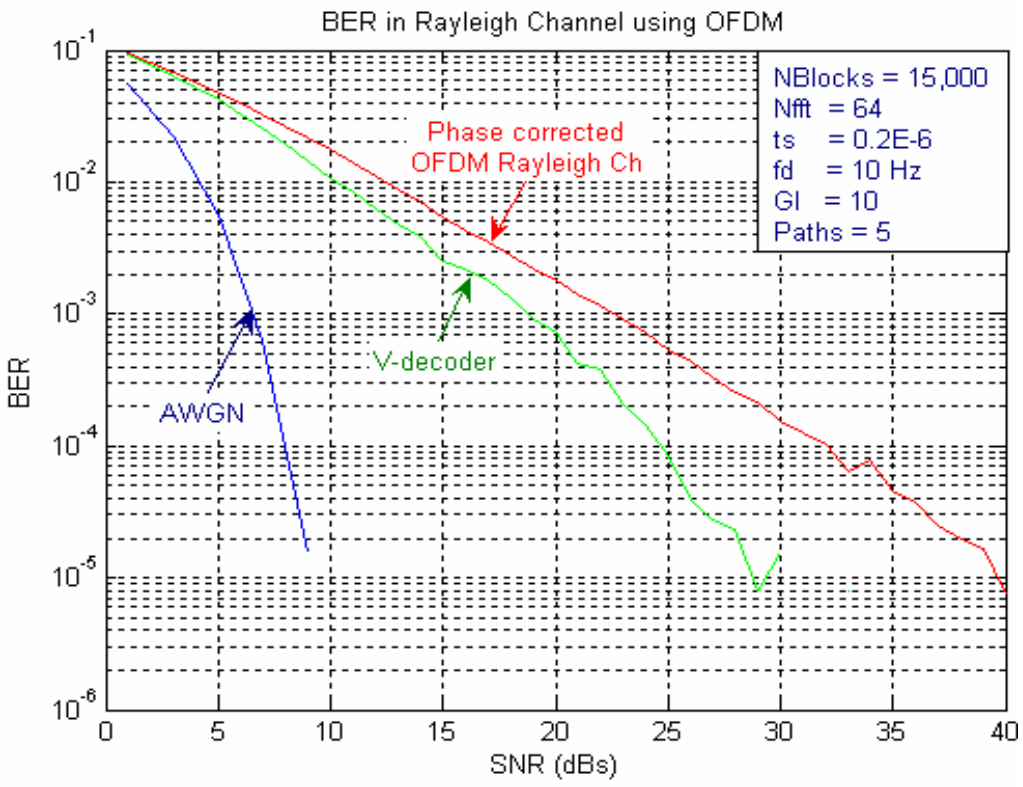

Figure 7.6: Effect of V-decoder

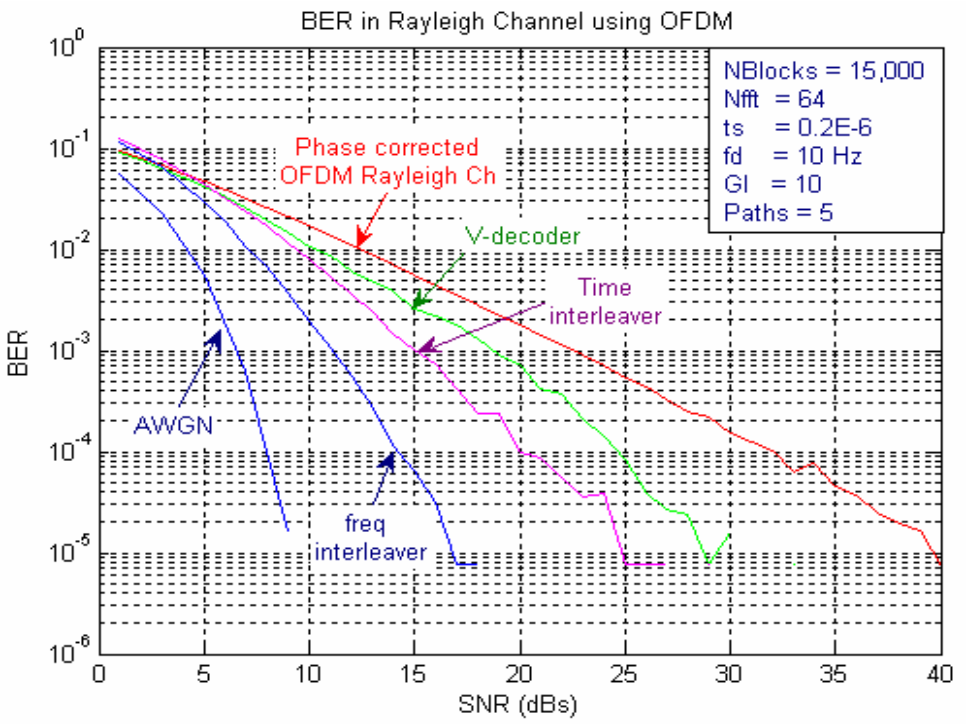

Figure 7.7: Comparison of V-decoder and interleavers on a OFDM System

7.8 Results Analysis

Figure 7.5 shows the BER performance of a phase corrected 5-paths Rayleigh faded channel of an OFDM system that uses a cyclic prefix to minimize the effect of the ISI due to the channel delay spread. It should be noted that conventional phase and amplitude compensation using pilot bits to estimate the amplitude and phase of each sub-carrier has been used. From the simulation results of a true Rayleigh faded channel, the characteristics curve indicates BER of 10^{-4} at SNR of 32dB. What is particularly important about this result is that the BER curve follows almost exactly, the curve expected of a single carrier system in a flat fading channel. What this indicates is that an OFDM system with a cyclic prefix and amplitude and phase correction of each sub-carrier does, indeed cause multipath fading to be treated by the OFDM system as frequency selective fading. Consequently, the result of Figure 7.5 is as expected. The bit error performance of this system may not be as good as for an AWGN channel, but it is far better than a single carrier system in multipath fading shown in Chapter 2.

Figure 7.6 shows that when Viterbi convolutional coder is used along with the cyclic prefix, the BER performance is improved i.e. the same BER of 10^{-4} is now achieved at SNR of 24dB as compared to 32dB without using Viterbi coding. Although the BER performance of about 8dB is improved by using the Viterbi coder but the data rate is halved. There is a compromise between data rate and BER performance.

The BER performance can be improved substantially by using interleavers as Figure 7.7 shows. When the time interleaver is used the BER of 10^{-4} is achieved at 20dB SNR, whilst with frequency interleaver the BER performance is further improved significantly i.e. the BER in that case is about 14 dB at SNR 10^{-4}. There is an improvement of 6dB with frequency interleaver.

It is clear from the simulation result how the use of the Viterbi coder in conjunction with both time and frequency interleaving improves the BER performance closely towards that of the AWGN channel. Note that to achieve these performance benefits both time and frequency interleaving must be used together. It is important to recognize that the true performance benefit of using OFDM in a multipath channel is only achieved when the time and frequency diversity provided by the memory of the convolutional coder is incorporated into the modulation scheme. The interleavers are necessary to make up for the shortcoming of the convolutional coder in burst errors.

7.9 MIMO-OFDM Systems

Chapter 3 and Chapter 4 has described how multiple transmit or receive antenna elements in the case of antenna arrays can be used in a communication system to improve the performance

of that system by forming highly directional beams in the wanted directions and deep nulls in the directions of interferers. The performance of such systems was analysed in Chapter 3 and chapter 4. However, within the past decade, an entirely different method of using multiple antennas has been developed which exploits spatial diversity that exists in richly scattered wireless channels, typical of mobile cellular radio channels and indoor wireless LANs [126]. In this new approach, multiple, spatially separated antennas are used at either the transmitter or the receiver or both to provide space diversity. In this chapter, the use of such diversity techniques is combined with the inherent frequency diversity found in OFDM to produce a communication system that is highly robust to multipath fading.

This type of use of multiple antennas is now referred to as multiple-input multiple-output (MIMO) communication systems and this was described in detail in Chapter 6 for the case of a single carrier communication system. By employing wideband technology, such as OFDM, that is used to reduce the inter-symbol interference (ISI) over multipath fading channel with MIMO techniques this promises to provide an extremely robust system. And this approach to frequency and space diversity is considered in the rest of this chapter. A MIMO-OFDM system is used to mitigate the inter symbol interference (ISI) and enhance the capacity of system [157][125]. In the approach described in this thesis, a novel MIMO-OFDM system is described that uses two independent space time codes for two sets of two transmit antennas and at the receiving end these two sets of codes are decoded based on successive interference cancellation.

7.10 Space-time coded OFDM-MIMO system

The existence of frequency selective fading in a mobile channel is an indication that some of the OFDM signal sub-carriers are attenuated more than others and data carried on those sub-carriers would be lost. In order to avoid this type of problem the diversity inherent in the OFDM system can be fully exploited by using coding and interleaving across the sub-carriers [126][143]. This introduces a relationship between different information carried on different sub-carriers such that the same relationship is used at receiving end to recover the data affected by deep nulls in the channel frequency response.

Figure 7.9 shows the schematics of a STBC MIMO-OFDM system. The technique involved in the process of implementation of an OFDM system is the insertion of a guard interval, called cyclic prefix (CP) that has to be long enough to accommodate the delay spread of the channel. The use of the CP turns the action of the channel on

the transmitted signal from a linear convolution into a cyclic convolution, so that the resulting overall transfer function can be diagonalized through the use of an IFFT and FFT at the transmitting and receiving end as shown in Figure 7.9.

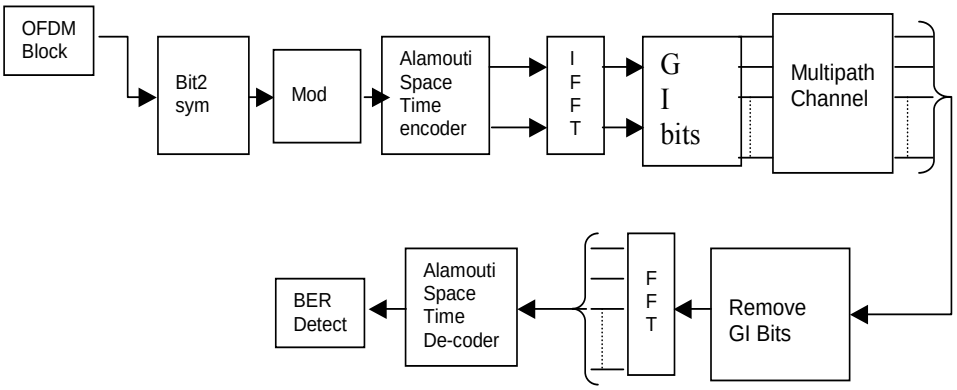

Figure 7.8: Block diagram of STBC OFDM-MIMO system

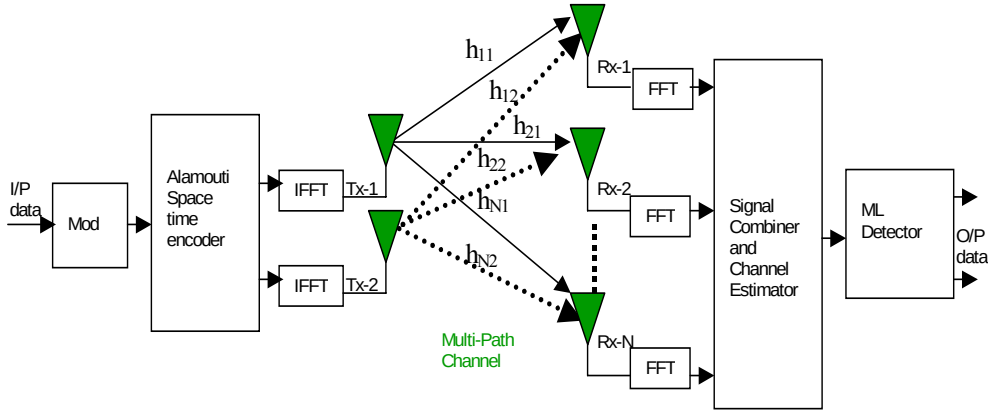

Figure 7.9: Schematic of STBC MIMO-OFDM System

For a MIMO-OFDM system, with *M* transmit antennas and *N* receive antennas the OFDM transmitted signal is expressed as [62].

$$\begin{aligned}\mathbf{x}(t) &= \sum_{k=0}^{K-1} a(k)\cos(\omega_k t) - b(k)\sin(\omega_k t) \\ &= \mathrm{Re}\left(\sum_{k=0}^{K-1} d(k)\exp(j2\pi k\Delta f_k t).\exp(j2\pi f_o t)\right) \\ &= \mathrm{Re}\left(\tilde{D}(t)\exp(j2\pi f_o t)\right)\end{aligned} \tag{7.15}$$

Where $a(k)$ and $b(k)$ are the real and imaginary parts of k^{th} symbol $d(k)$, $\omega_k = 2\pi f_k$ and $f_k = f_o + k\Delta f$, and $\tilde{D}(t)$ is the complex envelope of transmitted signal. The signals add up over the air and are received by multiple receive antennas and jointly processed to recover the transmitted information. The received signal at antenna *n*, in the presence of receiver noise $\mathbf{N}_{t,k}^{j}$, can be written as,

$$\mathbf{y}_{t,k}^{j} = \sum_{i=1}^{M} \mathbf{H}_{j,i}^{t,k} \mathbf{x}_{t,k}^{i} + \mathbf{N}_{t,k}^{j} \tag{7.16}$$

Where $\mathbf{H}_{j,i}^{t,k}$, is the quasi-static multipath channel coefficient from transmitter i to receiver j and $\mathbf{N}_{t,k}^{j}$ is the noise at the output of the receiver.

7.10.1 Channel and Receiver section

Consider that the signal $\tilde{\mathbf{x}}_n[k]$ is transmitted over the time-varying linear channel $h(t,\tau)$ without additional noise. If we call $h[k]$ the sampling version of the channel, then the output of obtained by the channel is:

$$\tilde{y}_n[k] = \sum_{l=0}^{N+L-1} \tilde{\mathbf{x}}_n[l] h[k-l] \tag{7.17}$$

where, $k = 0, 1, \ldots, N+L-1$ (i.e. the total number of samples)

The receiver basically does the reverse operation to the transmitter. The signal received is $\tilde{y}_n[k]$ that has $N+L-1$ samples, before the demodulation, we have to drop the L last samples of the received signal, and then remove the guard interval, in order to use correctly the Fourier Transform properties. Indeed the demodulation operation is a simple FFT according to the IFFT used as modulation. We need to find out N samples (one per carrier) as at the modulator input, Applying FFT to the signal $\tilde{y}_n[k]$, we get:

$$\tilde{Y}_n[k] = \sum_{l=0}^{N-1} \tilde{y}_n[l] \exp\left(-2\pi j k \frac{l}{N}\right) \tag{7.18}$$

$$\tilde{Y}_n[k] = \sum_{l=0}^{N-1} \left(\sum_{m=0}^{N+L-1} \tilde{x}_n[k] h[l-k] \right) \exp\left(-2\pi j k \frac{l}{N}\right) \tag{7.19}$$

$$\tilde{Y}_n[k] = \left(\sum_{m=0}^{N+L-1} \tilde{x}_n[k] \right) \sum_{l=0}^{N-1} h[l-k] \exp\left(-2\pi j k \frac{l}{N}\right) \tag{7.20}$$

$$\tilde{Y}_n[k] = \left(\sum_{m=0}^{N+L-1} \tilde{x}_n[k] \exp\left(-2\pi j k \frac{l}{N}\right) \right) \Im(h[k]) \tag{7.21}$$

The first term of the multiplication above looks like a Fourier Transform expression. In fact, if we restrict the summation index from m = 0 to $k = N$-1 it is equivalent to drop the L last samples of the signal $\tilde{y}_n[k]$. So the signal produced by the demodulator is given as:

$$\tilde{Y}_n[k] = \left(\sum_{m=0}^{N-1} \tilde{x}_n[k] \exp\left(-2\pi j k \frac{l}{N} \right) \right) \Im(h[k]) \tag{7.22}$$

$$\tilde{Y}_n[k] = \Im(x_n[k]) \Im(h[k]) \tag{7.23}$$

$$\tilde{Y}_n[k] = X_n[k] H[k] \tag{7.24}$$

A simple division by the channel frequency response gets back the transmitted signal. This modulation does not need any equalization and the data samples are then combined back to the same size as the original data.

7.11 Pilot assisted channel estimation and detection for OFDM-MIMO System

A pragmatic approach used for estimation of channel state information is based on the pilot symbols transmitted from two transmit antennas. Both the streams of pilot symbols transmitted are drawn from two rows of Hadamard matrix, The Hadamard matrix represented as $\mathbf{H}ad_n$, where $n = 2^i$ and i is an integer. The Hadamard matrix as a symmetric square-shaped matrix where every row of $\mathbf{H}ad_n$ is orthogonal to all the other rows. If we consider $n=8$ then Hadamard matrix of dimension 8x8 is as shown below:

$$\mathbf{H}ad_{8x8} = \begin{bmatrix} 1 & 1 & 1 & 1 & 1 & 1 & 1 & 1 \\ 1 & -1 & 1 & -1 & 1 & -1 & 1 & -1 \\ 1 & 1 & -1 & -1 & 1 & 1 & -1 & -1 \\ 1 & -1 & -1 & 1 & 1 & -1 & -1 & 1 \\ 1 & 1 & 1 & 1 & -1 & -1 & -1 & -1 \\ 1 & -1 & 1 & -1 & -1 & 1 & -1 & 1 \\ 1 & 1 & -1 & -1 & -1 & -1 & 1 & 1 \\ 1 & -1 & -1 & 1 & -1 & 1 & 1 & -1 \end{bmatrix} \tag{7.25}$$

From the Hadamard matrix it is observed that first column is all 1's and the second column is an alternating sequence of 1's and -1's. Let $\mathbf{H}ad_8[i]$ and $\mathbf{H}ad_8[j]$, $i, j = 0 \cdots\cdots 7$, be the two sequences formed from the i^{th} and j^{th} rows of Hadamard matrix. Then it can be verified that $\mathbf{H}ad_8[i]$ and $\mathbf{H}ad_8[j]$ are orthogonal to each other. Mathematically it can be represented that if two rows are transmitted from two transmitting antennas then they are orthogonal to each other if the inner product of the two rows of Hadamard matrix is zero, i.e.

$$\mathbf{H}ad^{Tx-1}.\mathbf{H}ad^{Tx-2} = \mathbf{H}ad_1\mathbf{H}ad_2^* - \mathbf{H}ad_2^*\mathbf{H}ad_1 = 0 \tag{7.26}$$

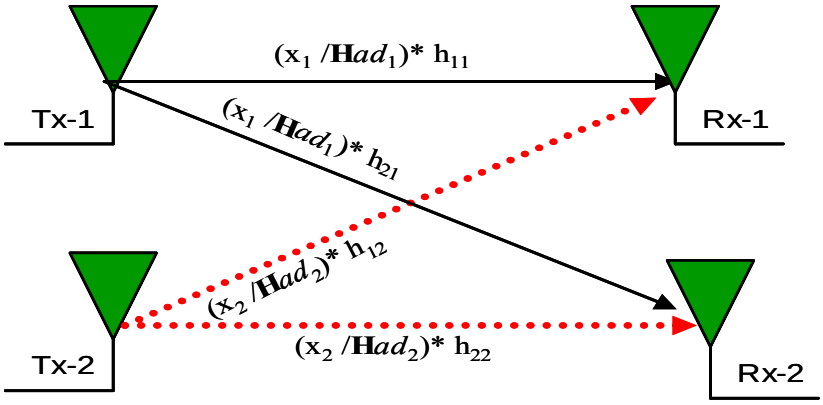

Therefore for the estimation of channel state information of 2x2 MIMO-OFDM system as shown in Figure above an OFDM frame of pilot symbols is sent from two transmit antennas denoted as $\mathbf{H}ad_1$ considered as one row of Hadamard matrix being transmitted from antenna-1 and $\mathbf{H}ad_2$ as the other row of Hadamard matrix being transmitted from antenna-2. The length of Hadamard matrix is same as that of the length of an OFDM frame of actual data symbols.

For OFDM implementation these Hadamard sequences are modulated using inverse FFT at the transmitting end given as:

$$X_{1-Pilot} = IFFT\left(\mathbf{H}ad_1\right) \tag{7.27}$$

$$X_{2-Pilot} = IFFT\left(\mathbf{H}ad_2\right) \tag{7.28}$$

When these sequences of pilot bits are sent across channel they are assumed to be known by the receivers, these are corrupted by the channel in addition to the contribution of AWGN at the receiving end, therefore the corrupted data symbols received from two antennas at the receiving end are represented as:

$$\hat{s}_1 = \mathbf{X}_{1-Pilot}h_{11} + \mathbf{X}_{2-Pilot}h_{12} + n_1 \tag{7.29}$$

$$\hat{s}_2 = \mathbf{X}_{1-Pilot}h_{21} + \mathbf{X}_{2-Pilot}h_{22} + n_2 \tag{7.30}$$

Where $\hat{s}_1$ and $\hat{s}_2$ are the corrupted signals received at receiver-1 and receiver-2. Now in order to obtain the individual channel coefficients associated with the received antennas, the

received signals in (7.29) and (7.30) are OFDM-demodulated by taking the Fourier transform of the received signals at the receiving end, which can be written as:

$$Y_{rx-1} = FFT(\hat{s}_1) \tag{7.31}$$

$$Y_{rx-2} = FFT(\hat{s}_2) \tag{7.32}$$

These OFDM demodulated signals are then correlated with the two replica of original Hadamard orthogonal pilot sequences to obtain the individual channel coefficients between transmitter and receiver given as:

$$\hat{h}_{1i} = Y_{rx-1} * conj(\mathbf{H}ad_i) \tag{7.33}$$

$$\hat{h}_{2i} = Y_{rx-2} * conj(\mathbf{H}ad_i) \tag{7.34}$$

Where, $i = 1,2$ i.e. Number of transmit antennas

In case of coherent detection the actual data symbols transmitted from two transmit antennas can be detected by removing the effect of channel from actual data symbols $\mathbf{x}_1$ and $\mathbf{x}_2$ transmitted from transmitter-1 and transmitter-2. The actual faded data signals received at receiver-1 and receiver-2 are given as:

$$\hat{s}_{1-faded} = \mathbf{x}_1 h_{11} + \mathbf{x}_2 h_{12} + n_1 \tag{7.35}$$

$$\hat{s}_{2-faded} = \mathbf{x}_1 h_{21} + \mathbf{x}_2 h_{22} + n_2 \tag{7.36}$$

These faded signals are OFDM demodulated by taking the FFT of the received signals, So the demodulated actual data symbols received at receiver-1 and receiver-2 are then represented as:

$$r_1 = FFT(\hat{s}_{1-faded}) \tag{7.37}$$

$$r_2 = FFT(\hat{s}_{2-faded}) \tag{7.38}$$

The resultant received estimated symbols are then achieved by convolving the estimated channel coefficients from (7.33) and (7.34) with the actual received OFDM demodulated data symbols from (7.37) and (7.38) using STBC decoder at the receiving end:

$$\hat{x} = \left[conj(\hat{h}_{11}) \quad \hat{h}_{12};\ conj(\hat{h}_{12}) - \hat{h}_{11}\right] * r_1 + \left[conj(\hat{h}_{21}) \quad \hat{h}_{22};\ conj(\hat{h}_{22}) - \hat{h}_{21}\right] * r_2 \tag{7.39}$$

This $\hat{x}$ stream of received data symbols is then demodulated using MPSK demodulator and converted to binary numbers to be compared with transmitted stream to find the error rate of the system.

7.12 Channel estimation for STBC MIMO-OFDM System

Channel estimation plays a vital role in all forms of coherent communication system [143]. This is especially true for MIMO systems, where multiple transmitters communicate, simultaneously, with multiple receivers. Because MIMO systems rely on the space diversity that is provided by the multipath channel, they can only successfully operate if all the different channel characteristics of each path are known perfectly so that the mutual interference caused by each co-channel link can be successfully removed using interference cancellation techniques. In an earlier section, three broad methods of channel estimation were outlined. In this thesis, because of the complexity of the STBC MIMO-OFDM system, a pragmatic approach to channel estimation has been taken that is based on the use of pilot symbols. In such an approach, an OFDM frame of data symbols is sent in which all the data symbols are known to the receiver. The transmitted pilot symbols are corrupted by the channel. However, since the receiver knows the sequence of symbols it is able to deconvolve the channel state information from the corrupted data. In this way the amplitude and phase perturbations can be estimated in the frequency domain for each sub-carrier. In this approach, it is vital that the pilot symbols are neither coded nor interleaved as it is the raw symbol that contains the channel information, not the decoded bits. Once the frame of pilot bits has been used to estimate the channel, the following frames can contain payload symbols, using the estimated channel characteristics to recover these frames. However, because the channel characteristics are time varying, the channel starts to change after the channel estimate has been made. This is set by the coherence time of the channel which is related to the velocity of the mobile handset. It is therefore necessary to re-estimate the channel periodically within a time period that is shorter than the coherence time of the channel by resending the pilot symbols. This approach is used in the results shown in Figure 7.10 to Figure7.15 to estimate the frequency selective fading for each sub-carrier.

For a MIMO system, the problem is made far more complex because a coded OFDM signal is sent over many different channels simultaneously, (i.e. from each transmitter

to each and every receiver antenna). It is vital that the channel characteristics of every path are estimated at the same time. In order to achieve this, a method of channel estimation was devised in which transmissions from each transmitter used a unique sequence of pilot symbols that were orthogonal to all other pilot symbol sequences for the other transmitter elements forming the MIMO system. In this case the pilot sequences were drawn from a set of orthogonal Hadamard sequences obtained by selecting rows from a Hadamard Matrix. The length of the Hadamard sequence matched the OFDM frame length. To simplify deconvolution of the channel state information from the received Hadamard sequences, BPSK modulation was used for the pilot symbols, irrespective of the type of modulation used for the payload bits. For example, for the case of a two transmitter STBC MIMO-OFDM system using an OFDM block length of 64 symbols, a Hadamard matrix of order 64 was used in which two rows of the Hadamard matrix were picked at random to represent the two pilot sequences for the two transmitters. This approach was implemented in Matlab and was found to work extremely well for the MIMO-OFDM system.

In STBC MIMO-OFDM systems channel estimation can also be done by RLS channel estimation algorithm [148], where first of all relationship between input and output is obtained and then channel transfer function is concluded in frequency domain and then IFFT is performed to obtain channel parameter matrix in time/delay domain. In second step an adaptive filter such as LMS/RLS is used to estimate the channel, Finally FFT is performed to draw the channel transfer matrix in time/frequency domain.

7.12.1 Criteria for determination of use of Communication System

As in case of wideband communication system, the channel is mostly frequency selective and time varying, so there is a requirement of estimating the channel continuously before the process of demodulation of an OFDM signals. Moreover before using communication system in a particular environment it is necessary to determine the channel matrix because it's the channel matrix '' **H** '' that decides which method of communication, whether ***Beam forming, MIMO, Opportunistic Communication system, OFDM or OFDM*** system is to be used.

7.12.1.1 Criteria for selection of channel matrix ($\mathbf{H}$)

If two rows of channel matrix $\mathbf{H}$ are identical then one of the rows is selected while other is deleted because both rows being identical carry the same information. In case one of the rows has different power then row with highest power is selected while one with low power is deleted [155][156].

If rows of $\mathbf{H}$, are not identical, then two rows with highest correlation are chosen, and one with highest correlation is deleted, while the other one is selected.

Hence estimated channel matrix $\widetilde{\mathbf{H}}$ is selected with rows of maximum power and maximum uncorrelated rows.

$\mathbf{H} * \mathbf{H}^H = 0$ indicates the uncorrelation of $\mathbf{H}$, whereas $\mathbf{H} * \mathbf{H}^H = 1$ indicates the fully correlation of $\mathbf{H}$.

The channel coefficients are generated to determine the correlation of channel matrix $\mathbf{H}$. If the channel coefficients are correlated then is a ***flat fading case***, which dominates the LOS environment, as a result ***Beamforming, MIMO or the Opportunistic communication*** system could be used.

Beamforming uses ***SDMA*** technique that relies on AoA estimation and is most effective. ***MIMO*** with antenna elements sufficiently spaced a part technique depends heavily on the spatial correlation of antenna elements, terminals with limited space resources. MIMO gives very good performance when that terminal is at location where decorrelation distance is very short. ***Opportunistic communication*** system could also be used in flat fading case because when a null is formed then fair sharing of resources is required which can be performed by use of a switch.

When the channel coefficients are determined to be uncorrelated, the channel exhibits the property of frequency selectivity (delay spread) and is said to be a ***frequency selective channel***. The delay-spread results into inter symbol interference (ISI) that can cause serious performance degradation. ***OFDM or OFDM*** systems are used to mitigate the effect of ISI in case of frequency selective channel as these techniques eliminate the need for equalisation and offer higher spectral efficiency. ICI is also created when delay spread is longer than cyclic prefix. When channel varies between OFDM symbol period, the time variation of the channel usually come from mobility or frequency offset between transmitter and receiver.

When fading is fast and BER does not improve with increase in SNR, it may be due to the fact of poor estimation of the channel in fast fading environment thereby the system performance is not improved. BER also increases with increase of Doppler spread because of severe ICI.

7.12.2 Diversity

Spatial or the antenna diversity is achieved when multiple antennas are used at transmitting and receiving end. Because of multiple antennas multiple channels are created between transmitters and receivers and is expected that it is not common that all the channels will go into fade simultaneously.

Diversity gain [124][146] is achieved when data signal is transmitted on these independent multiple channels in time, frequency and space and proper combining of the signals is done at the receiving end. Spatial or the antenna diversity has an edge over time or frequency diversity because it does not involve the use of transmission time or bandwidth. Space-time coding [146] is one of the techniques that provide the spatial diversity gain in systems with multiple antennas at the transmitting end In frequency-selective fading MIMO channels, two types of diversities like frequency and spatial diversity can be exploited by using space time coding technique.

7.13 Spatial Multiplexing in MIMO-OFDM Systems

In an OFDM-based MIMO system [146], transmitting independent data streams on a tone-by-tone basis with the total transmit power split uniformly across antennas and tones perform spatial multiplexing. The spatial multiplexing aims at increasing spectral efficiency by transmitting independent data streams [124]. Although the use of OFDM eliminates ISI, the computational complexity of MIMO-OFDM spatial-multiplexing receivers can still be high. This is because the number of data-carrying tones typically ranges between 48 (as in the IEEE 802.11a/g standard) and 1728 (as in the IEEE 802.16e standard) and spatial separation has to be performed for each tone.

7.14 Simulation of STBC OFDM-MIMO Systems

Here two STBC OFDM-MIMO systems are implemented in Matlab using Rayleigh channel and spatial channel models in frequency selective environment. The design parameters for the simulation of both the channel models compatible to specification requirement of IEEE 802.20 are given in Table 7-2 below.

Parameters	***Values***	
Channel	SCM	Rayleigh
N_blocks	20,000	20,000
FFT bins	64	64
Symbols/block	64	64
Environment	flat/freq selective fading	flat/freq selective fading
Antenna spacing	0.5	λ /2
SNR	1: 40 dB	1: 40 dB
Carrier frequency	2.4 GHz	2.4 GHz
Doppler frequency	10/50/100/141.6 Hz (63.720kmph)	100/141.6 Hz (63.720kmph)
Sampling time/symbol	0.2 µsec	0.2 µsec
Bandwidth	10 MHz	10 MHz
Modulation order (M)	2,4,16	2,4,16
Modulation type	PSK/QAM	PSK/QAM
Paths/link	2	2/3/4/5
Subpaths/path	20	-
GI bits	10	10
Maximum delay	5µsec	5µsec
Coding rate	½ Rate convolutional	½ Rate convolutional
Constraint length	3	3
Trace back length	5* Constraint length	5* Constraint length

Table 7-2: Simulation Parameters of OFDM-MIMO Systems

7.15 STBC OFDM-MIMO systems (Matlab Rayleigh channel model)

7.15.1 CASE-1

Here STBC OFDM-MIMO system that significantly increases the bit rate while decreasing the co-channel and inter-symbol interference has been implemented in time varying multipath Matlab Rayleigh (flat fading and frequency selective faded) channel model. The BER versus SNR simulation results implemented in Matlab using Alamouti STBC scheme with different number of antennas in order to analyze the diversity effect are shown below in Figure 7.10.

The design parameters for simulation of the OFDM-MIMO systems implemented are given in Table 7-2 above.

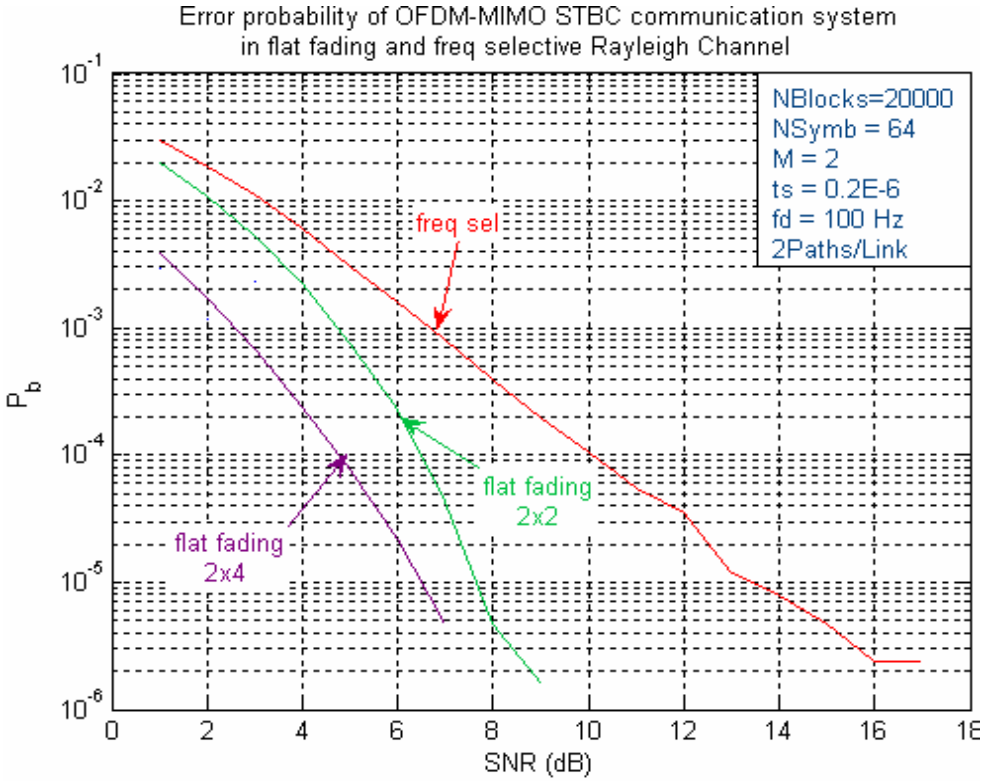

Figure 7.10: BER vs SNR over Rayleigh fading Channels

7.15.1.1 Simulation results

Here in this case two systems with antenna configuration as (2x2) and (2x4) have been implemented. The nomenclature of the configuration is such that (2x4) system means, 2 antenna elements are used at transmitting end, while 4 antenna elements have been used at receiving end.

Figure 7.10 shows the simulation results for BER performance characteristics curve using OFDM-MIMO (2x2) system in pure Rayleigh channel model with flat fading and frequency selective environment.

The simulation is performed with BPSK modulator. The number of FFT bins used are 64 and length of symbols sent per block is also 64. Total numbers of blocks sent per iteration are 20,000. From the simulation results it is seen that BER performance in case of flat fading environment is better than frequency selective fading environment.

In case of flat fading environment the BER of 10^{-5} at SNR of 7.5dB is achieved, whereas the same BER of 10^{-5} is achieved at SNR of 13dB in case of frequency selective environment employing 2-paths per link. This performance degradation in case of frequency selective fading is due to the effect of multipath with intersymbol interference.

In the same graph the BER performance characteristic curve for (2x4) system in flat fading environment is also shown, that dictates the improvement in the BER performance of the system by using 4-antennas at the receiving end in order to exploit the effect of diversity at the receiving end thereby improving the system's performance. It is seen that with (2x4) system BER of 10^{-5} is achieved at 6.8dB SNR as compared to (2x2) system where same BER was achieved at 7.8dB SNR. There is an improvement of 1dB at BER of 10^{-5} with (2x4) system.

7.15.2 CASE-2

In this case again (2x2) STBC OFDM-MIMO system is used in frequency selective environment of Rayleigh faded channel. Here the BER performance of the system is improved by using frequency interleaver in case of 2-paths. Then the same system is implemented with 3 and 4 paths to see the effect of multipath environment on BER performance.

The design parameters for simulation of the OFDM-MIMO systems implemented are given in Table 7-2 above.

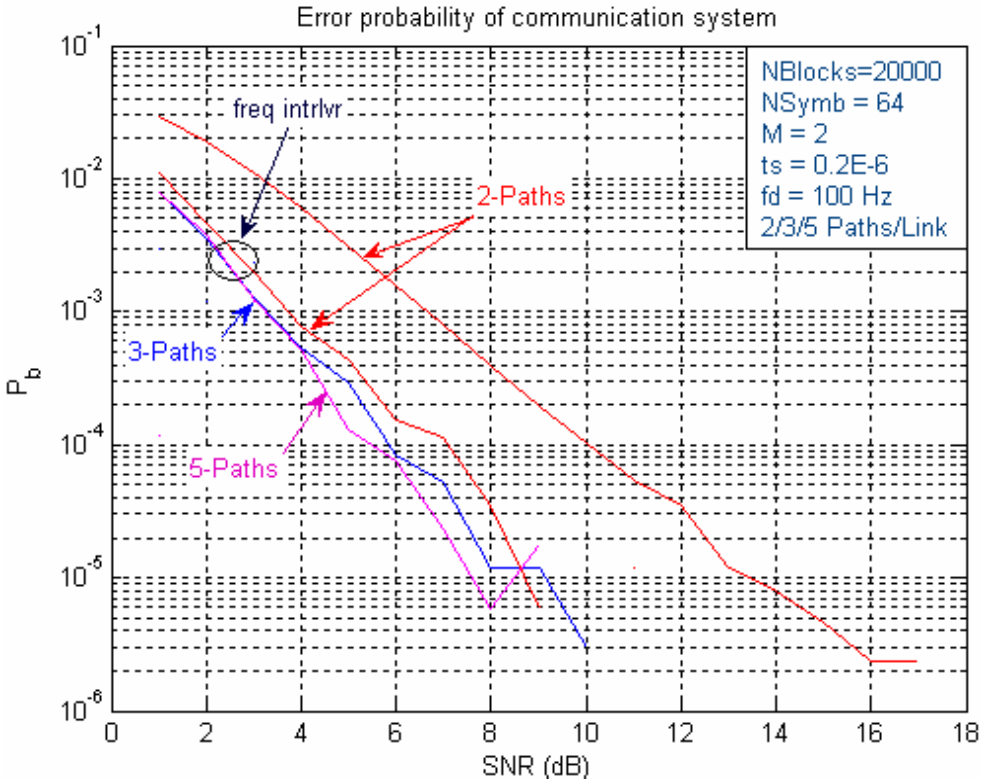

Figure 7.11: Multi-Path effect on BER

7.15.2.1 Results Analysis

Here the simulation graph of Figure 7.11 shows the BER performance of 2-Path frequency selective Rayleigh faded channel along with guard interval bits. The characteristics curve indicates BER of 10^{-5} at SNR of 13dB.

In this case it is realized that in order to gain the maximum benefit from frequency diversity, frequency interleaver is used along with viterbi-decoder, where it is observed that there is significant improvement in BER performance i.e. the same BER of 10^{-5} is now achieved at SNR of 9dB as compared to 13dB without using interleaver thereby giving a difference of 4dB improvement at same BER rate.

In addition to that Figure 7.11 also compares the effect of multipath and is seen from simulation results that in this case the BER performance is improved with more number of paths as shown in blue and magenta colours. This also verifies the property of an OFDM system that it mitigates the effect of multipath. The BER performance with 3 and 4 paths could even be improved by using time and frequency interleavers.

7.15.3 CASE-3

In this case again (2x2) STBC OFDM-MIMO system is used in frequency selective environment of Rayleigh faded channel. Here the BER performance of the system is improved by using viterbi-decoder and frequency interleaver in case of 2-paths,

The design parameters for simulation of the OFDM-MIMO systems implemented are given in Table 7-2 above.

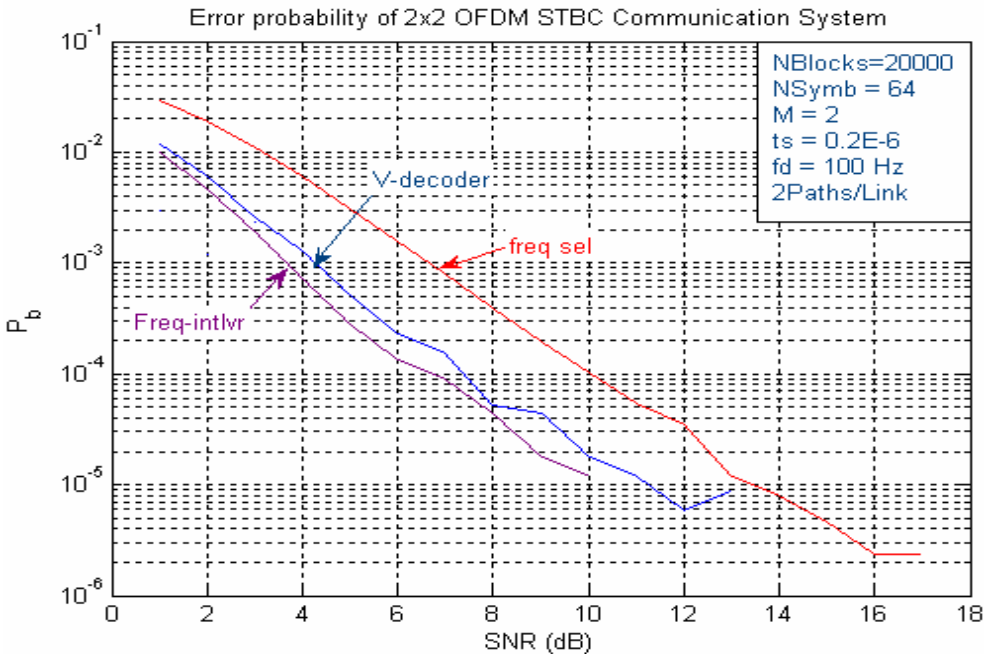

Figure 7.12: Comparison of V-decoder and interleavers

7.15.3.1 Results Analysis

Here the simulation graph of Figure 7.12 shows the BER performance of 2-Path frequency selective Rayleigh faded channel along with guard interval bits. The characteristics curve indicates BER of 10^{-5} at SNR of 13dB.

In this case it is realized that in order to gain the maximum benefit from frequency diversity, frequency interleaver is used along with viterbi-decoder, where it is observed the there is significant improvement in BER performance i.e. the same BER of 10^{-5} is now achieved at SNR of 9dB when using frequency interleaver and 10dB while using viterbi-decoder as compared to 13dB in case of true Rayleigh faded channel characteristic curve without using interleaver thereby giving a difference of 3-4dB SNR improvement at same BER rate. This indicates that maximum benefit from frequency diversity is achieved by using frequency interleaver.

Here it is interesting to note that although BER performance is improved by using viterbi-decoder but data rate is halved, so there is a compromise between data rate and BER performance.

CASE-4

In this case two (2x2) and (2x4) STBC OFDM-MIMO systems are implemented in frequency selective environment of Rayleigh faded channel. Here the BER performance of the system is improved by using viterbi-decoder and frequency interleaver in case of 2-paths. The performance of (2x2) system is then compared with (2x4) system.

The design parameters for simulation of the OFDM-MIMO systems implemented are given in Table 7-2 above.

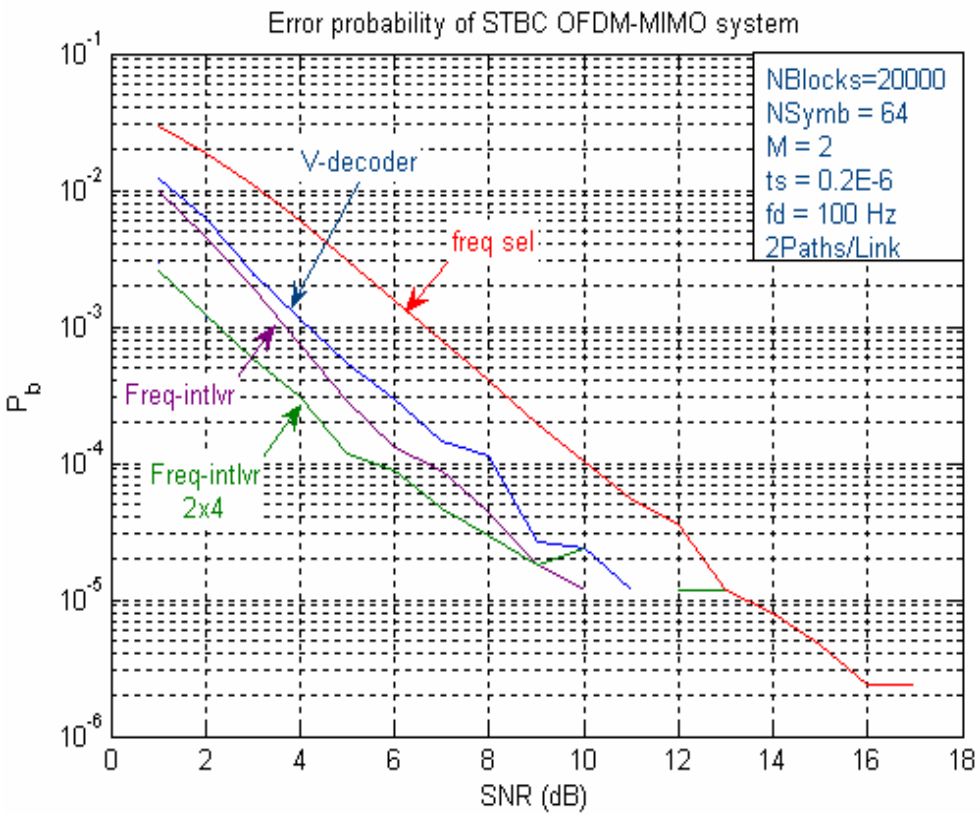

Figure 7.13: Effect of diversity on BER Performance

7.15.3.2 Results Analysis

Here since two systems are implemented, the results of (2x2) system are already discussed in CASE-3 above. Now the comparison of BER performance is made with (2x4) system.

From simulation results in Figure 7.13 it is seen that when 4-antennas are used at receiving end along with interleavers, BER performance is even improved as compared to (2x2) system, where in (2x4) system the BER of 10^{-5} is achieved at SNR of 8dB. This shows an improvement by using 4-antennas at receiving end as compared to 2-antennas and exploits the effect of diversity by increasing the order of diversity at receiving end.

7.16 STBC OFDM-MIMO systems (SCM)

7.16.1 CASE-1

Here a novel and dynamic system using STBC OFDM-MIMO (2x2) technology that takes into account the realistic propagation environment by using a realistic spatial channel model in flat fading and frequency selective fading environment has been implemented. This STBC OFDM-MIMO system significantly increases the bit rate while decreasing the co-channel and inter-symbol interference. The BER versus SNR simulation results implemented in Matlab using Alamouti STBC scheme with different system parameters in order to analyze the effect

of Doppler, modulation schemes and interleavers are shown below in Figure7.14 to Figure7.16.

The design parameters for simulation of the systems implemented are given in the Table 7-2 above.

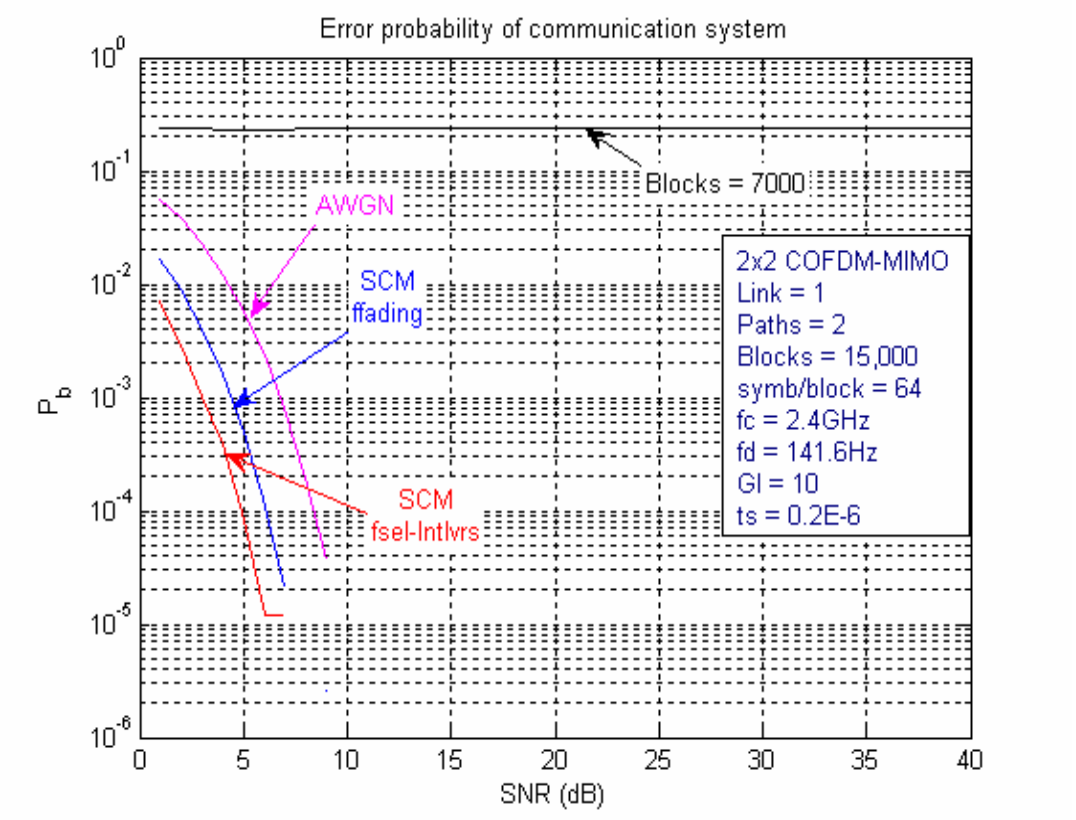

Figure 7.14: BER vs SNR over SCM STBC OFDM-MIMO System

7.16.1.1 Results Analysis

From simulation results of SCM system model it is seen that BER performance is better in case of frequency selective fading environment as compared to flat fading environment. Where BER of 10^{-4} at SNR of 5dB is achieved in case of frequency selective fading environment and same BER rate is achieved at SNR of 6dB in case of flat fading environment with 2-paths per link. This BER performance improvement is achieved due to use of freq/time interleavers in case of freq selective fading environment, where BER curve is pulled down from flat curve in black colour without using interleavers.

The simulation results shown are better than AWGN channel because of the use of MIMO systems and exploitation of diversity by frequency interleaver.

7.16.2 CASE-2

Here STBC OFDM-MIMO (2x2) system in multipath propagation environment using a realistic spatial channel model in frequency selective fading environment with different modulation schemes is implemented. The simulation is performed with PSK and QAM modulation schemes considering modulation order *M* as 2, 4 and 16 to see the difference of BER performance.

The design parameters for simulation of the systems implemented are given in the Table 7-2 above.

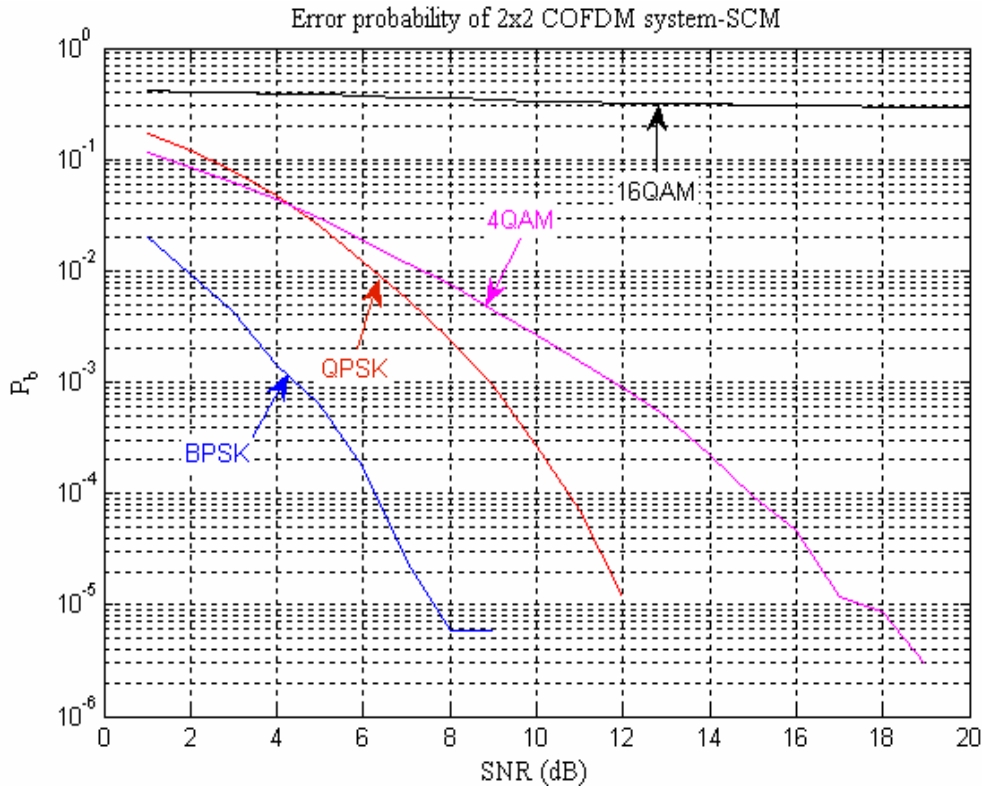

Figure7.15: Comparison of Modulation Schemes (SCM)

7.16.2.1Results Analysis

The simulation results of the system with different modulation schemes implemented are shown in Figure7.15 above.

It is seen that BER performance in case of QAM is not better than PSK scheme because in case of QAM the constellation points lie on square shape. This phenomenon has been described in chapter 2, where the power of constellation points is same in case of QPSK and 4-QAM but is not same in case of 16 QAM. For 16 QAM the constellation expands and power of constellation points on the outer circle is more than unity as compared to points on the inner circle. In case of 16 PSK still the power of all constellation points is unity as all points are lying on the same circle. As a result when using QAM scheme in case of deep null

when the likely point is closer to (0,0) axis will not be able to see the constellation points on the outer circle thereby giving more error in the data as seen in Figure7.15 above a black flat line with 16 QAM in the simulation result.

In case of 4 QAM simulation the power is same to all constellation points in one square as that of QPSK on a unit circle. Therefore BER performance is better at low SNR but at high SNR again BER performance is deteriorated due to multipath effect, rapid change of channel characteristics due to high Doppler Effect and poor channel estimation.

With BPSK modulation scheme the BER of 10^{-5} is achieved at SNR of 7.8dB, whilst comparing QPSK and 4-QAM it is seen that BER of 10^{-5} is achieved at SNR of 12dB in case of QPSK, while same BER of 10^{-5} at SNR of 17dB is achieved with 4QAM system. This difference of 5dB is due to power of constellations points in two modulation schemes.

It is further realized that in this system 16QAM system does not work because of the expansion of constellation and distribution of power to the points.

7.16.3 CASE-3

Here STBC OFDM-MIMO (2x2) system in multipath propagation environment using a realistic spatial channel model and frequency selective fading environment with different modulation schemes is implemented. The simulation is performed with PSK and QAM modulation schemes considering modulation order *M* as 2 and 4 to see the difference of BER performance while changing the Doppler which makes the channel characteristics to change more rapidly.

The design parameters for simulation of the systems implemented are given in Table 7-2 above.

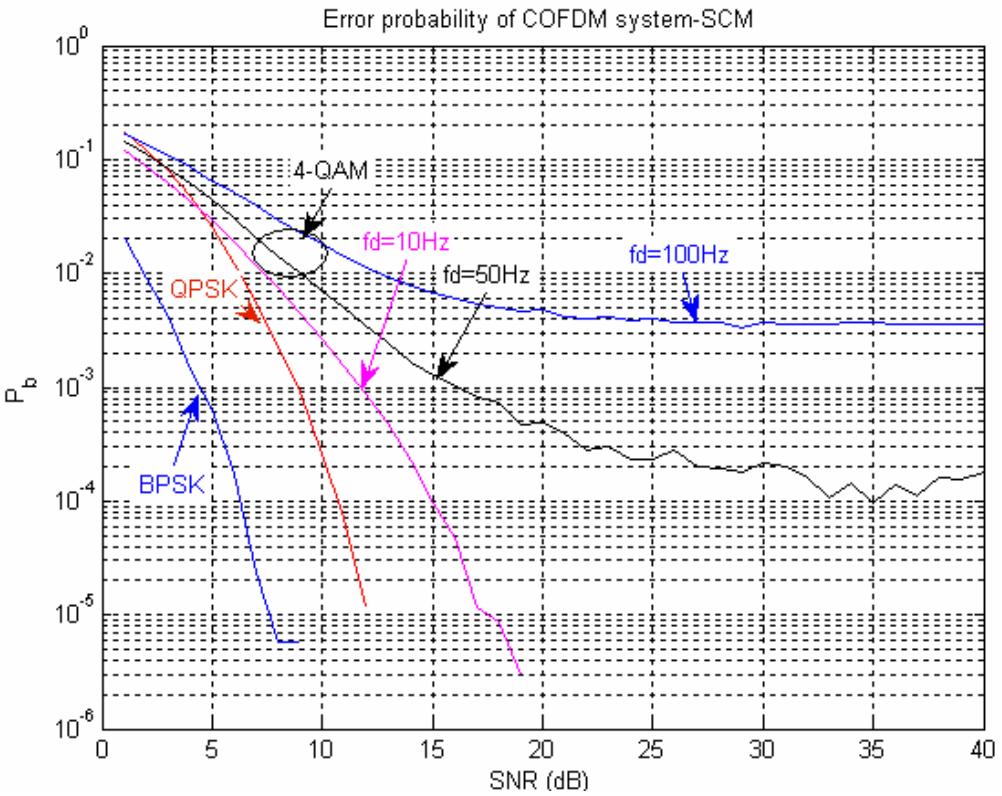

Figure7.16: Effect of Doppler on BER (SCM)

7.16.3.1 Results Analysis

Here the simulation results of the system implemented dictate the effect of Doppler on BER performance of the systems with different modulation schemes.

When QPSK and 4QAM are considered with 10Hz doppler it is seen that QPSK is better than QAM due to the power distribution of constellation points as explained above in CASE-2 for SCM implementation.

When QAM is considered with different values of Doppler frequency, it is seen that by increasing Doppler the BER performance of the system is deteriorated because of change in channel characteristics at high Doppler.

There is an irreducible BER floor achieved at high SNR due to rapid change in channel characteristics and multipath environment implemented. At low SNR the BER performance is compatible to 10Hz Doppler but then it is deteriorated.

7.17 Spatial correlation in SCM

In case of SCM implementation, when (2x2) MIMO system is used in case of time varying frequency selective channel the coefficients generated for different paths are shown in Figure 7.17 below. Here only coefficients of two paths are shown and is observed from simulation results of *Urban_Micro, Urban_Macro and Suburban_Macro* environment as shown in Figure 7.17 that by decreasing the distance between MS antenna elements the paths get more and more correlated. When the distance between antenna elements is sufficiently apart then the paths are de-correlated. This affects the error rate at receiving end in the sense that when paths are correlated, BER performance observed is poor as compared to the case when paths are de-correlated and system's performance is better in terms of BER observed at the receiving end. This validates the BER performance results of the systems simulation in Figure 7.18 below.

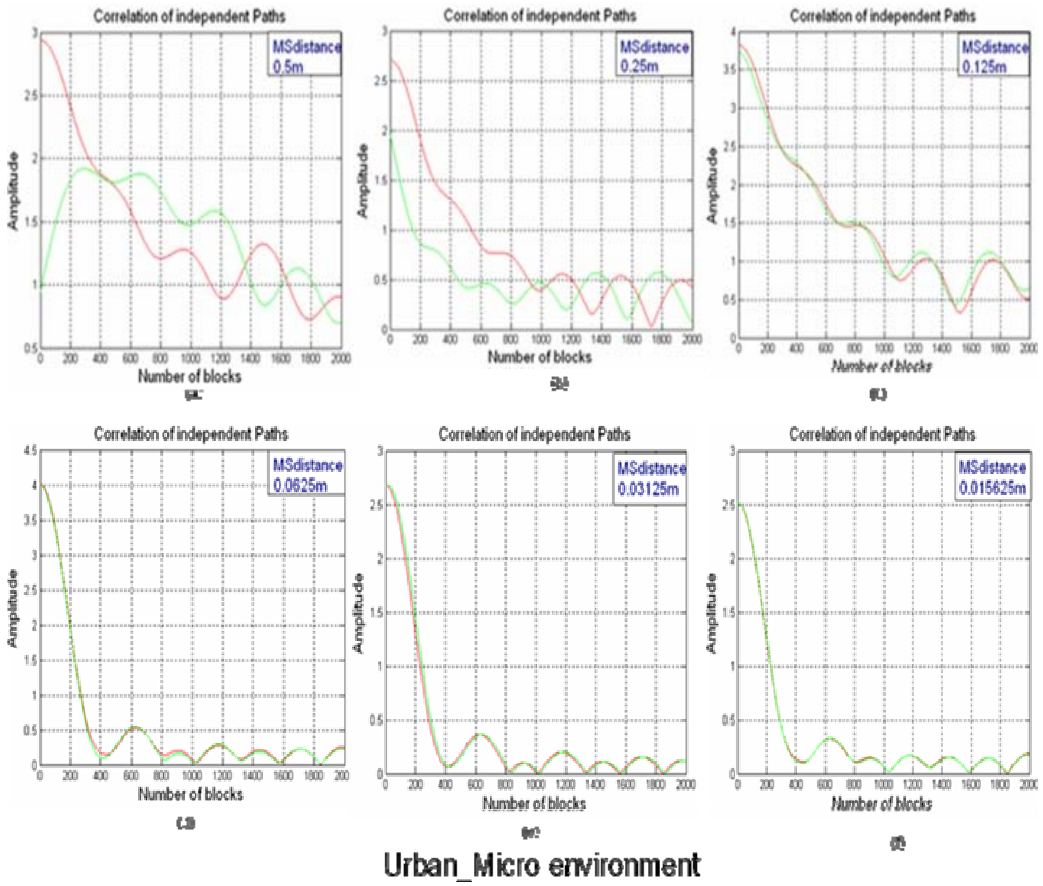

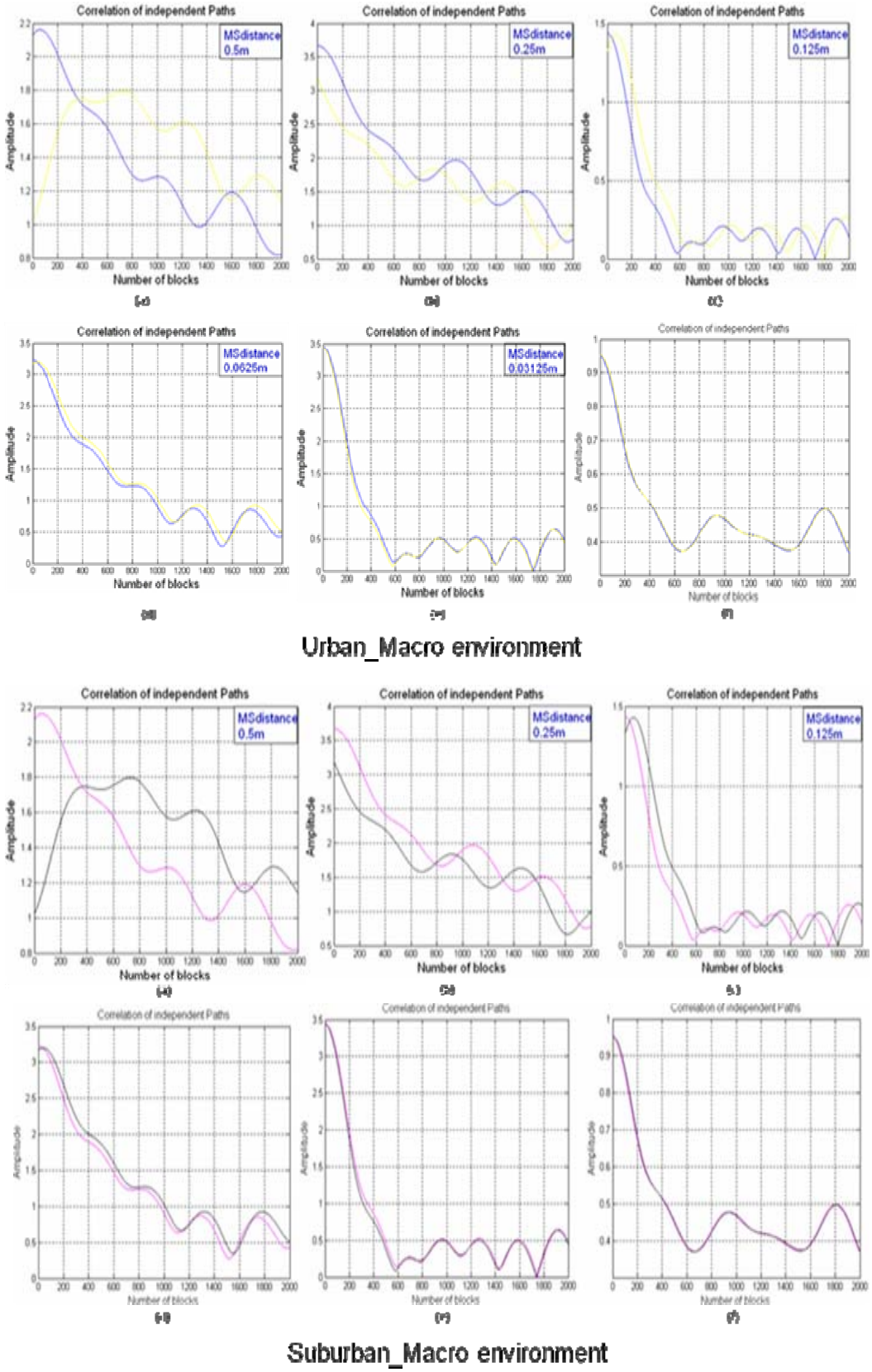

Figure 7.17: Spatial correlation of SCM in different environments

7.18 Effect of spatial correlation on BER Performance

Here in this case frequency selective STBC OFDM-MIMO (2x2) system is implemented using SCM model with carrier frequency f_c as 2.4GHz and mobile user traveling at speed of 63.720kmph. Spatial correlation is simulated by varying antenna spacing at MS while spacing between antenna elements at BS is kept constant.

The design parameters for simulation of the system implemented are given in the Table 7-2 above.

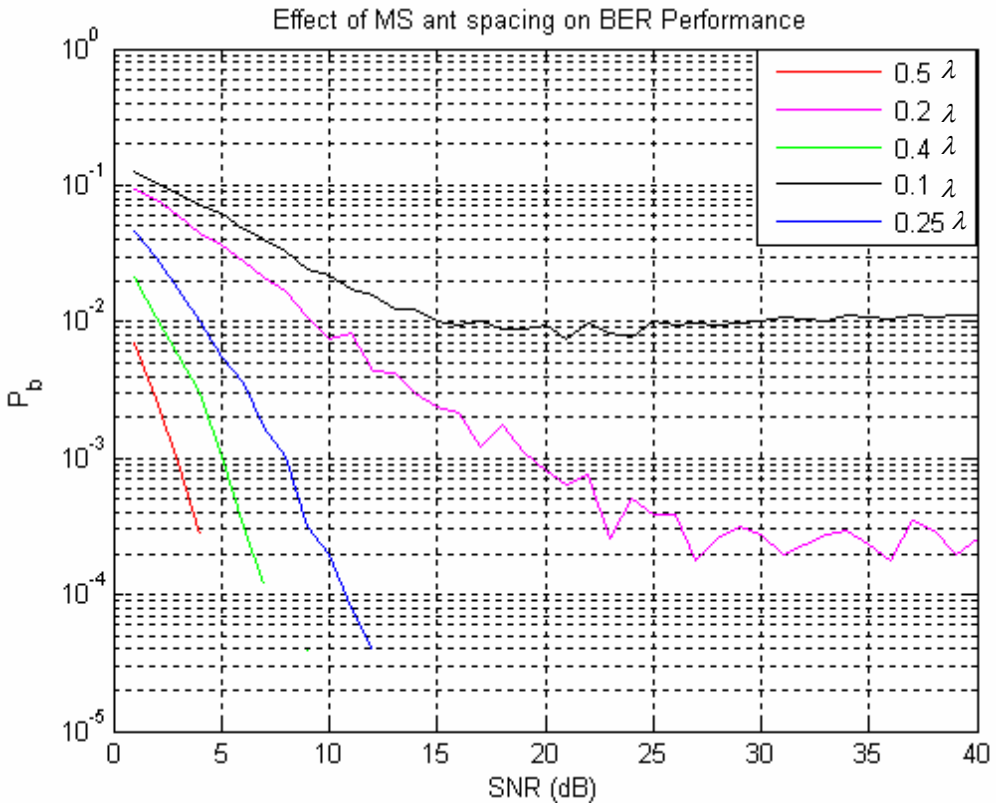

Figure 7.18: Effect of spatial correlation on BER

7.18.1 Results Analysis

Figure 7.18 shows the simulation of STBC OFDM-MIMO (2x2) system implemented using spatial channel model with different spacing between antenna elements at transmitting end, while keeping the spacing of received antenna elements constant.

It is seen from the simulation results that when the MS antenna spacing is 0.5λ then BER performance of 10^{-3} is achieved at SNR of 3dB as shown in red curve that is because of the fact that both antennas at MS are widely spaced and signals received are de-correlated and BER performance is better.

When the antenna spacing is decreased the BER performance is deteriorated as indicated in simulation results with different curves having different antenna spacing values, if the antenna spacing is 0.25λ then same BER of 10^{-3} is now achieved at SNR of 8dB thereby deteriorating the BER performance by almost 5dB.

This degradation in BER performance mainly happens due to the reason that when antennas are closely spaced, signals received by the antennas are severely correlated and both antennas at MS see the same fading channel. Hence by decreasing the spacing between antennas the bit error rate gets worse due to the effect of correlated received signals.

7.19 Summary

In this chapter the concept of frequency division multiplexing and orthogonal frequency division multiplexing is also described along with key components used in the implementation of an OFDM system. The essential feature of an OFDM system is that the serial data at the input is divided into parallel data and then the same parallel data is transmitted simultaneously to achieve the high rate of data transmission. Another advantage of OFDM system observed is the division of channel bandwidth into number of sub-channels decreases the bandwidth of each sub-channel thereby diminishing the need for use of equalizer at the receiving end.

It has also been shown that in order to prevent the orthogonality between the subcarriers and prevent the intersymbol interference, the use of guard intervals is necessary. Different simulations of OFDM and OFDM-MIMO systems have been implemented using Matlab Rayleigh and Spatial Channel models to compare the results of performance of systems in repect of BER. In order to avoid the delay spread that gives rise to intersymbol interference, guard interval bits were used and in order to overcome the problem of timing synchronization, channel estimation was used by the pilot assisted symbols. Channel estimation plays a vital role in all forms of coherent communication system. This is especially true for MIMO systems, where multiple transmitters communicate, simultaneously, with multiple receivers. The importance of coding and interleaving in frequency selective fading channel was examined by implementing the techniques such as viterbi-decoding, time interleaving and frequency interleaving to improve the system performance in terms of BER, which is shown with the help of simulation graphs.

The effect of Doppler and spatial correlation on BER performance of OFDM system has also been demonstrated with the help of simulations. It has been shown that by increasing Doppler the BER performance of the system is degraded. If the antenna spacing between the antenna elements is decreased the degradation in BER performance is observed which mainly happens due to the reason that when antennas are closely spaced, signals received by the antennas are severely correlated and both antennas at Mobile user see the same fading channel. Hence by decreasing the spacing between antennas the bit error rate gets worse due to the effect of correlated received signals.

Chapter 8

8 Summary and Conclusions

This thesis has been concerned with exploitation of diversity offered by the channel. The diversity could be space diversity that is exploited by a smart communications system using different techniques such as i) *SDMA* that forms highly directional beam towards wanted user and a null towards an interferer thereby isolating them in space ii) *MIMO* systems that uses dumb antennas and clever signal processing at the receiving end to resolve the problem of interference iii) Time diversity is exploited by the opportunistic communication system using omnidirectional and an adaptive antennas, that transmits to a user only when the channel conditions to that particular user are good. Frequency diversity is exploited by OFDM and OFDM systems. Finally a new system has been developed that uses a novel combination of smart antenna MIMO techniques based on OFDM technology using a realistic channel model that provides an advanced system configuration, which could be exploited by IEEE 802.20 user specification approach for broadband wireless networking.

8.1 Summary of the work

Chapter one described the evolution of the wireless communications and requirements for the fourth generation wireless cellular systems. A brief description of the different multiplexing techniques such as FDMA, TDMA, CDMA and WCDMA used in wireless communication systems was also covered. In addition this chapter covered research work already carried out using smart antennas in SDMA and MIMO techniques employing STBC and BLAST systems. Finally aims and objectives of the Thesis were given in the same chapter.

In chapter two the mechanism of transmission through the mobile radio channel, modelling digital communication system, deterministic and stochastic model of digital communication system and computer simulations of digital communication systems have been described. It was shown with the help of simulations how the multipath phenomenon severely degrades the quality of the transmitted signal and affects the performance of a digital communication link. The worst scenario of a mobile radio channel is when there is no line of sight in which case the channel is considered to be a Rayleigh faded channel. The multipath effect is worsened when the mobile user is moving due to the Doppler spread thereby making it difficult for the receiver to track the carrier frequency of the transmitted signal. In wideband systems, the phenomenon of multipath gives rise to intersymbol interference and imposes a constraint on the maximum transmission rate thereby reducing the performance of a system in terms of BER. Intersymbol interference can be reduced by the use of guard intervals and different

techniques like error correction coding and interleaving may be used to achieve the acceptable performance of communication link in terms of bit error rate. The concept of line of sight and plane earth propagation is also described and path loss variation has been described as to how does it vary with increase in distance between transmitter and receiver. The signal fading resulting from the distance travelled by the signal and the multipath effect may be divided into two categories, namely, fast fading and slow fading. Fast fading refers to the instantaneous changes in the signal's amplitude and may be approximated to be Rician if line of sight exists, otherwise Rayleigh distributed in case of non line of sight environment. Slow fading, on the other hand, refers to the variations in the average signal's field strength and may be approximated to have a log normal distribution.

The COST 207 channel's delay profiles for a typical urban and hilly terrain environments have been outlined for a discrete GWSSUS tapped delay line channel model. The time varying properties of the channel is modelled by generating time varying complex multiplicative coefficients. These are produced by using pairs of uncorrelated AWGN generators, where each pair represents the real and imaginary part of one coefficient. The Doppler Effect is simulated by passing the coefficients through a low-pass filter with a frequency response defined by the Doppler spectrum. Spatial channel model has also been described in detail along with advantages and weaknesses of the model.

A number of techniques like equalisation, convolutional coding, multicarrier modulation and interleaving for combating the channel's imposed limitations have been briefly reviewed and demonstrated with the help of simulation results that there is significant improvement in performance of a system by using convolutional encoder with different constraint lengths. A spatial channel model considered as realistic physical channel model has the capability of configuring the system with multiple antenna elements at transmitting and receiving end with applicability in different outdoor propagation like urban micro, suburban macro and urban macro environments has been described in detail along with factors that form the basis of selection of the channel model.

In chapter three method of conventional beamforming with the help of array processing starting with fundamentals of antenna elements and covering the description of spatial matched filter and optimum beamformer techniques using ULA were developed. A model for spatial signal received by ULA is presented with simulations. The concept of beamforming with the help of spatial matched filter, which maximises the gain in the direction of wanted user, is discussed along with simulation results presented. It is observed that spatial matched filter is only used to form main beam in the direction of a wanted user by increasing the gain and makes no attempt to not null out the interferer at all. In addition to that optimum

beamforming technique is also discussed that cancels the interferer by placing a null in the direction of an interferer and does not cater for the main beam to be directed towards the wanted user. The method for optimisation of weights for spatial matched filter and optimum beamformer is also presented in this chapter. Difference between spatial matched filter and an optimum beamformer has been shown with help of simulation results that give the graphs of isolation of wanted user from interferers operating from closer and farther angular positions. It is observed from the simulation results that it is important to recognise that the optimum beamformer makes no attempt to form main beam by maximising the gain in the wanted direction but to null out the interfering signals.

In chapter four different adaptive algorithms such as the LMS, NLMS and RLS algorithms have been implemented to get the optimum output by forming main beam pattern in wanted direction while nulling out the interferers. A comparison and result analysis of all the algorithms is also described after the simulation of these algorithms to see the efficiency and performance of each algorithm in terms of convergence to get the optimum output. It is observed that rate of convergence of each adaptive algorithm is dependent on the value defined for the forgetting factor which needs to have a small value in the range of 0 to 1. The convergence of RLS algorithm is quite fast compared to LMS and NLMS algorithm because of the involvement of computational complexity of correlation matrix **R**. In this chapter it is also highlighted that while implementing block adaptive method (SMI), the number of samples needed to obtain the correlation matrix, (i.e. the array support) is very important. When fewer samples are used, the estimate of $\mathbf{R}_{i+n}$ becomes progressively poorer and this impacts on the computation of the optimum weight vector. The sidelobe structure becomes increasingly random and the depth of the null in the direction of the interferer also becomes much reduced. In addition to that simple genetic algorithm is also implemented. Finally novel method of RLS based genetic algorithm is implemented to show the simulation results for forming deep nulls in the direction of interferers operating from closer angular distances about 5^{o} apart from each other, which can not be achieved with traditional gradient based search algorithms. The implemented RLS based GA has proved to be successful, where the algorithm places deep nulls very quickly by minimising the output power to reject the interferers.

Chapter five covers the opportunistic communications systems, where resources are allocated to the users depending upon the condition of channel. Different scenarios of opportunistic communication systems have been implemented. Where common and dedicated links in flat fading, non frequency selective and frequency selective fading environments using omni-directional and adaptive antennas are implemented in order to see the effect of BER performance with different antenna design in flat fading and multipath fading environment to

be compared with the ideal characteristic curve of additive white Gaussian noise channel. Here degradation of BER performance due to the amplitude distortion and phase rotation of the signal in the channel was rectified with implementation of different techniques using zero forcing equalizer to improve the BER performance of the system. The simulations are implemented using Matlab Rayleigh and spatial channel models to compare the BER performance of both channels. It is observed that under all circumstances opportunistic systems have better BER performance than non-opportunistic systems and in some cases the performance of an adaptive antenna is better than omnidirectional antenna when operating in multipath frequency selective environment with three co-channel users communicating with common BS. In addition to that simulation for correlated channels have also been implemented to see the effect of BER performance of the systems and is observed that if the channels are correlated there is degradation in the BER performance of the system.

In chapter six different types of MIMO systems are covered and then implemented to investigate the effect of diversity on the performance of MIMO systems in terms of BER. The space time block coded system and Layered space time architecture systems with different parameters of multipath channels are implemented to compare the performance of both systems. Simulations of Matlab Rayleigh and Spatial channel models using MIMO systems have been implemented to show the BER vs SNR performance of the systems. From simulations it is observed that BER performance is significantly improved with MIMO systems as more number of antennas are used to exploit the effect of diversity in the system. It is also observed from simulations, that by using layered space time architecture the BER performance with MIMO systems is not improved much as compared to STBC systems but data rate in that case is doubled due to multiplexing of data at the transmitting end. It is also seen from the simulations that overall LST systems using interference suppression and successive cancellation technique have better BER performance than systems without cancellation of interference. It is worth to note that STBC systems are better if BER performance improvement is required for fixed data rate, while LST systems are better for improvement of data rate depending on the number of transmit antennas as the data on all the transmit antennas is multiplexed.

In chapter seven transmission of signal through mobile radio channel is described under different environments like flat fading and frequency selective fading. The effect of an environment when there is no LOS and user is affected due to multipaths in the environment is covered and is observed that multipath effect gives rise to intersymbol interference as a result the transmission rate is affected. It has also been shown that in order to prevent the orthogonality between the subcarriers and prevent the intersymbol interference, the use of

guard intervals is necessary. In addition to that a situation is also covered when the user is moving and due to the Doppler Effect the BER performance is deteriorated since is difficult for the receiver to track the channel characteristics of fast moving channel. The concept of frequency division multiplexing and orthogonal frequency division multiplexing is also described along with key components used in the implementation of an OFDM system. Different simulations of OFDM MIMO and OFDM MIMO systems have been implemented using Matlab Rayleigh and spatial channel models. The importance of coding and interleaving in frequency selective fading channel was examined in addition to that techniques such as viterbi-decoding, time interleaving and frequency interleaving have been implemented to improve the system performance in terms of BER, that is shown with the help of simulation graphs. The effect of Doppler and spatial correlation on BER performance of OFDM system has also been demonstrated with the help of simulations. It has been shown that by increasing the Doppler and decreasing the spatial distance between antenna elements the BER performance of the system is degraded. The degradation in BER performance mainly happens due to the reason that when antennas are closely spaced, signals received by the antennas are severely correlated and both antennas at mobile station see the same fading channel. Hence by decreasing the spacing between antennas the bit error rate gets worse due to the effect of correlated received signals.

8.2 Future Work

The considerations for future work are presented below:

a. Novel system model developed can be practically implemented and introduced as a system level simulator.
b. A system could be implemented to optimise the selection of different diversity systems like SDMA, MIMO, and OFDM or coded OFDM depending upon the existing environments dictated by the channel conditions.
c. The SCM model can be used with the implemented system by incorporating the far scatterer clusters into account.
d. Neural network algorithms may be used to recognise the pattern of selection of various diversity systems implemented.
d. Using same implemented system the spatial temporal correlation properties of the SCM model can be compared with other outdoor channel models.

References

1. Christos Christodoulou and Naftali (Tuli) Herscovici, “Smart Antenna Systems for Mobile Communication Networks: Part 1: Overview and Antenna Design”, IEEE Antennas and Propagation Magazine, Vol. 44, No 3, pp.35-43, June 2002.
2. I. Rubin, ‘‘Message delay in FDMA and TDMA communication channels’’, IEEE transactions on communications, Vol. COM27, no. 5, pp.769-777, May 1979.
3. GSM Europe, ‘‘History of GSM’’, October 2000, published online at: www.gsmworld.com.
4. Samuel D. Stearns, “Digital Signal Processing with Examples in MATLAB”, by CRC Press LLC Edition 2003.
5. Dimitris G. Manolakis, Vinay K. Ingle, Stephen M. Kogon, “Statistical and Adaptive Signal Processing”, McGraw-Hill International Editions 2000.
6. P. Nicopolitidis, M. S. Obaidat and A. S. Pomportsis, ‘‘Wireless Networks’’, John Wiley & Sons, Ltd.
7. Simon Haykin, “Adaptive Filter Theory”, 3_{rd} edition Printice Hall, New Jersey 1996.
8. R. W. Chang, “Synthesis of Bandlimited Orthogonal Signals for Multichannel Data Transmission”, Bell Systems Technical Journal, Vol. 46, pp. 1775-1796, Dec. 1966.
9. B. R. Saltzberg, “Performance of an Efficient Parallel Data Transmission System”, IEEE Transactions on Communication Technology, Vol. COM-15, No. 6, pp. 805-811, Dec. 1967.
10. S. B. Weinstein and P. M. Ebert, “Data Transmission by Frequency Division Multiplexing using the Discrete Fourier Transform”, IEEE Transaction on Communications, Vol. COM-19, pp. 628-634, Oct. 1971.
11. W. T. Webb and L. Hanzo, “Modern Quadrature Amplitude Modulation”, IEEE Press, 1995.
12. R. Steele. “Mobile Radio Communications”, 3rd edition, IEEE Press, Vol. 55, No. 6, pp.1179-1187, May 1992.
13. W. C. Jakes, “Microwave Mobile Communications” John Wiley and Sons, 1974.
14. E. C. Ifeature and B. W. Jervis, “Digital Signal Processing, A Practical approach”, Addison Wesley publishers ltd, 1993.
15. D. I. Laurenson, D. G. M. Gruickshank and G. J. Povey, “A computationally Efficient Multipath Channel Simulator for the Cost 207 Models”, IEEE conference proceedings, vol. 6, pp. 48-51, July 1996.

16. A. J Viterbi, ‘‘CDMA principles of spread spectrum communications’’, Addison-Wisley wireless communications series, 1996.
17. F. Alam, F. Tariq and Brian D. Woerner, ‘‘Beamformng vs Diversity combining in 2-D receivers for third generation CDMA systems’’, 6th international conference on computer and information technology (ICCIT), vol. 11, pp. 58-65, 2003.
18. Warren L. Stutzman and Gary A. Thiele, “Antenna theory and design”, by John Wiley & Sons, Inc 1981.
19. http://en.wikipedia.org/wiki/Genetic_algorithm.
20. R.L. Haupt, “The development of smart antennas”, IEEE Antennas and Propagation Society International Symposium, vol. 4, pp. 48-51, July 2001.
21. Goldberg, David E, “Genetic algorithms”, Addison-Wesley, New York 1989
22. R.L. Haupt, J. Menozzi and Christopher J. McCormack, “Thinned Arrays Using Genetic Algorithms”, Antennas and Propagation Society International Symposium, 1993. AP-S. Digest , 28 June-2 July 1993, pp 712 – 715.
23. Christos Christodoulou and Naftali (Tuli) Herscovici, “Smart Antennas”, IEEE Antennas and Propagation Magazine, Vol.42, No 3, pp.39-47, June 2000.
24. Lal C Godara, “Applications of Antenna Arrays to Mobile Communications, Part I: Performance Improvement, Feasibility and System Considerations”, Proceedings of IEEE, Vol.85, No. 7, pp. 1031-1060, July 1997.
25. Lal C Godara, “Applications of Antenna Arrays to Mobile Communications, Part II: Beam Forming and Direction of Arrival Considerations”, Proceedings of IEEE, Vol.85, No. 7, pp. 1195-1245, August 1997.
26. J. H. Holland, “Genetic algorithms”, *Sci. Amer.*, pp. 66–72, July 1992
27. Robert A. Monzingo, Thomas W. Miller, “Introduction to Adaptive Arrays”, John Wiley & Sons , New York:1980
28. Theodore S. Rappaport, “Smart Antennas, Adaptive Arrays, Algorithms and wireless position location” 1988.
29. Iqbal Jami, and Richard F. Ormondroyd, “Joint angle of arrival and angle-spread estimation of multiple users using an antenna array and modified MUSIC algorithm”, IEEE 2001.
30. Christos Christodoulou and Naftali (Tuli) Herscovici, “Smart Antennas in Wireless Communications: Base-Station Diversity and Handset Beamforming”, IEEE Antennas and Propagation Magazine, vol.42, No 5, pp.45-53, October 2000.
31. G. V. Tsoulos, “Smart Antennas for Mobile Communication systems: benefits and challenges”, Electronics and Communication Engineering Journal April 1999.

32. Garret T. Okamoto, “Smart antenna systems”, Santa Clara, California
33. Shiann-Shiun Jeng, Guanghan Xu, Lin, and J. Vogel, “Experimental studies of spatial signature variation at 900 MHz for smart antenna systems”, IEEE Transactions on Antennas and Propagation, Vol.46, No 7, pp.75-83, July 1998.
34. Christos Christodoulou and Naftali (Tuli) Herscovici, “Potentials of Smart Antennas in CDMA systems and uplink improvements”, IEEE Antennas and Propagation Magazine, Vol.43, No 5, pp.38-46, October 2001.
35. S. Ghoshray, K. K. Yen, “More Efficient genetic algorithm for solving optimization problems”, IEEE International conference on systems, man and cybernatics, vol. 5, pp, 367-375, 22-25 Oct 1995.
36. Joseph Shapira and Samuel Miller, “A Novel Polarization Smart Antenna”, IEEE Vehicular Technology Conference, Vol.01, pp. 69-75, July 2001.
37. Joseph Shapira and Samuel Miller, “Transmission Considerations for Polarization-Smart Antennas”, IEEE Vehicular Technology Conference, Vol.01, pp. 438-745, 2001.
38. Ling Li, Hongbin Li and Yu-Dong Yaor, “Transmit Diversity and Equalization for Frequency Selective Fading Channels”, IEEE Vehicular Technology Conference,Vol. 3, pp.135-143, May 2001
39. Defne Aktas and Hesham El Gamal, “Multiple user Scheduling for MIMO Wireless Systems,” IEEE Vehicular Technology Conference, Vol. 3, pp.65-73, 2003.
40. Wei Li and T. Aaron Gulliver, “Smart Antennas and Transmit Diversity for GSM Systems”, Communications, Computers and signal Processing, PACRIM. 2003 IEEE Pacific Rim Conference vol. 1, pp.25-33, Aug 2003.
41. Sheng, J.G. Nallanathan, A. Tjhung, “Channel estimation for space-time block coded system under spatially correlated Rayleigh fading channel”, Personal, Indoor and Mobile Radio Communications, PIMRC 2003. IEEE Proceedings on Volume 3, pp.87-95, 2003.
42. Iraji, S. Lilleberg, “Interference cancellation for space-time block-coded MC-CDMA systems over multipath fading channels”, Vehicular Technology Conference, VTC Volume 2, pp.65-73, Oct. 2003.
43. G. J. Foschini, “Layered space-time architecture for wireless communication in a fading environment when using multi-element antennas”, Bell Labs Tech Journal, vol. 1, pp.335-343, 1996.

44. Frohlich. F, Martin, U, "Frequency-domain MIMO interference cancellation technique for space-time block-coded single-carrier systems", 2004 ITG Workshop on Smart Antennas.
45. Richad. B. Ertel, Paulo Cardieri, Kevin W. Sowerby, Rappaport. T.S, and Reed. J.H, "Overview of spatial channel models for antenna array communication systems", Personal Communications, IEEE Volume 5, Issue 1, pp.77-86, Feb. 1998
46. Spatial Channel Measurement and modelling, "http://www.techonline.com/community/related_content/14707''.
47. Propagation Models for Urban Measurement, "http://www.wtech.org/loyala/wireless/04_02.htm''.
48. Hui Liu, Guanghan Xu ''Smart antennas in wireless systems: Uplink Multiuser blind channel and sequence detection", IEEE Transactions on Communications Volume 45, No. 2, pp.98-105, February. 1997.
49. Multiple Input Multiple Output (MIMO) Systems for Wireless Communications, "http://www.signaluu.se/Research/rdiversity.html''.
50. Fugen, T. Kuhnert, C. Maurer, J. Wiesbeck, "Performance of multiuser MIMO systems under realistic propagation conditions", Smart Antennas, 2004. ITG Workshop, 2004.
51. Understanding MIMO, "http://www.commsdesign.com//printableArticle''
52. Web Proforum Tutorials, "http://www.iec.org''
53. Adel A. M. Saleh and Reinaldo A. Valenzuela, "A statistical model for indoor multipath propagation", IEEE journal on selected areas of communications, SAC-5, Feb. 1987.
54. German. G, Spencer. Q, Swindlehurst. L, Valenzuela. R, "Wireless indoor channel modelling: statistical agreement of ray tracing simulations and channel sounding measurements", Acoustics, Speech, and Signal Processing, IEEE Proceedings Volume 4, pp.135-143, May 2001.
55. Oh-Soon Shin; Kwang Bok Lee, "Packet scheduling for MIMO cellular systems", Vehicular Technology Conference, Volume 3, pp.335-343, April 2003.
56. Junqiang Li; Letaief, K.B.; Zhengxin Ma; Zhigang Cao, "Spatial multiuser access with MIMO smart antennas for OFDM systems", IEEE 54th Vehicular Technology Conference, VTC, Volume 3, pp.245-253, Oct. 2001.
57. J.B Anderson, T.S Rappaport, "Propagation measurement and models for wireless communications channels", IEEE Comm. Mag., Vol. 33, no. 1, Jan. 1995.
58. Matthias Paetzold, "Mobile Fading Channels", John Wiley & Sons, Ltd, 2002

59. U. Lambrette, S. Fechtel, and H. Meyer, "A frequency domain variable data rate frequency hopping channel model for the mobile radio channel", IEEE 47th VTC'97, Arizona, USA, May 1997.
60. M. Paetzold, U. Killat, and F. Laue, "A frequency selective Rayleigh fading channel simulator with given correlation properties", IEEE Int. Workshop on Intelligent Signal Processing and Communication Systems, ISPACS'97, Kuala Lumpur, Malaysia, Nov. 1997.
61. http://en.wikipedia.org/wiki/Kolmogorov-Smirnov_test
62. B. Vucetic and J. Yuan, "Space-Time Coding", John Wiley and Sons, Chichester, UK,2003
63. J. G. Proakis, Digital Communications. McGraw Hill, New York, 4th edition, 2000
64. http://en.wikipedia.org/wiki/Multiple-input_multiple-output_communications
65. Tom Feist Director, DSP Tools Marketing, "Rapid Prototyping and verification of MIMO systems", DSP magazine May 2006.
66. G. J. Foschini and M. J. Gans, "On the limits of wireless communications in a fading environment when using multiple antennas", Wireless Personal Communications, vol. 6, pp. 311-335, 1998.
67. G. D. Golden, G. J. Foschini, R. A. Valenzulea and P. W. Wolniansky, "Detection Algorithm and Initial Results using VBLAST Space-Time Communication Architecture", IEEE Electronics Letters, vol. 35, no. 1, pp.635-643, Jan. 1999.
68. http://www1.bell-labs.com/project/blast/.
69. G. J. Foschini, P.W. Wolniansky, G.D. Golden and R.A. Valenzuela, "V-BLAST: An Architecture for Realizing very High Data Rates over the Rich Scattering Wireless Channel", Bell Labs, Lucent Technologies.
70. Christos Christodoulou and Naftali (Tuli) Herscovici, "Space Time Adaptive Processing Using Circular Arrays", IEEE Antennas and Propagation Magazine, Vol, 43, No. 1, pp.65-77, February 2001.
71. Christos Christodoulou and Naftali (Tuli) Herscovici, "Simulation of Mobile Fading Channels", IEEE Antennas and Propagation Magazine, Vol.44, No. 6, pp.745-756, December 2002.
72. Molina, Domingo, Jose-Victor and Leandro, "A Distributed MIMO Scheme for open Areas and Urban Street Microcells", IEEE, No 3, pp.335-343, 2004.
73. Matthias Stege, Marcus and Fettweis, "On the Performance of Space-Time Block codes", Vehicular Technology Conference, VTC, Volume 3, pp.785-793, May. 2001.

74. Kiyoshi Hamaguchi and Lajos Hanzo, "Multi-stage Multi-user detection assisted asynchronous Fast-FH/MFSK", Vehicular Technology Conference, VTC, 2003.
75. Kiyoshi Hamaguchi, Lie-Liang Yang and Lajos Hanzo, "On the Performance of Multi-stage Multi-user detection assisted Fast-FH/MFSK", Vehicular Technology Conference, VTC, pp.86-98, 2003.
76. Jari Helkkonen, Timo, Jyri, Korpi and Mikko Saily, "Capacity gain from Transmit diversity Methods in limited Bandwidth GSM/EDGE networks", Vehicular Technology Conference, VTC, pp.756-767, 2003.
77. Hong-Cheol Kim, Yoan shin and Won-Cheol Lee, "Performance enhancement of Transmit diversity Schemes using Subarray Transmit Eigen-beamformer", Vehicular Technology Conference, VTC, pp.935-943, 2003.
78. Jia Hou, Moon Ho Lee and Ju Yong Park, "Simple Correlation cancelling algorithm for Space time Block Codes", Vehicular Technology Conference, VTC, pp.25-33,2003.
79. Lizhong Zheng and David N. C. Tse, "Diversity and Multiplexing: A fundamental Tradeoff in Multi-antenna Channels", IEEE Transactions on Information Theory, Vol. 49, No. 5, pp.76-87, May 2003.
80. David N. C. Tse, Pramad Viswanath and Lizhong Zheng, "Diversity-Multiplexing Tradeoff in Multi-access Channels", IEEE Transactions on Information Theory, Vol. 50, No. 9, pp.835-846, September 2004.
81. Gerhard Bauch and Javed Shamim Malik, "Orthogonal Frequency Division Multiple Access with Cyclic Delay Diversity", 2004 ITG workshop on Smart Antennas.
82. Kai-Kit Wong, R.D. Murch and K.B. Lataief, "MIMO antenna system for frequency selective fading channels", IEEE Personal indoor and Mobile Radio Communications 2000.
83. V. Pohl, V. Jungnickel, T. Haustein and Helmolt, "Antenna spacing in MIMO indoor Channels", IEEE Vehicular Technology Conference, Vol. 3, pp.46-53, 2002.
84. Hiroki Inokura, Noriyoshi Kuroyanagi, Mitsuhiro Tomita and Naoki Suehiro, "A CDMA MIMO system with Multiple-Dimension decorrelating detectors", IEEE, 2003.
85. Juha Laurila, Klaus Kopsa, Robert Schurhuber and Ernst Boneck, "Semi-blind separation and detection of co-channel signals", IEEE, 1999.
86. M.F. Siyau, P. Nobles and R.F Ormodroyd, ''Channel estimation for layerd space-time systems", Proceedings of 4th IEEE Workshop on SPAWC, pp 482-486, 2003.

87. M.F. Siyau, P. Nobles and R.F Ormodroyd, “Performance of a layered space-time cellular system used with a fractionally spaced channel estimator operated in a time-varying, frequency-selective wireless channel”, IEEE Proceedings VTC2004-Fall. Vol. 4, pp 2467-2472, 2004.
88. J. Michael Johnson, “Genetic Algorithm Design of a Switchable Shaped Beam Linear Array with Phase only Control”,.
89. R. L. Haupt, “An Introduction to Genetic Algorithms for Electromagnetics”, IEEE Antennas and Propagation Magazine, Vol. 37, No. 2, April 1995.
90. R. L. Haupt, “Genetic Algorithm Design of Antenna Arrays”, IEEE Transactions on Antennas and Propagation, Vol. 43, No. 8, pp 1466-1472, June 1996.
91. R. L. Haupt, “Phase-Only Adaptive Nulling with Genetic Algorithm”, IEEE Transactions on Antennas and Propagation, Vol. 45, No. 6, pp 2576-2582, June 1997.
92. R. L. Haupt and J. Michael Johnson, “Dynamic Phase-Only Array Beam Control using a Genetic Algorithm”, IEEE Transactions on Antennas and Propagation, Vol. 25, No. 4, pp 2868-2875, June 1998.
93. R. L. Haupt, “Adaptive antenna arrays using a Genetic Algorithm”, IEEE Transactions on Antennas and Propagation, Vol. 25, No. 4, pp 4457-4462, 2006.
94. Ralph O. Schmidt, “Multiple Emitter Location and Signal Parameter Estimation”, Proc. RADC Spectral Estimation Workshop, pp 243-258, 1979.
95. R. Roy, A. Paulraj, T. Kailath, ‘‘ESPRIT- A subspace rotation approach to estimation of parameters of Cisoids in noise’’, IEEE Transactions on Acoustics, Speech and signal processing, Vol. 32, pp. 1340-1342, May 1986.
96. Michael D. Zoltowski, Seth D. Silverstein and Cherain P. Mathews, “Beamspace Root-Music for Minimum Redundancy Linear Arrays”, IEEE Transactions on Signal Processing, Vol. 41, No. 7, pp 467-472, July 1993.
97. Richard Roy and Thomas Kailath, “ESPRIT- Estimation of Signal Parameters via Rotational Invariance Techniques”, IEEE Transactions on Acoustics, Speech and Signal Processing, Vol. 37, No. 7, pp 760-772, July 1989.
98. Jo Verhaevert, Emmanuel Van Lil and Antoine Van de Capelle, ‘‘Analysis of the SAGE DOA parameter extraction with 1.8 GHz indoor measurements’’, VTC 2003-Fall. IEEE 58th, Vol 1, pp 659-668, 6-9 Oct 2003.
99. I. Jami, M. Ali and R. F Ormondroyd, “Comparison of methods of locating and Tracking cellular mobiles”, IEEE colloguium on 17 May 1999.

100. DeGroat, Dowling and Darel A. Linebarger "The Constrained Music Problem", IEEE Transactions on Signal Processing, Vol. 41, No. 3, pp 2367-2372, July 1993.

101. Michael D. Zoltowski, Seth D. Silverstein and Gregory M. Kautz "Beamspace Root-Music", IEEE Transactions on Signal Processing, Vol. 41, No. 1, pp 6567-6572, January 1993.

102. Christos Christodoulou and Naftali (Tuli) Herscovici, "Smart Antenna Systems for Mobile Communication Networks: Part 2: Beamforming and Network Throughput", IEEE Antennas and Propagation Magazine, Vol. 44, No 4, pp 5267-5272, August 2002.

103. Christos Christodoulou and Naftali (Tuli) Herscovici, "On the Design of Switched-Beam Wideband Base Stations", IEEE Antennas and Propagation Magazine, Vol. 46, No 1, pp 7667-7675, February 2004.

104. Tobias J. Oechtering and Aydin Sezgin, "A new Transmission Scheme using Space-Time Delay Code", ITG Workshop on smart Antennas 2004.

105. Jihoon Choi, Heejung Yu and Yong H. Lee, "Adaptive MIMO decision feedback Equalization for Receivers in Time-Varying Channels", IEEE 2003.

106. J. Nicholas Laneman, Gregory W. Wornell and David N. C. Tse" Diversity in Wireless Networks: Efficient Protocols and Outage Behavior", IEEE Transactions on Information Theory, Vol. 50, No. 12, pp 3577-3582, December 2004.

107. W. Su, A. K. Sadek and K. J. R. Liu, ''SER performance analysis and allocation for decode-and forward cooperation protocol in wireless networks'', IEEE WCNC, New Orleans, LA, pp. 984-989, Mar 2005.

108. E. C. Van Der Meulen, ''Three terminal communication channels'', Advances in applied Probability, pp. 120-154, 1971.

109. T. M. Cover and A. El Gamal, ''Capacity theorems for the relay channel'', IEEE Transactions on Information Theory, Vol. 25, pp. 572-584, September 1975.

110. Ahmed S. Ibrahim, Ahmed K. sadek, Weifing Su and K. J. Ray Liu, ''Cooperaitve with channel state information: when to cooperate'', IEEE Globecom 2005.

111. Sang Wu Kim and Ravi Cherukuri " Spatial Multiplexing for High-rate wireless communications", IEEE 6th workshop on signal processing advances in wireless communications, 2005.

112. Pramod Viswanath, David N. C. Tse and Rajiv laroia "Opportunistic Beamforming using Dumb antennas", IEEE Transactions on Information Theory, Vol. 48, No. 6, pp. 4256-4265, June 2002.

113. Aria Nosratinia, Todd E. Hunter and Ahmadreza Hedayat "Communications in Wireless Networks", IEEE Communication Magazine. October 2004.
114. R. L. Haupt, "The development of smart Antennas", IEEE Transactions on Antennas and Propagation, 2001.
115. Keizo Cho, Yasushi Takatori, Kazuhiro Komiya, Kentaro Nishimori and Hideki Mizuno, "Novel Smart antennas for applying SDMA to cellular mobile communication systems", IEEE 2002.
116. Keizo Cho, Kazuhiro Komiya, Kentaro Nishimori and Hideki Mizuno, "Effectiveness of directivity and Polarization control SDMA systems in a cellular environment", IEEE 2002.
117. J. D. Parsons, "The Mobile Radio Propagation Channel", 2_{nd} John Wiley & Sons, 2000.
118. 3rd Generation Partnership Project (3GPP), "Spacial channel model for multiple input multiple output (MIMO) simulations (3gpp TR 25.996 version 6.1.0 (2003-09)''.
119. J. Salo, G. Del Galdo, J. Salmi, P. Kyosti, M. Milojevic, D. Laselva, and C. Schneider, "MATLAB implementation of the 3GPP Spatial Channel Model (3GPP TR 25.996)", on-line, Jan. 2005, http://www.tkk.fi/Units/Radio/scm/.
120. EURASIP Journal on wireless communications and networking 2007.
121. Tapan K. Sarkar, Michael C. Wicks, Magdalena Salazar-Palma, and Robert J. Bonneau "Smart Antennas", John Wiley & Sons, 2003.
122. Q.spencer, "A statistical model for Angle of Arrival in Indoor Multipath Propagation", IEEE VTC, 1997.
123. P. A. Bello, "Characterization of Randomly Time-Variant Linear Channels", IEEE transactions on communications systems, Vol. CS-11, pp. 336-393, Dec 1963.
124. A. J. Paulraj, D. A. Gore, R. U. Nabar and Helmut Bolcskei, "An Overview of Communications- A Key to Gigabit Wireless", Proceedings of IEEE, vol. 92, No.2, pp 5624-5637, February 2004.
125. Hemanth Sampath, Shilpa Talwar, Jose Tellado A. J. Paulraj and Vinko Ercig, "A Fourth-generation MIMO-OFDM Broadband wireless system: Design, Performance and field trial results", IEEE Communication Magazine, Vol.4, pp 7845-7857, September 2002.
126. D. Gesbert, M. Shafi, Da-Shan Shiu, P. J. Smith and Ayman Naquib, "From Theory of Practice: An Overview of MIMO Space-Time coded Wireless Systems", IEEE

Journal on selected Areas in Communications, vol. 21, No.3, pp. 6598-6607, April 2003.

127. J. H. Winters, "On the capacity of radio communication systems with antenna diversity in Rayleigh fading environment", IEEE Journal on selected Areas in Communication, Vol. 5, pp 267-276, June 1987.
128. I. E. Telatar, "Capacity of multiantenna Gaussian Channels", AT&T Bell Laboratories, Tech. Memo, June 1995.
129. I. E. Telatar, "Capacity of multiantenna Gaussian Channels", IEEE ISIT 2001, Washington. D. C. June 24-29, 2001.
130. Jack Salz, "Digital transmission over cross coupled linear channel", Bell Systems Tech Journal, Vol. 64, pp 5457-5462, July-Aug 1985.
131. G. Rayleigh and J. M. Ciioffi, "Spatial-temporal coding for wireless communications", IEEE transactions on communications systems. Vol. 46, pp 3437-3446, 1998.
132. S. M. Alamouti, "A simple transmit diversity technique for wireless communications", IEEE J. Special Areas in Communications, vol. 16, no 8, pp 1451-1458, 1998.
133. V. Tarokh, N. Seshadri and A.R. Calderbank, "Space-time codes for high data rate wireless communication: Performance criteria and code construction", IEEE transactions on information theory Mar 1998.
134. J. Foschini, "Layered Space-time architecture for wireless communications in fading environment", Bell Labs Technical Journal, Vol. 1, No 2, pp 1367-1372, autumn, 1996.
135. C. Waldschmidt, C. Kuhnert, S. Schulteis, and W. Weisbeck "On the Integration of MIMO Systems into Handheld Devices", 2004 ITG Workshop on Smart Antennas.
136. Aydin Sezgin, Eduard A. Jorsweik and Volker Jungnickel "Maximum Diversity Detection for Layered Space-Time Codes", IEEE VTC 2003.
137. Keun Chul HWANG and Kwang Bok (Ed) LEE "Joint Transmitter-Receiver Optimization for Multiple Input Multiple Output (MIMO) Systems", IEEE VTC 2003.
138. N. Seshadri and J. H. Winters, "Two Schemes for Improving the Performance of Frequency Division Duplex (FDD) Transmission Systems using transmitter antenna diversity", Int. Journal. Wireless Information Networks, Vol. 1, pp 7467-7472, Jan 1994.

139. I.A. Glover and P.M. Grant, "*Digital Communications*", Prentice Hall Europe, Second edition 2004.
140. L. Hanzo, B. J. Choi and T. Killer, "OFDM and MC-CDMA for Broadband Multi-user Communications", John Wiley & Sons, 2003.
141. L. Hanzo, "Bandwidth-efficient wireless multimedia communications", Proceedings of the IEEE, Vol. 86, pp. 1342-1382, July, 1998.
142. H. Chen, X. Deng and A. Haimovich, "Layered turbo space-time coded MIMO-OFDM systems for time varying channels", IEEE 2003.
143. Gordon L. Stuber, John R. Barry, Steve W. Mclaughlin, YE (Geoffrey) Li, Marry Ann Ingram and Thomas G. Pratt, ''Broadband MIMO-OFDM wireless Communications'', Proceedings of IEEE, Vol. 92, No. 2, pp 9427-9432, February 2004.
144. Enrique Ulffe Whu, ''MIMO-OFDM systems for high data rate wireless networks'', Project repor EE60 advanced wireless networks at Stanford university.
145. R.M. Rao and B. Daneshrad, "Analog impairments in MIMO-OFDM systems", IEEE transactions on wireless communications, vol. 5, pp. 3382-3386, Dec. 2005.
146. H. Bolcskei and ETH Zurich, "MIMO OFDM wireless systems: Basics, Perspectives and Challenges", IEEE wireless communications, pp. 31-37, Aug 2006.
147. Sinem Coleri, Mustafa Ergen, Anuj Puri and Ahmad Bahai, ''Channel estimation techniques based on pilot arrangement in OFDM systems'', IEEE transactions on Broadcasting, Vol. 48, No. 3, pp 15-24, September 2002.
148. Y. Liang, H. Luo, R. Liu and C. Yan, "RLS channel estimation and data detection in space –time coded MIMO-OFDM system", IEEE 2006.
149. Feng Yang, Lin Gui and Ling Na Hu, ''Semiblind Channel estimation in OFDM systems'', IEEE 20007.
150. Tao Cui and Chintha tellambura, "Superimposed pilot symbols for channel estimation in OFDM systems", IEEE Globecomm 2005.
151. Y. Li, ''Pilot-symbol aided channel estimation for OFDM in wireless systems'', IEEE transactions on vehicular technology, Vol 49, pp. 1207-1215, July 2000.
152. E. Al-Susa and R. Ormondroyd, ''A predictor based decision feedback channel estimation method for OFDM with high resilience to rapid time-variations'', IEEE proceedings of vehicular technology conference, Vol. 1, pp. 273-278, September 1999.

153. M. Necker and G. Stuber, ‘‘Totally Blind channel estimation for OFDM over fast varying mobile channels’’, IEEE proceedings of international conference on communications, April 28-May 2 2002.
154. P. L. Jiangping and X. B. R. Zhou, “Channel estimation in MIMO OFDM system by tracking the delay-subspace”, IEEE 2007.
155. Andreas F. Molisch and Moe Z. Win, ‘‘MIMO systems with antenna selection’’, IEEE microwave magazine, March 2004.
156. Y. S. Choi, A.F. Molisch, M.Z. Win and H.H. Winter, ‘‘Fast antenna selection algorithms for MIMO systems’’, IEEE proceedings of vehicular technology conference, 2003.
157. Ye (Geoffrey) Li, Jack H. winters and Nelson R. Sollenberger, ‘‘MIMO-OFDM for wireless communications: Signal detection with enhanced channel estimation’’, IEEE transactions on communications, Vol. 50 No.9, pp 7942-7957, September 2002.
158. Application note on “Channel estimation for WCDMA Rake Receiver”, Nov 2004. http://www.freescale.com.